Assessing the impacts of the Oyster Creek Nuclear Generating Station and its closure on gelatinous zooplankton and planktonic community structure

Paul Bologna, John Gaynor, Robert Meredith, and Matthew Schuler

Department of Biology, Montclair State University

Prepared for:

New Jersey Department of Environmental Protection

Division of Science and Research

Project Manager: Joseph Bilinski

April 2023

State of New Jersey
Phil Murphy, Governor

Department of Environmental Protection
Shawn M. LaTourette, Commissioner

Division of Science & Research
Nicholas A. Procopio, Ph.D., Director

Visit the DSR website:
https://dep.nj.gov/dsr

Please cite as: **Bologna, P., Gaynor, J., Meredith, R. and Schuler, M. 2023.** Assessing the impacts of the Oyster Creek Nuclear Generating Station and its closure on gelatinous zooplankton and planktonic community structure. Final Report. New Jersey Department of Environmental Protection. Trenton, NJ. 146 pages.

Executive Summary

For the last decade we have been monitoring and investigating the gelatinous zooplankton community in Barnegat Bay, New Jersey. During this time frame, Barnegat Bay was severely impacted by Superstorm Sandy, which directly impacted the density of the top predator the Bay Nettle (*Chrysaora chesapeakei*), allowing a more diverse community of gelatinous zooplankton species to flourish after the storm. In addition, the operation of the Oyster Creek Nuclear Generating Station (OCNGS) has put significant stresses on the health of Barnegat Bay for over 50 years through direct destruction of planktonic organisms, redirection of water flow used in cooling the plant, and a chronic thermal stress. This research looked at determining the changes associated with the closure of the plant on the zooplankton community to assess whether the closure resulted in improved ecological conditions to support the recovery of Barnegat Bay after this chronic stress.

A sampling protocol was established to assess the spatial and temporal distribution of gelatinous zooplankton from Barnegat Bay to determine the potential impact that the closure of OCNGS would have. Sampling occurred between May and September of 2018, 2019, and 2021. Water quality measurements generally follow a typical seasonal pattern, but evidence of hypoxia was observed for the Oyster Creek Route 9 site (OCNGS Outflow site) in 2021, suggesting that the water quality dynamics have been impacted by the closure. Linked with this change, was the elevated (>1C) temperatures observed at the Forked River Route 9 site in 2021 as well. It may be possible that the reduction in flow associated with the closure has allowed thermal exchange to occur in the system, potentially leaching back into the Forked River due to lack of flow toward the uptake of the plant. However, these minor changes in 2021 pale in comparison to the significant thermal loading observed in 2018. As such, the closure of OCNGS has resulted in improved temperature regimes for Barnegat Bay and likely play a critical part in the improved biological conditions observed in 2021.

Assessing the multi-year sampling program provides insight into the changes observed in the bay from the closure of the plant. When evaluating the changes from 2018 to 2021, lift net sampling demonstrated an increase in density of the two major gelatinous zooplankton in the bay, the comb jelly *Mnemiopsis leidyi* and the scyphozoan, *Chrysaora chesapeakei*. While *M. leidyi* densities increased, the increase was not significant. However, a significant increase in *C. chesapeakei* densities did occur increasing on average six-fold from 2018 to 2021. In contrast, these results are slightly different from the plankton sampling effort, which showed significant increases in *M. leidyi* densities from 2018 to 2021, reflecting the ability of the plankton nets to collect the smallest individuals. However, for *C. chesapeakei*, no differences were observed among years, which may be an artifact of the sampling process. As predicted, the plant closure did result in increases in major gelatinous zooplankton species.

Plankton tows were also able to document significant increases in the density of many critical species for which the plant was known to have a substantial impact on. Specifically, significant increases in Calanoid Copepod densities were recorded, as well as significant increases in Fish Eggs, and *Menidia menidia* (Atlantic Silverside). This suggests that with the closure of OCNGS, several key groups of organisms are showing increases in their populations. As copepods, fish eggs, and silversides are important in the support of coastal food webs and recreationally and commercially important species, the future of Barnegat Bay looks promising as it recovers from the substantial thermal and biological impacts the plant exerted on the bay.

Analysis of molecular samples has yielded tremendous insight into the presence of species in Barnegat Bay. With over 300 taxa identified from NEXGEN sampling and confirmation of species

identities through molecular analyses of micro-medusa, a better foundation of the taxa richness and community structure has been gained. This includes the identification of numerous non-native species, some of which are well established now like the hydrozoan *Eucheilota maculata*, as well as the identification of new locations where the invasive hydrozoan *Gonionemus vertens* has spread to, prior to collecting live adults in subsequent sampling events. NEXGEN analyses demonstrated significant differences in community structure that existed between areas of direct impact from the OCNGS and external controls during its operation in 2018. After the closure of the plant, significant changes in community structure were evident, and with corroborating evidence from the significant increases in fish eggs, fish larvae, copepods, and several other taxa seen in the plankton tow samples, demonstrate that Barnegat Bay is beginning to recover from the long-term stresses placed on it. Supporting the recovery of the faunal communities, NEXGEN sampling data showed no significant differences were seen among sites using the compiled taxonomic information from 2021, suggesting a more robust and diverse Barnegat Bay. Continued monitoring of the abundance and community structure of the zooplankton is needed to evaluate the recovery and assess how the bay may fare under future climate change scenarios. However, it appears that the closure of the OCNGS has had a positive impact on the zooplankton community in Barnegat Bay, New Jersey.

In summary, the closure of OCNGS has resulted in improved environmental and ecological conditions for Barnegat Bay. The elimination of the chronic thermal stress due to cooling needs of the plant has provided an opportunity for the recovery of organisms and communities in the surrounding waters. While this is a critically important part of the recovery, the greatest positive impact was the near elimination of organism loss due to entrainment and impingement. While recovery of the zooplankton community improved, but was muted in 2019, the results from 2021 clearly indicate a system in recovery. Specifically, for calanoid copepods, which are an essential link in the trophic web of Barnegat Bay, we saw a five-fold increase in densities by 2021 when compared to 2018. More encouraging though was the order of magnitude increase in fish egg density and the two orders of magnitude increase in density of the Atlantic Silverside (*Menidia menidia*). These massive increases come despite the increases in their predators (i.e., *C. chesapeakei* and *M. leidyi*), indicating that during the timeframe of this work substantial improvements in the health of Barnegat Bay are occurring and hopefully in time we will continue to see planktonic communities flourish. Continuing efforts to monitor and evaluate the changes are needed to ensure that the health and wellbeing of Barnegat Bay continues to improve in the face of every growing urbanization and commercial development occurring in the region.

Table of Contents

List of Figures

List of Tables

Statement of the Problem:

Increasing coastal development has created environments which favor species that are tolerant of various pollutants and degraded water quality. Additionally, the hardening of shorelines and elimination of natural vegetated regions creates the potential that tolerant fouling organisms can colonize and expand in these degraded systems. Many developed coastal estuaries are plagued by poor water quality and increasing inclusion of non-native species. As such, developed coastal estuaries are being defined by lowered species richness and diversity as invaders monopolize available space (Ruiz et al. 1997, Cohen & Carlton 1998); quantity and toxicity of pollutants (Long et al. 1996); loss of natural habitats (Lathrop & Bognar 2001); and simplification of food webs through redirection of energy, species introduction, and overfishing (Byrnes et al. 2007). In particular, the relative increase in gelatinous zooplankton in many regions of the ocean has led to a phase shift from 'textbook' planktonic communities dominated by zooplanktivorous fish and higher apex predators to ones dominated by ctenophores, cnidarians, and pelagic tunicates. While the apparent global increase in gelatinous zooplankton is actively debated (see Condon et al. 2013), many specific regional locations have strong documentation of elevated abundances (Fuentes et al. 2010) often leading to food web disruption and fisheries crashes (Roohi et al. 2010).

In addition to the general development of coastal systems, power generation has led to significant thermal impacts on communities, as well as entrainment and impingement issues related to biological resources. The Oyster Creek Nuclear Generating Station (OCNGS) is one of these coastal developments which has had profound impacts on the Barnegat Bay Estuary through thermal loading and direct mortality of a variety of coastal species which have been entrained through the plant. Many of these organisms are small planktonic taxa or represent egg/larval stages of benthic and pelagic taxa. With the shut-down of the plant, this research will utilize a BACI (Before-After, Control-Impact) design to ascertain the current impacts of OCNGS on gelatinous zooplankton communities and the projected changes associated with decommissioning of the plant.

2021 Scope of Project

1. **Assess the distribution of gelatinous zooplankton and potential impacts of Oyster Creek Nuclear Generating Station (OCNGS) on planktonic community structure.**
2. **Assess community structure across temporal scales: comparing baseline data from 2012-2014 with community structure data from 2018-2021.**
3. **Metagenomic Composition assessment of planktonic communities and impacts of OCNGS.**

Project Methods

Objective 1: Assess the distribution of gelatinous zooplankton and potential impacts of Oyster Creek Nuclear Generating Station (OCNGS) on planktonic community structure.

To complete Objective 1, we divided our sampling approach into bi-monthly regional surveys, and targeted coastal development (i.e. lagoon) sampling.

Table 1. Sampling Site Locations & Designations

Sampling Site	Abbreviation	GPS Coordinates	Site Designation
Toms River West	TRW	N39.93296, W74.13198	Control
Sunrise Beach Open Water	SB	N39.83807, W74.15535	Control
Sunrise Beach Lagoon	SBL	N39.84025, W74.15052	Control
Forked River Lagoon	FRL	N39.82283, W74.18880	Impact
Forked River West	FRW	N39.82166, W74.16698	Impact
Forked River Rt.9	FRR9	N39.82065, W74.20147	Impact
Forked River East	FRE	N39.81217, W74.12657	Control
Oyster Creek Rt.9	OCR9	N39.81032, W74.24298	Impact
Oyster Creek Mouth	OCM	N39.80896, W74.16871	Impact
Double Creek East	DCE	N39.78779, W74.15613	Control
Double Creek West	DCW	N39.78574, W74.20119	Control
Bay Shore Lagoon	BSL	N39.76658, W74.19637	Control

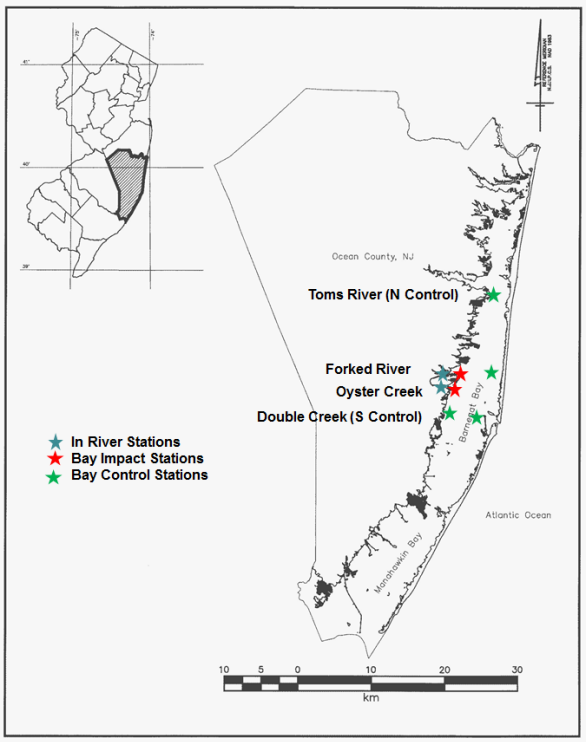

Figure 1. Bay Sampling Sites

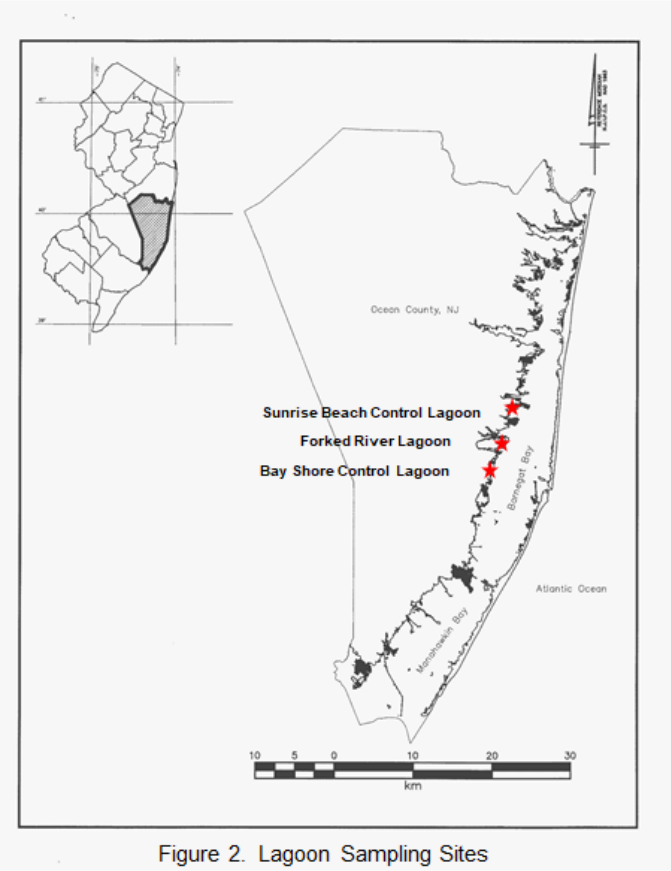

Figure 2. Lagoon Sampling Sites

a. Bi-Monthly assessment in Barnegat Bay

We established 9 sampling sites in Barnegat Bay which were sampled between May 25 and September 25, 2021 (Table 1, Figure 1). Specifically, we sampled the river and bay regions of the Forked River and Oyster Creek region (n=4). These sites represent the communities directly impacted by the plant in the intake and outflow regions of OCNGS. Five external sites were established to act as control regions for comparison. These include two stations to the south (Double Creek East and West) previously used in our bay-wide work from 2012-14, one site east of Forked River used as an eastern control point (also previously used in our bay-wide work from 2012-14), one just north of Forked River (Sunrise Beach) and one northern control point at Toms River (Figure 1). This provides essential data regarding the spatial and temporal distribution surrounding the OCNGS in Barnegat Bay. A combined sampling program of lift nets (n=10) and plankton tows (n=4, 3 for direct counts, 1 for metagenomics analyses, Objective 3) allowed us to assess the distribution of gelatinous zooplankton, as well as zooplankton. These data provide the broad-based distribution and identify potential relationships among various zooplankton groups and the potential impacts of the OCNGS on the relative abundance and taxa richness of these organisms.

b. Targeted coastal development sampling

Cnidarian polyps are known to settle on various hard substrates and increasing coastal development has increased the amount of available surface for settling larvae. As these polyps are the ultimate source of new adult medusae, we are planning to sample developed regions in Barnegat Bay to gain an understanding of the distribution within these communities and the potential impacts of OCNGS. Three sites were sampled monthly in June, July, and August using lift nets and plankton nets to assess gelatinous zooplankton (Figure 2). Specifically, the Forked River Lagoon system lies between the intake and outflow

region of the OCNGS and has the greatest potential to show impacts on the relative abundance of gelatinous zooplankton. In addition, a northern control lagoon system will be sampled (Sunrise Beach Lagoon) as well as a southern control lagoon (Bay Shore Lagoon).

c. Intensive OCNGS Sampling

It is recognized that both tidal and nocturnal status of zooplankton communities can change dramatically. To address this temporal variability in gelatinous zooplankton communities, we conducted a targeted day-night sampling program associated with the OCNGS. Specifically, we sampled the river and bay regions of the Forked River and Oyster Creek region (n=4). These sites represent the communities directly impacted by the plant in the intake and outflow regions of OCNGS. Intensive sampling occurred once in July 2021. The sampling regime encompassed day and night sampling events during a 24-hour period. In this way, we can capture diel comparisons which may impact zooplankton communities. A combined sampling program of lift nets and plankton tows will allow us to assess the distribution of gelatinous zooplankton, as well as zooplankton during these sampling events.

d. Molecular Identification of Cnidarians from Plankton tows

Zooplankton tows done in the field are immediately assessed for ctenophores and large medusae. All plankton tows are preserved in ethanol and returned to the lab for a more careful and thorough enumeration of all organisms captured to the lowest taxonomic unit. Invariably, we find small medusae (< 1 mm) and unknown ephyrae. Due to their small size and lack of distinguishing features, these are often difficult to assess using traditional taxonomic tools (Dawson & Jacobs, 2001; Schroth et al., 2002) and we isolated these unknowns and identified them using DNA barcoding. Individual unknown cnidarians were transferred in ethanol and DNA isolated as described by Gaynor et al. (2016). DNA was quantified and subjected to PCR amplification using the common barcoding regions of 16S and COI (Gaynor et al., 2016). Samples that generated clean amplicons of the predicted size were sequenced in-house using our ABI 3130 Automated DNA Sequencing Platform. Unknown DNA samples were then subjected to BLAST searches (Altschul et al., 1990) to identify the organism using both barcoding loci. We consider this to be especially useful in light of our recent discoveries of non-native cnidarians in NJ coastal systems (Gaynor et al., 2016; Restaino et al., 2018a, 2018b).

Objective 2: Assess community structure across temporal scales: comparing baseline data from 2012-2014 with community structure data from 2018-2021.

During 2012-2014, we collected gelatinous zooplankton data describing the conditions in Barnegat Bay, including stations near the OCNGS (Bologna et al. 2015, 2017). These data include conditions prior to Super-storm Sandy (2012) and two years of community assessment afterwards (2013-2014). Results from these data indicated that the significant reduction in the dominant predator, *Chrysaora chesapeakei* (formerly *C. quinquecirrha*), occurred post Sandy and caused dramatic shifts in the structure of the gelatinous zooplankton community with increased species richness and diversity (Bologna et al. 2017). Our proposed sampling sites replicate five of these stations including: Forked River East (East Control) Forked River West (Impact), Double Creek East and Double Creek West (Southern Controls), as well as Toms River West. In order to bridge these data and ascertain whether changes in baseline are present and to assess the changes associated with the closure of the plant; the comparable site data will be analyzed to compare the density of gelatinous zooplankton among years (2012-2014 to 2018-2021).

Objective 3: Metagenomic Composition assessment of planktonic communities and impacts of OCNGS

Next generation sequencing (NGS) platforms provide a wealth of DNA sequence information and have revolutionized the biological sciences. As compared to traditional sequencing methods, NGS allows for the rapid and accurate development of genomic resources. NGS targeted sequencing (barcoding) has

proven useful for revealing patterns of marine benthic biodiversity on a large scale (e.g. Leray and Knowlton 2015).

DNA Extraction

Planktonic samples were collected from OCNGS as indicated in Objective ## Samples for NGS analysis were immediately mixed with 100% ethanol to yield a final concentration of 70% (v/v) ethanol. Samples were labeled and stored on ice until returned to the laboratory where they were stored at -20C until extracted. Each sample was concentrated by centrifugation (15,000 x g for 10 min @4C) and pellets briefly dried in a Speed-Vac and weighed to determine the fresh weight of each sample. Total genomic DNA was isolated from each pellet using a CTAB/NaCl protocol (Winnepenninckx et al., 1993 as modified by Gaynor et al., 2016). A complete protocol is detailed in Appendix A of this document. Genomic DNA was quantified by fluorescence with Qubit 3.0 and by UV spectroscopy using a Nanodrop 1000.

NGS Library Preparation

NGS sequence analysis of these samples was carried out using amplified targeted regions in metazoan DNA (cytochrome c oxidase subunit I (COI) primers). A library was generated for each metagenomic DNA sample using PCR employing a cocktail of COI primers. The 5 degenerate primers used were:

>dgLCO1490
TCGTCGGCAGCGTCAGATGTGTATAAGAGACAGGGTCAACAAATCATAAAGAYATYGG

>dgHCO2198
GTCTCGTGGGCTCGGAGATGTGTATAAGAGACAGTAAACTTCAGGGTGACCAAARAAYCA

>jgLCO1490
TCGTCGGCAGCGTCAGATGTGTATAAGAGACAGTITCIACIAAYCAYAARGAYATTGG

>jgHCO2198
GTCTCGTGGGCTCGGAGATGTGTATAAGAGACAGTAIACYTCIGGRTGICCRAARAAYCA

>mlCOIintF-XT (Internal COI primer)
TCGTCGGCAGCGTCAGATGTGTATAAGAGACAGGGWACWRGWTGRACWITITAYCCYCC

All primers were synthesized by IDT-DNA (Integrated DNA Technologies | IDT (idtdna.com)) and included either the forward or reverse Illumina adaptor sequences on the 5' end of each primer. PCR amplifications were performed using I-5 2X Taq DNA polymerase Master Mix (https://www.mclab.com/I-5-2X-High-Fidelity-PCR-Master-Mix.html) according to manufacturer's directions with the exception that we used 20 µL reaction volumes. Primers used for amplification of the COI loci are listed above. PCR was carried out in a ProFlex Thermal Cycler (Applied Biosystems, Inc.) according to the following parameters: 98C for 2 min (1X); 98C for 20 s, 50C for 30 s, and 72C for 30 s (40X); 72C for 7 min (1X); followed by a hold at 4C. Positive and negative template controls were always run and typically 10 µL of each amplicon was run on a 1.25% (w/v) agarose gel to assess purity and yield of PCR product.

NextGen Sequence Analysis

NGS sequencing was run in-house using the Illumina MiSeq platform. The MiSeq platform can typically yield ~25 million 300 base pair (bp) reads per run (using the V3 cartridge with paired-end reads). Prior to pooling, each library was quantified using a Qubit 3 fluorometer and normalized to 20 pM. Once pooled, normalized libraries were spiked with 20% PhiX as recommended by the manufacturer as a control for low diversity libraries and loaded onto the cell at a final concentration of 4 pM. Typically, multiple libraries (~30 to 45) were pooled and indexed (which allows for sample identification) per run (see 16S Metagenomic Sequencing Library Preparation, Illumina). This sequencing scheme should allow for all

species present in a given sample to be amplified. Output was generated as raw fastq files that were processed as described below.

Bioinformatic Analyses

PEAR

Raw demulitplexed fastq files from the MiSeq runs were first processed using the paired-end read merger PEAR (Zhang et al. 2014). Forward and reverse sequences were merged prior to all analyses because our targeted COI sequences range from approximately 350 bp to 900 bp. All resultant sequences from a given collection site analyzed by PEAR (paired, unpaired forward, unpaired reverse) were subsequently concatenated into a single fastq file.

Categorical Sample Groupings

All samples, which were amplified for 2019, were analyzed and categorically grouped for faunal statistical analyses and taxonomic identification as implemented in QIIME2 (Bolyen et al. 2019). Major groupings include:

- **Location** (Bayshore Lagoon [n=3], Double Creek East [n=6], Double Creek West [n=7], Forked River East [n=7], Forked River Lagoon [n=7], Forked River RT9 [n=8], Forked River West [n=8], Oyster Creek Mouth [n=8], Oyster Creek Outflow RT9 [n=8], Sunrise Beach Lagoon [n=3], Sunrise Beach Open Water [n=7], Toms River [n=5]);
- **Geography** (East [n=13], West [n=46], Lagoon [n=13], North [n=5]);
- **Circulation** (Lagoon [n=13], River [n=19], Tidal open [n=43]);
- **Impact_1** (Control [n=38], Impact [n=39]);
- **Impact_2** (Control [n=27], Far Control [n=11], Impact [n=39]);
- **Site-group** (Inflow [n=23], Lagoon [n=6], Near Control [n=27], Outflow [n=16]), Far Control [n=5];
- **Time of Day** (Night [n=4], Day [n=73]);
- **Temperature regime** (Low [n=25], Medium [n=23], High [n=21], Extreme [n=8]); and
- **Salinity Regime** (Euryhaline [n=20], Polyhaline [n=52], Mesohaline [n=5]).
- See BarnegatBay_2019-metadata.xlsx for more details of categorical binning,

Additional combined analyses were performed that combined the 2018 and 2019 samples. Likewise, all of these samples were analyzed and categorically grouped for faunal statistical analyses and taxonomic identification as implemented in QIIME2 (Bolyen et al. 2019). These analyses either grouped data into categories regardless of collection year or compared each category by year. Major groupings include:

- **Location** (Bayshore Lagoon [n=6], Double Creek East [n=9], Double Creek West [n=11], Forked River East [n=12], Forked River Lagoon [n=11], Forked River RT9 [n=13], Forked River West [n=14], Oyster Creek Mouth [n=14], Oyster Creek Outflow RT9 [n=14], Sunrise Beach Lagoon [n=6], Sunrise Beach Open Water [n=12], Toms River [n=10]);
- **Geography** (East [n=21], West [n=78], Lagoon [n=23], North [n=10]);
- **Circulation** (Lagoon [n=23], River [n=37], Tidal open [n=72]);
- **Impact_1** (Control [n=66], Impact [n=66]);
- **Impact_2** (Control [n=45], Far Control [n=21], Impact [n=66]);
- **Site-group** (Inflow [n=38], Lagoon [n=12], Near Control [n=44], Outflow [n=28]), Far Control [n=10];
- **Time of Day** (Night [n=7], Day [n=125]);
- **Temperature regime** (Low [n=43], Medium [n=38], High [n=37], Extreme [n=14]);
- **Salinity Regime** (Euryhaline [n=32], Polyhaline [n=90], Mesohaline [n=10]); and
- **Power Plant Closing** (After [n=77], Before (n=55).

QIIME2 Analyses – Statistical Analyses of Species Diversity

The site-specific PEAR sequences were imported and analyzed as single end read files in QIIME2 (Bolyen et al. 2019). The q2-demux plugin was used to determine the number of sequences obtained per sample and their quality. Sequences were then denoised using DADA2 (via q2-dada2 plugin) (Callahan et al. 2016) with the following settings: trim-left 10, trunc-len 290, trunc-q 20. DADA2 allows for the detection and correction of Illumina sequence data as well as the removal of phiX reads and chimeric sequences. The amplicon sequence variants (ASVs) were subsequently aligned using mafft (Katoh et al. 2002) and the phylogenetic tree was inferred using fasttree2 (Price et al. 2010) implemented in the q2-phylogeny plugin. ASV's are single DNA sequences representing the sequenced COI amplicons. ASV's are used in all analyses as they provide a more accurate estimate of sequence variation than do operational taxonomic units (OTUs). OTUs represent clusters of sequences based on some threshold of sequence similarity.

The alpha diversity metric Enspie (Chase and Knight 2013) as implemented in the alpha diversity plugin was used to explore the composition of the zooplankton samples. All samples were subsampled without replacement (i.e. rarefied) to 3254 sequences per sample (2019) and 1988 (2018-2019 combined analysis) based off of the sample with smallest number of sequences. These values were chosen so as to retain as many samples as possible with high sequence counts for downstream analyses. Two samples were excluded from both analyses (one from Double Creek East and the other from Toms River West). All Toms River samples were also excluded in two additional analyses due to it being more of a freshwater ecosystem as compared to all other sites.

Taxonomic Analyses

A custom COI reference database and corresponding taxonomic classifications was created for all taxonomic analyses using a series of custom scripts and R 3.6.2 (R Core Team, 2019). Only metazoan taxa were included. All metazoan COI fasta sequences were downloaded from the NCBI database searching on COI, COX1, and CO1 for Annelida, Arthropoda, Bryozoa, Chordata, Cnidaria, Echinodermata, Mollusca, Nematoda, Platyhelminthes, Rotifera, and Porifera. The longest sequence for each taxon was kept when multiple sequences for the same species was present and where possible only vouchered sequences were kept. Custom scripts concatentated the fasta files from each of the individual searches and renamed each fasta sequence with its corresponding accession number only. The NCBI taxonomy was then assigned to each sequence using R 3.6.2 (R Core Team, 2019) and the Taxonomizr (v0.5.3; Sherrill-Mix, 2019) package. Additional custom scripts then converted the Taxonomizr IDs to the QIIME2 taxonomy format. The q2-feature-classifier fit-classifier-naive-bayes was used to train the classifier on the full-length COI sequences (unique NCBI COI sequences and associated taxonomy created above). The feature-classifier classify-sklearn (Bokulich et al. 2018). Each ASV was then assigned a taxonomic ranking at 0.7 confidence using the feature-classifier classify-sklearn (Pedregosa et al. 2011).

Results

Water Quality

Bay Wide Sampling Sites: Salinity, temperature, and dissolved oxygen water quality parameters were collected on each sampling event. Samples were collected on May 25, June 10, June 23, July 15, July 27, August 10, and September 25, 2021. Water quality showed substantial variation among sites. In regard to salinity, several sampling trips occurred on days following substantial rain events, so riverine sites showed reduced salinities on those dates (Figure 3). In general, Toms River West showed the lowest average salinity, but both Forked River Route 9 and Oyster Creek Route 9 (in-flow and out-flow of OCNGS) showed substantial freshwater inputs during sampling (Figure 3). With regards to temperature, all sites showed seasonal patterns of increases then cooling during the last sampling events (Figure 4). Incredibly, average water temperature was highest at Forked River Lagoon and Forked River Route 9 site. In fact, these temperatures were >1C higher than the Oyster Creek Route 9 site, where the greatest thermal loading was observed during the operation of OCNGS in 2018. When dissolved oxygen was investigated, most sites maintained relatively high concentrations of oxygen and little evidence of hypoxia (Figure 5), with the exception of Forked River Lagoon and Oyster Creek Route 9 sampling in August, where values were below 5mg/l. Additionally, Oyster Creek Route 9 showed evidence of hypoxia in September (Figure 5), which may indicate the change in circulation due to closure is impacting water quality in unexpected ways.

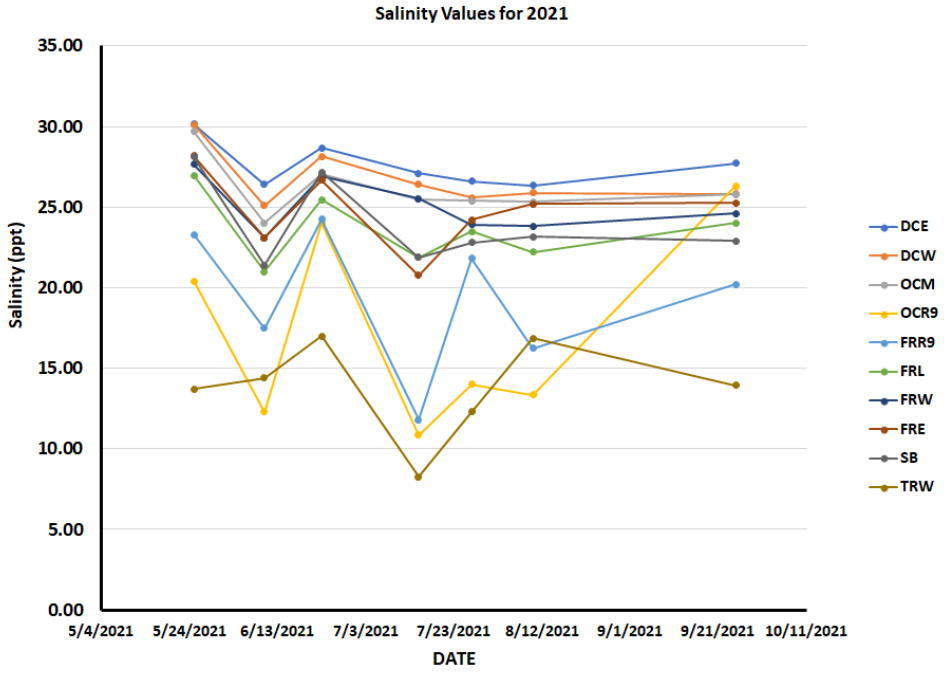

Figure 3. Salinity concentrations among Bay sites in 2021.

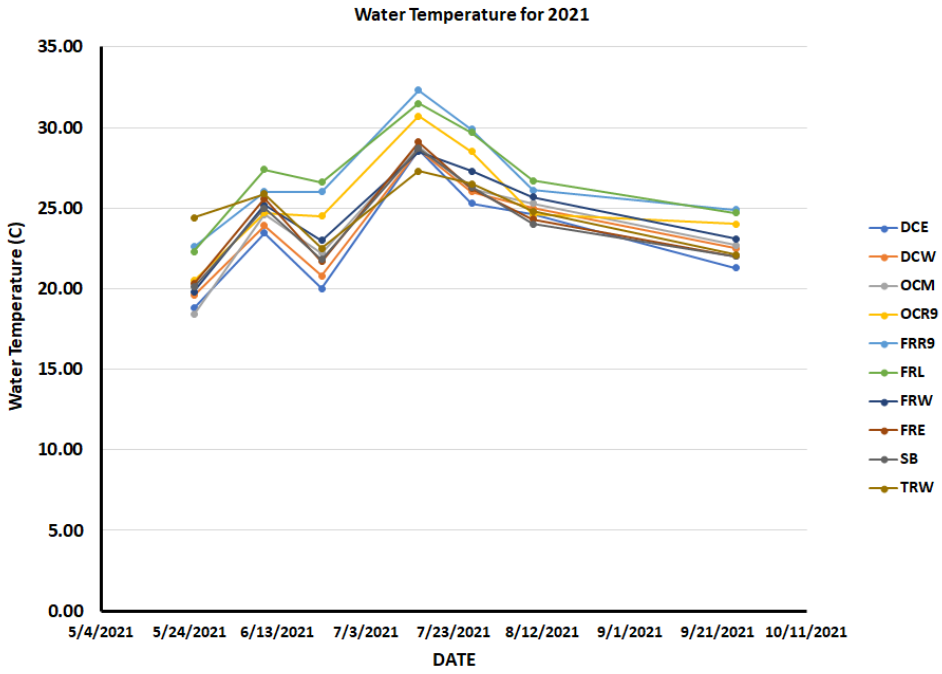

Figure 4. Water temperature among Bay sites in 2021.

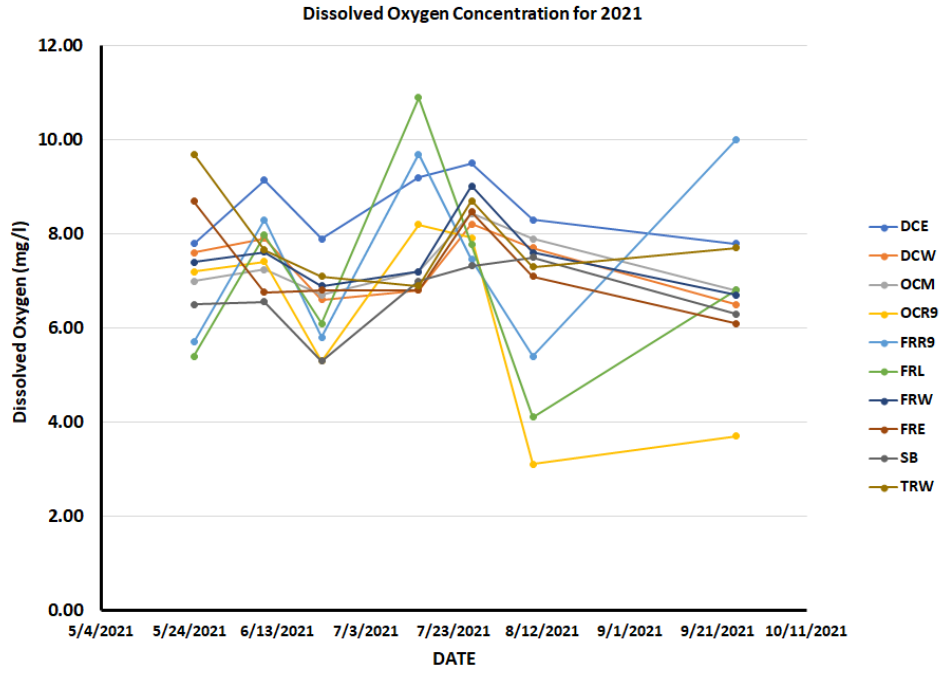

Figure 5. Dissolved oxygen concentrations among Bay sites in 2021.

Day-Night Water Quality:

During 2021, day and night sampling occurred only in July, since the August sampling event was compromised by COVID among the crew and PI. Sampling occurred on July 27th during the day and then at night into July 28th. Salinity values represent typical estuarine conditions (Figure 6), with the lowest salinity observed at the Forked River Route 9 site, demonstrating that reduced water circulation from the plant has minimized salinity at that site. What is perplexing is the relatively high water temperatures observed at this same site (Figure 7), almost 2C greater, and this greater temperature was also evident in the bay-wide sampling (Figure 4). When assessing dissolved oxygen, all sites for both day and night showed high oxygen concentrations and no evidence of hypoxia (Figure 8).

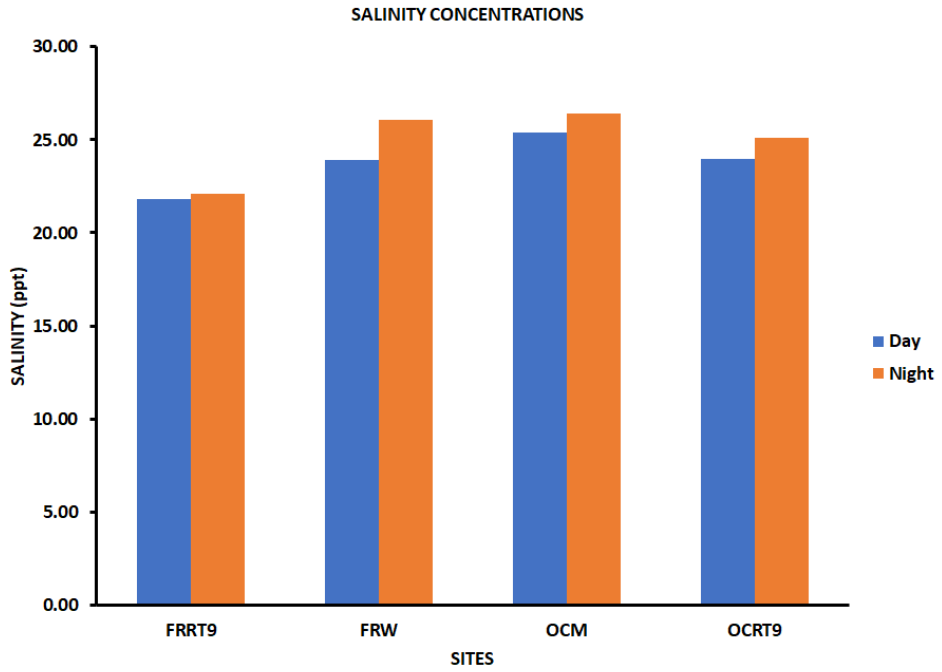

Figure 6. Day-Night Comparisons of Water Salinity among Bay sites on July 27-28, 2021.

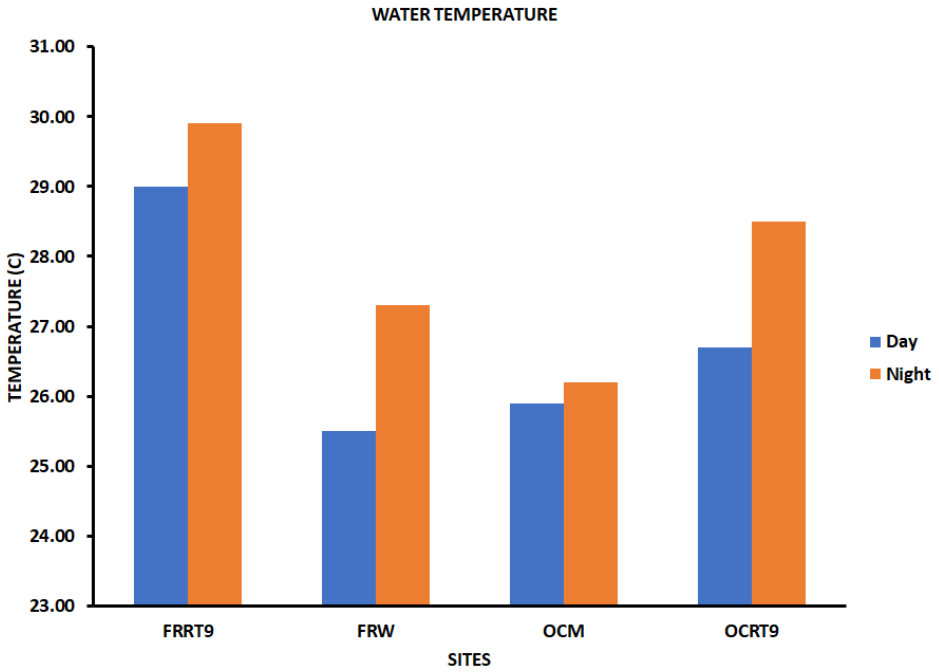

Figure 7. Day-Night Comparisons of Water temperature among Bay sites on July 27-28, 2021.

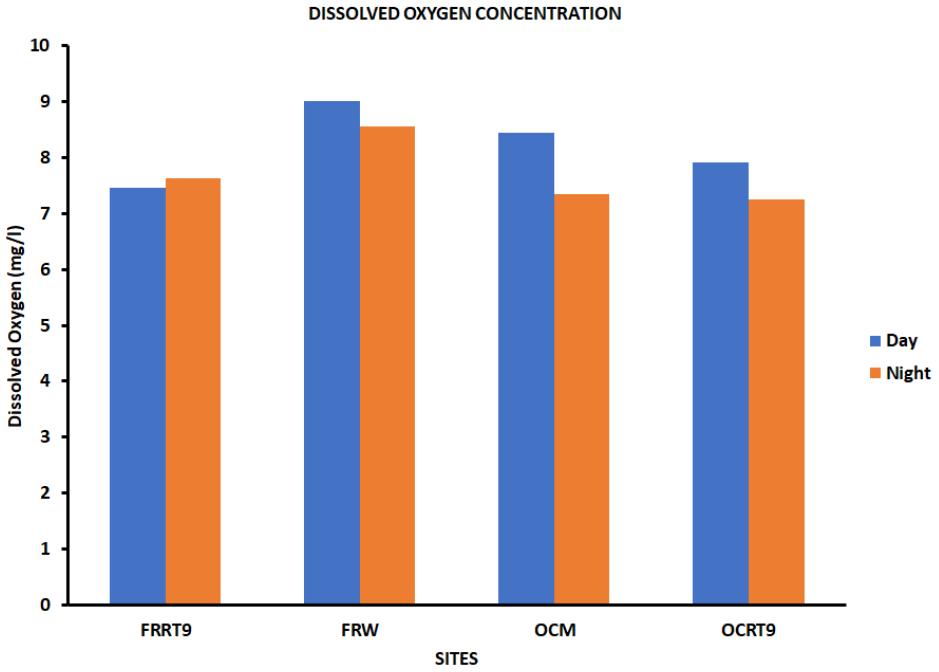

Figure 8. Day-Night Comparisons of Dissolved Oxygen concentrations among Bay sites on July 27-28, 2021.

Water Quality Lagoon Sampling Sites:

Water quality measurements in the lagoons varied among sites in 2021. Salinity at Bayshore Lagoon began at high values in June, but steadily decreased during sampling and was greatly reduced in August (Figure 9). Lagoon water temperature showed a seasonal increase and was similar among all sites (Figure 10). Dissolved oxygen showed some unusual patterns in Forked River Lagoon showing extremely high values in July, but hypoxia in August (Figure 11). The other sites showed relatively stable oxygen concentrations with no evidence of hypoxia.

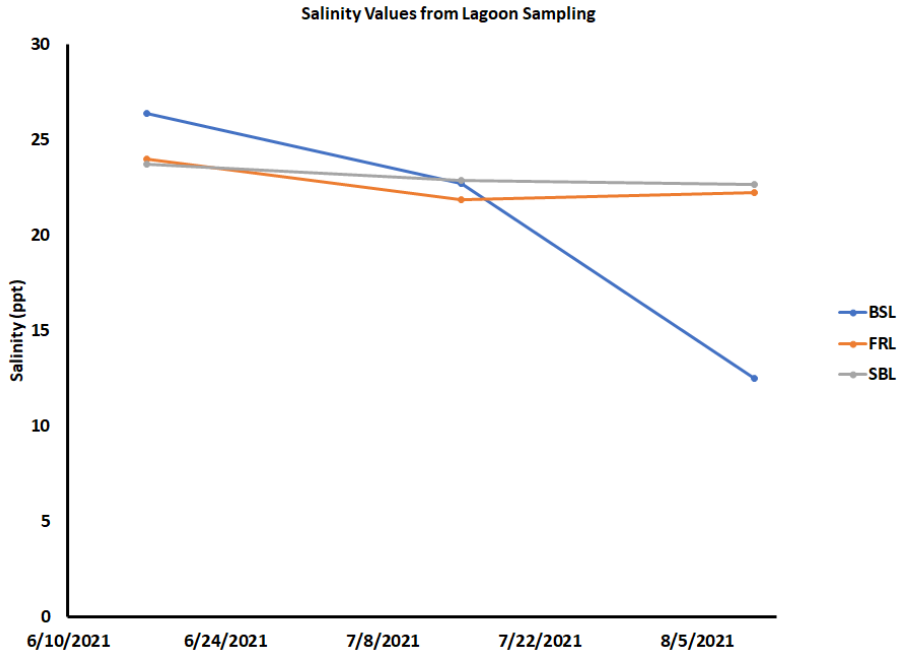

Figure 9. Salinity concentrations among lagoon sites in 2021.

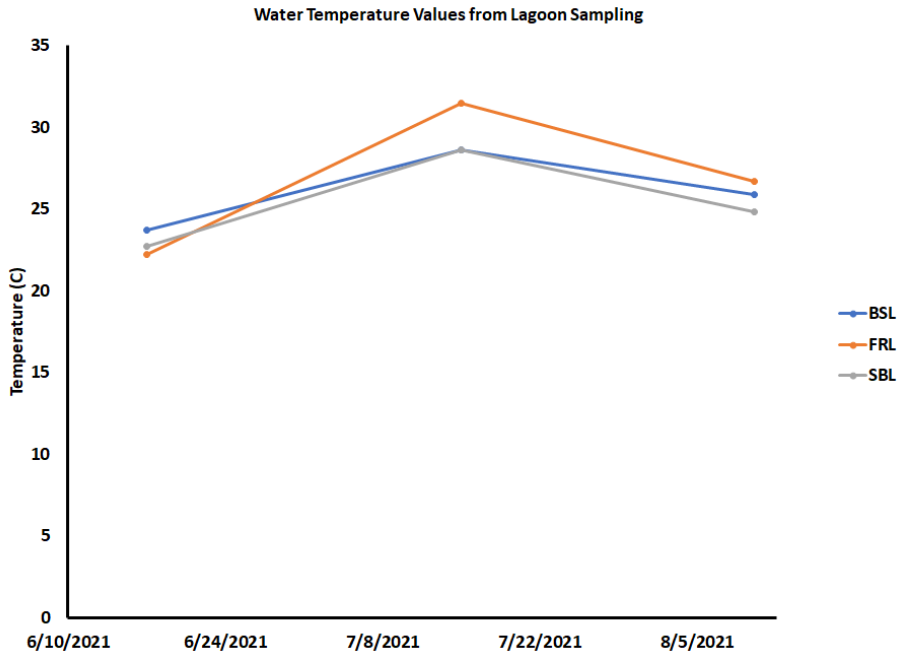

Figure 10. Water temperature among lagoon sites in 2021.

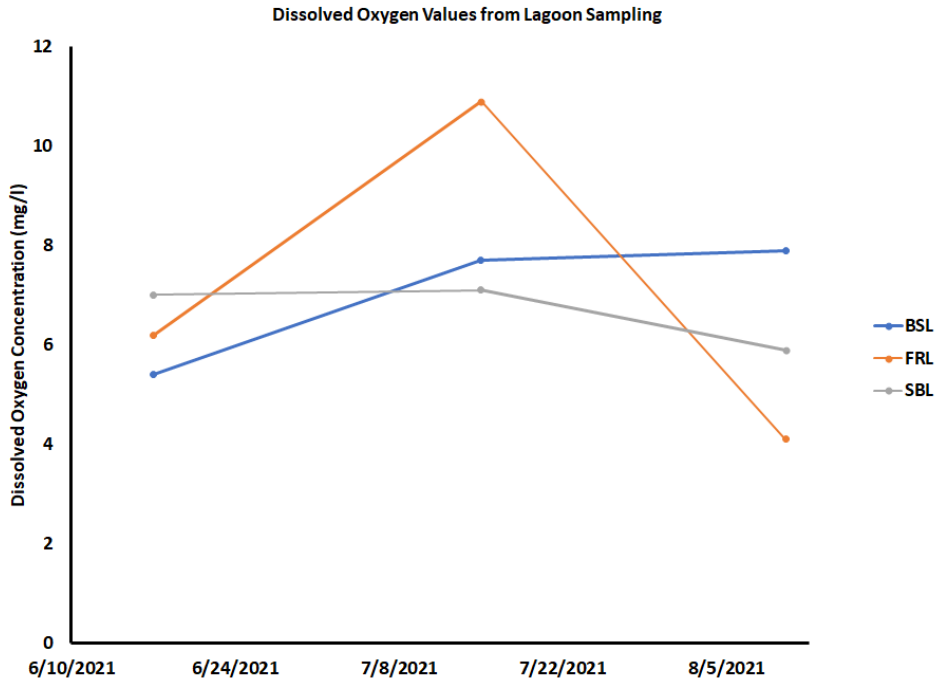

Figure 11. Dissolved oxygen concentrations among lagoon sites in 2021.

2021 Lift Net Results

Bay-Wide Sampling:

Lift net sampling resulted in the identification of seven gelatinous zooplankton species including *Chrysaora chesapeakei*, *Nemopsis* spp., *Mnemiopsis leidyi*, *Salpa salpa*, *Gonionemus vertens*, *Aequora* spp. and *Pleurobrachia pileus*. Numerically, *M. leidyi* was the most abundant species (Figure 12) and differed significantly among sites in the ANCOVA for 2021 ($F_{9,728} = 5.81$, $P < 0.0001$). *Chrysaora chesapeakei* also differed significantly among sites ($F_{9,728} = 7.53$, $P < 0.0001$), with significantly greater densities at Forked River Lagoon, Forked River Rt. 9, and Toms River West compared to all other sites, while *Nemopsis bachei* density was significantly greatest at Forked River East and Toms River West (Figure 12) compared to all other sites ($F_{9,728} = 7.06$, $P < 0.0001$).

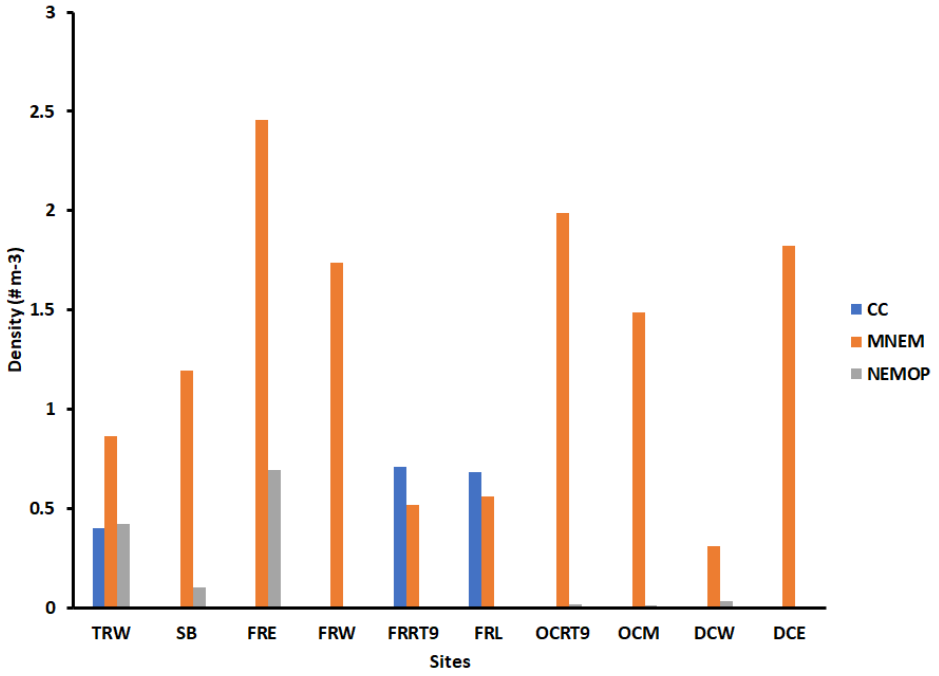

Figure 12. Average density of the three major gelatinous zooplankton species among all sites. Taxa abbreviations: CC = *Chrysaora chesapeakei*, MNEM = *Mnemiopsis leidyi*, NEMOP = *Nemopsis bachei*.

Lagoon Sampling:

During 2021, Lagoons were sampled on June 17, July 15, and August 10. Lift net sampling yielded only two gelatinous species in abundance, which included *M. leidyi* and *C. chesapeakei* (Table 2). For *M. leidyi*, overall density was significantly higher in July that other months ($_{F2,80}$ = 4.5, P < 0.014), but none were collected from FRL in July leading to a significant interaction between site and month (P < 0.0001). For the Bay Nettle, they were only recorded from the Forked River Lagoon and were greatest in June compared to July and August, leading to another significant interaction between month and site (P < 0.0001). The only other species to be identified from the lift nets were single occurrences of *Nemopsis bachei* and *Pleurobrachia pileus*.

Table 2. Densities of *M. leidyi* and *C. chesapeakei* from Lagoon sampling sites in 2021.

M. leidyi density (# m^{-3})			
Site	June 17	July 15	August 10
Sunrise Beach Lagoon	0.18	1.19	0.71
Forked River Lagoon	1.10	0.00	0.75
Bay Shore Lagoon	0.25	1.65	0.29
C. chesapeakei density (# m^{-3})			
Site	June 17	July 15	August 10
Sunrise Beach Lagoon	0	0	0
Forked River Lagoon	2.01	0.07	0.07
Bay Shore Lagoon	0.00	0.00	0.00

2021 Plankton Tow Results

Bay-wide Sampling

Plankton samples were collected on seven dates from May to September 2021. Numerically, samples were dominated by Calanoid copepods and several crustacean taxa including shrimp and crab larvae (Table 3). Among these taxa, results from the ANCOVA showed significant differences in density among sites for Calanoid copepods ($F_{11,217} = 3.3$, $P < 0.0005$), *Podon* spp. ($F = 2.19$, $P < 0.017$), *Evadne* spp. ($F = 2.7$, $P < 0.003$), Shrimp larvae ($F = 2.72$, $P < 0.003$) and Crab larvae ($F = 1.87$, $P< 0.05$). Significant differences in density for dates of collection were observed for Calanoid copepods ($P < 0.0001$), *Podon* spp. ($P < 0.0001$), *Evadne* spp. ($P <0.0001$), and shrimp larvae ($P < 0.0003$). Three species of gelatinous zooplankton were also abundant including *M. leidyi*, *C. chesapeakei*, and *N. bachei* (Table 3). *Mnemiopsis leidyi* showed significant differences among dates of collection ($F_{1, 217} = 4.4$, $P < 0.03$), *C. chesapeakei* medusa showed no differences among sites or date, but *C. chesapeakei* ephyrae showed significant differences in density among sites ($F = 5.49$, $P< 0.0001$) and collection dates ($F = 4.8$, $P < 0.04$), while *N. bachei* also showed significant differences among sites ($F = 2.7$, $P < 0.002$) and dates of collection ($F = 4.2$, $P < 0.04$). Other important taxa that had the potential to be negatively impacted by OCNGS include fish eggs and larvae, which both showed significant differences among sites ($P < 0.0017$, $P < 0.002$, respectively) and dates ($P < 0.0002$, $P < 0.0001$, respectively). Two fish species were sufficiently abundant to evaluate their densities and for *Anchoa mitcheli*, they showed significant differences among sites ($P< 0.02$), while *Menidia menidia* showed significant differences among sites and date ($P < 0.03$, $P < 0.0001$).

Table 3. Density of the abundant taxa and critical species collected during the Bay-wide plankton sampling in 2021. Taxa abbreviations: CC = *Chrysaora chesapeakei*, MNEM = *Mnemiopsis leidyi*, CCEPH = *C. chesapeakei* ephyrae, NEMOP = *Nemopsis bachei*, CALCOP = Calanoid Copepods, PODON = *Podon* spp., EVADNE = *Evadne* spp., FEGG = Fish Eggs, FISHLARV Fish Larvae (total), ANCHMIT = *Anchoa mitchelli*, MENIDIA = *Menidia menidia*, SHRLARV = Shrimp Larvae, CRABLARV = Crab Larvae.

TAXA	DCE	DCW	FRE	FRW	FRL	FRRT9	OCM	OCRT9	SB	TRW
CC	0.02	0.00	0.00	0.00	0.47	0.06	0.01	0.00	0.00	0.00
MNEM	3.90	0.81	1.92	3.29	3.44	2.62	3.01	1.26	1.72	1.73
CCEPH	0.00	0.00	0.03	0.06	3.35	0.29	0.03	0.00	0.00	0.02
NEMOP	0.00	0.06	1.12	0.04	0.00	0.01	0.01	0.05	0.26	0.25
CALCOP	1343.9	608.3	637.9	488.0	2.45	4.45	269.3	7.34	135.5	23.8
PODON	4.15	0.31	3.85	0.07	0.01	0.03	1.35	0.01	0.12	0.00
EVADNE	11.44	0.54	14.30	0.04	0.01	0.08	1.25	0.03	0.14	0.03
FEGG	56.28	2.17	6.36	2.23	0.06	0.69	3.20	0.06	25.40	3.00
FISHLARV	1.42	2.10	3.58	0.74	0.09	0.03	0.85	0.04	1.32	0.25
ANCHMIT	0.01	0.00	0.01	0.00	0.02	0.01	0.00	0.00	0.00	0.08
MENIDIA	0.27	0.88	1.68	0.56	0.04	0.02	0.21	0.01	0.93	0.07
SHRLARV	21.89	4.38	8.34	0.25	0.29	0.23	2.17	0.88	0.88	0.35
CRABLARV	39.93	111.86	0.41	2.15	0.30	2.60	2.39	3.23	8.09	2.23

2021 Lagoon Plankton Sampling

Density of abundant taxa from the three lagoons is listed in Table 4. While *M. leidyi* was abundant in all three lagoons, *C. chesapeakei* was only collected in the Forked River Lagoon site where it also had substantially greater densities of *C. chesapeakei* ephyrae (Table 4). Other taxa of note were moderate abundances of Calanoid copepods, shrimp larvae, and crab larvae, but both fish eggs and fish larvae were generally very low in lagoon samples compared to the open bay samples (Table 3).

Table 4. Density of the abundant taxa collected during the Lagoon plankton sampling in 2021. Taxa abbreviations: CC *Chrysaora chesapeakei*, MNEM = *Mnemiopsis leidyi*, CCEPH = *C. chesapeakei* ephyrae, CALCOP = Calanoid Copepods, FEGG = Fish Eggs, FISHLARV Fish Larvae (total), SHRLARV = Shrimp Larvae, CRABLARV = Crab Larvae.

TAXA	BL	FRL	SBL
CC	0.00	0.47	0.00
MNEM	1.28	3.44	0.89
CCEPH	0.02	3.35	0.00
CALCOP	0.29	2.45	0.99
FEGG	0.07	0.06	0.07
FISHLARV	0.02	0.09	0.04
SHRLARV	0.52	0.29	0.27
CRABLARV	1.06	0.30	1.59

Molecular Identification of Unknown Cnidarian Taxa

During 2021, 119 unknown cnidarians were analyzed for molecular identification. 105 samples amplified and provided sequence coverage sufficient to identify individuals and 14 samples failed to amplify. 11 different taxa (and relative % of identifications) were identified from samples including *Turritopsis dohrnii* (31.43%), *Aequorea* sp. (27.62%), *Eucheilota maculata* (16.19%), *Laodicea undulata* (10.48%), *Nemopsis bachei* (6.67%), *Bougainvillia* sp. (1.90%), *Chrysaora chesapeakei* (1.90%), *Corymorpha floridana* (0.95%), *Proboscidactyla ornate* (0.95%), *Helgicirrha malayensis* (0.95%), and *Obelia geniculate* (0.95%) (Figure 13). While most of these species are native to the region, two species, *Eucheilota maculata* (Figure 14) and *Helgicirrha malayensis* (Figure 15), are non-native species. *Eucheilota maculata* was a common hydrozoan in some samples with densities ranging from 0.18-0.84 m^{-3}, and as such, this represents a substantial presence in Barnegat Bay and a successful invasion. For *Helgicirrha malayensis*, its only known distribution is in the tropical Indo-Pacific Ocean. These new additions to non-native hydrozoans in Barnegat Bay is now at five different taxa.

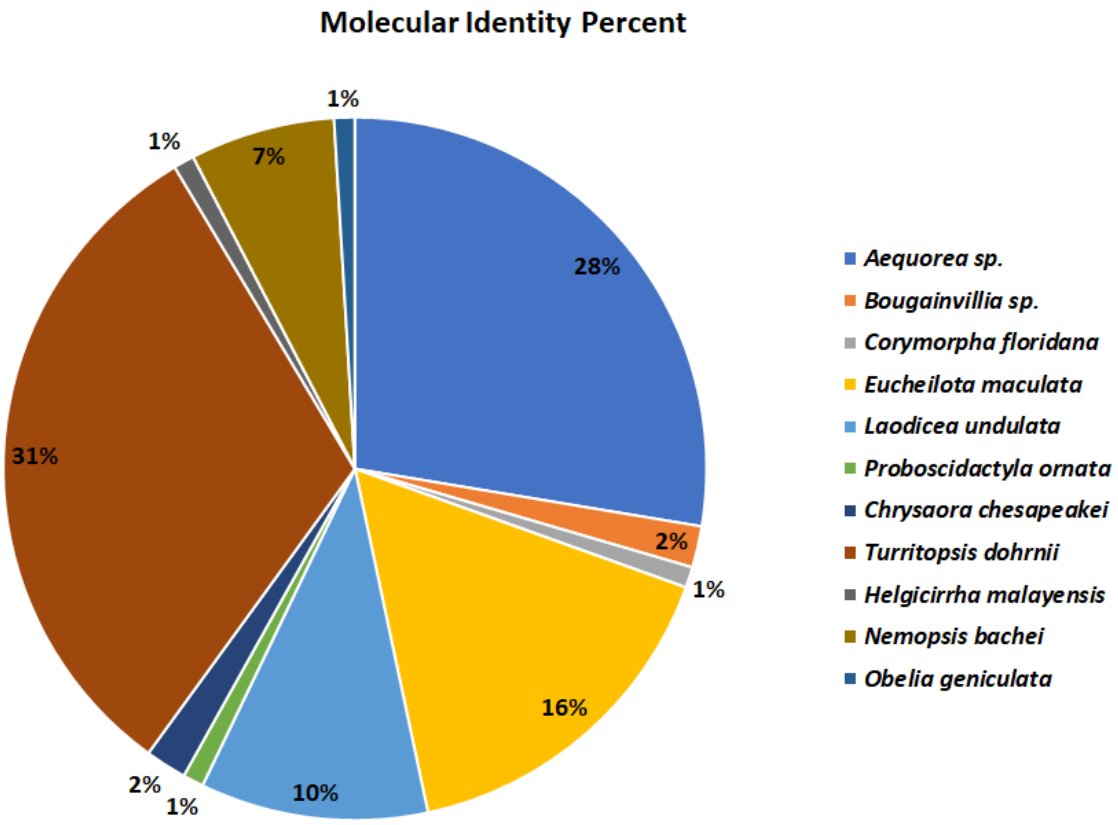

Figure 13. Molecular identification of unknown species collected during sampling in 2021

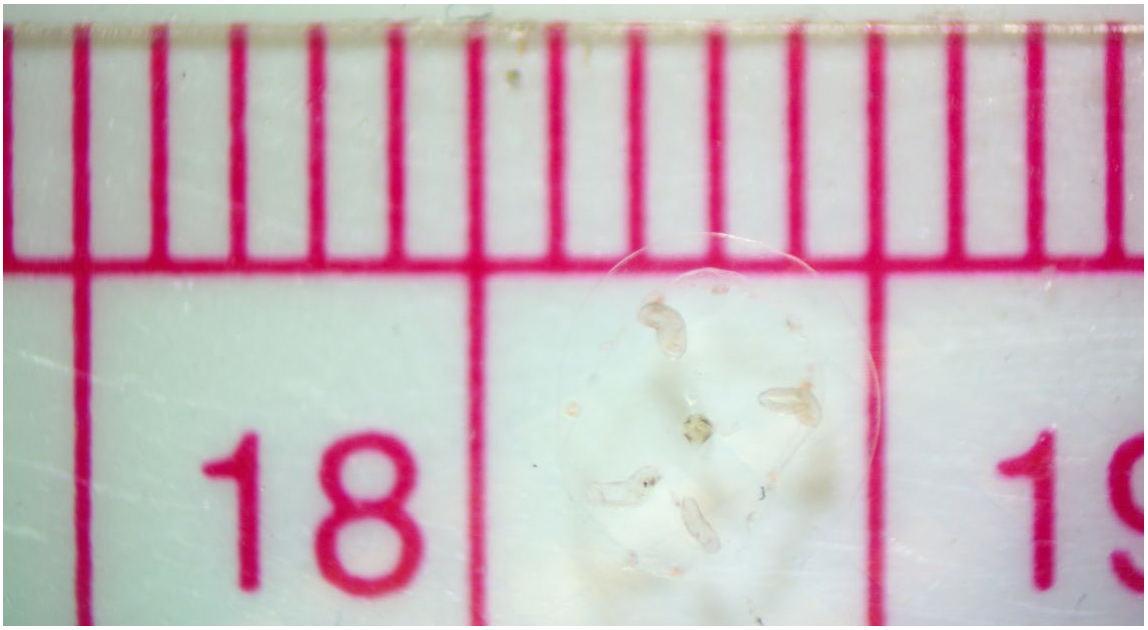

Figure 14. Image of *Eucheilota maculata* collected from samples in 2021. Image scale is in mm.

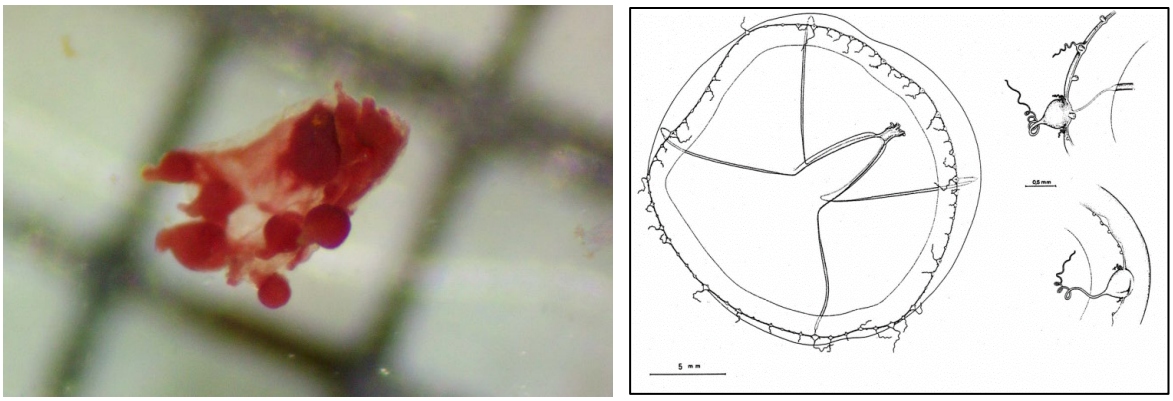

Figure 15. Image of *Helgicirrha malayensis* collected from samples in 2021 (left) and line drawing of the species from Bouillon et al. 1988 (right). For reference, the scale in the left image (square below the specimen) is 1mm and the scale in the line drawing is 5mm.

Metagenomic Composition assessment of planktonic communities and impacts of OCNGS.

Statistical Analyses of Species Diversity

Samples from 2021 contained anywhere from ~700 reads to ~800,000 reads. Over six thousand ASVs were identified across all samples. Of these 1365 were assigned to Metazoa. Samples from the combined dataset (consisting of both the 2018, 2019, and 2021 samples) contained anywhere from ~700 reads to ~4,100,000 reads. Over twenty-five thousand ASVs were identified across all samples. Of these 5012 were assigned to Metazoa.

Statistically significant differences in species diversity as identified by Enspie are given below for analyses with and without Toms River for 2021 samples (Table 5). "All groups" refers to a comparison between all members of a category and pairwise is between two categories. X=No statistical significance; q-value= p-value with a Benjamini & Hochberg correction (Benjamini & Hochberg 1995).

Table 5. Significant differences among categorical analyses for 2021 Samples only from NEXGEN Sequencing.

	Toms River Included				**Toms River Excluded**		
CATEGORY		**Enspie (Kruskal-Wallis)**				**Enspie (Kruskal-Wallis)**	
	All Groups (p-value)	**pairwise**	**q-value**		**All Groups (p-value)**	**pairwise**	**q-value**
Location Name	X		X		X		X
Geography	X		X		X		X
Circulation	X		X		X		X
Impact_1	X		X		X		X
Impact_2	X		X		X		X
Site-group	X		X		X		X
Time of Day	X		X		X		X
Temperature Regime	X		X		X		X
Salinity Regime	X		X		X		X

Taxonomic Analyses

In the 2021 sample analysis, two-hundred and twenty-eight unique taxa were identified to species level at 0.70 confidence or greater. The combined 2018, 2019, 2021 sample analysis identified three hundred and eighty-four unique taxa at 0.70 confidence or greater. Some of the specie identifications refer to unique sequences on GenBank that are only given a designation and no assigned species name (see accompanying data files BarnegatBay_Identified_Species_2018_2019_.2021_.7_confidence.xlsx). Anywhere from 43 (e.g. Sunrise Beach Lagoon) to 114 (e.g. Double Creek East) species were identified from each of the collection sites in 2021. Of the 228 identified metazoan taxa, 193 had defined Genera in the 2021 data set. Of the 384 identified metazoan taxa, 325 had defined Genera in the combined 2018, 2019, and 2021 data set.

Multi year comparisons: 2018, 2019, 2021

Water Temperature

Since the primary goal of this work was to evaluate how the gelatinous zooplankton and associated pelagic community might change in accordance with the closure of the OCNGS, we present findings incorporating data among all years of collection to provide an evaluation of systemic changes when present. One of the first necessary assessments regards the temperature differences associated with the discharge from the plant. Initial data collections from 2018 show a consistent and significantly elevated water temperature in the outflow region of the OCNGS (Figure 16). After the shutdown of the plant and the reduction in water flow and heat discharge, it is apparent that temperatures in the fall of 2018 (post-shut down) were similar between the intake and outflow of the plant (FRRT9 and OCRT9, respectively; Figure 17). When water temperature was again evaluated using data loggers at these two sites during the 2021 sampling season, no significant difference in temperature was observed (Figure 18).

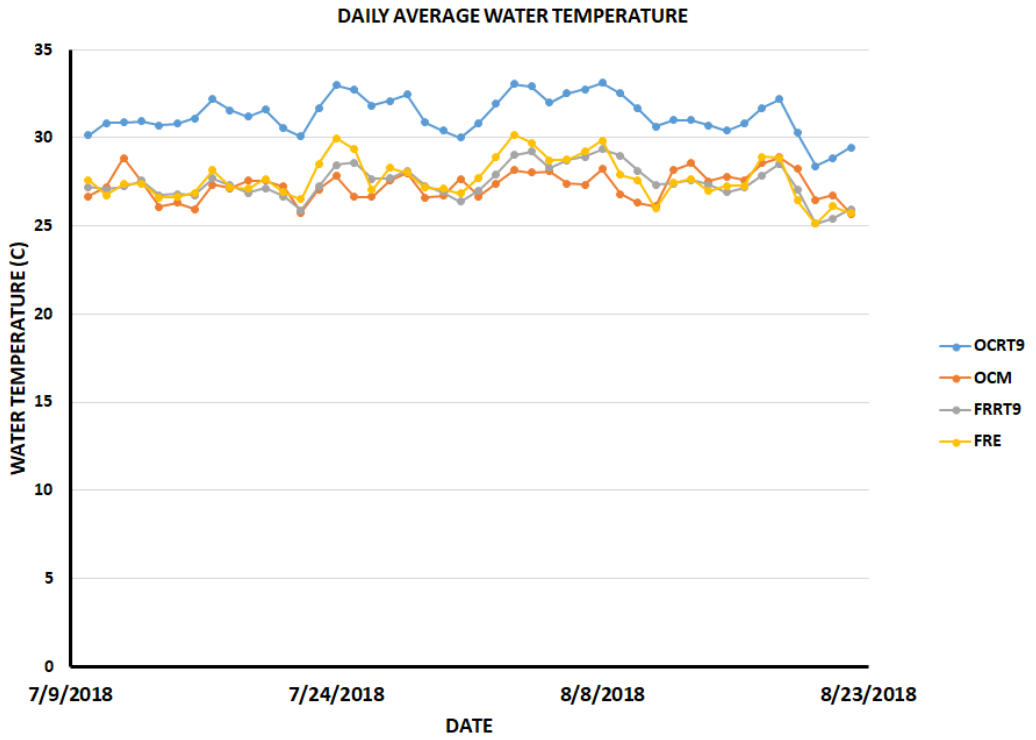

Figure 16. Daily average water temperatures prior to OCNGS shutdown in 2018. Data presented represent the temperature at the inflow sampling site Forked River Rt. 9 (FRRT9), Forked River East (FRE), Oyster Creek Mouth (OCM), and the OCNGS outflow sampling site (OCRT9). A significant temperature difference was observed during the plant operation among sites with the outflow region demonstrating significantly greater water temperatures.

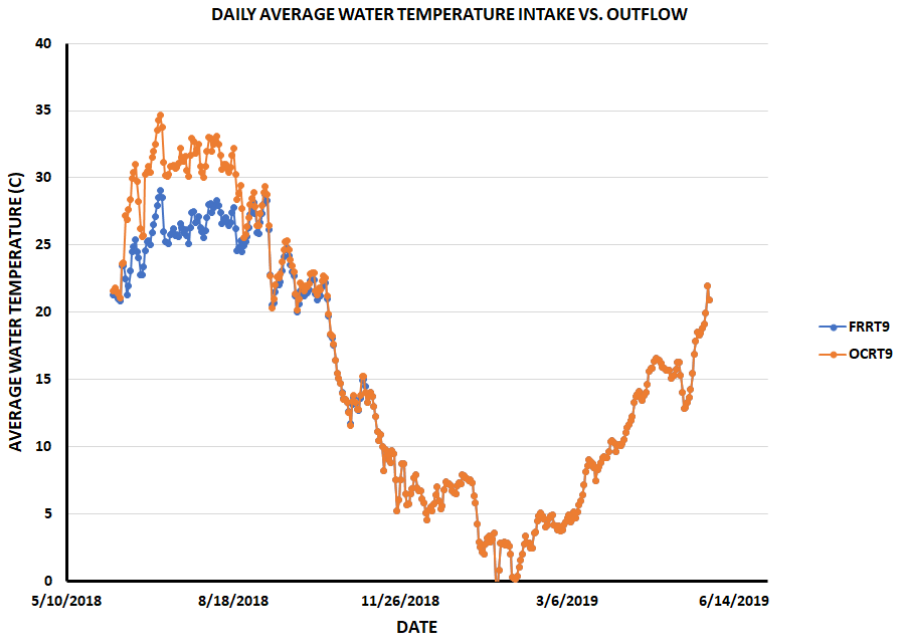

Figure 17. Daily average water temperatures prior to OCNGS shutdown in 2018 and following the shutdown and into the spring of 2019. Data presented represent the temperature at the inflow sampling site Forked River Rt. 9 (FRRT9) and the OCNGS outflow sampling site (OCRT9). A significant temperature difference was observed during the plant operation, but no differences following the closure.

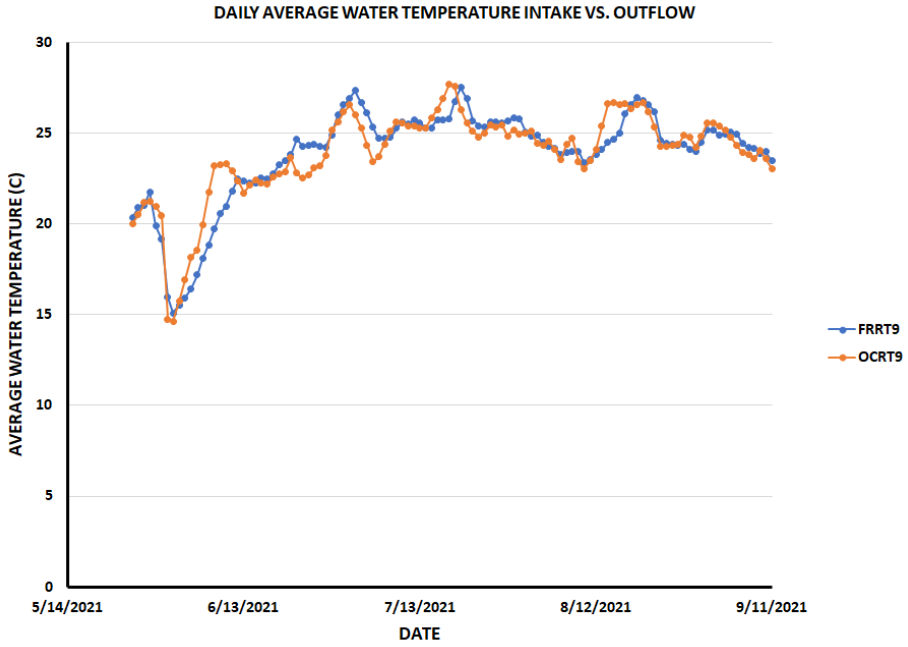

Figure 18. Daily average water temperatures during the spring and summer of 2021, 2-years post shut down. Data presented represent the temperature at the inflow sampling site Forked River Rt. 9 (FRRT9) and the OCNGS outflow sampling site (OCRT9). No significant temperature difference was observed between sites.

Lift Net Analyses of Gelatinous Species

Three gelatinous zooplankton were abundant in lift net samples among all three years and include *Chrysaora chesapeakei*, *Mnemiopsis leidyi*, and *Nemopsis bachei* (Table 6). A mixed model ANOVA was used to assess differences in the density of species among Years, Months (nested within years), and Sites. Statistical analyses indicate significant increases in the density of *C. chesapeakei* among years ($F_{2,2358}$ = 8.68, P < 0.0002) as well as significant differences among months of collection (Month (Year), $F_{10,\ 2358}$ = 5.6, P < 0.0001) and sites ($F_{11,2358}$ = 16.3, P < 0.0001). For *M. leidyi*, density increased from 2018 to 2021, but was not significantly greater, however, density did differ significantly among months of collection (Month (Year), $F_{10,\ 2358}$ = 13.2, P < 0.0001) and sites ($F_{11,2358}$ = 5.96, P < 0.0001). These generalized results were the same for *N. bachei* with no difference among years, but density did differ significantly among months of collection ($F_{10,\ 2358}$ = 15.4, P < 0.0001) and sites ($F_{11,2358}$ = 10.6, P < 0.0001).

Table 6. Comparative densities of the three dominant gelatinous zooplankton species collected by lift nets among years. Values in table represent average density (#m^{-3}) + SE.

Year		*C. chesapeakei*	*M. leidyi*	*N. bachei*
2018		0.023 ± 0.006	0.91 ± 0.07	0.129 ± 0.027
2019		0.09 ± 0.14	1.07 ± 0.23	0.11 ± 0.016
2021		0.15 ± 0.03	1.26 ± 0.09	0.11 ± 0.27

Since all of the gelatinous zooplankton showed significant differences among sites, we provide the following spatial and temporal analyses of these taxa among the sites where they were observed.

Chrysaora chesapeakei

The Bay Nettle, *Chrysaora chesapeakei,* was not observed at Sunrise Beach, Forked River East, Oyster Creek Mouth, Double Creek East, or Double Creek West during all three sampling years leading to the significant differences in density observed in the Mixed-model ANOVA. For sites with observed *C. chesapeakei* individuals, general trends among sites showed that bay nettle densities peak somewhere between June and July, suggesting early summer conditions are optimal for nettles to mature into medusa life stages. This corresponds to the trends observed for ephyrae who emerge during the spring and were abundant in May through July. While three sites showed their presence in August, densities were generally much lower than the peaks observed in June and July for all years. The declines seen in August and into September may relate to natural mortality and advection from the system.

Site Specific Patterns in Abundance

Toms River West

At Toms River West, a few bay nettles (*Chrysaora chesapeakei*) were seen in 2018, though none were observed during the 2019 sampling. However, they returned once again in July 2021, where they were observed at their highest densities (Figure 19).

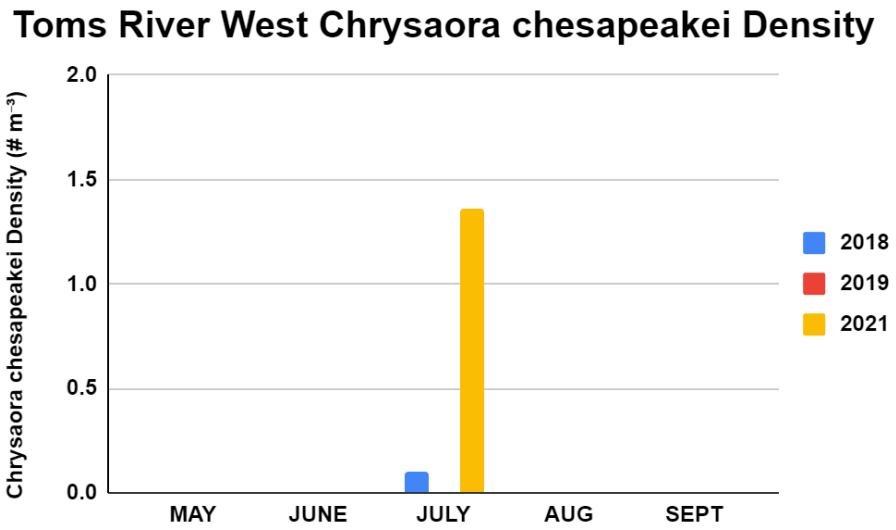

Figure 19. Lift Net Density of *Chrysaora chesapeakei* from Toms River West for all years.

Sunrise Beach Lagoon

Sunrise Beach Lagoon showed the presence of bay nettles on only one date in 2019 (Figure 20).

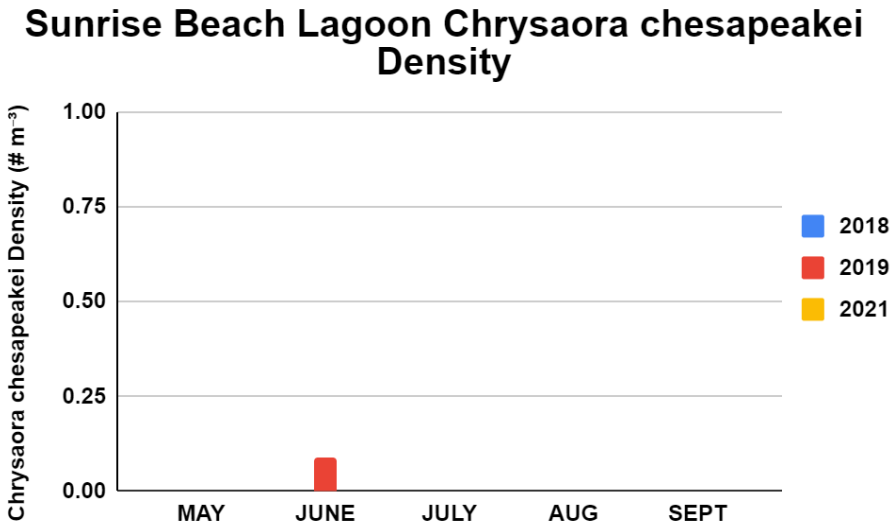

Figure 20. Lift Net Density of *Chrysaora chesapeakei* from Sunrise Beach Lagoon for all years.

Forked River West

Bay nettles were mostly absent at Forked River West during sampling efforts from 2018 to 2021, with the only exception being a collection of individuals in July 2021 (Figure 21).

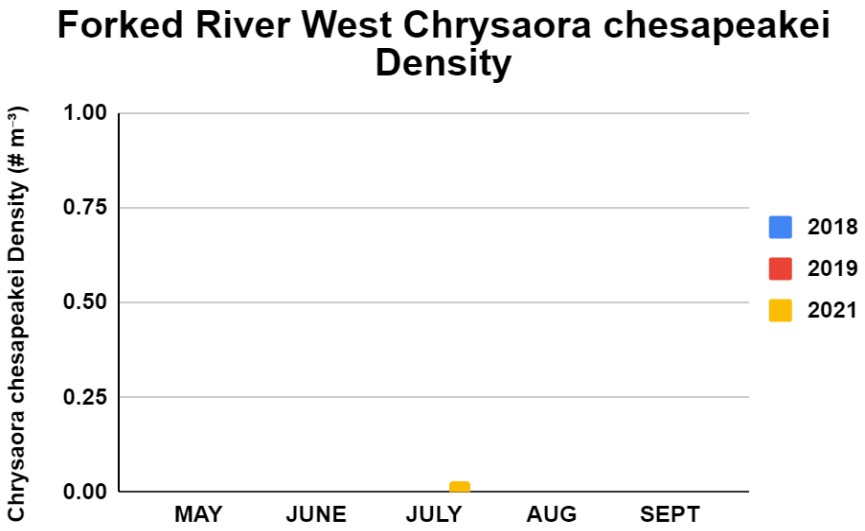

Figure 21. Lift Net Density of *Chrysaora chesapeakei* from Forked River West for all years.

Forked River Rt. 9

At Forked River Rt. 9, bay nettles were spotted at relatively similar densities from June 2019 to August 2019 (0.5 m^{-3}), with a slight increase in density as the summer progressed (Figure 22). The following year, bay nettles were only seen in July 2021, yet with more than triple the density of June, July, or August 2019.

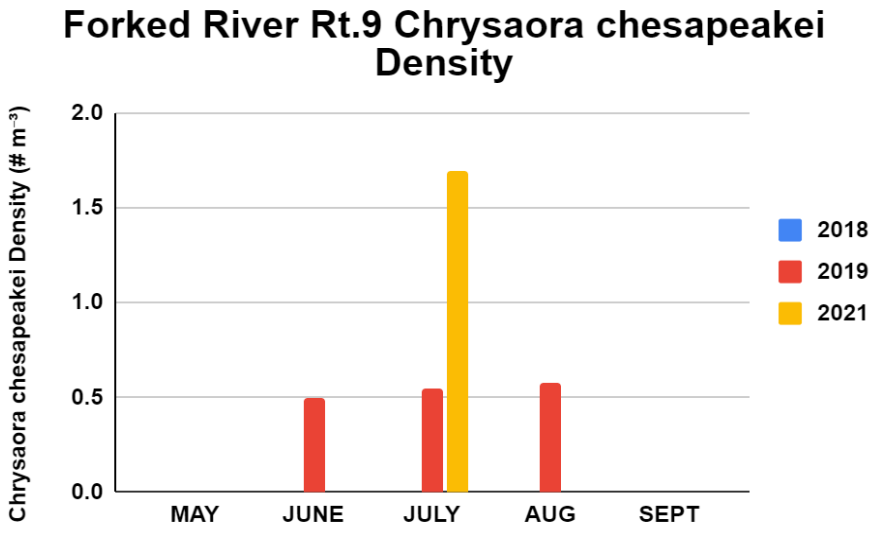

Figure 22. Lift Net Density of *Chrysaora chesapeakei* from Forked River Rt. 9 for all years.

Forked River Lagoon

Bay nettle densities varied greatly among 2018, 2019, and 2021 at Forked River Lagoon (Figure 23). In 2018, nettles were seen in small densities in July and even smaller densities the following month. In 2019, nettles were observed as early as June, instead of July as in the previous year, with densities increasing rapidly and peaking in July, but lingering in presence until September 2019. In 2021, nettles were seen at their greatest densities in June before declining greatly by July, but remaining present through to September.

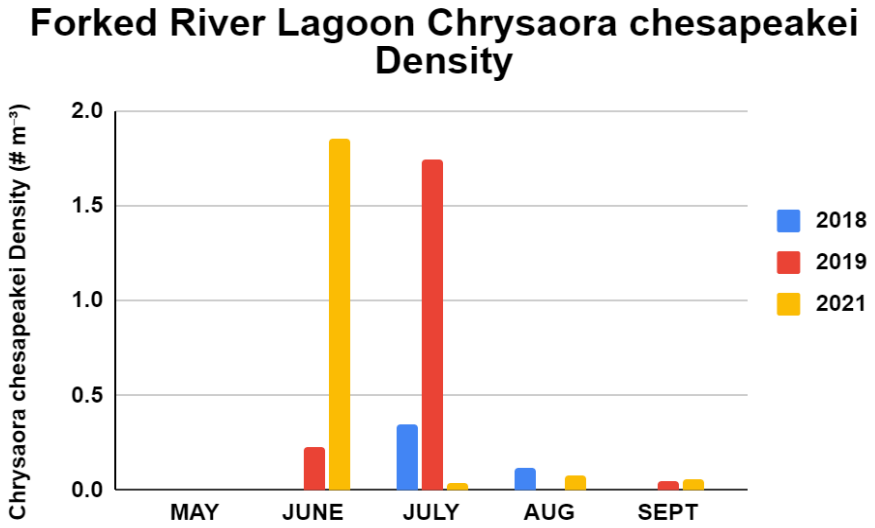

Figure 23. Lift Net Density of *Chrysaora chesapeakei* from Forked River Lagoon for all years.

Oyster Creek Rt. 9

Bay nettles were observed only in June and July of 2019 at the Oyster Creek Rt. 9 sampling station (Figure 24). Nettle densities increased somewhat from June to July, although there were still low densities in July. Bay nettles were not observed at Oyster Creek Rt. 9 in either 2018 or 2021. Their absence in 2018 might reflect the active nature of the OCNGS in destroying gelatinous species, but this does not account for their absence in 2021.

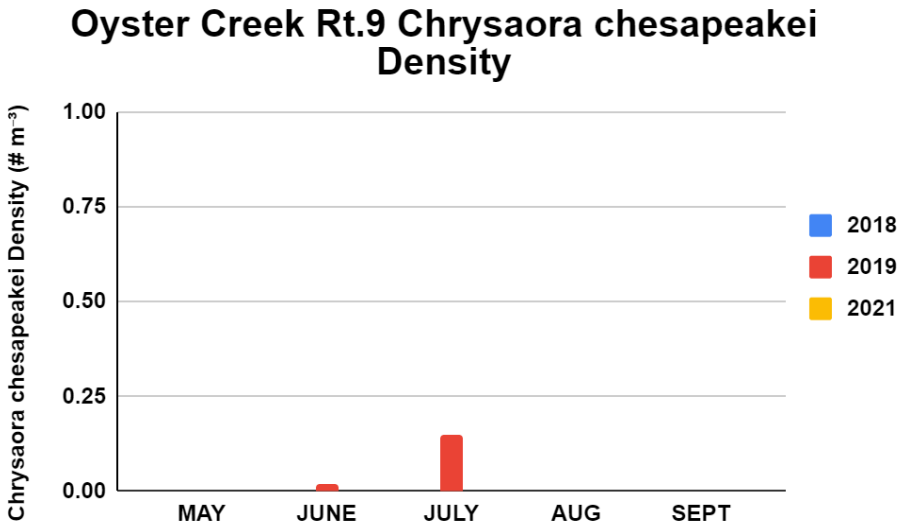

Figure 24. Lift Net Density of *Chrysaora chesapeakei* from Oyster Creek Rt. 9 for all years.

Bayshore Lagoon

At Bayshore Lagoon, Bay Nettles were present in July during 2018 and 2019, but absent in 2021 (Figure 25). They were present in August of 2018 as well, but at very low densities.

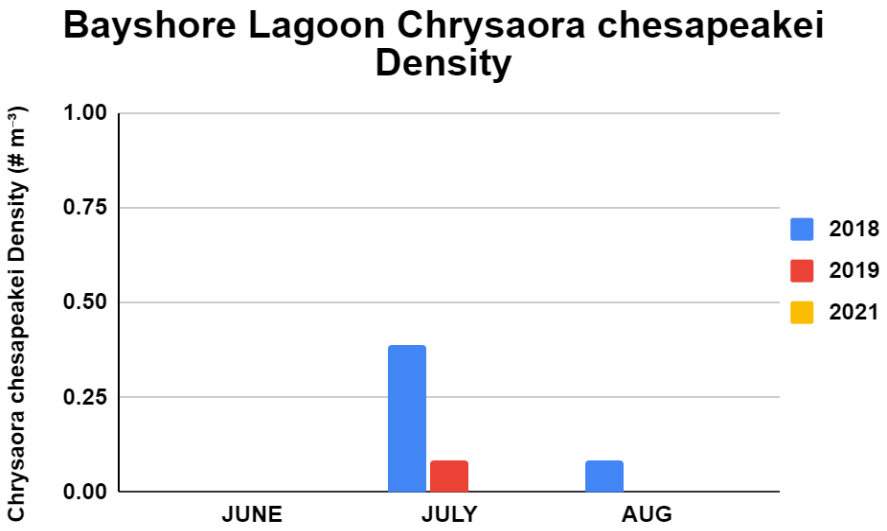

Figure 25. Lift Net Density of *Chrysaora chesapeakei* from Bayshore Lagoon for all years.

Nemopsis bachei

Nemopsis bachei were observed at all sites except for the Forked River Lagoon site during all three sampling years. For sites with observations, general trends showed that *N. bachei* were most abundant in June among all sites and years leading to significantly greater densities in June compared to other months ($P < 0.0001$). High densities in June suggest that *N. bachei*'s sexual reproductive season begins in late spring, leading to a bloom in June. Some sporadic reports in late summer months, such as September, possibly suggest that some sites may have had a secondary bloom of medusae in the fall, in alignment with fall phytoplankton and zooplankton blooms.

Site Specific Patterns in Abundance

Toms River West

For Toms River West, *N. bachei* was only observed in May and June for all three sampling years (Figure 26). In 2018, *N. bachei* was observed only in June and no other months. In 2019, densities were also only observed in June, however densities were roughly four times as great as the previous year. In 2021, *N. bachei* were observed as early as May in small densities, then reported the following month with considerably higher densities.

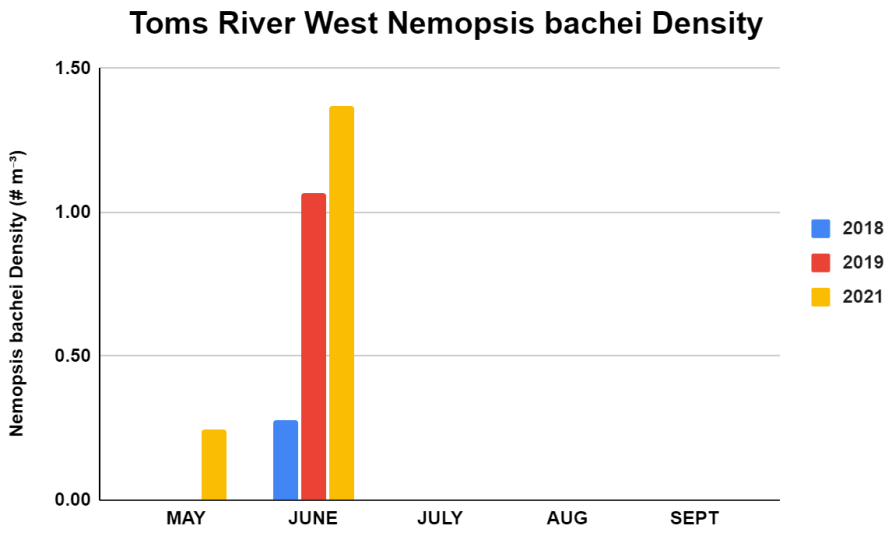

Figure 26. Lift Net Density of *Nemopsis bachei* from Toms River West for all years.

Sunrise Beach

For Sunrise Beach, *N. bachei* were seen only in May and June during the three sampling years (Figure 27). In 2018, *N. bachei* were observed in June with a substantially high density. In 2019 and 2021, observations were made in May and increased densities were seen by June, however there were relatively fewer *N. bachei* individuals in comparison to 2018.

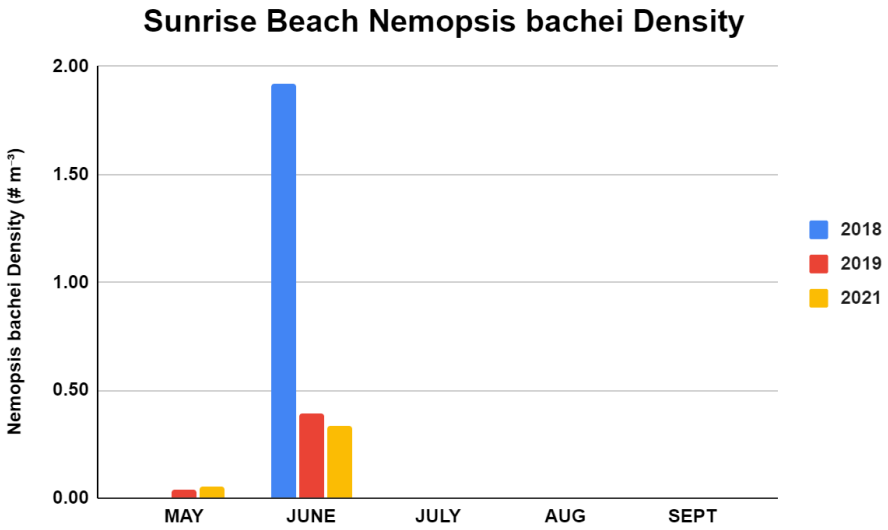

Figure 27. Lift Net Density of *Nemopsis bachei* from Sunrise Beach for all years.

Sunrise Beach Lagoon

At Sunrise Beach Lagoon, *N. bachei* was only observed in June of 2019 at very low densities (Figure 28). This was unexpected as they were abundant in all three years in the adjacent waters at our Sunrise Beach sampling location.

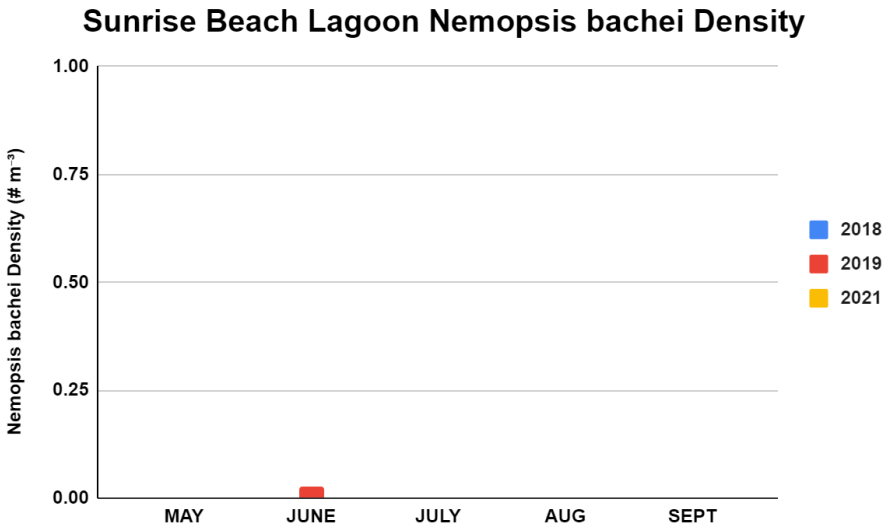

Figure 28. Lift Net Density of *Nemopsis bachei* from Sunrise Beach Lagoon for all years.

Forked River East

For Forked River East, *N. bachei* individuals were generally seen in June, however some observations were made in September of 2019 (Figure 29). The greatest density was recorded in June of 2021 with densities exceeding 2 m^{-3}.

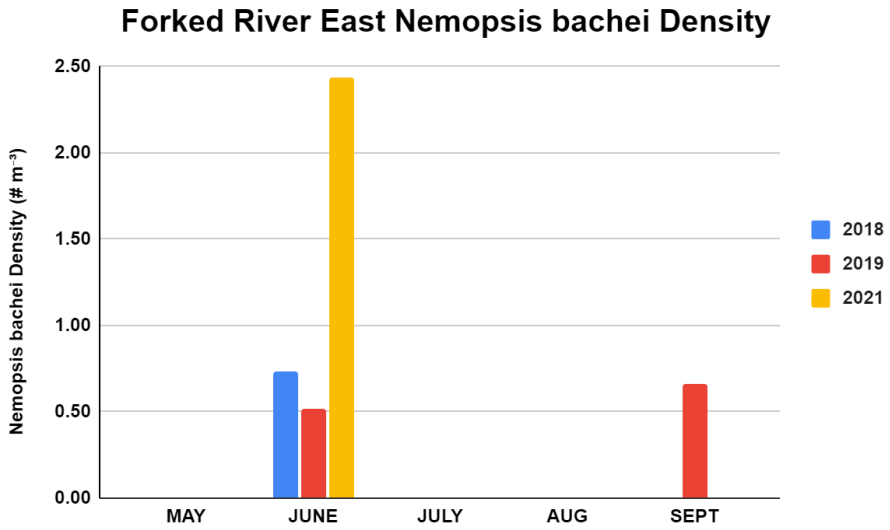

Figure 29. Lift Net Density of *Nemopsis bachei* from Forked River East for all years.

Forked River West

For Forked River West, a few *N. bachei* were seen in June of 2018 and 2019, but none were observed in 2021 (Figure 30).

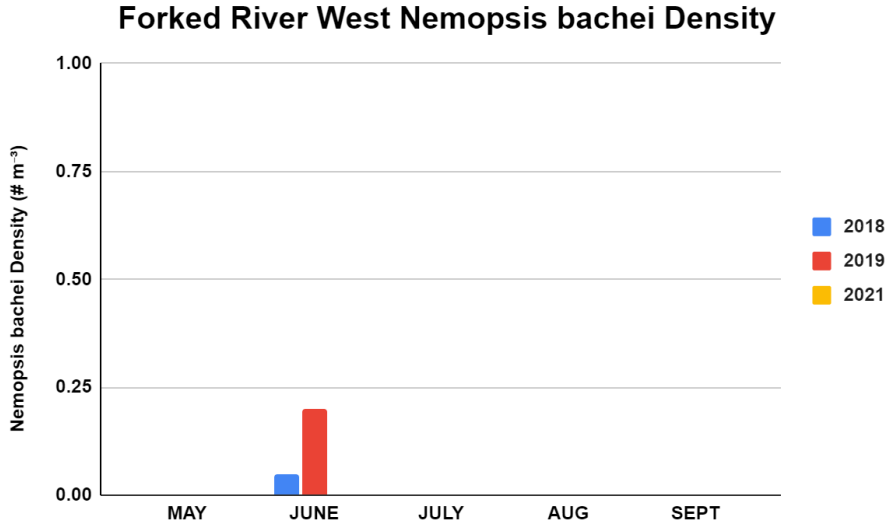

Figure 30. Lift Net Density of *Nemopsis bachei* from Forked River West for all years.

Forked River Rt. 9

For Forked River Rt. 9, *N. bachei* individuals were seen only in June 2018 and 2019 at Forked River Rt. 9 (Figure 31). 2019 densities were considerably larger than 2018 densities by a factor of roughly four. No reports of *N. bachei* were made in 2021 for this site.

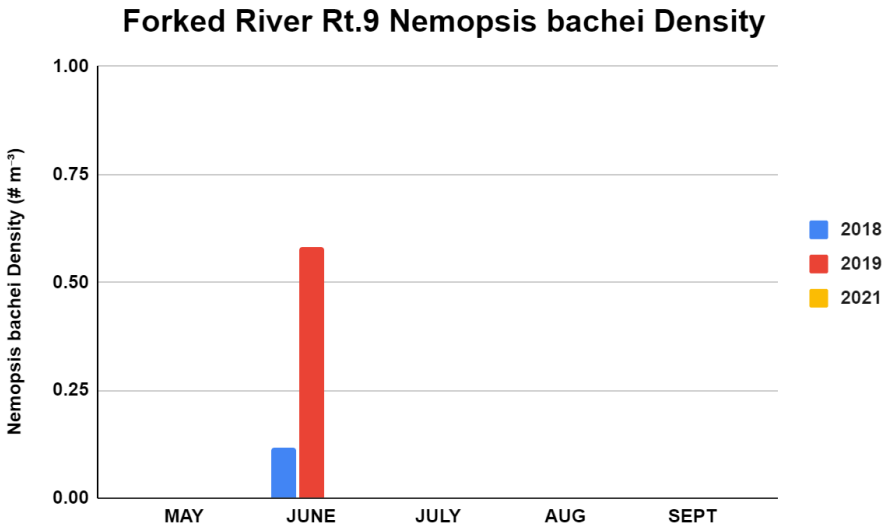

Figure 31. Lift Net Density of *Nemopsis bachei* from Forked River Rt. 9 for all years.

Oyster Creek Rt. 9

For Oyster Creek Rt. 9, low densities were observed for *N. bachei* in June of all years, but they were also present in July of 2018 (Figure 32). This suggests that the polyp stage must reside within the lagoonal community surrounding the outflow.

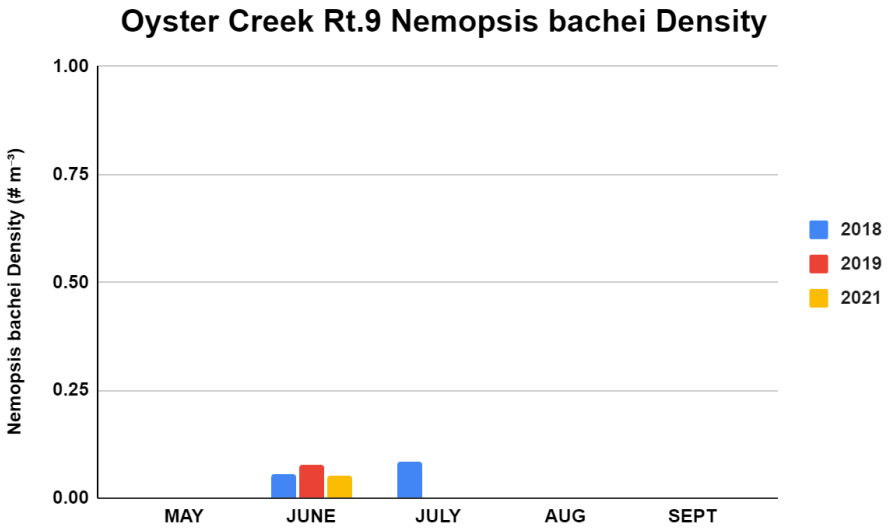

Figure 32. Lift Net Density of *Nemopsis bachei* from Oyster Creek Rt. 9 for all years.

Oyster Creek Mouth

For Oyster Creek Mouth, *N. bachei* densities in 2018 and 2019 were substantially greater in June than 2021 (Figure 33). Sampling in 2019 yielded low densities in May before increasing in June.

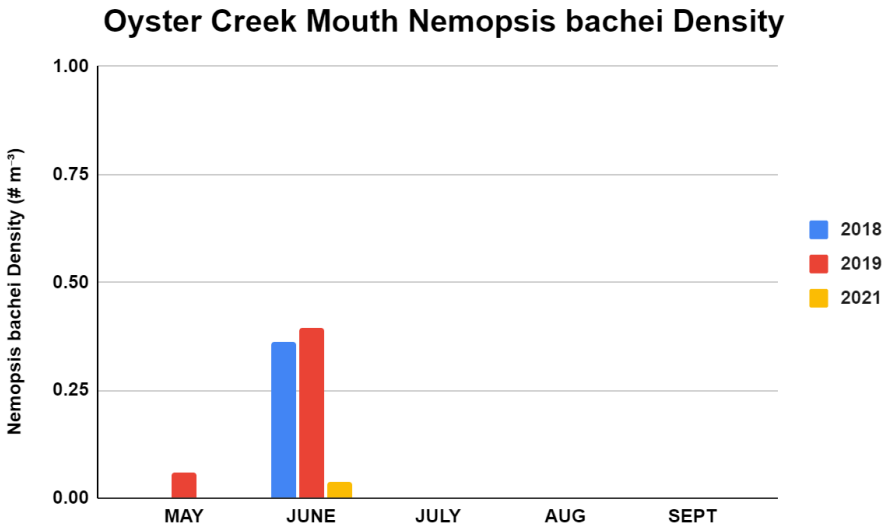

Figure 33. Lift Net Density of *Nemopsis bachei* from Oyster Creek Mouth for all years.

Double Creek East

At Double Creek East during the months of June 2018 and 2019, the first appearance of *N. bachei* were seen and collected with there being a slightly greater amount in June of 2019 (Figure 34). However, the greatest density seen was in September 2019, where there was an abundance of *N. bachei* at Double Creek East. This high density is counter to the spring bloom observed elsewhere in the bay and may suggest a complex reproductive strategy, as no individuals were recorded in 2021 for this site.

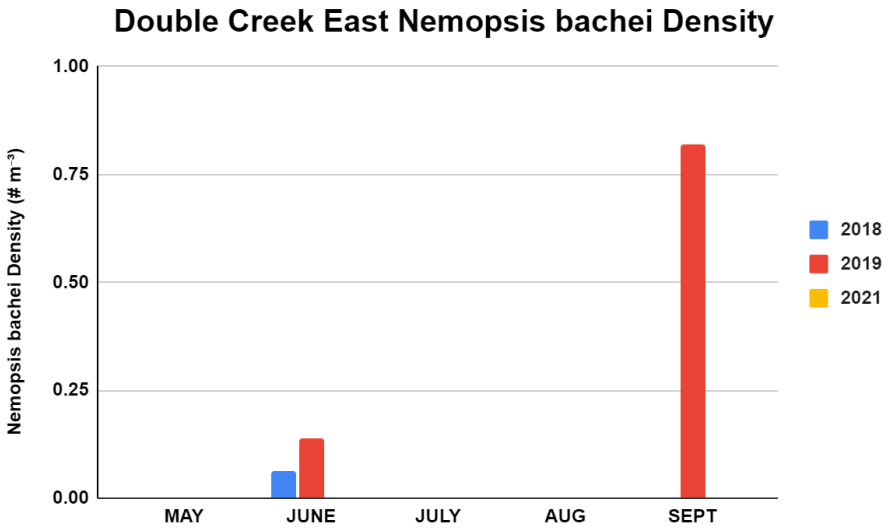

Figure 34. Lift Net Density of *Nemopsis bachei* from Double Creek East for all years.

Double Creek West

For Double Creek West in June of 2018, 2019, and 2021, there was a low recorded density for *N. bachei* (Figure 35). In September of 2019, *N. bachei* was observed again during sampling, not to the degree seen in Double Creek East.

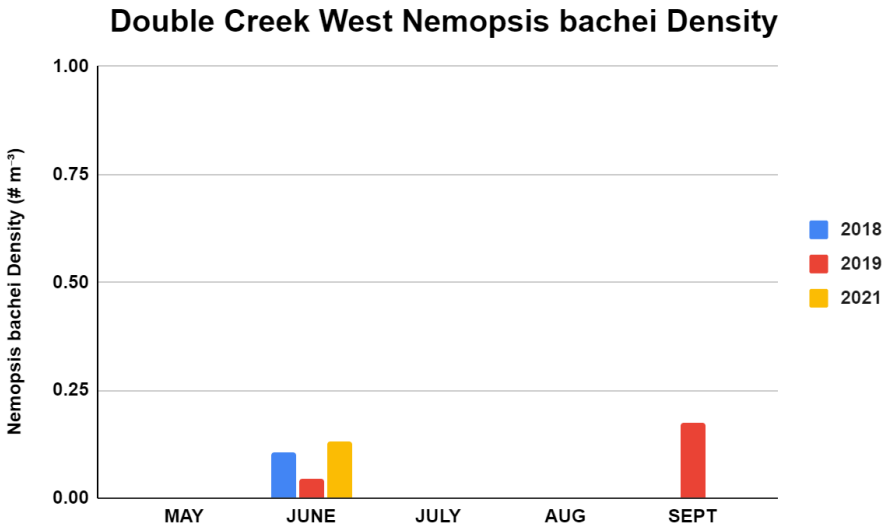

Figure 35. Lift Net Density of *Nemopsis bachei* from Double Creek West for all years.

Bayshore Lagoon

At Bayshore Lagoon in June 2021, there was a small presence of *N. bachei* at this location (Figure 36). However, for all of 2018 and 2019 there was no presence of *N. bachei* recorded.

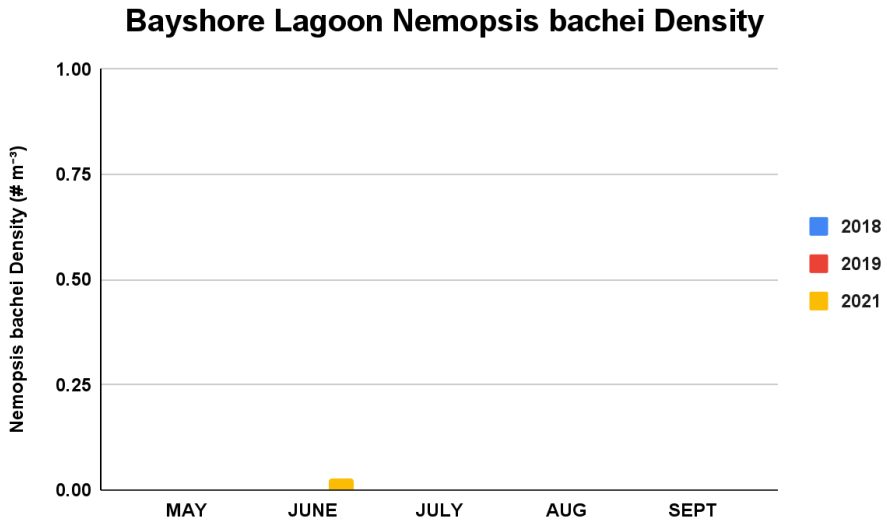

Figure 36. Lift Net Density of *Nemopsis bachei* from Bayshore Lagoon for all years.

Mnemiopsis leidyi Trends among Sites

All sites sampled during the three years had at least one observation of *Mnemiopsis leidyi*, and thus had observable density to be investigated. Analysis of the three years of density data for *M. leidyi* among the sites sampled demonstrated significant differences among sites ($P < 0.0001$) and months of collection ($P < 0.0001$). Additionally, there was a non-significant overall increase in density from $0.91 m^{-3}$ in 2018 to $1.26 m^{-3}$ in 2021. However, patterns of temporal abundance among sites varied. One striking feature was the lack of individuals observed during May sampling events for all sites.

Site Specific Patterns in Abundance

Toms River West

At Toms River West, *M. leidyi* were seen in very low densities in 2018, however greater densities were observed as the years progressed, but never exceeded 2 m^{-3} (Figure 37). However, no temporal pattern of abundance was observed among all the years, but likely reflects the relatively unique low salinity water quality characteristics of this site compared to the others.

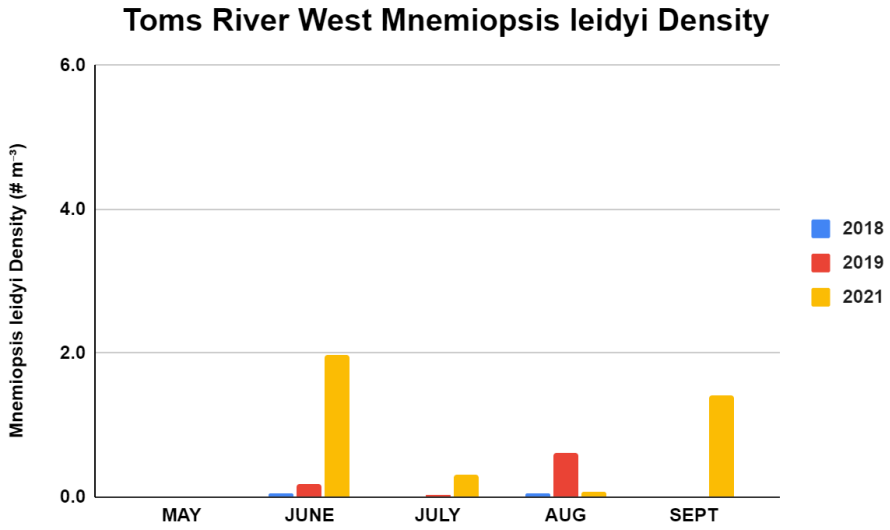

Figure 37. Lift Net Density of *Mnemiopsis leidyi* from Toms River West for all years.

Sunrise Beach

For Sunrise Beach, *M. leidyi* densities were seen to increase steadily throughout the summer in 2018, however this pattern shifted in the following years to one where declines occurred mid-summer between peak densities (Figure 38). The July decline trend was observed in 2019 and 2021, as high densities seen in June would decrease between July and August. This reduction in density corresponds to the increase of *C. chesapeakei*, one of *M. leidyi*'s major predators. In 2019, a bloom of individuals was recorded in September, possibly as a response in reduced predation pressure.

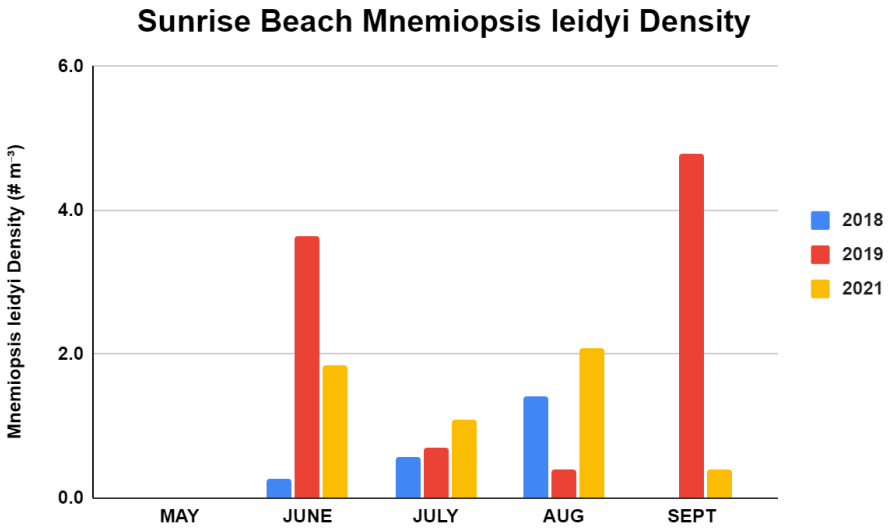

Figure 38. Lift Net Density of *Mnemiopsis leidyi* from Sunrise Beach for all years.

Sunrise Beach Lagoon

For Sunrise Beach Lagoon, the density of *M. leidyi* was the highest in July throughout all three years (Figure 39). Following a year of low densities observed throughout June-August 2018, in 2019 *M. leidyi* were only observed in July and in 2021 peak densities occurred in July. This is in stark contrast to the reductions in July observed for *M. leidyi* in the adjacent waters of Sunrise Beach (Figure 38).

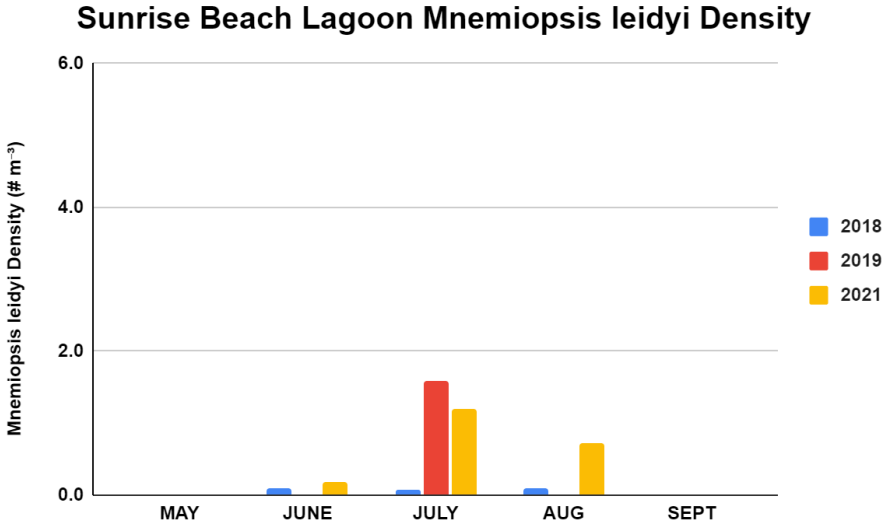

Figure 39. Lift Net Density of *Mnemiopsis leidyi* from Sunrise Beach Lagoon for all years.

Forked River East

Forked River East's *M. leidyi* population experienced a general pattern of gradual density decline throughout the summer, but in 2019 there was a massive bloom in September (Figure 40).

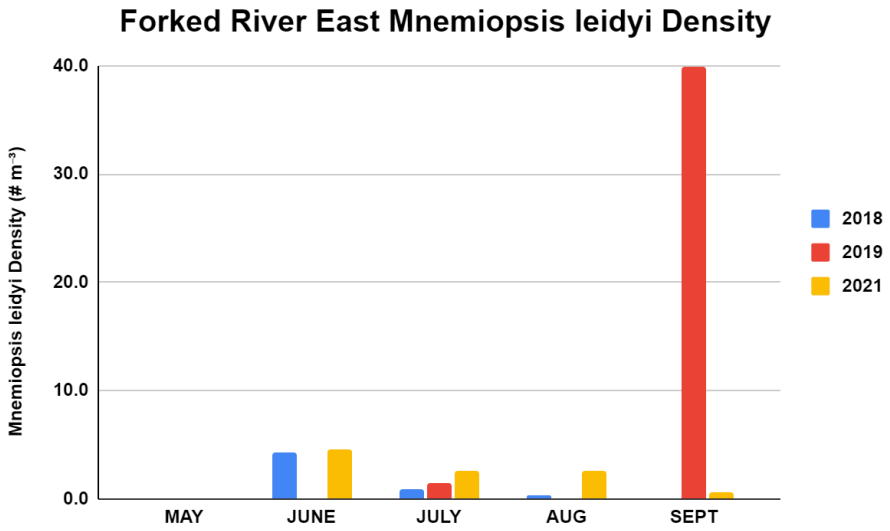

Figure 40. Lift Net Density of *Mnemiopsis leidyi* from Forked River East for all years.

Forked River West

For Forked River West, *M. leidyi* were seen to have density patterns which differed for each year, with peaks ranging from June in 2021 to July in 2018 and September in 2019 (Figure 41). This highly variable pattern suggests that *M. leidyi* populations are quite dynamic in the central regions of Barnegat Bay.

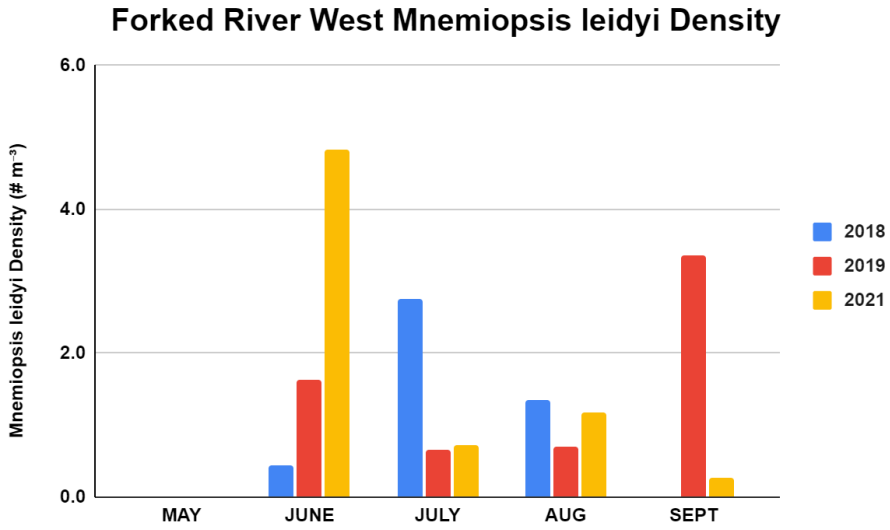

Figure 41. Lift Net Density of *Mnemiopsis leidyi* from Forked River West for all years.

Forked River Rt. 9

At Forked River Rt. 9, *M. leidyi* densities saw differing growth patterns between 2018, 2019, and 2021 (Figure 42). In 2018 while the OCNGS was in service, high densities were observed at the site which was the closest point to the intake. Densities then dropped off in 2019 dramatically after the shutdown, possibly relating to changes in the flow dynamics of the plant, with a late season peak in abundance in September. In 2021, peak densities were observed in June similar to 2018. This site likely has shown similar major changes as the Oyster Creek Rt. 9 site due to the plant closure.

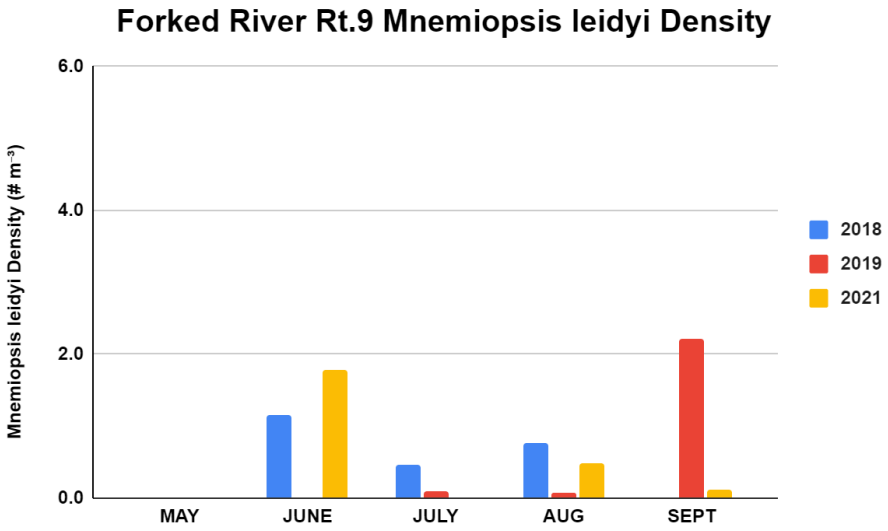

Figure 42. Lift Net Density of *Mnemiopsis leidyi* from Forked River Rt. 9 for all years.

Forked River Lagoon

At Forked River Lagoon, densities of *M. leidyi* were among the lowest of all sites for all years (Figure 43). Their almost complete absence in July does correspond to the increased densities of their primary predator in the system, *C. chesapeakei*, and when their densities declined during August, *M. leidyi* populations seemed to return to the lagoon.

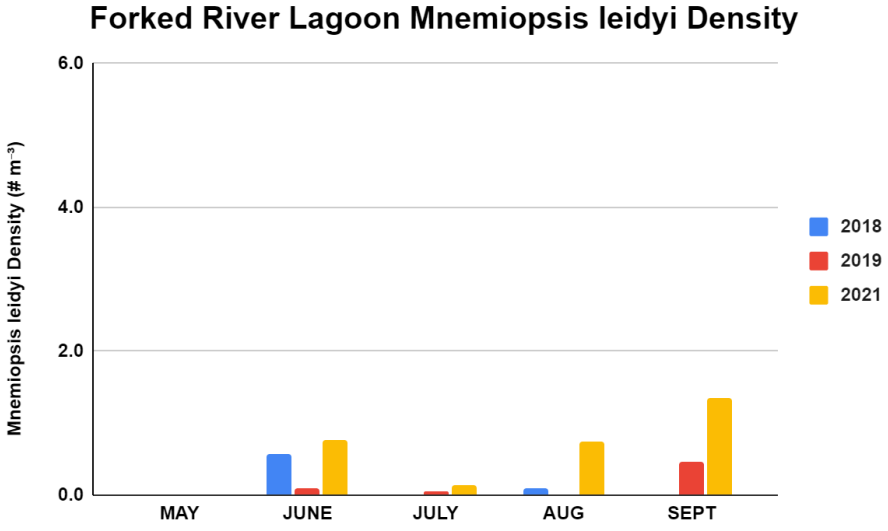

Figure 43. Lift Net Density of *Mnemiopsis leidyi* from Forked River Lagoon for all years.

Oyster Creek Rt. 9

For Oyster Creek Rt. 9, *M. leidyi* densities experienced a net increase by the end of sampling time. (Figure 44). In 2018, densities were initially seen in very low quantities before increasing considerably by July and somewhat into August. 2019 densities experienced a stall between June and July, were not observed in August, then reported once more in September with roughly three times the individuals since July. 2021 demonstrated a small peak in June that steadily declined until August, as a massive boom roughly three times as large was observed in September.

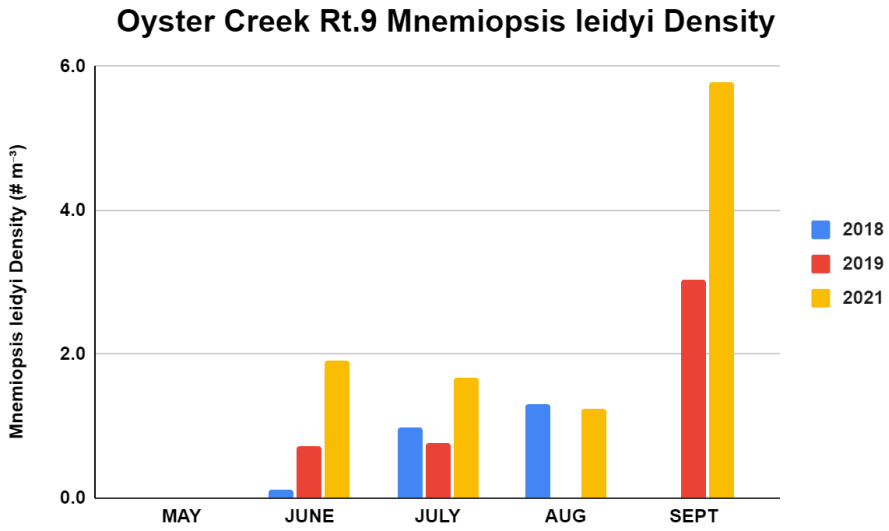

Figure 44. Lift Net Density of *Mnemiopsis leidyi* from Oyster Creek Rt. 9 for all years.

Oyster Creek Mouth

Oyster Creek Mouth's *M. leidyi* densities in 2018 were initially low in June, with gradual growth seen up to August (Figure 45). In 2019 and 2021, June densities were initially high with declines in the following months. Additionally, the pattern of abundance among months and years greatly differed from those observed just upstream at the Oyster Creek Rt. 9 that showed their greatest densities in September. However, the generalized increase in densities from 2018 to 2021 suggests that plant closure may have allowed this region to show some recovery in regards to *M. leidyi* population densities.

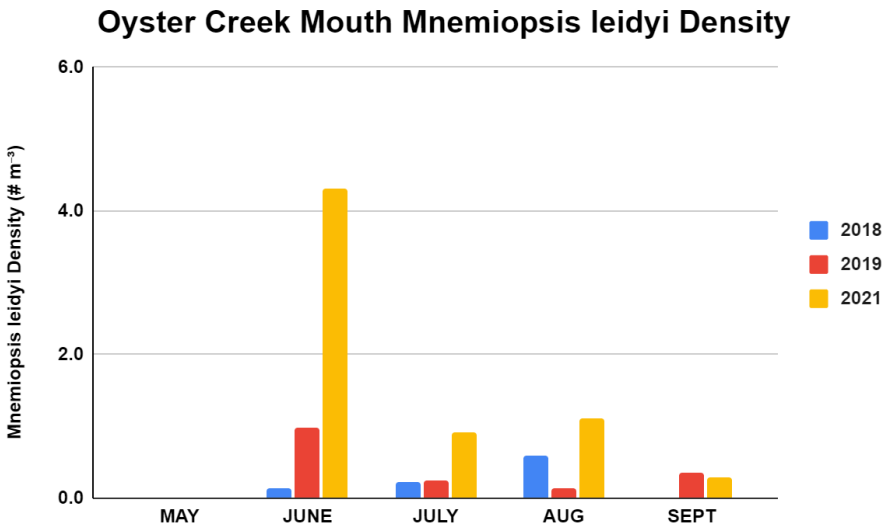

Figure 45. Lift Net Density of *Mnemiopsis leidyi* from Oyster Creek Mouth for all years.

Double Creek East

At Double Creek East, there was an abundance of *M. leidyi* observed in June during 2018 and 2021, but densities in 2019 were substantially less (Figure 46). The minimal density observed in 2019 was observed for some other sites, but not to the comparable level shown here. It is possible that since this site is the closest location to the Barnegat Inlet, that the tidal forces and oceanic influence impacted their density and distribution in 2019, but the densities observed at Double Creek West are almost opposite with the greatest densities observed in 2019 (Figure 47).

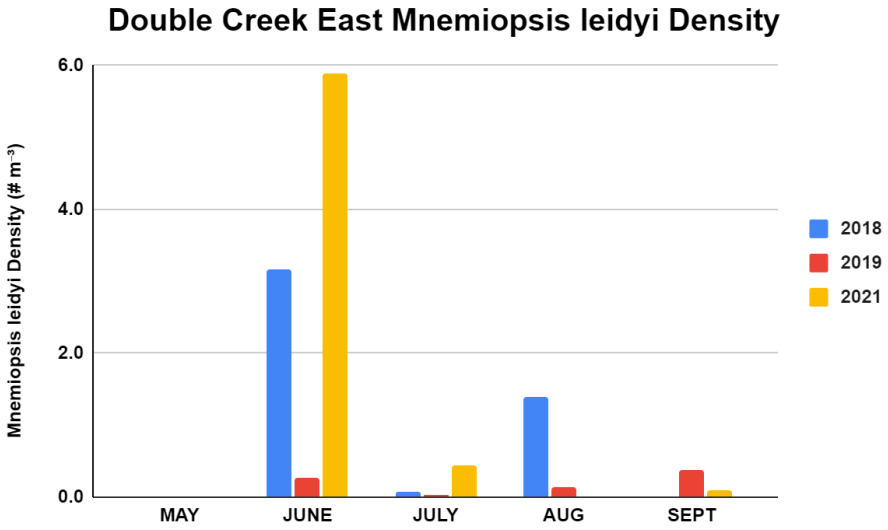

Figure 46. Lift Net Density of *Mnemiopsis leidyi* from Double Creek East for all years.

Double Creek West

At Double Creek West, *M. leidyi* densities in June for 2018 and 2019 were larger than the densities in the following months, but this was not the case for 2021 (Figure 47). In 2021, the densities were generally very low from June-August. In 2019, the resurgent bloom of *M. leidyi* was again present in September.

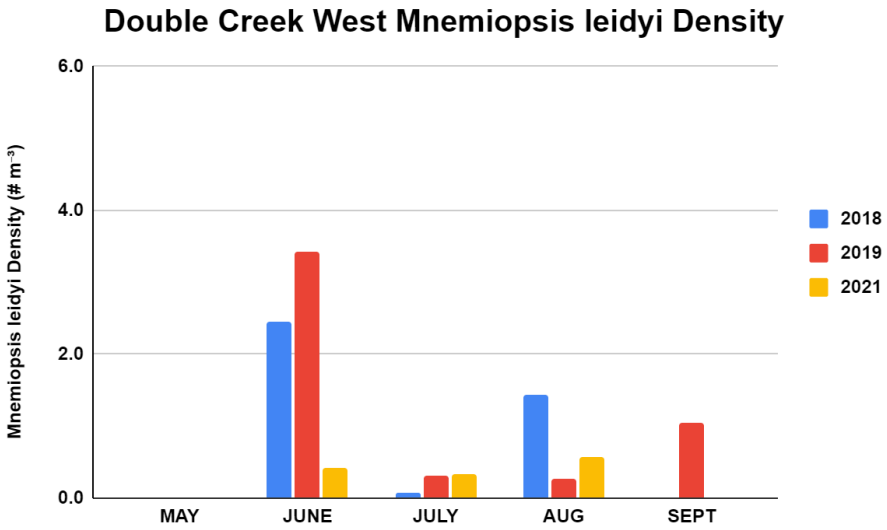

Figure 47. Lift Net Density of *Mnemiopsis leidyi* from Double Creek West for all years.

Bayshore Lagoon

In 2018, Bayshore Lagoon saw a slight increase in *M. leidyi* density between June and July before a larger increase appeared in August (Figure 48). The same thing is seen in 2019, where there were no observations made in June, but there were in July and August with August having a slightly higher density. In 2021, there was a fluctuation in the abundance that was observed from June-August with July having the highest density present in all three years.

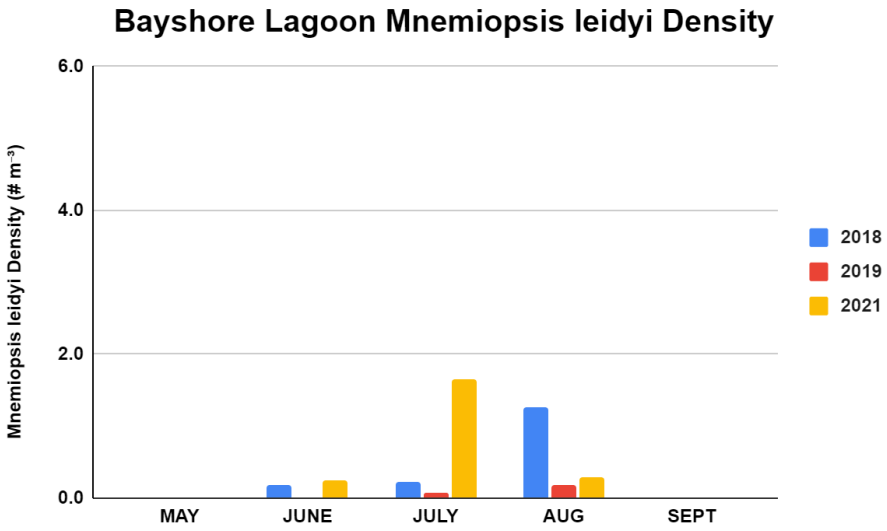

Figure 48. Lift Net Density of *Mnemiopsis leidyi* from Bayshore Lagoon for all years.

Plankton Tow Analyses of Gelatinous Species

During plankton tow sampling for the project, numerous species of gelatinous species were identified including: the comb jellies *Mnemiopsis leidyi* and *Pleurobrachia pileus;* the scyphozoans *Chrysaora chesapeakei, Cyanea capillata,* and *Aurelia spp*.; the hydrozoans *Turritopsis spp., Bougainvillia spp., Obelia spp., Aequora spp., Clytia spp., Nemopsis bachei, Rathkea octopunctata, Sarsia tubulosa, Gonionemus vertens,* and *Corymorpha spp*.; and the Salp *Thalia* spp. Several of these taxa showed significant differences in density among years, sites, and months based on the Mixed-Model ANOVA. The most abundant species are assessed for each individual site where they occurred.

Chrysaora chesapeakei

For plankton tow sampling, *Chrysaora chesapeakei* were not observed at Toms River West and Forked River West during all three sampling years. This was unexpected, as these are regions with known high population levels of *C. chesapeakei*. After considering all sampling years, most of the individuals seen during the sampling season were observed somewhere between June and August, especially mid-summer around July, leading to significant differences in densities among months ($F_{10,614} = 2.66$, $P < 0.004$). In general, *C. chesapeakei* densities were relatively low at most sites, but did differ significantly among sites ($F_{11,614} = 5.9$, $P < 0.0001$) with the Forked River Lagoon site having the greatest density followed by the Forked River Rt. 9 site. Both sites saw dramatic increases in 2019 compared to 2018 after the OCNGS was shut down.

Site Specific Patterns in Abundance

Sunrise Beach

There was a low density of *Chrysaora chesapeakei* observed at Sunrise Beach and they were only collected in August 2018 (Figure 49). In the following two years, they were not observed at this location, although they were collected in 2021 from the adjacent Sunrise Beach Lagoon.

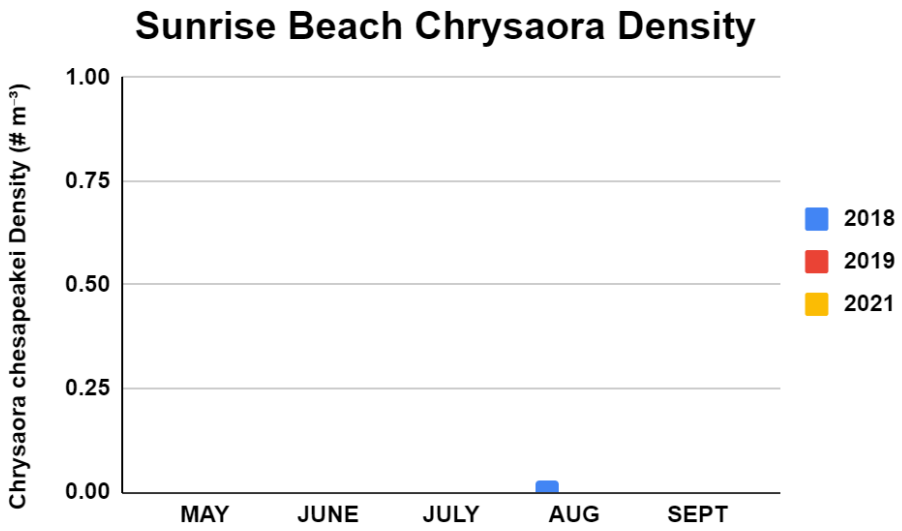

Figure 49. Plankton tow density of *Chrysaora chesapeakei* from Sunrise Beach for all years.

Sunrise Beach Lagoon

C. chesapeakei individuals at Sunrise Beach Lagoon were seen only in August of 2018 and June of 2021, both in very sparse numbers (Figure 50). August 2018 yielded a slightly larger density than June 2021.

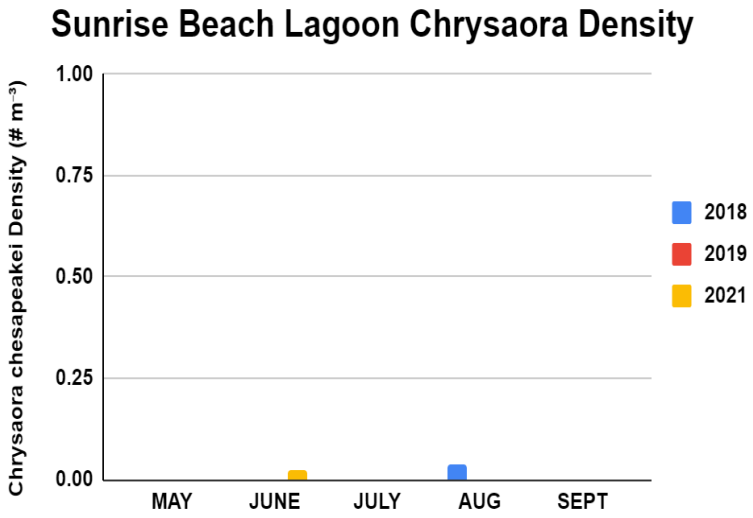

Figure 50. Plankton tow density of *Chrysaora chesapeakei* from Sunrise Beach Lagoon for all years.

Forked River East

At Forked River East, *C. chesapeakei* was not observed in 2018 and 2021 (Figure 51). There was a low density seen in July 2019 and no observations were made for August that same year. There was a substantial increase in density in September 2019, which may reflect the adult medusae swimming and moving within the Bay.

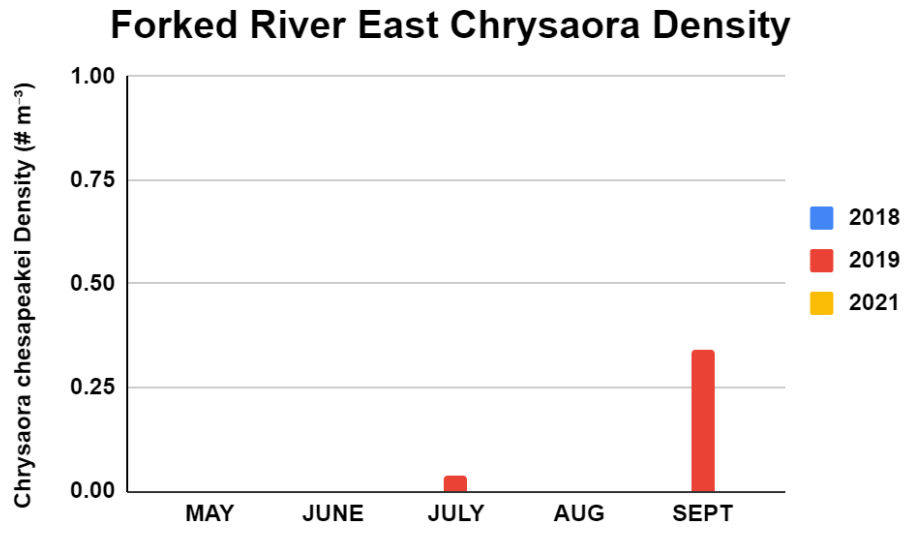

Figure 51. Plankton tow density of *Chrysaora chesapeakei* from Forked River East for all years.

Forked River Rt. 9

For Forked River Rt. 9, no *C. chesapeakei* individuals were seen throughout the 2018 sampling season during the active operation of the plant, however a considerable increase was observed in 2019 the year after the plant stopped active operation (Figure 52). June, July, and August of 2019 had the highest densities recorded for this site, with a noticeable bloom occurring into July and a slight decline by August. In 2021, no individuals were recorded in June, but low densities were observed in July and August and this likely reflects the change in water circulation patterns at this site following the shutdown.

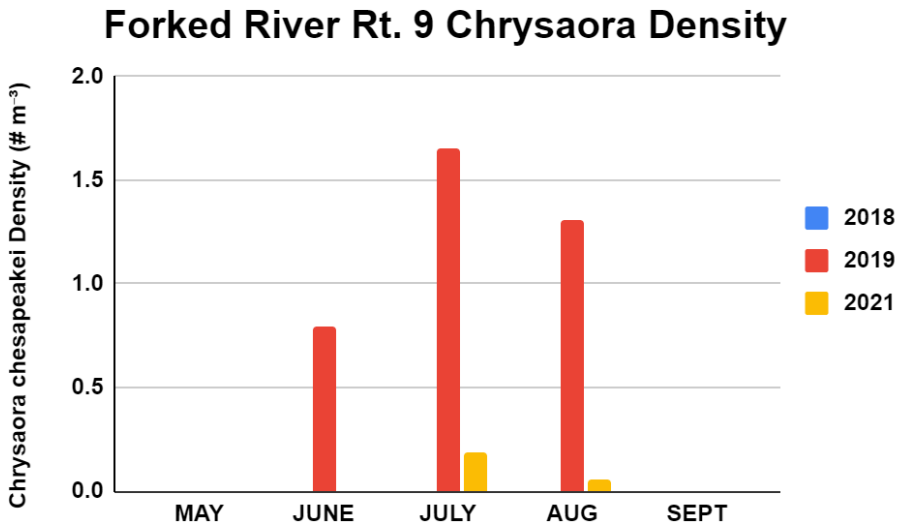

Figure 52. Plankton tow density of *Chrysaora chesapeakei* from Forked River Rt.9 for all years.

Forked River Lagoon

In 2018, *C. chesapeakei* individuals at Forked River Lagoon were found in sufficient numbers in June, and bloomed to more than four times the size by July (Figure 53). By August, densities decline severely before becoming absent in later months. 2019 displayed a similar pattern where small June densities increased to much larger quantities by July before declining once again into August, however July 2019 recorded more individuals per cubic meter. 2021 saw large densities as early as May, with an absence in June and few individuals recorded in July. These declines seen after July may reflect the reduced production of ephyrae and movement of medusae out of the lagoon.

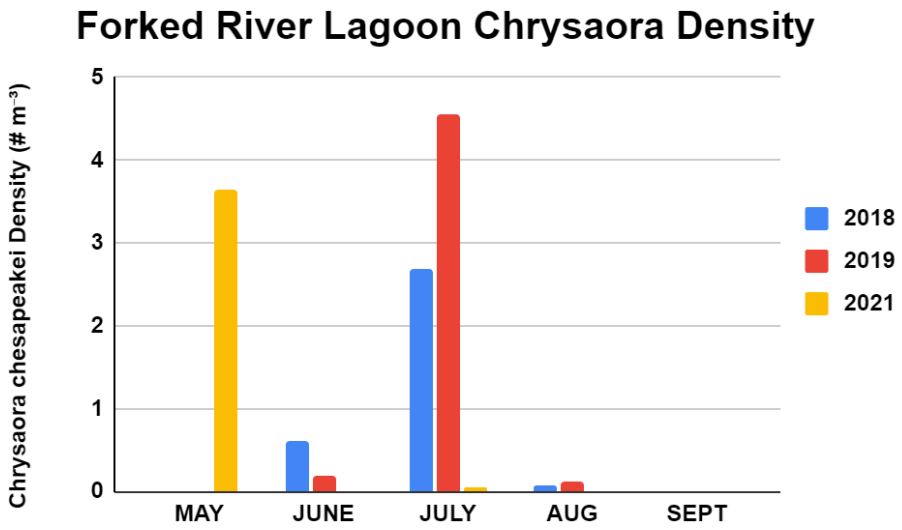

Figure 53. Plankton tow density of *Chrysaora chesapeakei* from Forked River Lagoon for all years.

Oyster Creek Rt. 9

At Oyster Creek Rt. 9, *C. chesapeakei* was only recorded in July of 2019 (Figure 54), the year following the shutdown. No other collections were made in 2019, nor 2018 or 2021. It is possible that the operation of the plant ensured no development of medusae in 2018, but does not explain their absence in 2021, except for the possibility that the nearby lagoon communities of Oyster Creek do not have substantial polyp populations.

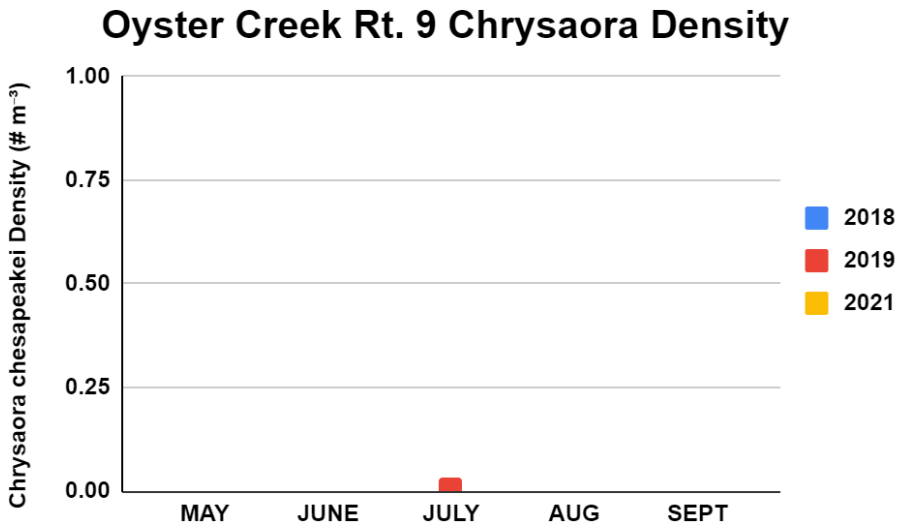

Figure 54. Plankton tow density of *Chrysaora chesapeakei* from Oyster Creek Rt.9 for all years.

Oyster Creek Mouth

Oyster Creek Mouth yielded very few individuals, observed only in July 2021; no other months in 2021 had reported observations, nor did the entirety of 2018 and 2019 (Figure 55). These observations correspond with the lack of medusae observed upstream at the Oyster Creek Rt. 9 site.

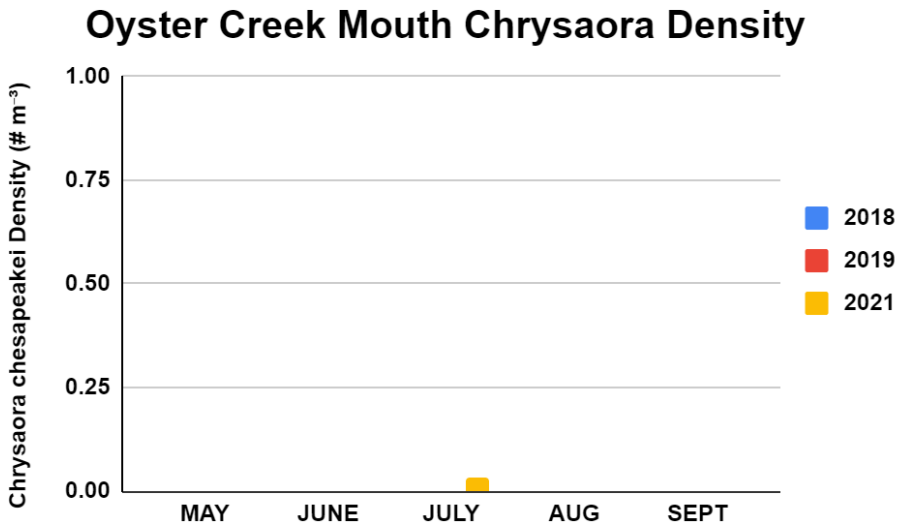

Figure 55. Plankton tow density of *Chrysaora chesapeakei* from Oyster Creek Mouth for all years.

Double Creek East

Double Creek East also saw few *C. chesapeakei* individuals throughout the sampling season, with densities recorded in June 2021 only (Figure 56). This pattern may reflect the site's proximity to the inlet and high rates of tidal flushing.

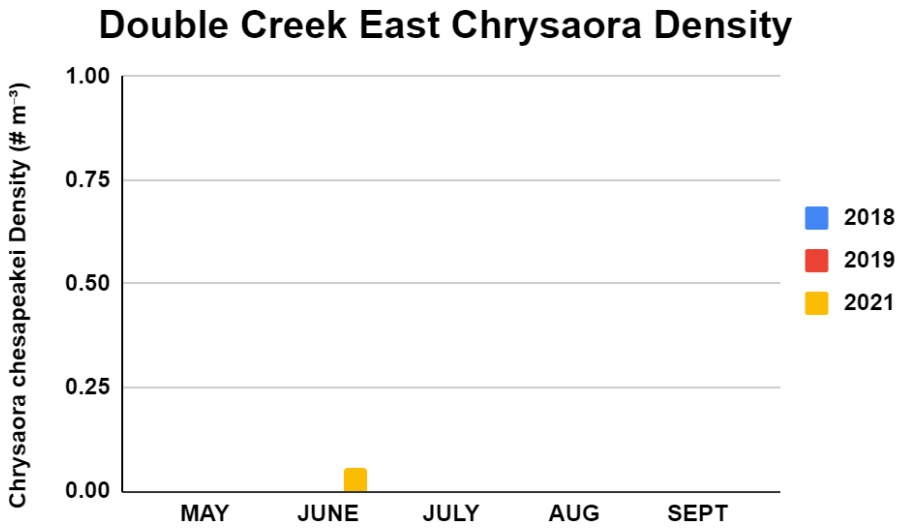

Figure 56. Plankton tow density of *Chrysaora chesapeakei* from Double Creek East for all years.

Double Creek West

Presence of *C. chesapeakei* was only observed in August of 2019 (Figure 57). There were no other recordings made for *C. chesapeakei* at Double Creek West in 2018, 2019, and 2021.

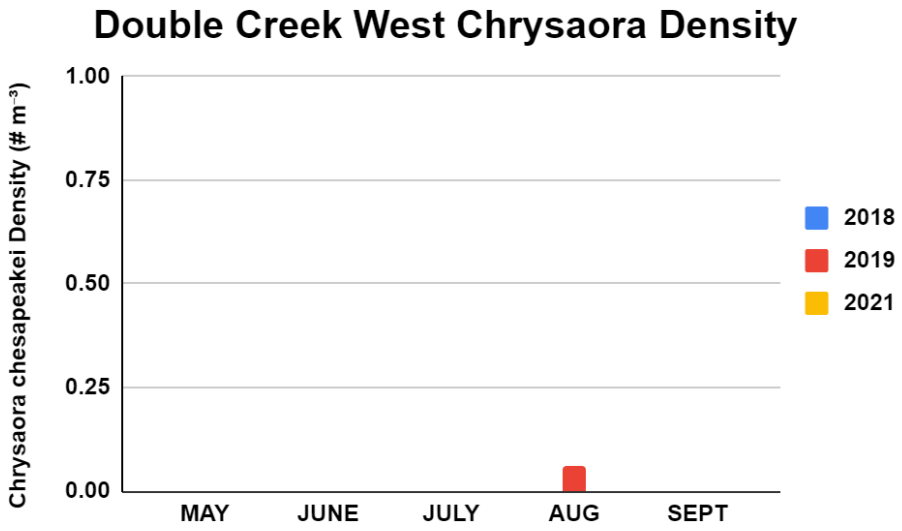

Figure 57. Plankton tow density of *Chrysaora chesapeakei* from Double Creek West for all years.

Bayshore Lagoon

At Bayshore Lagoon in July of 2018, a high density of *C. chesapeakei* was observed compared to the other data points (Figure 58). In 2019, *C. chesapeakei* was recorded during July and August, but no individuals were recorded in 2021.

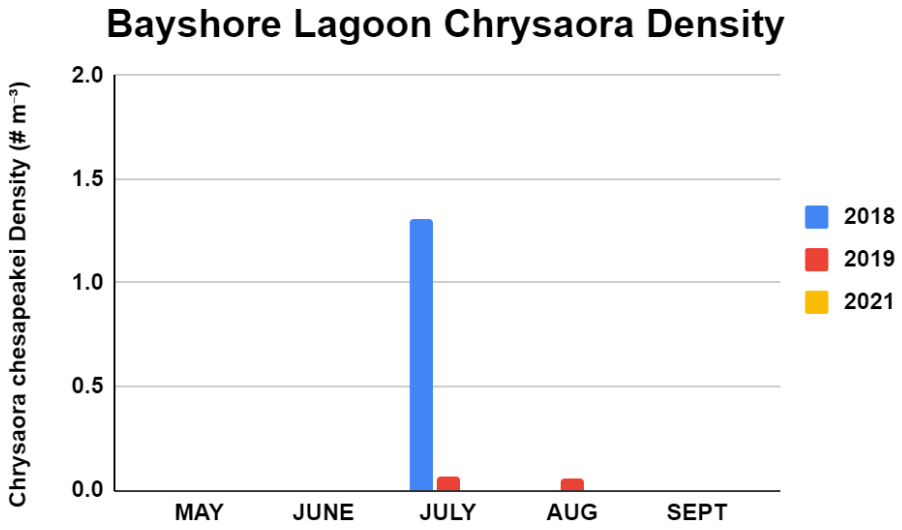

Figure 58. Plankton tow density of *Chrysaora chesapeakei* from Bayshore Lagoon for all years.

Chrysaora chesapeakei Ephyrae Trends

Similar to the results from the statistical analyses, ephyrae densities differed significantly among months of collection ($F = 2.6$, $P < 0.0005$) and sites ($F = 3.96$, $P < 0.0001$). Bay nettle ephyrae were not observed at Double Creek East and Double Creek West during all three sampling years, which could have contributed to the significant differences seen among sites. In general, ephyrae were observed during each month sampled, but the highest densities reflect the emergence of them in late spring and early summer, which corresponds to the increased densities of medusae observed in June through August.

Site Specific Patterns in Abundance

Toms River West

Bay nettle ephyrae were only detected in June of 2021 at Toms River West (Figure 59). No other observations were made.

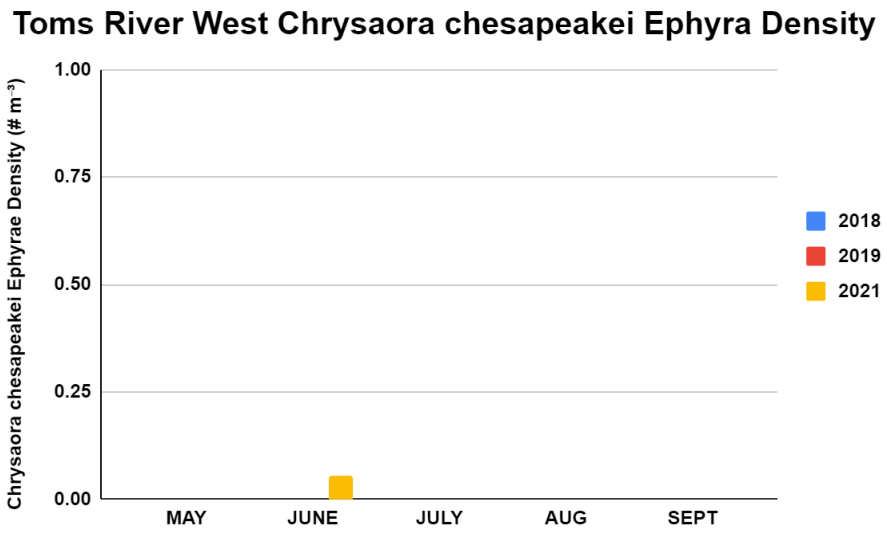

Figure 59. Plankton tow density of *C. chesapeakei* ephyrae from Toms River West for all years.

Sunrise Beach

The only observation made at Sunrise Beach was a considerably small density of bay nettle ephyrae in June 2019 (Figure 60).

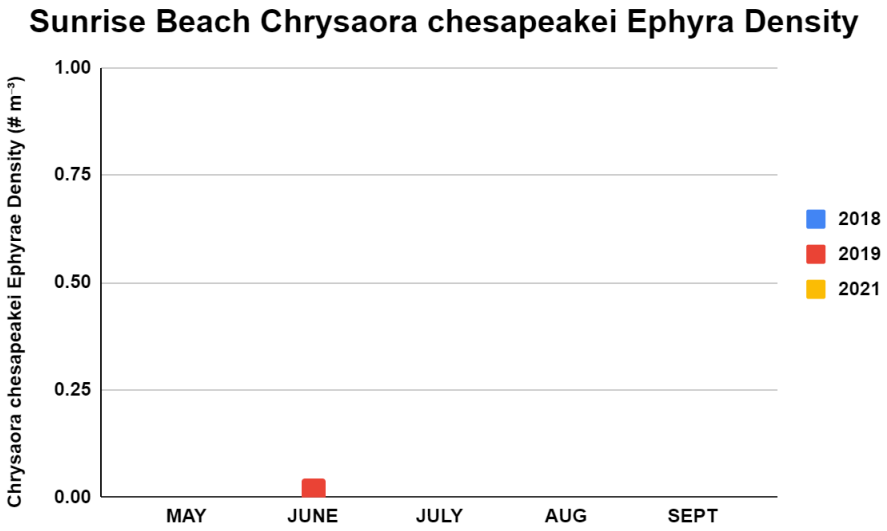

Figure 60. Plankton tow density of *C. chesapeakei* ephyrae from Sunrise Beach for all years.

Sunrise Beach Lagoon

There was an absence of bay nettle ephyrae for 2019 and 2021 entirely at Sunrise Beach Lagoon (Figure 61). The only recorded observations for this site were in July 2018 and as this is the likely source for ephyrae for Sunrise beach, the lack of ephyrae was unexpected.

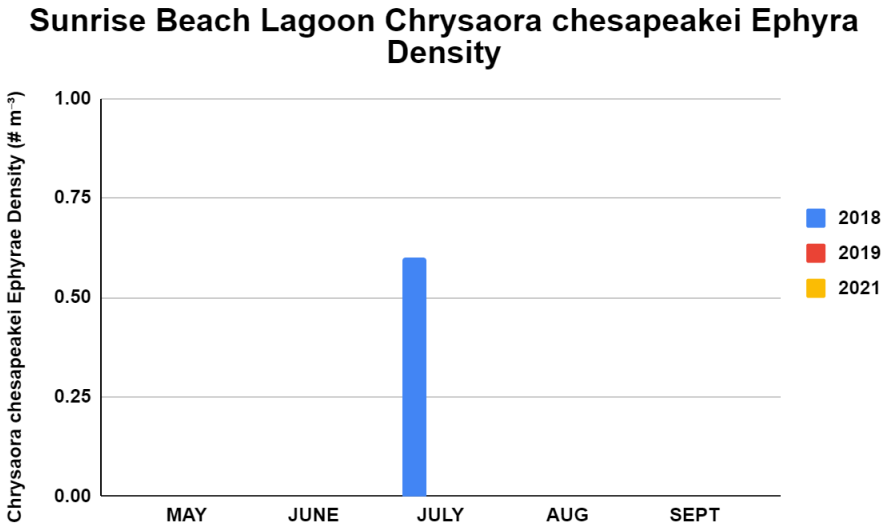

Figure 61. Plankton tow density of *C. chesapeakei* ephyrae from Sunrise Beach Lagoon for all years.

Forked River East

In May of 2019 and 2021, *C. chesapeakei* ephyrae were observed in low densities at Forked River East (Figure 62). For the remaining months, no other observations were made. It is possible that in 2018 the plant operation limited ephyrae dispersal from lagoon communities, but after the shutdown, ephyrae pulsed into the broader Barnegat Bay system.

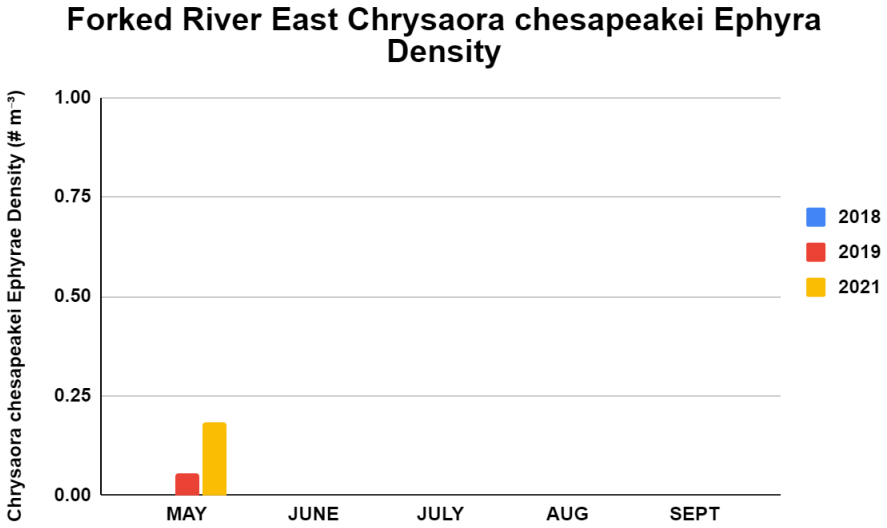

Figure 62. Plankton tow density of *C. chesapeakei* ephyrae from Forked River East for all years.

Forked River West

No ephyrae were collected in 2018 from this site while the plant was in operation (Figure 63). It is highly probable that ephyrae generated in nearby lagoons during the operation of the OCNGS were entrained into the cooling system. However, in both 2019 and 2021, post shutdown, ephyrae were collected in the late spring from this site and likely reflects fewer ephyrae being advected into the plant.

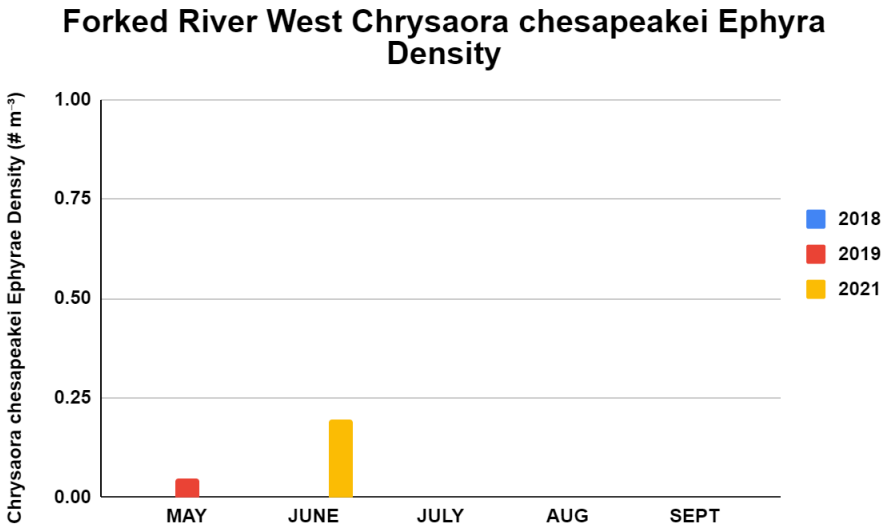

Figure 63. Plankton tow density of *C. chesapeakei* ephyrae from Forked River West for all years.

Forked River Rt. 9

In 2018, sea nettle ephyrae were exclusively present in July only (Figure 64) and corresponds to the pattern seen in 2018 for the Forked River Lagoon (Figure 65). The following year, bay nettle ephyrae were found in both June and July in similar densities, but during 2021 substantially more ephyrae were collected beginning in May and continuing into August. This pattern of increases after the shutdown of the plant suggests increasing polyp populations in the region.

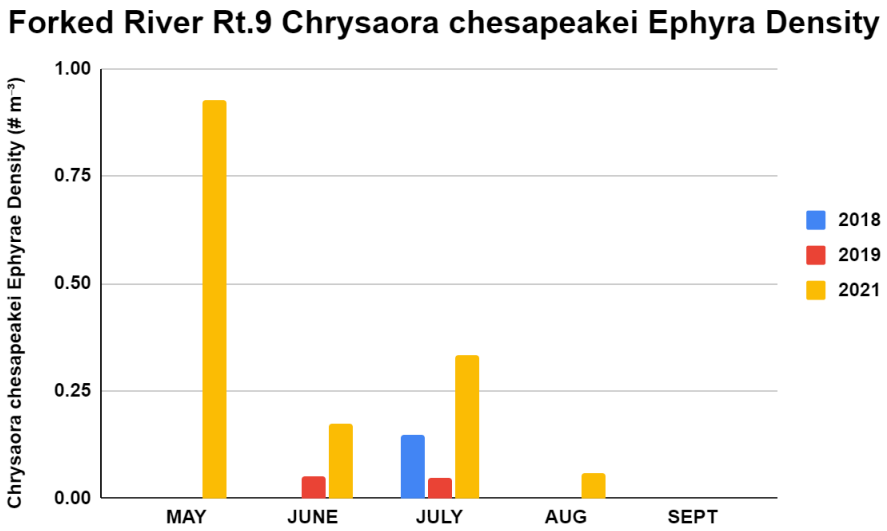

Figure 64. Plankton tow density of *C. chesapeakei* ephyrae from Forked River Rt. 9 for all years.

Forked River Lagoon

Densities of *C. chesapeakei* ephyrae are maximal at this site and exceeded 35 m^{-3} in July 2018 (Figure 65). While ephyrae densities were lower in the following years, the scale of abundance in this region is very high and represents a substantial source of ephyrae and ultimately medusae to the system. This source could be responsible for the significant increases in adult densities observed in 2021 during the lift net surveys in the bay.

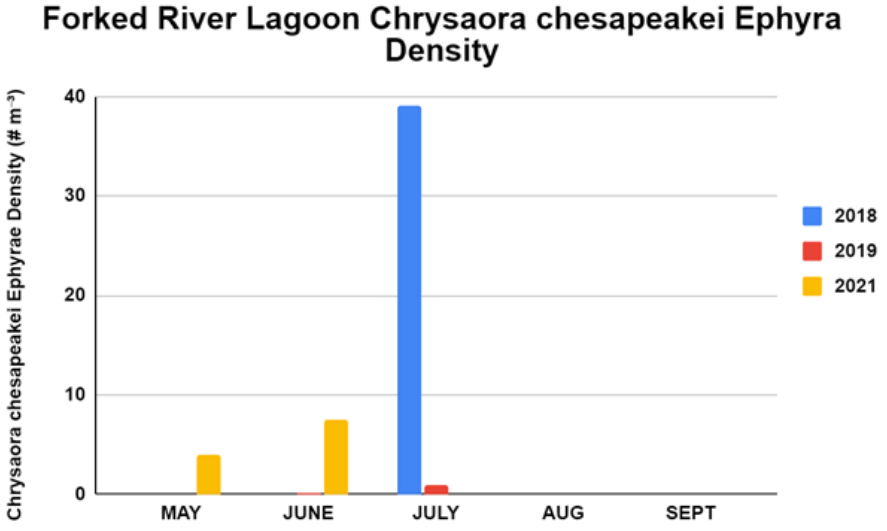

Figure 65. Plankton tow density of *C. chesapeakei* ephyrae from Forked River Lagoon for all years.

Oyster Creek Rt. 9

A small collection of *C. chesapeakei* ephyrae were observed in August of 2018 (Figure 66). Ephyrae were not observed for the remaining months of 2018, 2019, and 2021. This finding corroborates the low densities of adults observed at this site and may reflect low polyp populations in the nearby regions.

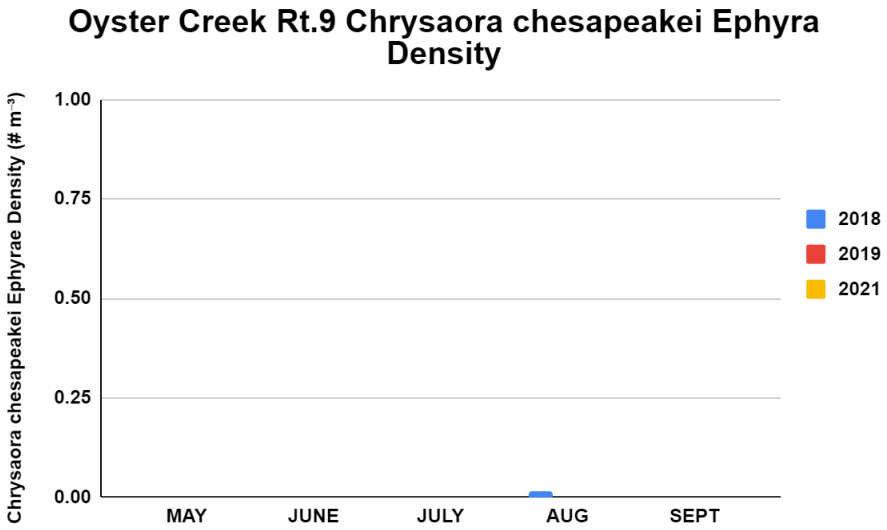

Figure 66. Plankton tow density of *C. chesapeakei* ephyrae from Oyster Creek Rt. 9 for all years.

Oyster Creek Mouth

Chrysaora chesapeakei ephyrae were not observed at Oyster Creek Mouth in 2018 (Figure 67), but they were recorded in June of 2019, as well as in May and August of 2021 after the shutdown. These results suggest that the change in flow dynamics in this region have allowed ephyrae from neighboring areas to be dispersed into this region.

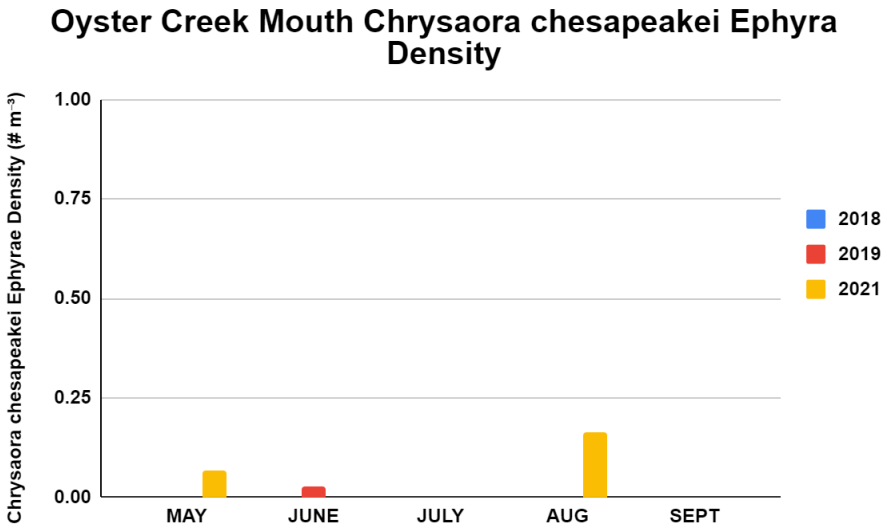

Figure 67. Plankton tow density of *C. chesapeakei* ephyrae from Oyster Creek Mouth for all years.

Bayshore Lagoon

At Bayshore Lagoon, *C. chesapeakei* ephyrae was not present during the sampling events in 2018 and 2019 (Figure 68). In June 2021, a low number of *C. chesapeakei* ephyrae were observed, but no subsequent bloom in adults was recorded here.

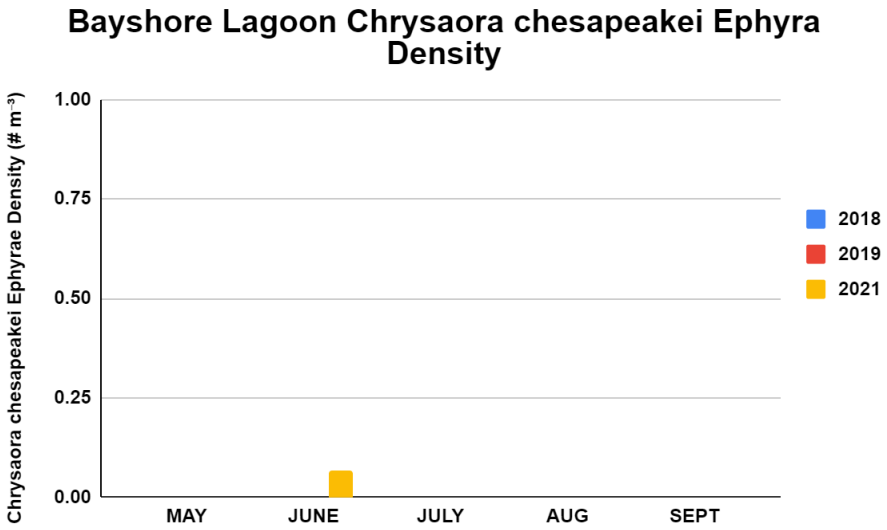

Figure 68. Plankton tow density of *C. chesapeakei* ephyrae from Bayshore Lagoon for all years.

Mnemiopsis leidyi Trends

General trends for the density and distribution of *Mnemiopsis leidyi* changed between 2018, 2019, and 2021. A significant increase in density was observed after the OCNGS went offline ($F_{2,613} = 14.2$, $P < 0.0001$) going from 0.55m^{-3} in 2018 to 1.87m^{-3} in 2019, and to 2.29m^{-3} in 2021. This differs from the results associated with the lift net analysis which did not show a significant increase in density among years, but lift nets do not collect the smallest *M. leidyi*, which are collected by the plankton nets. A similar seasonal trend was observed for plankton samples with lift nets, where densities of *M. leidyi* decreased in July and August resulting in significant density differences among months ($F_{10,613} = 23.26$, $P < 0.0001$), but densities rebounded in the fall. These results correspond to the increase in *C. chesapeakei* during this time, potentially exerting top-down predation pressure on *M. leidyi*.

Site Specific Patterns in Abundance

Toms River West

Toms River West's sampling years 2018, 2019, and 2021 demonstrated drastically different growth trends for *M. leidyi* (Figure 69). In 2018, very sparse numbers were observed in June, with a very slight increase to follow in July. In 2019, few individuals were not seen initially until July. *M. leidyi* densities were seen to increase to much higher densities in the following month. In 2021, initial densities were seen in June with the highest recorded numbers for the site, however those densities declined immensely into July. Population growth was seen between July and September with a recovery from July's decline.

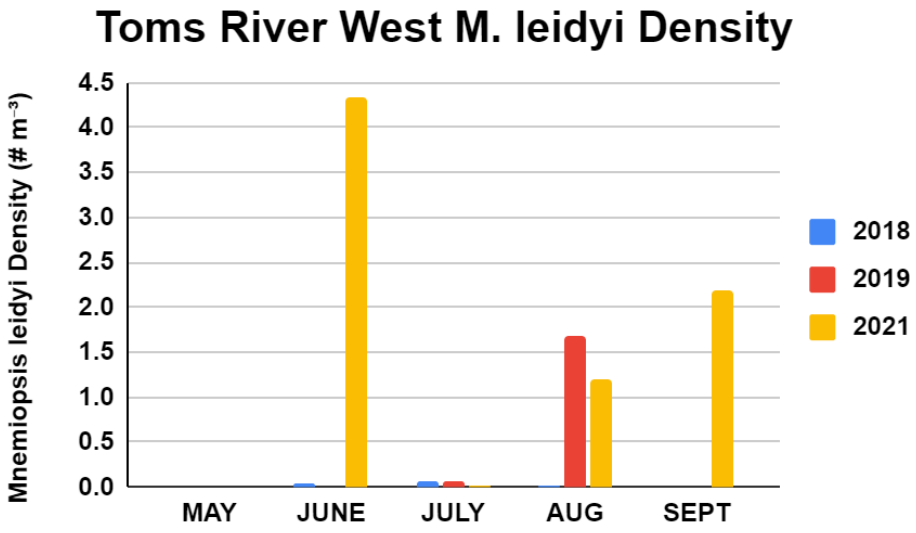

Figure 69. Plankton Tow densities of *Mnemiopsis leidyi* from Toms River West for all years.

Sunrise Beach

Sunrise Beach's *M. leidyi* population in 2018 demonstrated sufficient densities in July that declined somewhat into August (Figure 70). The following year, *M. leidyi* were seen first in June with ample numbers, then considerably fewer numbers in July that increased again into August. By September, densities increased to extremely high quantities. In 2021, very sparse numbers were observed as early as May, and greater quantities observed in June. Densities declined into July and recovered slightly into August, however densities declined once again into September.

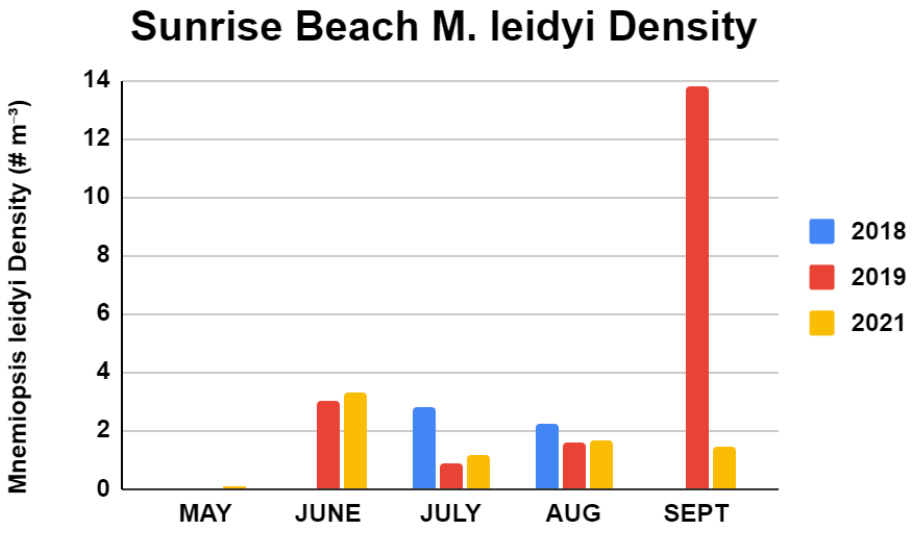

Figure 70. Plankton Tow densities of *Mnemiopsis leidyi* from Sunrise Beach for all years.

Sunrise Beach Lagoon

In 2018, low densities of *M. leidyi* were recorded only in June and August at Sunrise Beach Lagoon (Figure 71). The following year, there was a significantly high density of *M. leidyi* observed in July that drastically decreased in August. In 2021, densities were recorded for the months of June-August with the highest totals of *M. leidyi* in July.

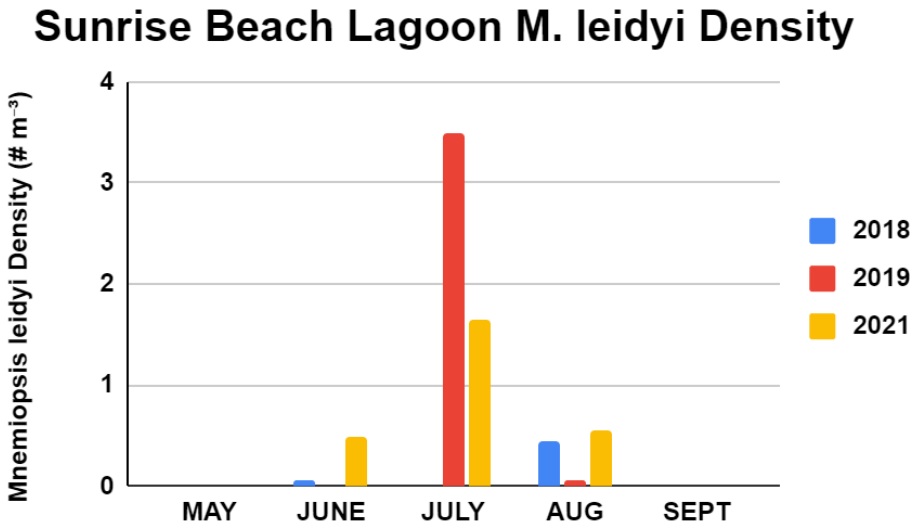

Figure 71. Plankton Tow densities of *Mnemiopsis leidyi* from Sunrise Beach Lagoon for all years.

Forked River East

M. leidyi at Forked River East in 2018 appeared in sufficient numbers starting from June, with some fluctuation through July and August (Figure 72). In 2019, very few individuals were seen in June and August, however blooms were observed in July and (especially) September. 2021 yielded considerably high

densities in June yet noteworthy declines in July; slight declines followed into August, then slight increases followed into September.

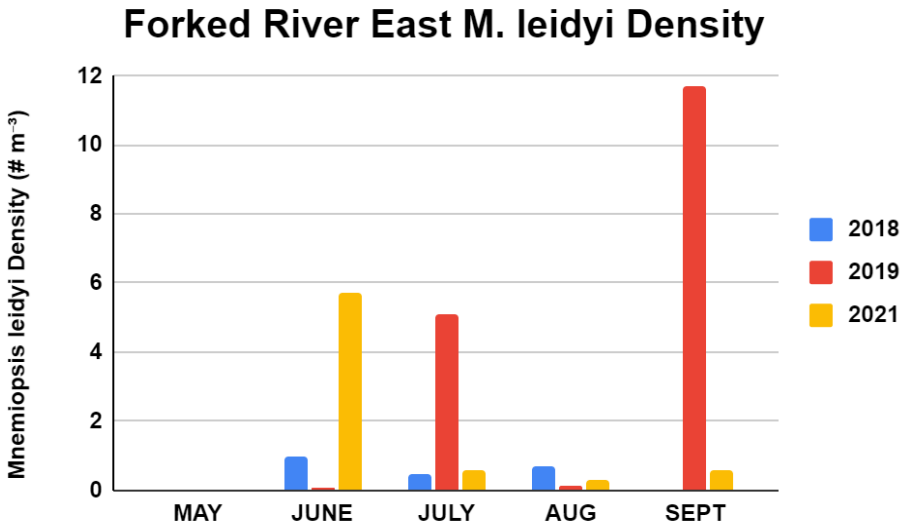

Figure 72. Plankton Tow densities of *Mnemiopsis leidyi* from Forked River East for all years.

Forked River West

M. leidyi at Forked River West in 2018 appeared in sufficient numbers starting in July with a significant decrease in August (Figure 73). In 2019, few individuals were seen in June with a slight increase in July and a decrease in August. September 2019 saw a significant increase of more than eight times the amount in August. In 2021, densities were considerably high in June then declined through August. September 2021 saw a slight increase from August.

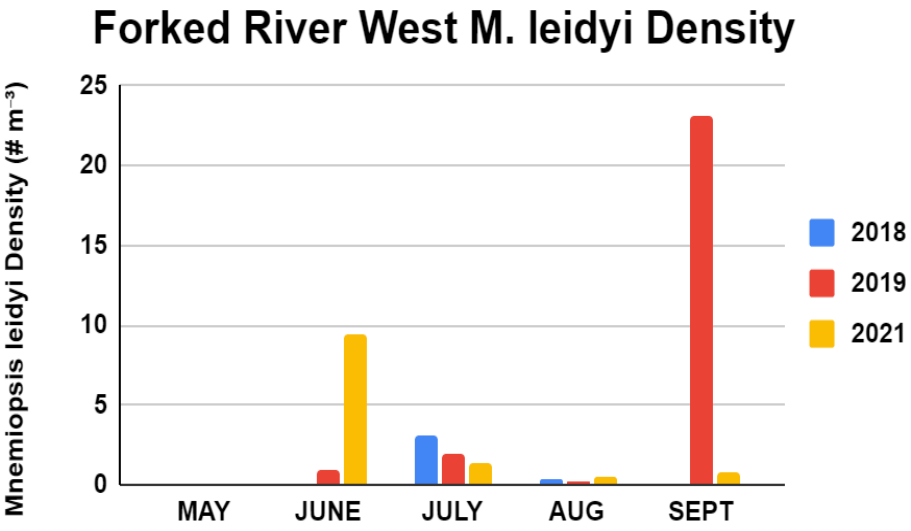

Figure 73. Plankton Tow densities of *Mnemiopsis leidyi* from Forked River West for all years.

Forked River Rt. 9

M. leidyi densities at Forked River Rt. 9 were very sparse starting in June 2018, yet increased into July before ultimately decreasing in August (Figure 74). In 2019, densities were more or less stable from June to August, however densities increased in September to more than eight times the amount in the previous month. In 2021, densities were initially at their highest in June, however they declined considerably by July. August had no reports of *M. leidyi* in 2021, but a small population was observed in September.

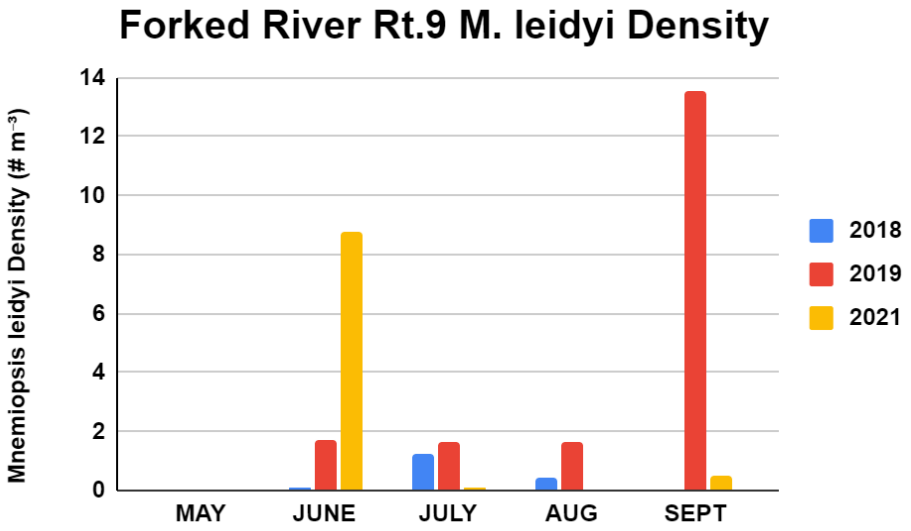

Figure 74. Plankton Tow densities of *Mnemiopsis leidyi* from Forked River Rt. 9 for all years.

Forked River Lagoon

At Forked River Lagoon, *M. leidyi* was scarce in 2018 and only observed in June and August (Figure 75). Densities did not increase in 2019, but *M. leidyi* was now seen in July and September and not in June and August. *M. leidyi* densities were highest in September and June 2021, respectively and demonstrated increasing densities throughout the field season.

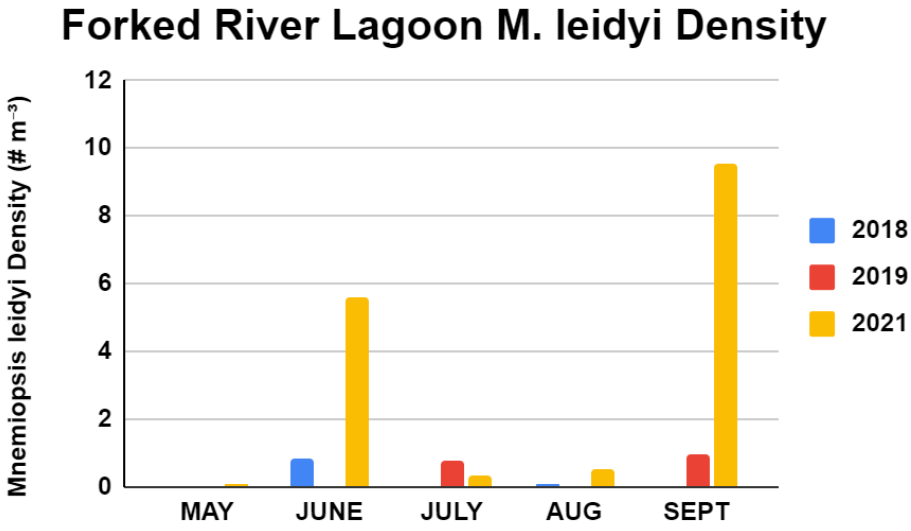

Figure 75. Plankton Tow densities of *Mnemiopsis leidyi* from Forked River Lagoon for all years.

Oyster Creek Rt. 9

M. leidyi at Oyster Creek Rt. 9 were very sparse in June 2018, with a significant increase observed in July. This trend was maintained through August, although with only a slight decrease (Figure 76). In 2019, June densities were entirely absent, yet July saw a significant increase. August saw a complete absence of *M. leidyi*, yet September once again saw a slight increase though not to the same level as July. In 2021, June saw somewhat high densities where July saw a significant decrease leading to a complete absence in August and September.

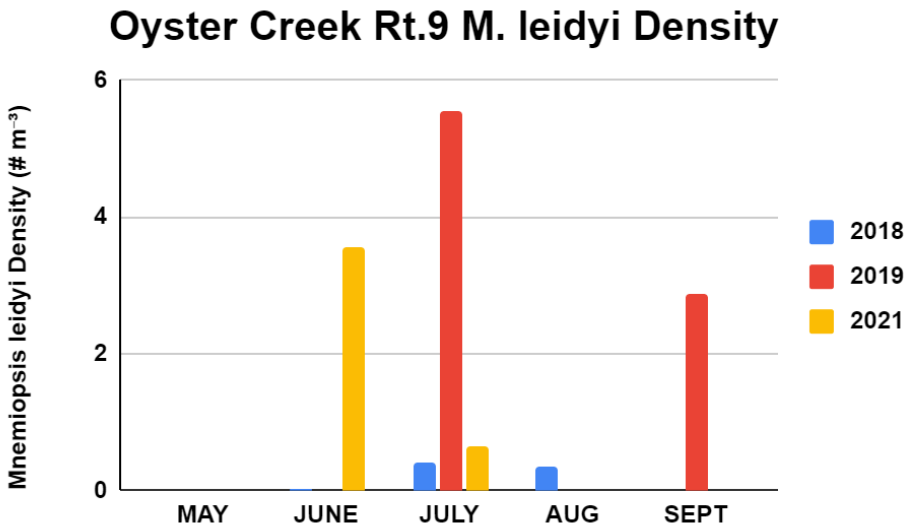

Figure 76. Plankton Tow densities of *Mnemiopsis leidyi* from Oyster Creek Rt. 9 for all years.

Oyster Creek Mouth

M. leidyi at Oyster Creek Mouth were very sparse in June 2018 with a minor increase in July and August, though not significant (Figure 77). In 2019, June densities were slightly higher than August of 2018 with densities continuing to decrease in both July and August. In contrast, September saw a significant increase as opposed to the decrease observed in earlier months. In 2021, June saw an abundance of individuals followed by a significant decrease in July. August saw a slight increase in individuals and September decreased to almost no individuals.

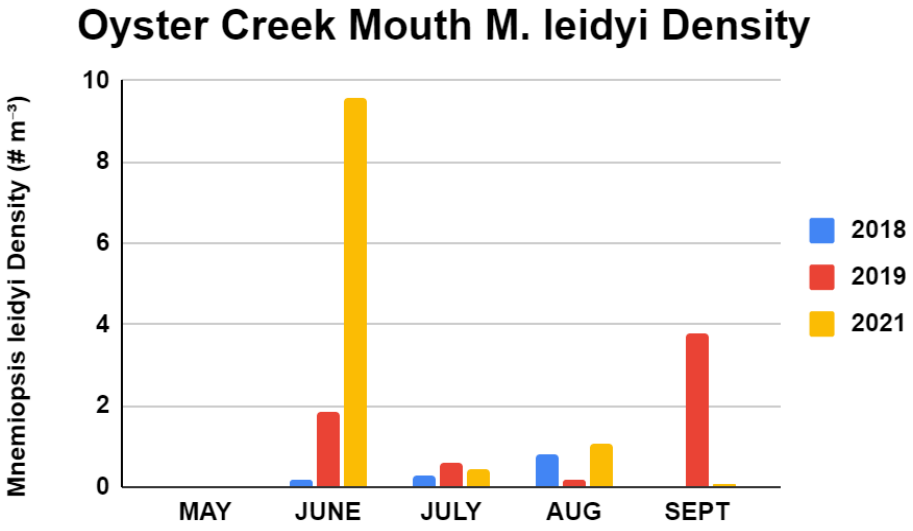

Figure 77. Plankton Tow densities of *Mnemiopsis leidyi* from Oyster Creek Mouth for all years.

Double Creek East

M. leidyi densities were scarce at Double Creek East from May to August 2018 with a significant decrease from June to July (Figure 78). In 2019, *M. leidyi* was seen in June in low numbers and was not recorded at all from July to August. In September 2019, density considerably increased. *M. leidyi* was abundant in June 2021 and density decreased as the summer progressed.

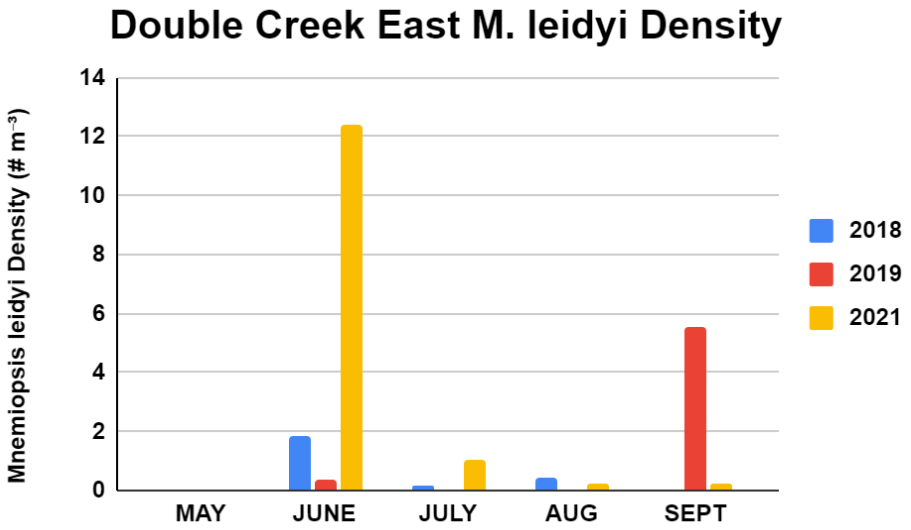

Figure 78. Plankton Tow densities of *Mnemiopsis leidyi* from Double Creek East for all years.

Double Creek West

Double Creek West experienced great densities of *M. leidyi* throughout all three years (Figure 79). In 2019, July had the highest density of *M. leidyi,* then decreased slightly in August and increased again in September. In contrast to the previous year, *M. leidyi* numbers were highest in September 2021 and lowest in July 2021.

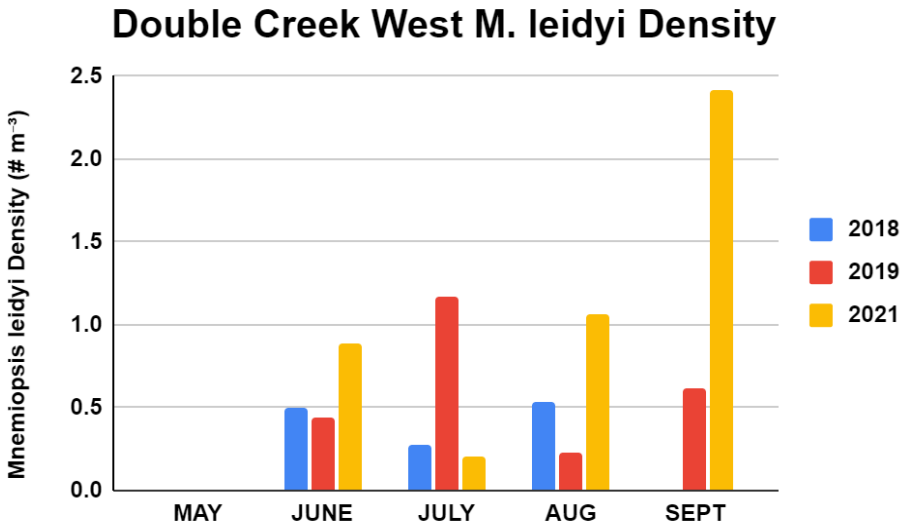

Figure 79. Plankton Tow densities of *Mnemiopsis leidyi* from Double Creek West for all years.

Bayshore Lagoon

Bayshore Lagoon's *M. leidyi* average densities increased between 2018 and 2021, with a higher overall abundance witnessed between the months of June and August (Figure 80). 2018 densities exhibited a small peak in July, however 2019's peak densities appeared in August. *M. leidyi* individuals were also only noted in July and August in 2019. By 2021, initially observed densities were relatively higher than the apex densities in previous years; the highest densities were recorded in July of this year, as well, before it declined into August.

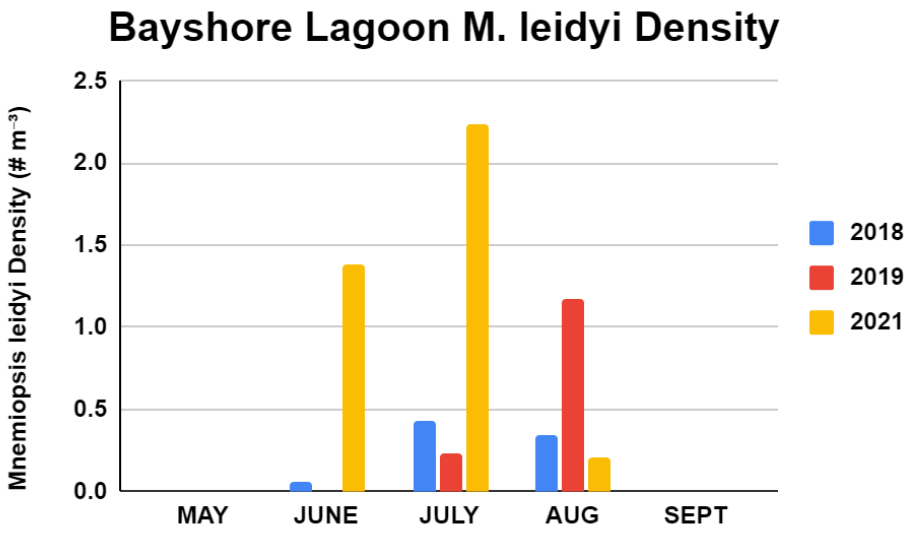

Figure 80. Plankton tow densities of *Mnemiopsis leidyi* from Bayshore Lagoon for all years.

Nemopsis bachei Trends

Plankton tow samples showed a generalized increase in overall density from 2018 (0.09 m^{-3}) to 2021 (0.17m^{-3}). While this was an approximate doubling in density, this difference was not significant. This is likely due to the significant differences among months observed in the analyses ($F_{10,614} = 6.1$, $P < 0.0001$) relating to the late spring bloom observed in May and June of each year. Additionally, there were significant differences among sites ($F_{11,614} = 2.75$, $P < 0.002$) with the greatest densities observed at Forked River East in 2021.

Site Specific Patterns in Abundance

Toms River West

In 2019 and 2021, there was a greater collection of *Nemopsis bachei* at Toms River West from May to July with June 2021 having the highest collection amount (Figure 81). Compared to June 2018, there was only one appearance made in the data, and for all years in the months of August and September, there were no *N. bachei* collected.

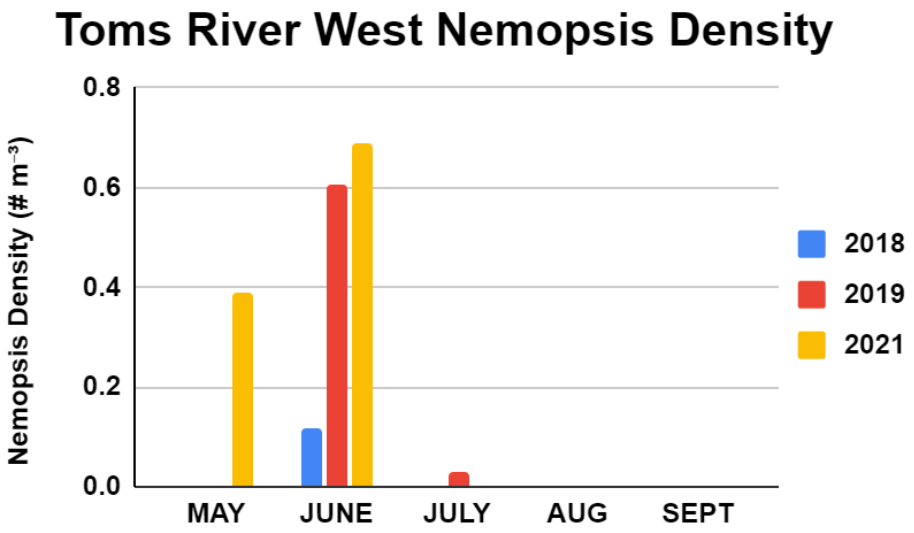

Figure 81. Plankton tow *Nemopsis bachei* densities from Toms River West for all years.

Sunrise Beach

N. bachei presence was marked from May to August at Sunrise Beach, where most were recorded to be below 0.4 individuals m^{-3} (Figure 82). For all years, June had the highest *N. bachei* density.

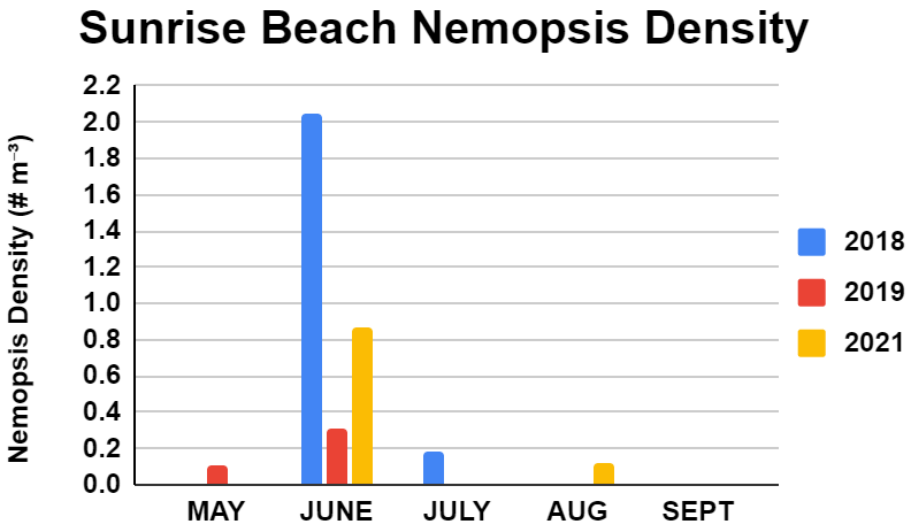

Figure 82. Plankton tow *Nemopsis bachei* densities from Sunrise Beach for all years.

Sunrise Beach Lagoon

There was a single observation of *N. bachei* made in June of 2019 at Sunrise Beach Lagoon (Figure 83).

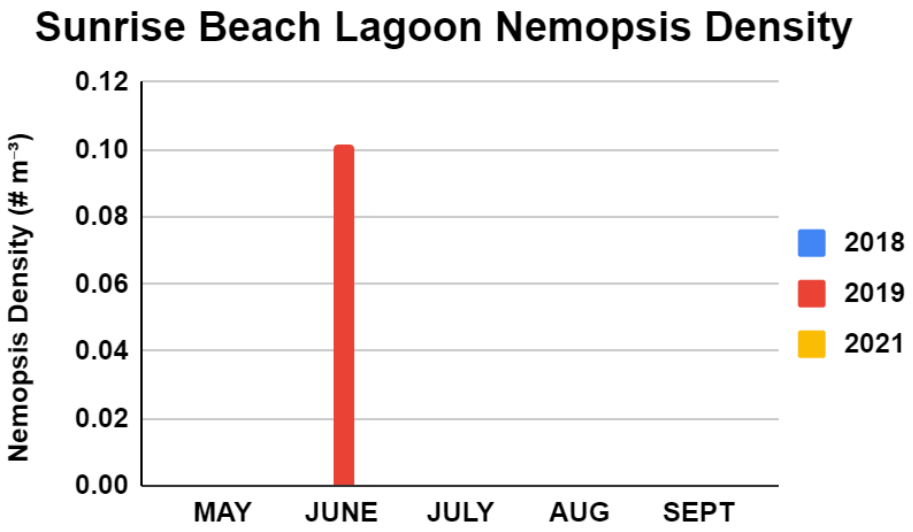

Figure 83. Plankton tow *Nemopsis bachei* densities from Sunrise Beach Lagoon for all years.

Forked River East

There were low recorded *N. bachei* densities for all years during select months at Forked River East, except for June of 2021 (Figure 84). No observations were recorded in May and August of any year, but a secondary bloom occurred in September of 2019.

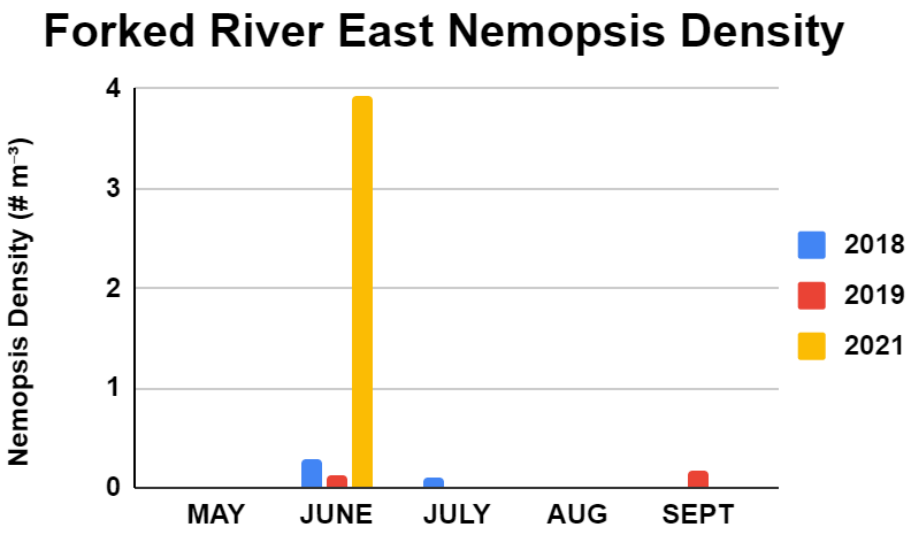

Figure 84. Plankton tow *Nemopsis bachei* densities from Forked River East for all years.

Forked River West

There were recorded observations for *N. bachei* in June for all years with the highest density occurring in 2019 at Forked River West (Figure 85) and 2019 was the only year where they were observed in May. This suggests a single late spring bloom for this species.

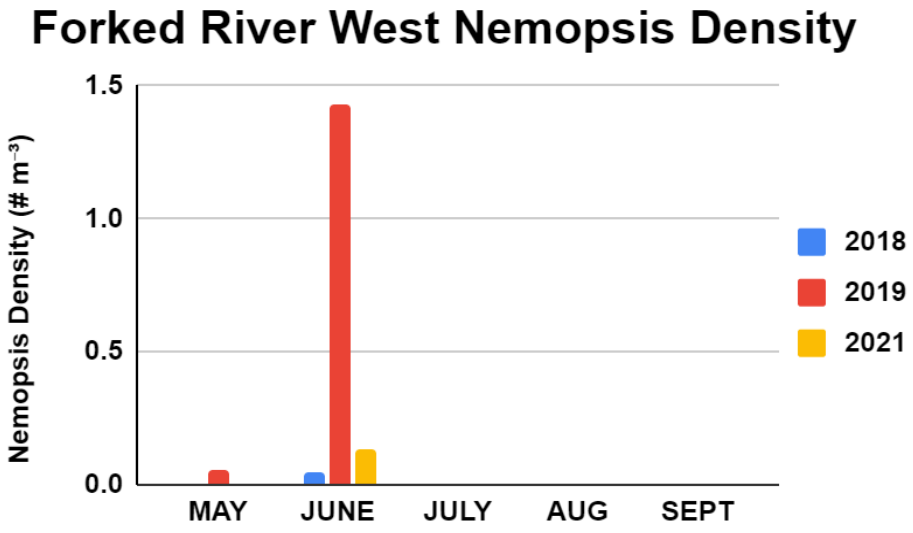

Figure 85. Plankton tow *Nemopsis bachei* densities from Forked River West for all years.

Forked River Rt. 9

At Forked River Rt. 9, June was the only month to have observed *N. bachei* densities in all three years (Figure 86). *N. bachei* presence was also observed in May and September of 2019, which corresponds to the late spring bloom and potential secondary bloom in September.

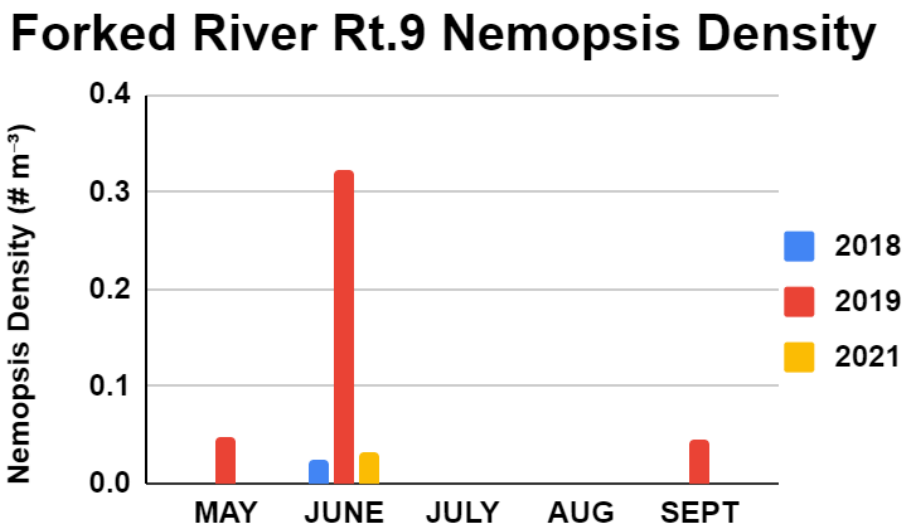

Figure 86. Plankton tow *Nemopsis bachei* densities from Forked River Rt. 9 for all years.

Forked River Lagoon

In June of 2019 at Forked River Lagoon, there was one observation made of *N. bachei*. No other recordings were noted (Figure 87).

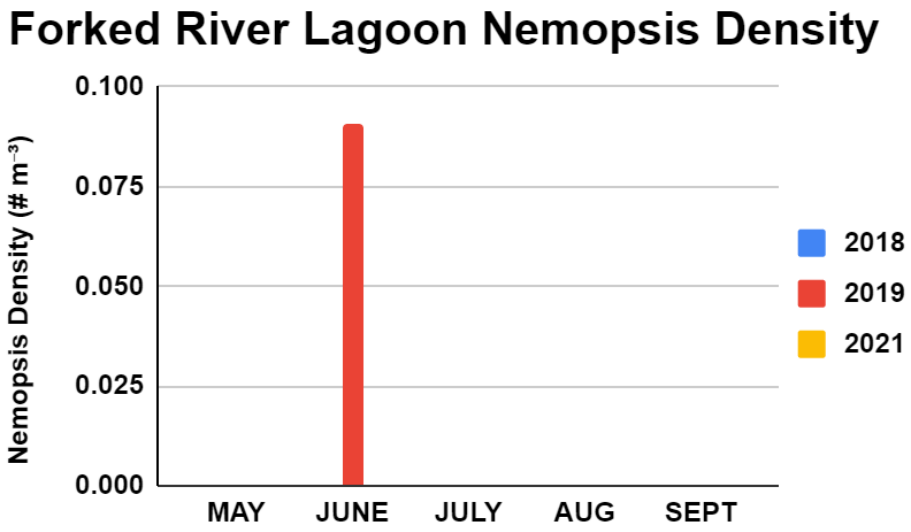

Figure 87. Plankton tow *Nemopsis bachei* densities from Forked River Lagoon for all years.

Oyster Creek Rt. 9

At Oyster Creek Rt. 9, there were two instances of recorded *N. bachei* densities in 2018 in the months of June and July, which compared to 2019 and 2021, had only seen one density recording (Figure 88). From these density recordings, the most abundant month that all three years can be seen in together is June, with 2021 having the highest *N. bachei* density. It is possible that the observation in July of 2018 reflect the operation of the plant and the water circulation.

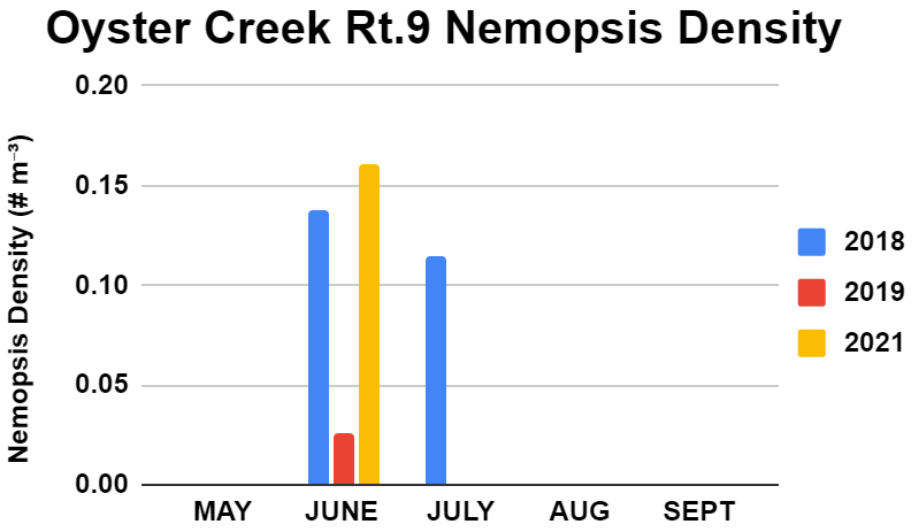

Figure 88. Plankton tow *Nemopsis bachei* densities from Oyster Creek Rt. 9 for all years.

Oyster Creek Mouth

The only observations of *N. bachei* made at Oyster Creek Mouth occurred in June of 2018, 2019 and 2021 (Figure 89), with the greatest density occurring in 2019. No other recorded densities were noted.

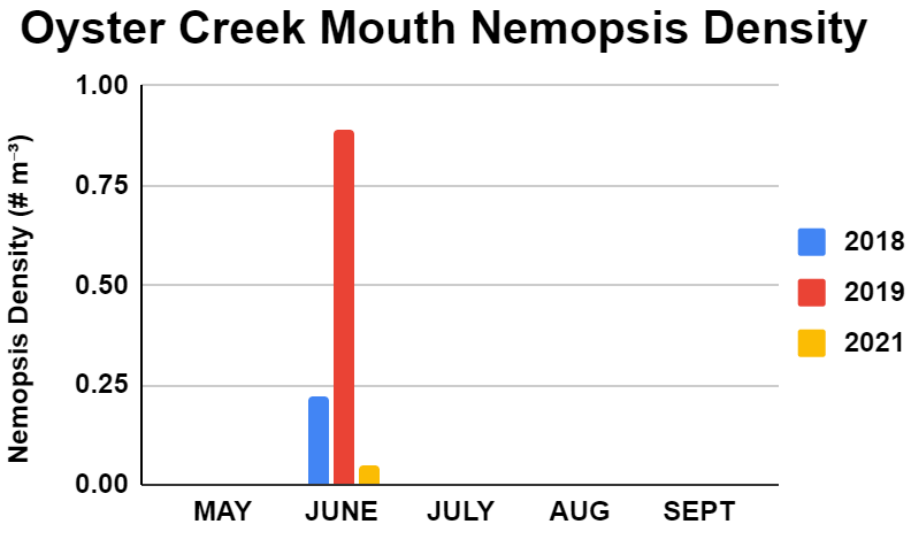

Figure 89. Plankton tow *Nemopsis bachei* densities from Oyster Creek Mouth for all years.

Double Creek East

2019 had the greatest densities for *N. bachei* in the months of June, July, and September at Double Creek East (Figure 90). Compared to 2018, the only density presence seen is in June. In 2021, there was no presence of *N. bachei*.

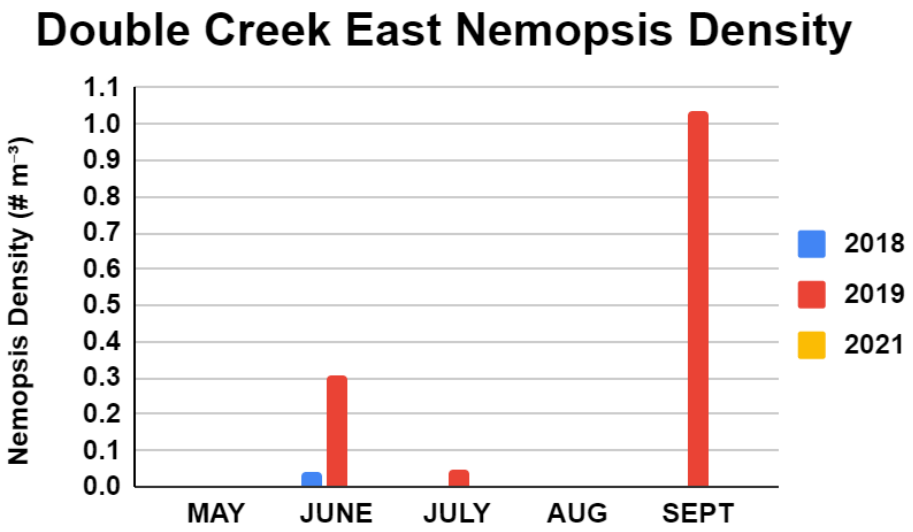

Figure 90. Plankton tow *Nemopsis bachei* densities from Double Creek East for all years.

Double Creek West

At Double Creek West, *N. bachei* were recorded from May to June throughout all three sampling years (Figure 91). In 2018, *N. bachei* were only found in June and July. In 2019, the largest density was observed in June and another recording in August. In 2021, densities were only observed in May and June.

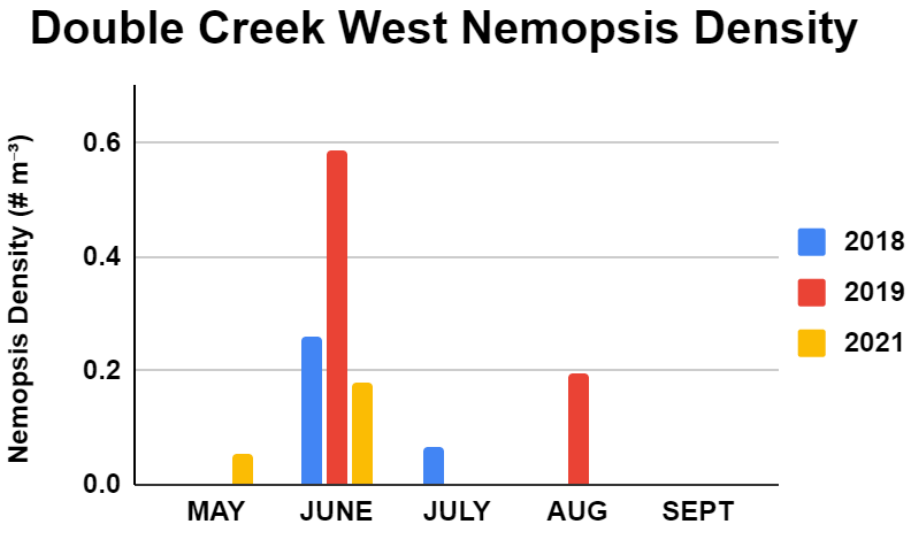

Figure 91. Plankton tow *Nemopsis bachei* densities from Double Creek West for all years.

Bayshore Lagoon

In June and July of 2018, there were recorded *N. bachei* densities at Bayshore Lagoon (Figure 92). No other observations were made in 2019 nor 2021.

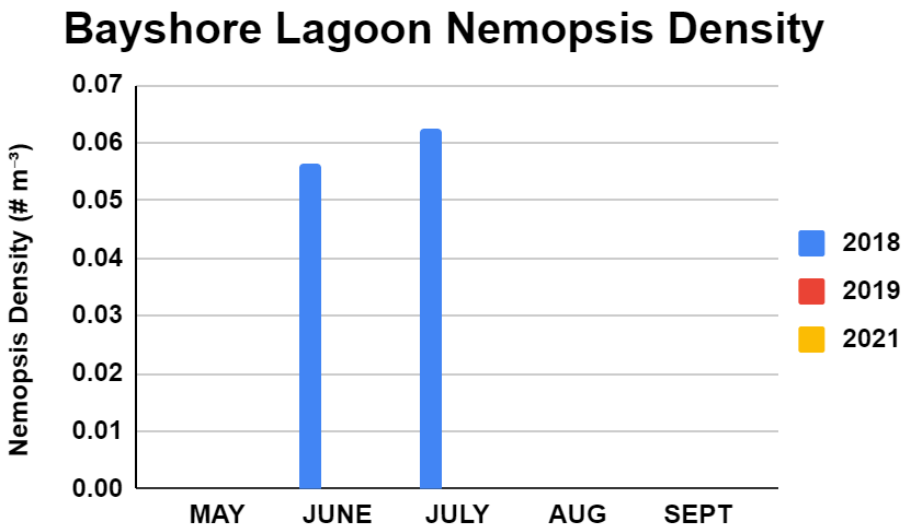

Figure 92. Plankton tow *Nemopsis bachei* densities from Bayshore Lagoon for all years.

Plankton tow Analyses of Major Non-Gelatinous Zooplankton Taxa

Calanoid Copepods

Results from plankton samples show that the taxa in highest abundance was the group Calanoid Copepods. Calanoid densities differed significantly among years, sites, and months of collection. In terms of differences, copepod densities increased significantly from 73.9m^{-3} in 2018 to 384.5m^{-3} in 2021 ($F_{2, 614}$ = 9.72, P < 0.0001). Densities differed significantly among sites ($F_{11,614}$ = 3.57, P < 0.0001) with densities in lagoons substantially lower than more open water sites. Differences among months of collection also differed significantly ($F_{10, 614}$ = 17.34, P < 0.0001) as copepod blooms occurred generally in May and June, with sharp declines in abundance during the rest of the summer.

Site Specific Patterns in Abundance

Toms River West

At Toms River West, copepods were seen in very small numbers in the months of May, July, and August in 2018, 2019, and 2021 (Figure 93). Throughout the specified years, Copepods were observed in much greater densities in the month of June, but were completely absent in September. The highest density recorded was in June 2019.

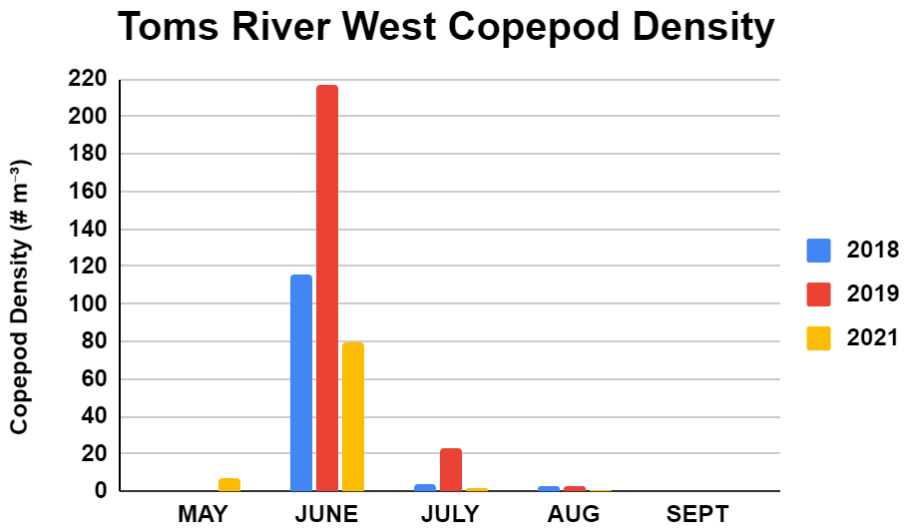

Figure 93. Plankton tow Copepod densities from Toms River West for all years.

Sunrise Beach

Copepods were only observed at Sunrise Beach in 2018 in the months of June and July (Figure 94). In 2019, copepods were recorded in all months except in August, with the peak abundance in June, while in 2021 peak density occurred in May.

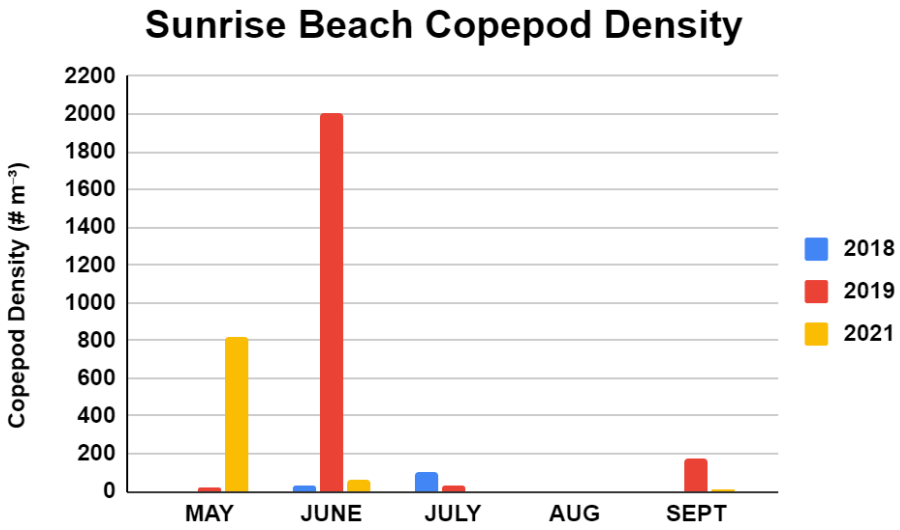

Figure 94. Plankton tow Copepod densities from Sunrise Beach for all years.

Sunrise Beach Lagoon

The greatest copepod density for Sunrise Beach Lagoon was observed in July of 2018 at approximately 83 individuals m^{-3} (Figure 95). A much lower density was recorded for the same year, but in June at approximately 7 individuals m^{-3}. In 2019, the copepod density observed in June was greater than 15 individuals m^{-3}. The following month of July exhibited numbers less than 5 individuals m^{-3}. The year 2021 had the lowest densities present in June, July, and August.

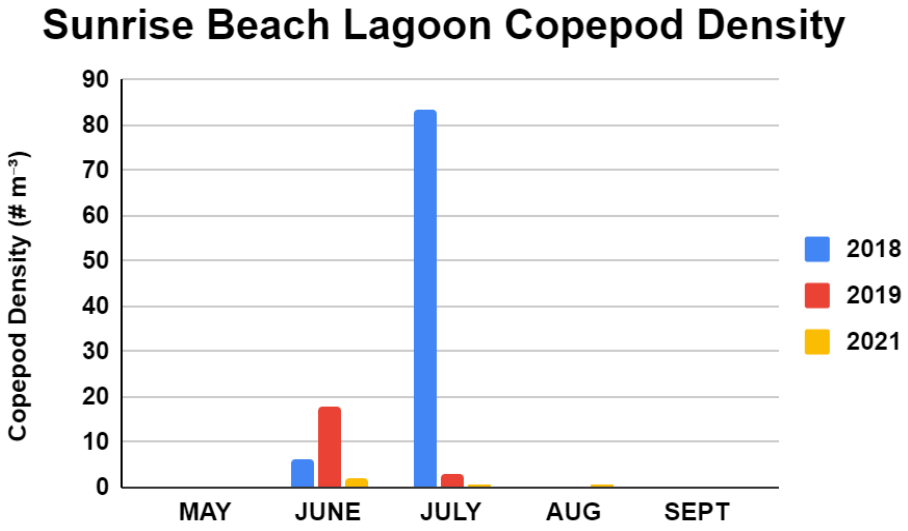

Figure 95. Plankton tow Copepod densities from Sunrise Beach Lagoon for all years.

Forked River East

In 2018 at Forked River East, copepods were seen in small numbers in June, and even smaller densities the following month (Figure 96). In 2019, copepods were also observed in small numbers from May through September, with the exception of August. The month of May contains the highest and only density of copepods recorded in 2021.

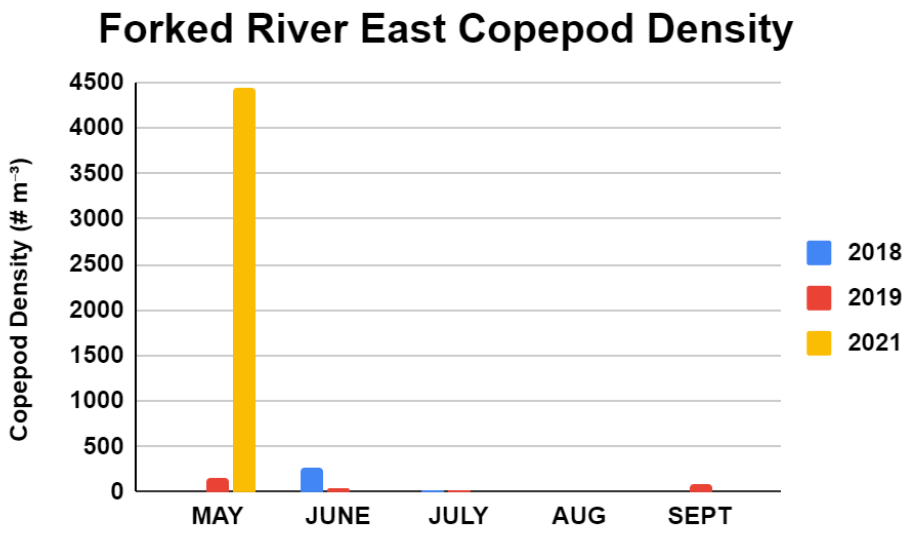

Figure 96. Plankton tow Copepod densities from Forked River East for all years.

Forked River West

At Forked River West, copepod densities varied between 2018, 2019, and 2021 (Figure 97). In 2018, the organisms were observed in relatively small numbers in June and August. In 2019, they had small densities in the months of May, June, July, and September. Copepods were then found in much greater numbers in May and June of 2021.

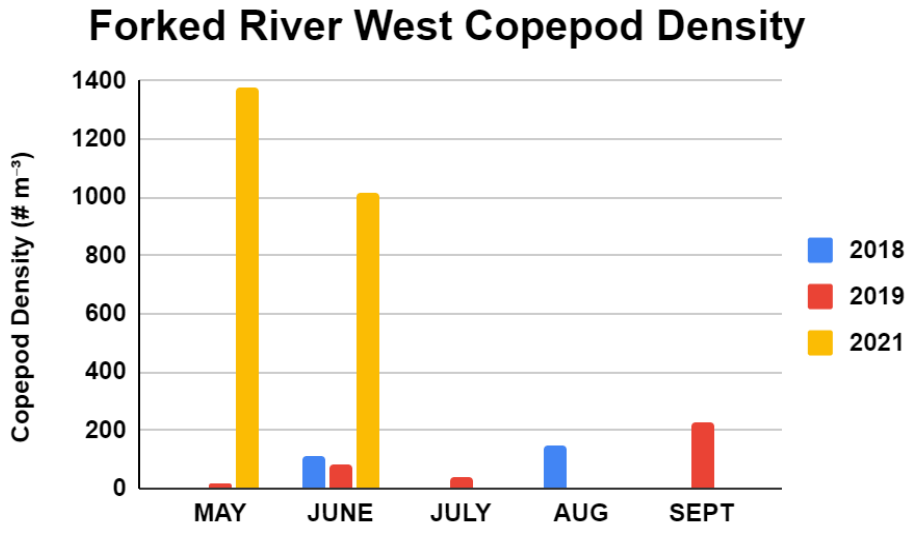

Figure 97. Plankton tow Copepod densities from Forked River West for all years.

Forked River Rt. 9

Forked River Rt. 9 exhibits a decline in copepod density over the course of the three years recorded (Figure 98). The greatest densities observed were in June, July, and August of 2018. The next year displayed a substantial increase in copepod density in the month of May, but was followed by much smaller numbers in the preceding month of June, July, August, and September. For 2021, the density continued to decrease, with smaller numbers being displayed from May to September.

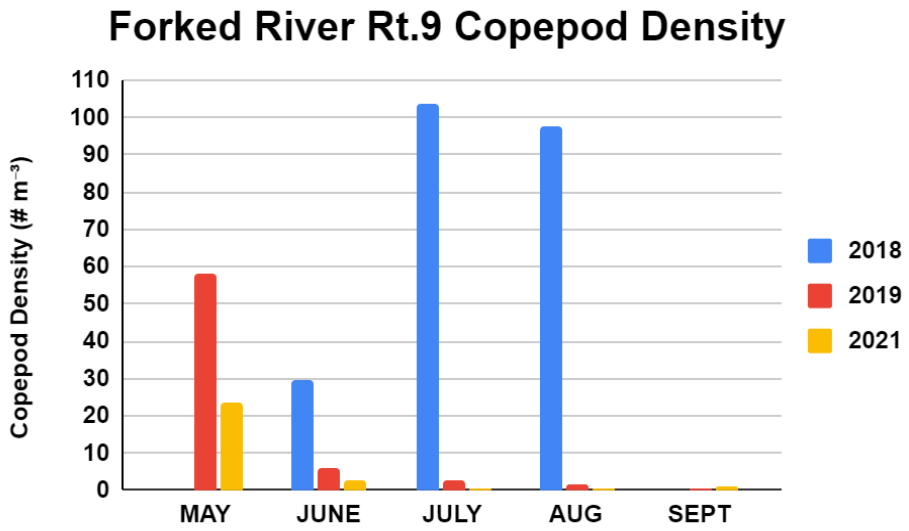

Figure 98. Plankton tow Copepod densities from Forked River Rt. 9 for all years.

Forked River Lagoon

At Forked River Lagoon, copepod densities were present in 2018 within the months of June, July, and August (Figure 99). In 2019, densities were observed additionally in May and September, however overall densities declined from the previous year with considerably lower peak densities. 2021 yielded early peak densities starting in May, however the following months experienced declines until August.

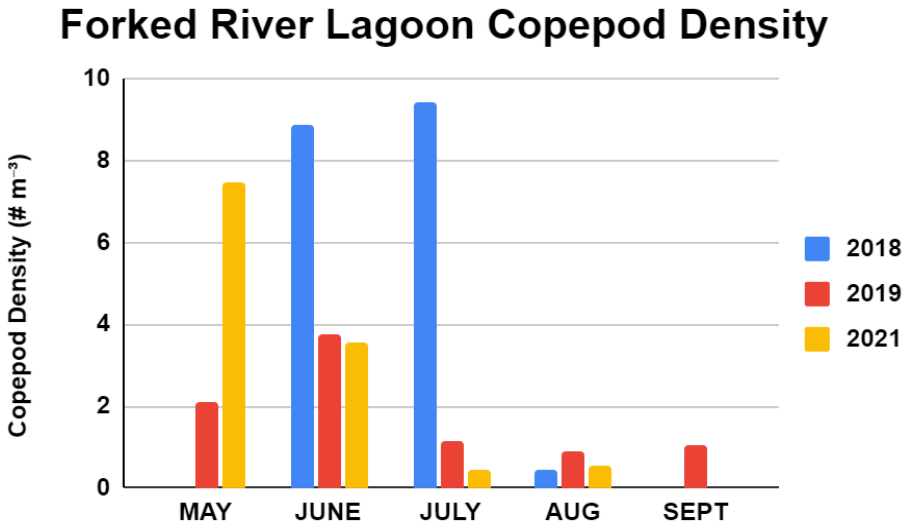

Figure 99. Plankton tow Copepod densities from Forked River Lagoon for all years.

Oyster Creek Rt. 9

The greatest copepod densities at Oyster Creek Rt. 9 were observed in July and August of 2018 (Figure 100). Overall density between 2019 and 2021 has declined as copepod numbers have steadily decreased from May to September.

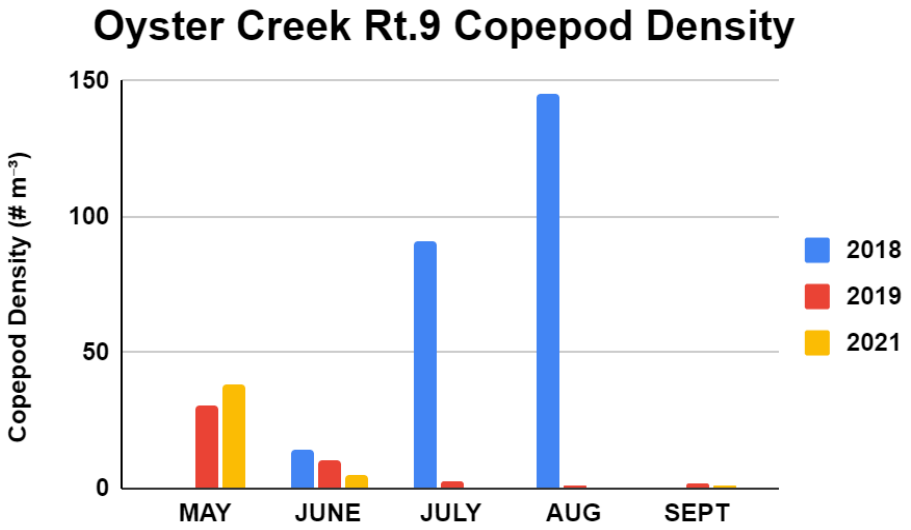

Figure 100. Plankton tow Copepod densities from Oyster Creek Rt. 9 for all years.

Oyster Creek Mouth

In May and June 2021 at Oyster Creek Mouth, copepod densities were significantly higher than in 2018 and 2019 (Figure 101). The lowest density recorded for 2021 is observed in September. In 2018, copepod densities varied, but maintained numbers below 200 individuals m^{-3}, with the highest density recorded appearing in August. In 2019, densities also varied and maintained numbers below 200 individuals m^{-3} with the highest being observed in the month of September.

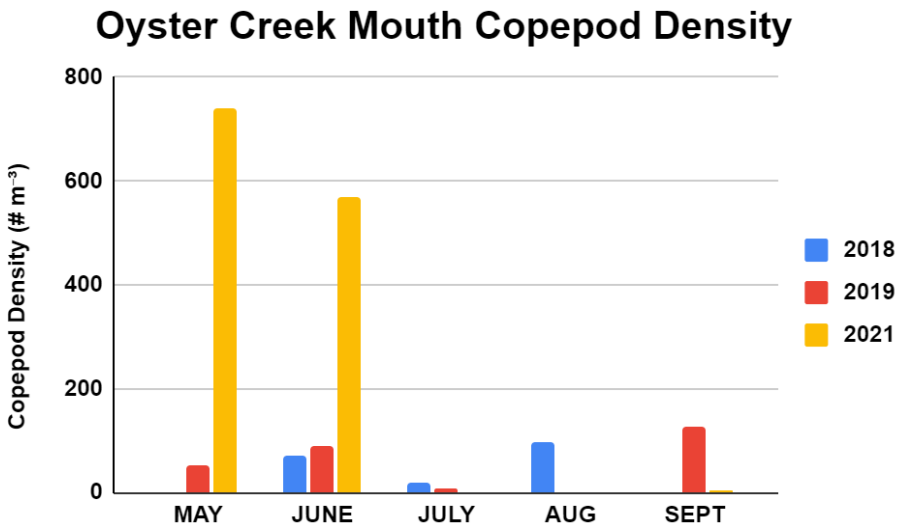

Figure 101. Plankton tow Copepod densities from Oyster Creek Mouth for all years.

Double Creek East

The largest copepod densities for Double Creek East were observed in May and June of 2021 (Figure 102). Significantly smaller densities were recorded in previous years. In 2018, copepod densities were only present in June and July and were less than 500 individuals m^{-3}. In 2019, copepod densities were observed in May, June, and September and were also less than 500 individuals m^{-3}. There were no copepods observed in the month of August for any of the three years.

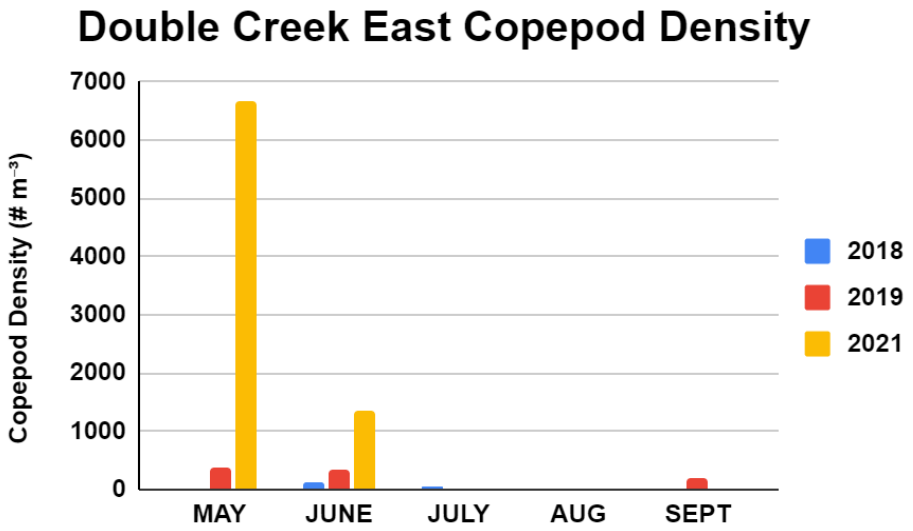

Figure 102. Plankton tow Copepod densities from Double Creek East for all years.

Double Creek West

In May and June 2021 at Double Creek West, copepod densities were significantly higher than in 2018 and 2019 (Figure 103). The lowest densities were observed in May, June, and September of 2019, with the smallest density appearing in May. In 2018, copepod densities were low and only observed in June and July.

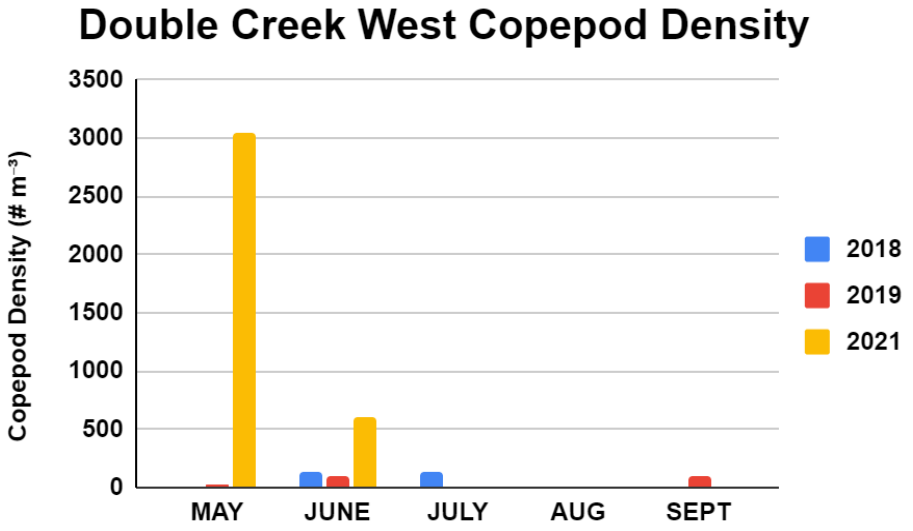

Figure 103. Plankton tow Copepod densities from Double Creek West for all years.

Bayshore Lagoon

Copepod densities were observed in June, July, and August for all three years at Bayshore Lagoon (Figure 104). July of 2018 yielded the highest density for the site between all years. There was no data recorded for the months of May and September from 2018-2021.

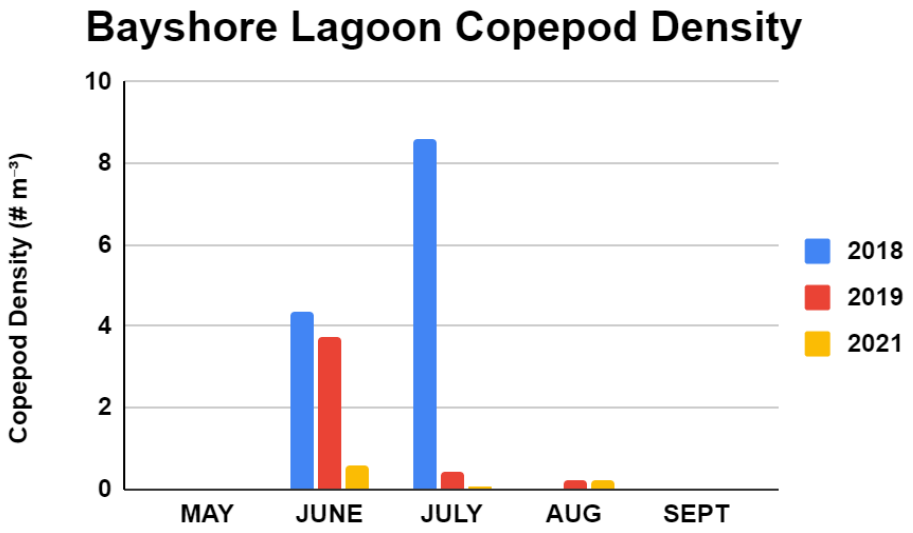

Figure 104. Plankton tow Copepod densities from Bayshore Lagoon for all years.

Fish Egg Trends

Critical resources which were known to have been impacted by the operation of OCNGS included fish, fish larvae, and fish eggs. In particular, the production of fish eggs and their entrainment and destruction in the cooling process of OCNGS operations was detrimental to populations. Analysis from our data indicate a significant increase in fish egg density from $1.37m^{-3}$ in 2018 to $5.44m^{-3}$ in 2019 and finally to $10.6m^{-3}$ in 2021 ($F_{2,614} = 4.15$, $P < 0.016$). Additionally, fish egg density differed significantly among months of collection ($F_{10,614} = 6.82$, $P < 0.0001$) and sites ($F_{11,614} = 2.96$, $P < 0.0008$), dominated by early season abundance of fish eggs in May and June, and very low densities observed in lagoon sites and sites around the OCNGS.

Site Specific Patterns in Abundance

Toms River West

Fish eggs were collected at Toms River West from May-August in all years with 2021 yielding the greatest densities in June with respect to other months (Figure 105). There were no recorded observations in September for any of the three years.

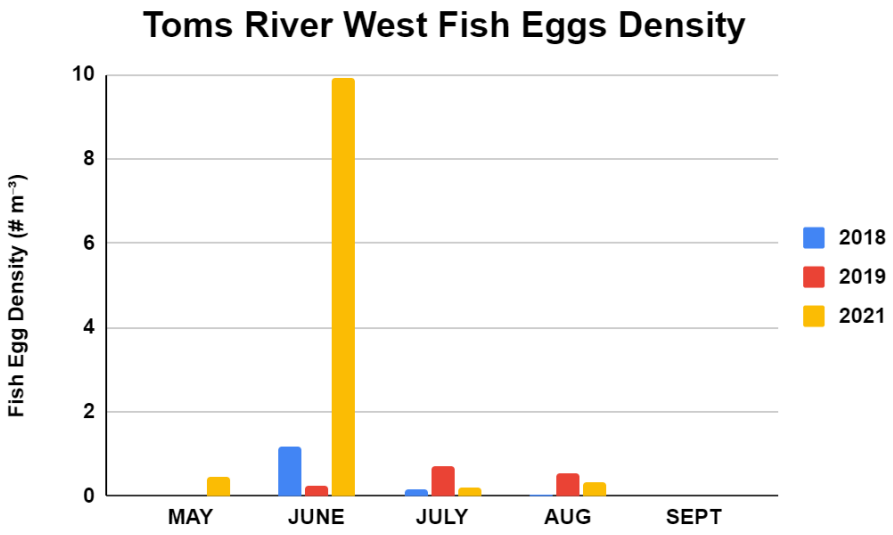

Figure 105. Plankton tow fish egg densities of various species from Toms River West for all years.

Sunrise Beach

At Sunrise Beach, few fish eggs were collected in 2018, but their abundance increased with each subsequent year, peaking in 2021 (Figure 106).

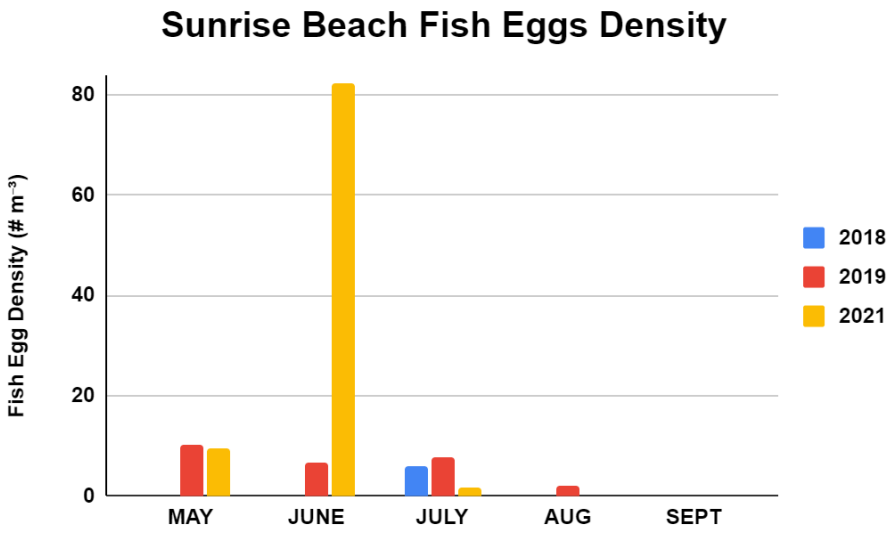

Figure 106. Plankton tow fish egg densities from Sunrise Beach for all years.

Sunrise Beach Lagoon

In both 2018 and 2019 at Sunrise Beach Lagoon, few fish eggs were recorded from samples and were almost absent from samples in 2021 (Figure 107). As this is a restricted lagoon system which is unlikely generating fish eggs and larvae, these low densities were expected.

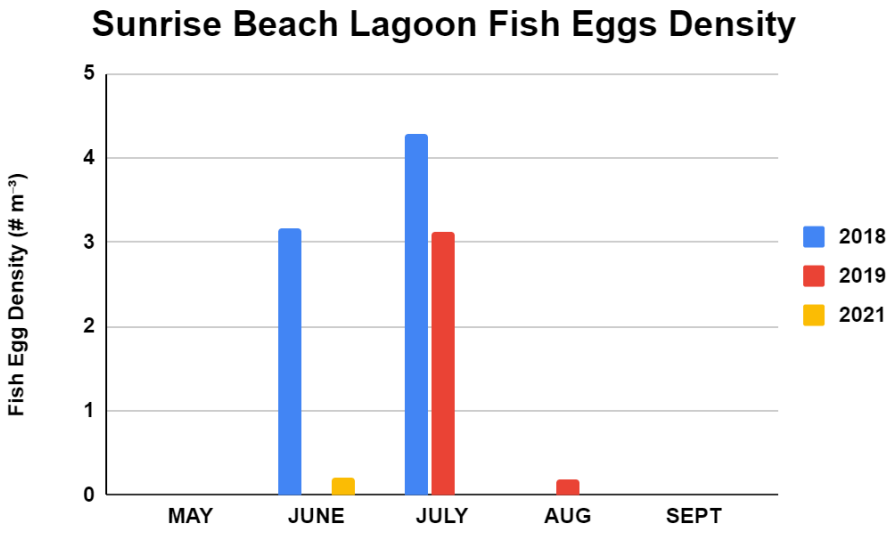

Figure 107. Plankton tow fish egg densities from Sunrise Beach Lagoon for all years.

Forked River East

Fish eggs were present throughout all three years at Forked River East (Figure 108). In 2018, July had the highest density of fish eggs and then substantially decreased throughout August and September. June 2019 had the highest recorded fish egg density for that year. In May 2021, fish egg density peaked at about 42 eggs per cubic meter and diminished throughout the remainder of the summer.

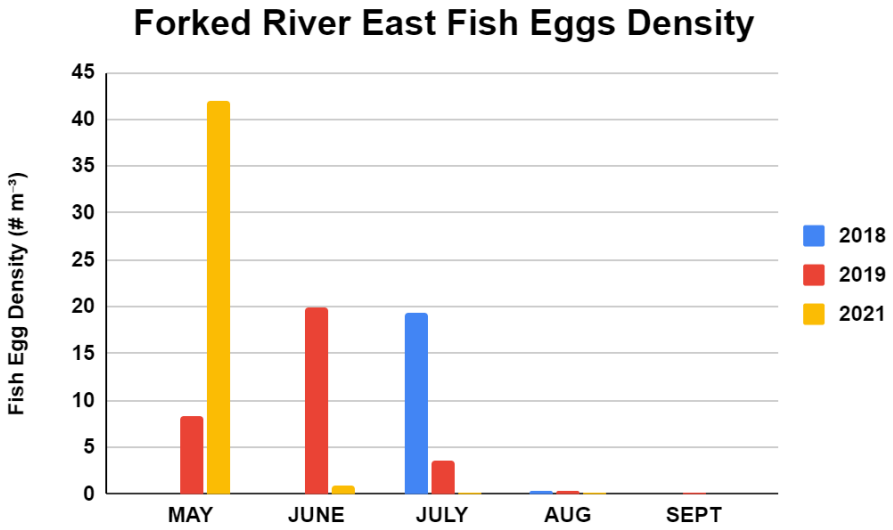

Figure 108. Plankton tow fish egg densities from Forked River East for all years.

Forked River West

At Forked River West, fish eggs were present all three years with the highest density being recorded in June of 2019 (Figure 109). Throughout 2018, 2019, and 2021, June samples had the greatest density of fish eggs, while densities dropped throughout July-September. The major increase in density from 2018 to subsequent sampling years clearly indicates that after the closure of the plant, fewer fish eggs were being entrained into the plant and the result was a rebound in fish egg densities at this site. As such, closure of the OCNGS resulted in a strong recovery of fish egg densities, pointing to the positive impact the closure has had on the bay.

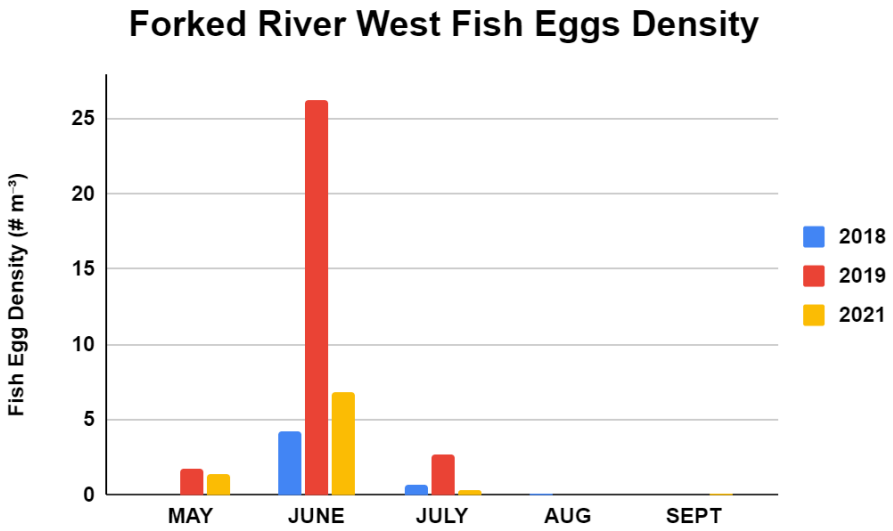

Figure 109. Plankton tow fish egg densities from Forked River West for all years.

Forked River Rt. 9

Fish eggs were present all three years at Forked River Rt. 9 in lower densities (Figure 110). In 2018, there were no observations made in May, but July was the peak month for fish egg density. May 2019 had the highest density at almost 16m^{-3}. That same year, density dramatically decreased in June. The same kind of trend was seen in 2021, with fish egg density peaking in May and dropping by June, although this year had a lower density to begin with.

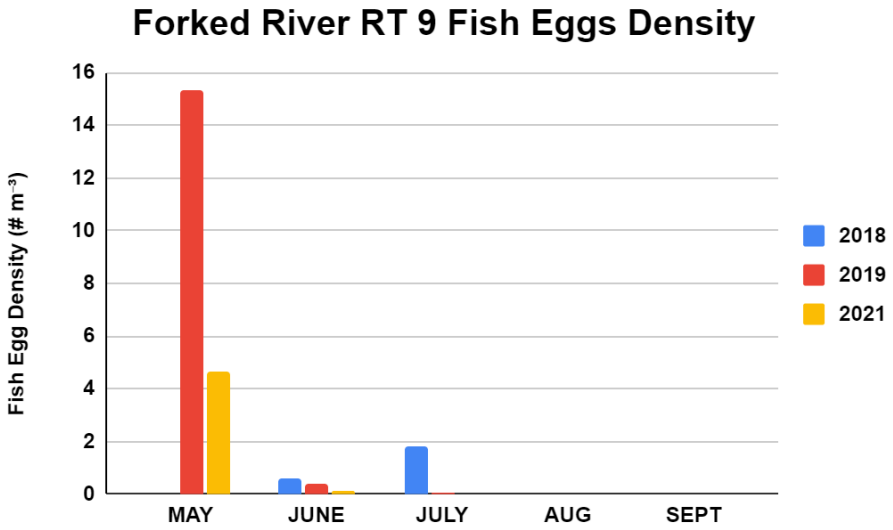

Figure 110. Plankton tow fish egg densities from Forked River Rt. 9 for all years.

Forked River Lagoon

The largest density of fish eggs recorded at Forked River Lagoon was in June of 2018, but this site had the lowest overall fish egg density (Figure 111). Fish eggs were not observed in 2019 at this site, but a few were recorded in May and June of 2021. As this is a dead-end lagoon with relatively elevated gelatinous zooplankton populations, it is likely that predation plays a critical role in reducing the abundance of fish eggs at this site.

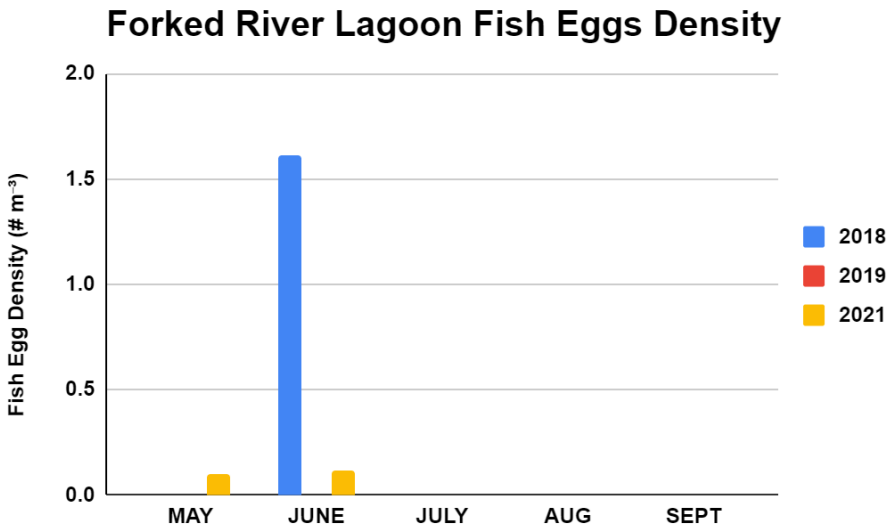

Figure 111. Plankton tow fish egg densities from Forked River Lagoon for all years.

Oyster Creek Rt. 9

Compared to other months, May 2019 and July 2018 had the most abundant fish egg densities recorded (Figure 112). Regardless of year, fish egg densities just outside the outflow of the plant were always low compared to other sites and likely reflect their destruction during operations in 2018 and the major hydrological changes occurring after the shutdown.

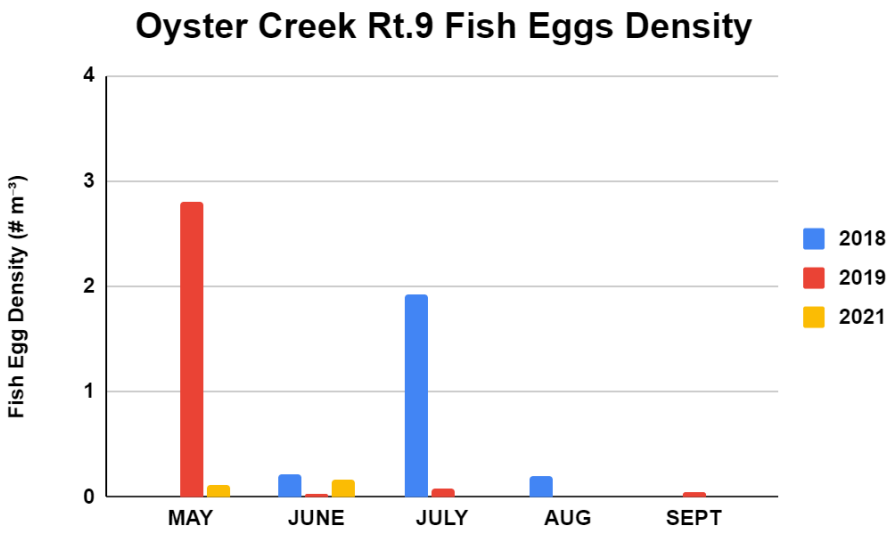

Figure 112. Plankton tow fish egg densities from Oyster Creek Rt. 9 for all years.

Oyster Creek Mouth

Oyster Creek Mouth had low densities of fish eggs in 2018, but substantial increases in density were recorded for 2019 and 2021 (Figure 113). In 2019, fish egg densities were high in June and July, while peak densities were observed in May and June of 2021.

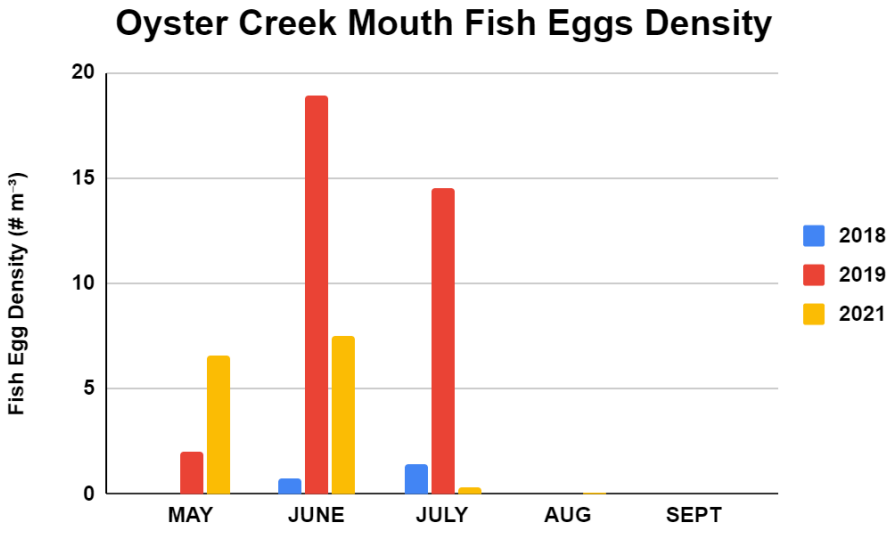

Figure 113. Plankton tow fish egg densities from Oyster Creek Mouth for all years.

Double Creek East

Double Creek East had a low presence of fish eggs throughout 2018 and 2019 (Figure 114). In May 2021, density rose exponentially from the previous years and then decreased greatly in June.

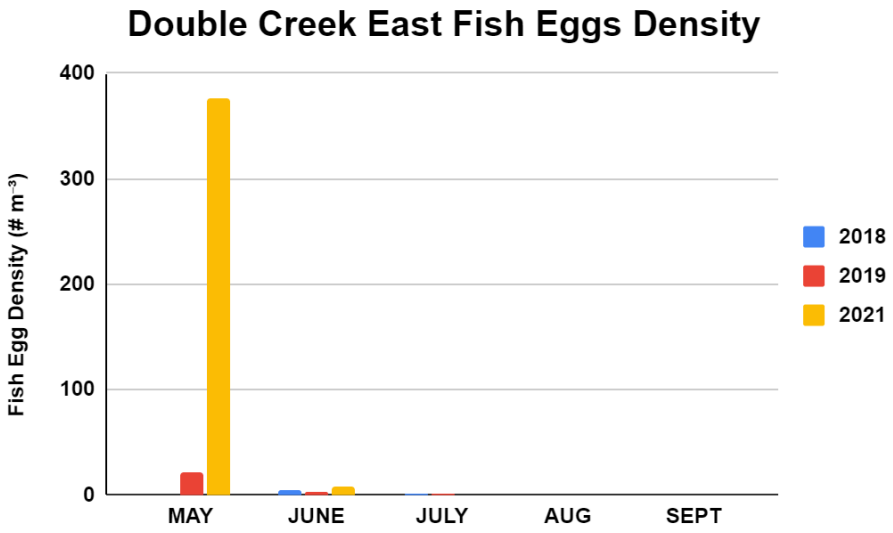

Figure 114. Plankton tow fish egg densities from Double Creek East for all years.

Double Creek West

Double Creek West had fish eggs present throughout all three years. Density was on the lower side (>5 individuals m^{-3}) in 2018, but rose substantially in 2019 and 2021 (Figure 115). June 2019 had the highest density of fish eggs recorded at this site and decreased by about half in July. In 2021, the highest density was seen in May, but fish eggs were still present throughout June and July.

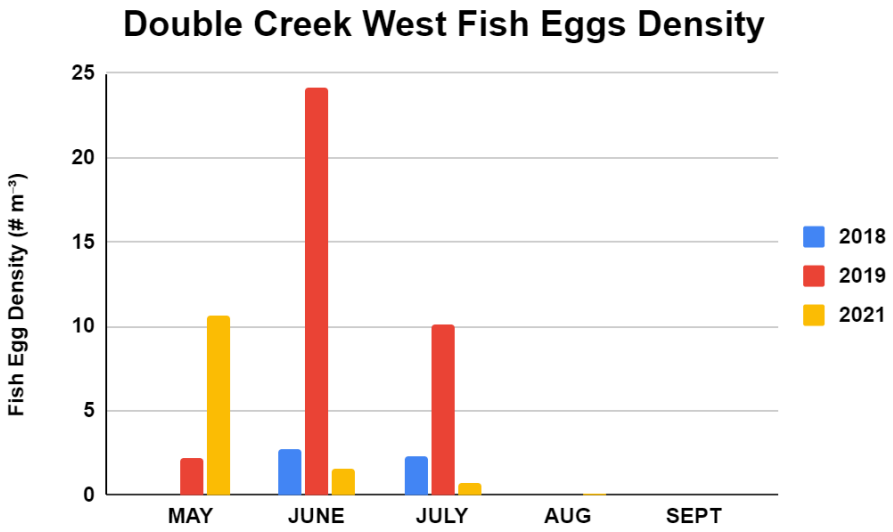

Figure 115. Plankton tow fish egg densities from Double Creek West for all years.

Bayshore Lagoon

All three years yielded observations of fish eggs in June at Bayshore Lagoon (Figure 116). Like the other lagoon communities, fish egg abundance was extremely low (<0.25m^{-3}) reflecting that these lagoon communities do not support early life history stages of fish.

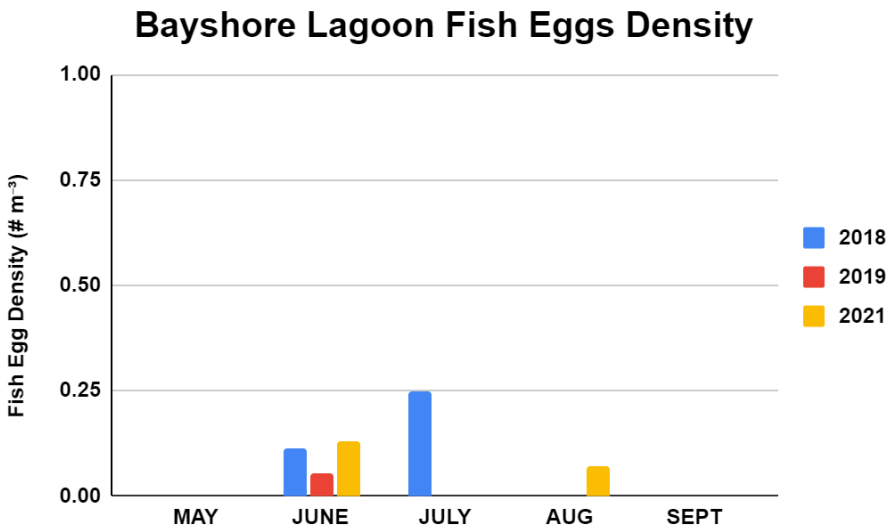

Figure 116. Plankton tow fish egg densities from Bayshore Lagoon for all years.

Atlantic silverside, *Menidia menidia*, Larval Trends

The Atlantic Silverside is an important forage fish species in Barnegat Bay, supporting the diet of commercially and recreationally important fin fish species. Compiled trends for *M. menidia* between the years 2018, 2019, and 2021 show varying trends among sites and months, however there is an obvious increase in average and maximum densities as the years progress starting from 2018, suggesting a successful recovery in Atlantic silverside populations after the shutdown of the OCNGS in 2018. Specifically, overall density increased significantly among years ($F_{2,614} = 13.14$, $P < 0.0001$) starting with an average density of $0.0054 m^{-3}$ in 2018, increasing to $0.029 m^{-3}$ in 2019, and finally increasing to an average of $0.51 m^{-3}$, an increase in density of two orders of magnitude! Additionally, there were significant differences in month of collection ($F_{10, 614} = 16.85$, $P < 0.0001$) and among sites ($F_{11,614} = 1.98$, $P < 0.03$). General growth patterns discerned from data showed that *M. menidia* spawned most frequently in late spring months such as May and June, where multiple sites have peak densities within these months, with declines in larval abundance throughout the summer reflecting their importance in supporting coastal food webs, as well as their ability as adults to avoid plankton nets.

Site Specific Patterns in Abundance

Toms River West

Observations of *Menidia menidia* at Toms River West occurred in all years during the month of June, with the highest density in 2021 (Figure 117). In July 2021, there were also observations of *M. menidia*.

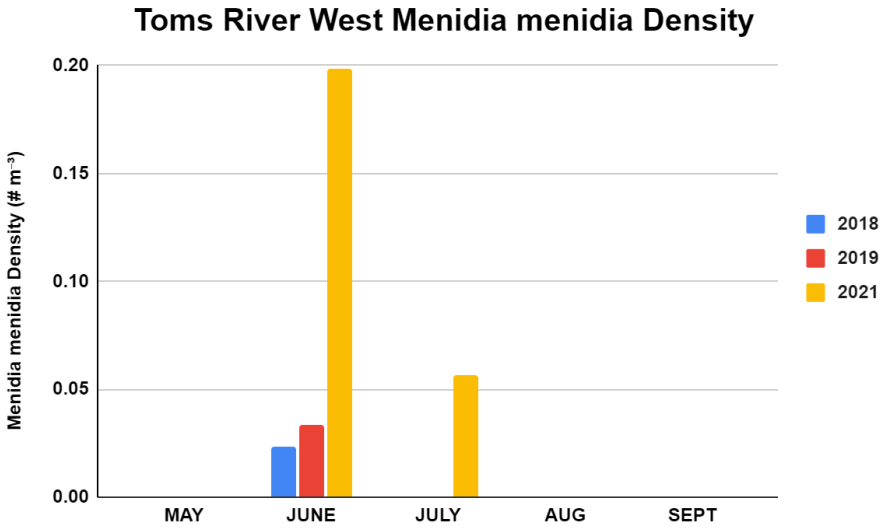

Figure 117. Plankton tow *Menidia menidia* densities from Toms River West for all years.

Sunrise Beach

Sunrise Beach yielded *M. menidia* observations in May and June of 2021 and June 2019 (Figure 118), but they did not occur in 2018. The peak in density in May of 2021 nicely documents the significant increases seen among all sites after the shutdown of the plant.

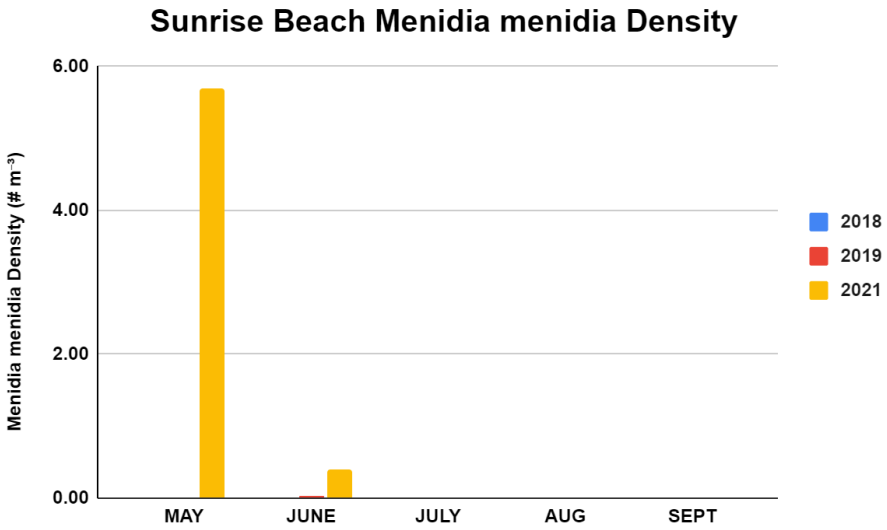

Figure 118. Plankton tow *Menidia menidia* densities from Sunrise Beach for all years.

Sunrise Beach Lagoon

At Sunrise Beach Lagoon, there were no observations made in 2018 for *M. menidia* (Figure 119). They were found only in August of 2019 and in 2021, they were only present in June.

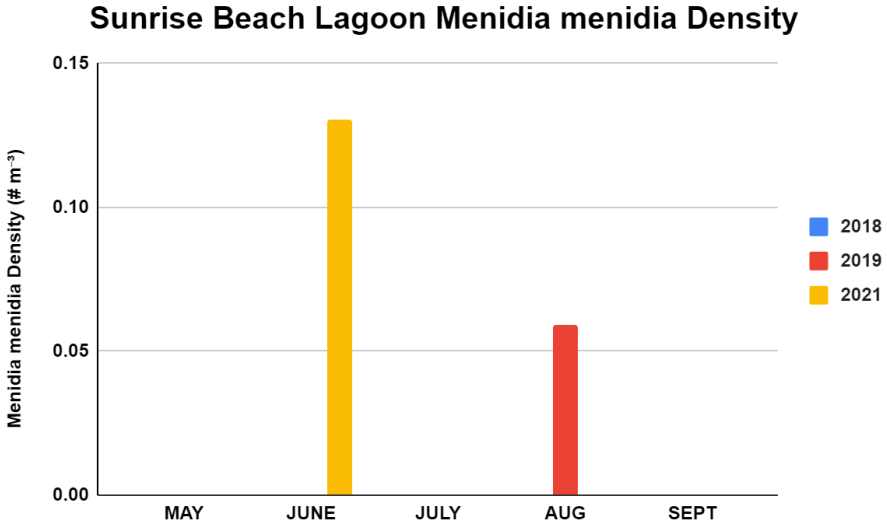

Figure 119. Plankton tow *Menidia menidia* densities from Sunrise Beach Lagoon for all years.

Forked River East

Forked River East also yielded *M. menidia* collections in May and June of 2021 (Figure 120), but their absence was noted in 2018 and 2019.

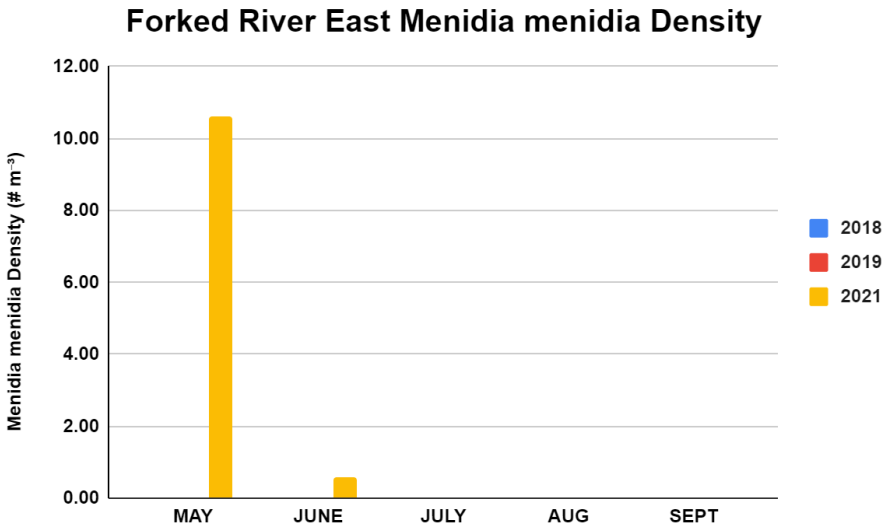

Figure 120. Plankton tow *Menidia menidia* densities from Forked River East for all years.

Forked River West

Forked River West displayed similar trends with Forked River East having *M. menidia* larvae in higher densities in May and June of 2021 (Figure 121), but absent in 2018. In June 2019, there was a small observation of *M. menidia*, possibly signaling the initial recovery of this species after the shutdown.

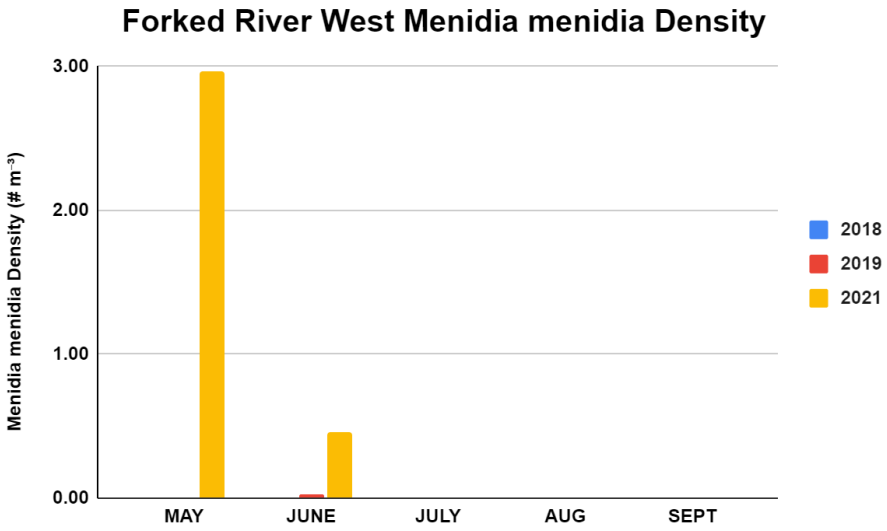

Figure 121. Plankton tow *Menidia menidia* densities from Forked River West for all years.

Forked River Rt. 9

Menidia menidia observations were made only in June and July of 2021 at Forked River Rt. 9 (Figure 122) and at extremely low densities. In the remaining months and years, there were no other collections.

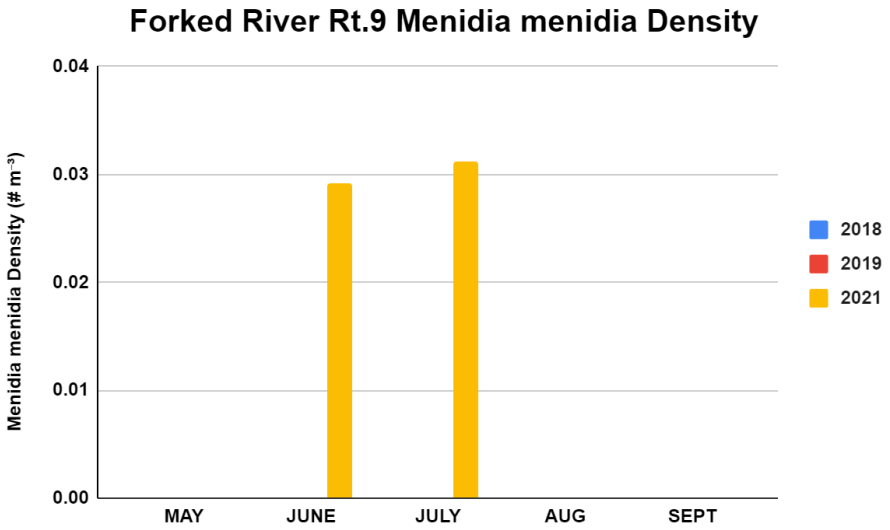

Figure 122. Plankton tow *Menidia menidia* densities from Forked River Rt. 9 for all years.

Forked River Lagoon

At Forked River Lagoon, *M. menidia* was not collected at this site in 2018, but was present at very low densities in 2019 and 2021 where peak abundance was recorded in June (Figure 123).

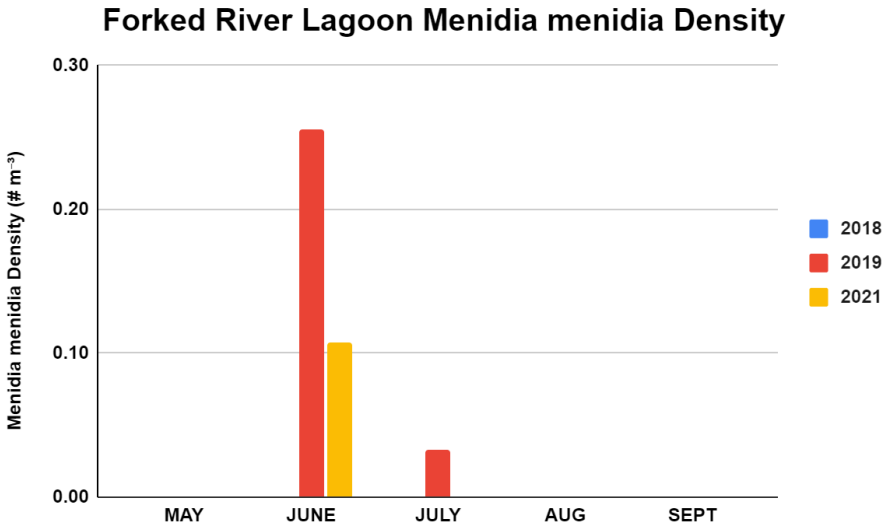

Figure 123. Plankton tow *Menidia menidia* densities from Forked River Lagoon for all years.

Oyster Creek Rt. 9

M. menidia observations were made each year in only one month, each different from other years, albeit at very low densities (Figure 124). In 2018, the only observation was made in June which consisted of the lowest observed density. The next year, 2019, the density was larger and occurred in September, but these were larger individuals who had grown toward adulthood. Lastly in 2021, the largest density recorded happened in May, reflecting the recovery and late spring spawning for this species.

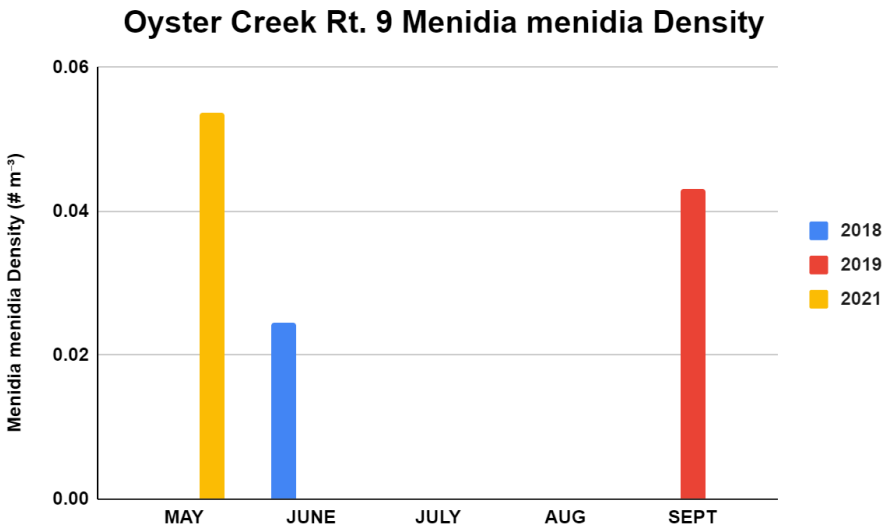

Figure 124. Plankton tow *Menidia menidia* densities from Oyster Creek Route 9 for all years.

Oyster Creek Mouth

The highest *M. menidia* density at Oyster Creek Mouth was recorded in May 2021, but decreased over the span of the sampling season (Figure 125). In 2019, *Menidia menidia* were found only in June. In 2018, silversides were observed in July and August, but these reflect the collection of a single adult *M. menidia* in plankton tows.

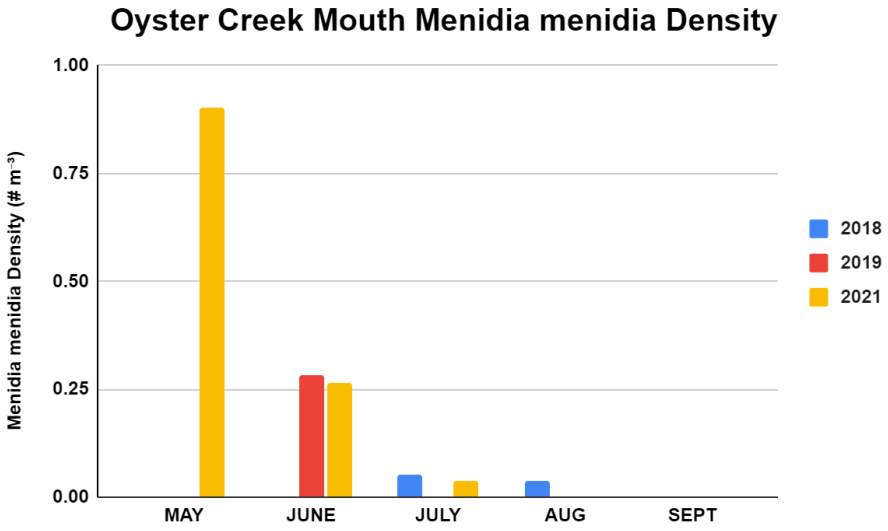

Figure 125. Plankton tow *Menidia menidia* densities from Oyster Creek Mouth for all years.

Double Creek East

M. menidia densities at Double Creek East were highest in May and June of 2021 (Figure 126). For 2018 and 2019, significantly lower densities were observed. Only in June and July were there small densities.

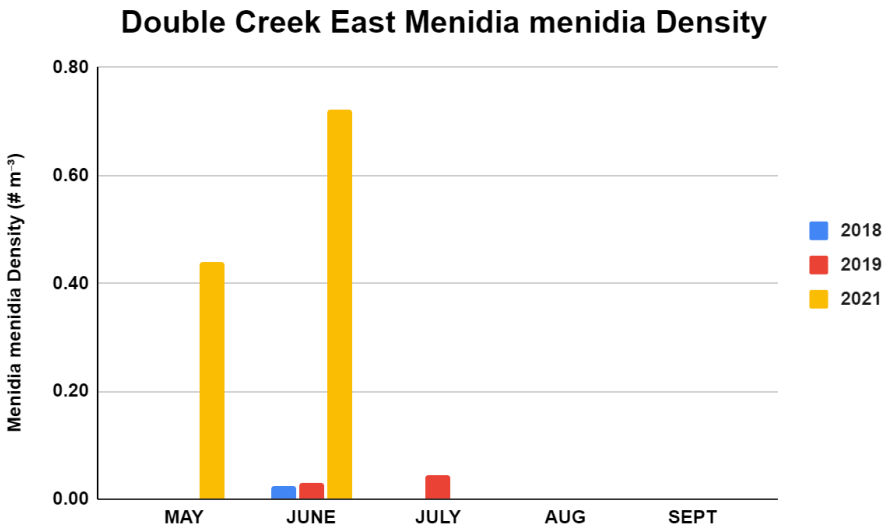

Figure 126. Plankton tow *Menidia menidia* densities from Double Creek East for all years.

Double Creek West

M. menidia was not observed in 2018 at Double Creek West (Figure 127). It was observed in June 2019 but at significantly low amounts. In 2021, May had the greatest density of Atlantic silversides and as the summer progressed, density decreased.

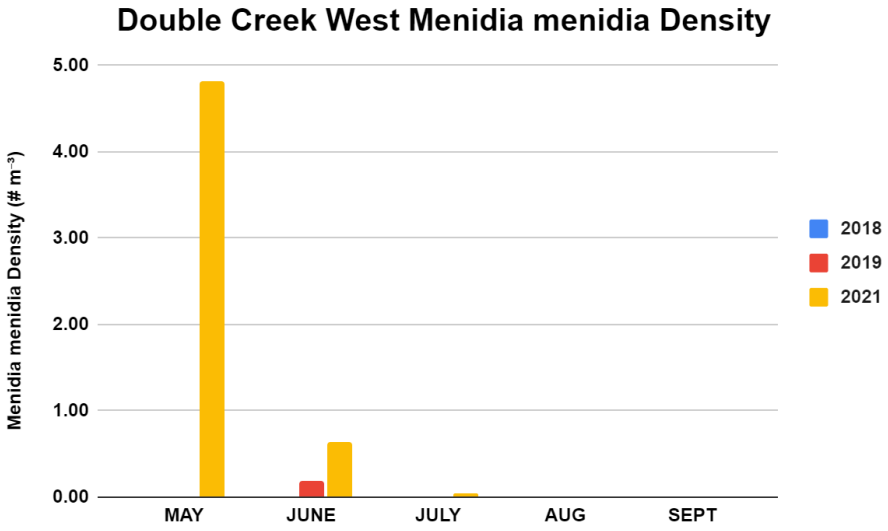

Figure 127. Plankton tow *Menidia menidia* densities from Double Creek West for all years.

Bayshore Lagoon

At Bayshore Lagoon, *M. menidia* was only observed in July 2019 (Figure 128). *M. menidia* was not found at Bayshore Lagoon for the remaining months of 2019, and was not seen through the entirety of 2018 and 2021.

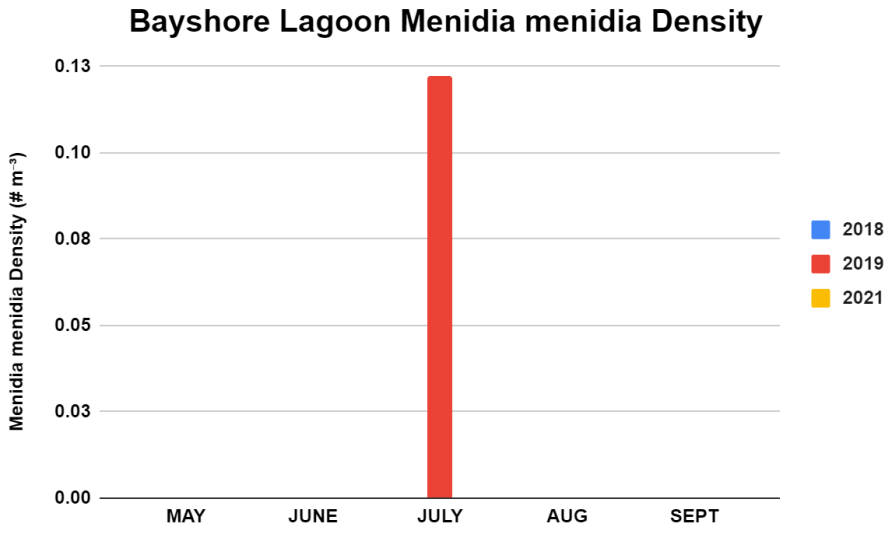

Figure 128. Plankton tow *Menidia menidia* densities from Bayshore Lagoon for all years.

Community Level Changes in the Zooplankton

After the closure of the OCNGS, changes in the abundance and density of organisms became apparent. This manifested itself in fundamental changes in a variety of community species compositional changes. Specifically, with regards to the average taxonomic richness observed among sites, certain opposing patterns could be seen (Figure 129). For some sites, taxa richness was not fundamentally impacted by the closure in 2018 and these sites include Toms River West and Forked River East, both of which were beyond the general impact zone of the plant. However, for many sites, taxa richness was greater in 2019 and 2021 compared to 2018, signaling an increase in the number of taxa identified from these areas after the shutdown. Only two sites, Forked River Rt. 9 and Oyster Creek Rt. 9, showed significant declines in taxa richness following the closing and is a direct result of the impacts the plant had on the zooplankton community. Prior to the shutdown, Forked River saw a major draw of water through this region to act as the primary cooling water for the plant. With the reduction in flow, fewer organisms were drawn into the river from the surrounding water bodies and taxa richness dropped. For Oyster Creek Rt. 9, the lack of flow would have disrupted the hydrodynamics of the river with more stagnation and reduced tidal fluxes leading to a reduction in taxa richness.

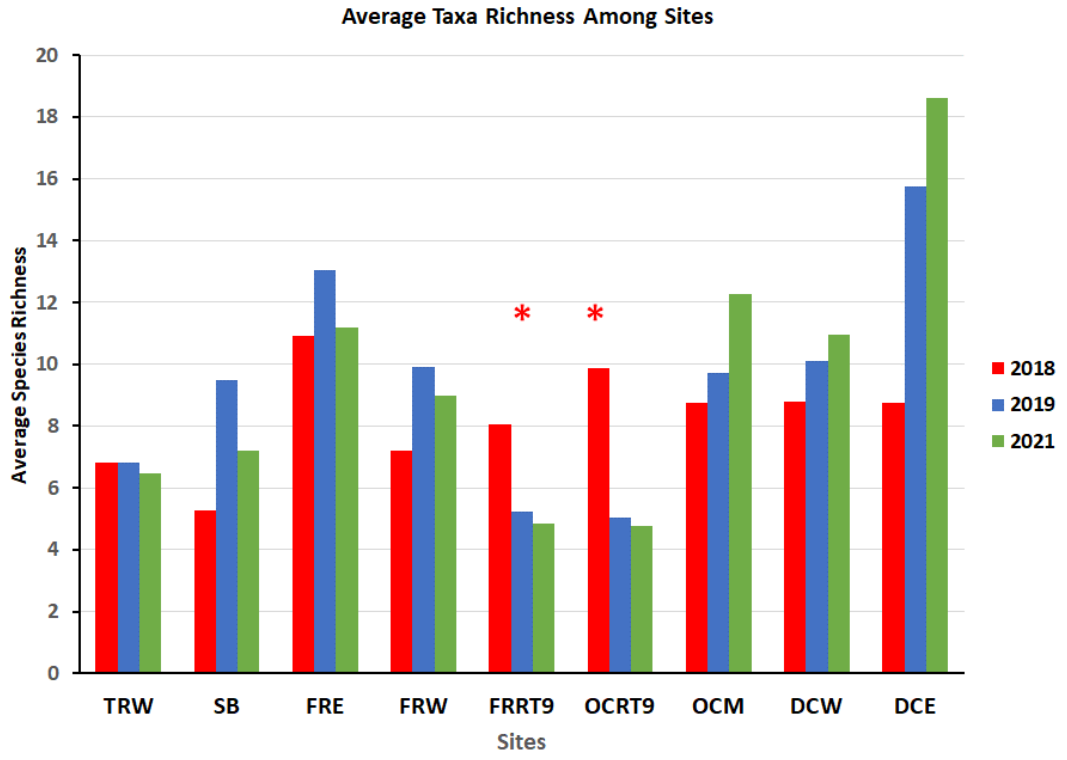

Figure 129. Average Taxonomic Richness among sites from 2018, 2019, and 2021 (* highlights significant declines in Taxa Richness among years).

Community structure was also evaluated using Primer® Software to evaluate how the overall zooplankton community changed due to the closure of the plant. To evaluate the impacts of the closure of OCNGS, a stratification of data was used to create comparable analyses among sites and years. To this end, only data collected from June through August was used, as samples in May 2018 did not occur as well as not all sites were sampled in September of all years. Additionally, since Toms River West was

substantially outside the impact region of the OCNGS, it was removed from these analyses to truly assess the community differences. A series of analyses was conducted to ascertain general dominance in community structure among years and sites. Specifically, a Similarity of Percentages Analysis (SIMPER) was conducted to assess the similarities and dissimilarities in community structure among years. Results showed that in 2018, site were characterized by four dominant groups including Calanoid copepods, Crab Larvae, Shrimp Larvae and the comb jelly *M. leidyi*. Numerically, these taxa constituted 95% of all organisms collected in plankton nets, with 44% relegated to copepods (Table 7), but the overall low Average Similarity of 20.02% suggests high variability among sites as well as temporal differences in the relative abundance of organisms. Similar results were observed in 2019 with an overall average similarity of 21.26%, but *M. leidyi* was replaced by Fish Eggs in the analysis, demonstrating the substantial increase in their abundance after the shutdown of OCNGS. Additionally, Copepod abundance increase by almost 150%, leading it to contribute to over 65% of all organisms identified in plankton tows and reflects the negative impact the plant had on copepod populations. Results from 2021 show some major differences, with only an 11.4% similarity among all sites, again dominated by a handful of abundant organisms (Table 7). The relatively low Average Similarity in 2021 reflects the dramatic changes in taxa richness among sites which occurred after the shutdown of OCNGS, which included significant declines in richness at FRRT 9 and OCRT9 sites, while OCM, DCW, and DCE all showed increases (Figure 129).

Table 7. SIMPER Analysis comparing dominant taxa defining general community structure among all sites for each of the three years of sampling.

2018					
Average similarity: 20.02					
Species	Av. Abund	Av. Sim	Sim/SD	Contrib%	Cum.%
Calanoid Copepod spp.	50.65	8.92	0.6	44.55	44.55
Crab Larvae (Brachyura)	10.57	7.51	0.6	37.52	82.07
Shrimp Larvae (Caridea)	4.98	1.37	0.34	6.83	88.9
Mnemiopsis leidyi	0.75	1.24	0.32	6.21	95.11
2019					
Average similarity: 21.26					
Species	Av.Abund	Av.Sim	Sim/SD	Contrib%	Cum.%
Calanoid Copepod spp.	123.01	13.85	0.81	65.14	65.14
Crab Larvae (Brachyura)	11.18	2.74	0.51	12.87	78.01
Fish Eggs	5.81	1.65	0.31	7.78	85.79
Shrimp Larvae (Caridea)	7.54	1.32	0.61	6.22	92.01
2021					
Average similarity: 11.40					
Species	Av.Abund	Av.Sim	Sim/SD	Contrib%	Cum.%
Calanoid Copepod spp.	410.62	4	0.39	35.1	35.1
Mnemiopsis leidyi	2.63	3.37	0.38	29.53	64.63
Crab Larvae (Brachyura)	20.06	1.79	0.33	15.67	80.3
Shrimp Larvae (Caridea)	4.61	0.7	0.34	6.13	86.43
Fish Eggs	11.33	0.26	0.14	2.32	88.75
Caprellidae	1.09	0.21	0.13	1.8	90.56

When a Two-Way Analysis of Similarity (ANOSIM) was conducted on the community level data, significant differences among years occurred (Global R = 0.168, P < 0.001) and all comparisons among years showed significant differences (2018 vs. 2019, R=0.184 P < 0.001; 2018 vs. 2021, R=0.113 P < 0.001; 2019 vs. 2021, R=0.19, P < 0.001). This corresponds to the significant increases in the density of several organisms including Calanoid Copepods, Fish Eggs, and Crab Larvae (Table 8) leading to the major differences among years. When individual sites were evaluated, most sites showed significant differences in their community composition when compared to the other sites (Table 8). Only 8 site comparisons showed no significant differences in community structure and these generally included sites that were adjacent to each other (e.g., DCW, OCM) and the similarity in water masses is a determining factor in the distribution of planktonic organisms. The only three exceptions to this involved DCW, which showed no difference with FRW, SB, and FRE. Among all the sites which did not differ significantly, four western sites along the bay including SB, FRW, OCM, and DCW are linearly adjacent to each other. However, the significant differences among the sites is likely the result of the changes which occurred after the closure of OCNGS.

Table 8. Results of a Two-Way Analysis of Similarity (ANOSIM) on plankton community structure evaluating the differences in zooplankton communities between sites. Non-significant differences between sampling sites are in bold.

Pairwise Tests Groups	R Statistic	Significance
DCE, DCW	0.11	0.002
DCE, FRE	0.115	0.001
DCE, FRL	0.503	0.001
DCE, FRRT9	0.365	0.001
DCE, FRW	0.105	0.004
DCE, OCM	0.103	0.003
DCE, OCRT9	0.386	0.001
DCE, SB	0.14	0.001
DCW, FRE	**0.019**	**0.149**
DCW, FRL	0.348	0.001
DCW, FRRT9	0.219	0.001
DCW, FRW	**-0.015**	**0.71**
DCW, OCM	**0.001**	**0.413**
DCW, OCRT9	0.235	0.001
DCW, SB	**0.023**	**0.133**
FRE, FRL	0.38	0.001
FRE, FRRT9	0.237	0.001
FRE, FRW	**-0.001**	**0.471**
FRE, OCM	0.053	0.02
FRE, OCRT9	0.253	0.001
FRE, SB	0.092	0.003
FRL, FRRT9	0.121	0.001
FRL, FRW	0.296	0.001
FRL, OCM	0.366	0.001
FRL, OCRT9	0.164	0.001
FRL, SB	0.319	0.001
FRRT9, FRW	0.186	0.001

FRRT9, OCM	0.2	0.001
FRRT9, OCRT9	**-0.008**	**0.599**
FRRT9, SB	0.168	0.001
FRW, OCM	**0.01**	**0.277**
FRW, OCRT9	0.2	0.001
FRW, SB	**0.017**	**0.182**
OCM, OCRT9	0.201	0.001
OCM, SB	0.041	0.041
OCRT9, SB	0.178	0.001

To evaluate whether sites showed significant changes in their community structure following the closure of OCNGS, an ANOSIM was conducted to assess individual sites and years to assess community changes. For most sites, significant differences between year comparisons were observed (Table 9). However, many sites did not show significant difference after the closure of the plant. Specifically, DCW showed no significant differences among years. It is possible that its location is remote enough that it was not being significantly impacted by the plants' operation. However, this could not explain the non-significance observed for FRW, which was in the uptake influence of the plant. It is possible that the increased flow in that general region would have resulted in greater diversity of organism moving through the region, but not being directly killed or impacted by the plant. Taxa richness did increase in 2019 and 2021, but perhaps not substantial enough to cause a shift in overall community structure. Similarly, both SB and TRW did not show significant changes, but they too could have been outside the major influence of OCNGS. A complete evaluation of all sites and year comparisons can be found in Appendix C.

Table 9. Results of an Analysis of Similarity (ANOSIM) on plankton community structure evaluating the operational period of the OCNGS (2018) and post-closure sampling. Results are presented for specific sites pre- and post-closure. Non-significant differences between sampling years are in bold.

Site-Year	Site-Year Comparison	R Statistic	Significance (P-value)
DCE 2018	DCE 2019	0.108	0.036
DCE 2018	DCE 2021	0.261	0.001
DCE 2019	DCE 2021	0.208	0.005
DCW 2018	**DCW 2019**	0.08	**0.083**
DCW 2018	**DCW 2021**	0.05	**0.142**
DCW 2019	DCW 2021	0.301	0.002
FRE 2018	FRE 2019	0.119	0.015
FRE 2018	FRE 2021	0.321	0.001
FRE 2019	FRE 2021	0.363	0.001
FRL 2018	FRL 2019	0.121	0.019
FRL 2018	FRL 2021	0.177	0.008
FRL 2019	FRL 2021	0.208	0.003
FRRT9 2018	FRRT9 2019	0.379	0.001
FRRT9 2018	FRRT9 2021	0.306	0.001
FRRT9 2019	FRRT9 2021	0.17	0.009
FRW 2018	**FRW 2019**	0.075	**0.093**
FRW 2018	**FRW 2021**	0.08	**0.062**

FRW 2019	FRW 2021	0.311	0.002
OCM 2018	**OCM 2019**	0.088	**0.054**
OCM 2018	OCM 2021	0.144	0.013
OCM 2019	OCM 2021	0.23	0.005
OCRT9 2018	OCRT9 2019	0.299	0.001
OCRT9 2018	OCRT9 2021	0.375	0.001
OCRT9 2019	**OCRT9 2021**	0.079	**0.073**
SB 2018	**SB 2019**	0.08	**0.083**
SB 2018	**SB 2021**	-0.019	**0.522**
SB 2019	SB 2021	0.084	0.047
TRW 2018	**TRW 2019**	-0.003	**0.397**
TRW 2018	**TRW 2021**	0.055	**0.132**
TRW 2019	TRW 2021	0.148	0.024

Subsequent to the community analyses, a Principal Component Analysis (PCA) was conducted on the complete zooplankton community (Figure 130) and stratified to include on the gelatinous zooplankton species (Figures 131, 132). Results from the community analysis among years indicated several key taxa driving the distribution of data in the PCA. Specifically, taxa defining differences among years included Calanoid Copepods, Shrimp Larvae, Crab Larvae, Fish Eggs and Salps. These taxa correspond to critical taxa observed in the SIMPER analyses (Table 7) as well as the significant increases in abundance for several of these taxa following the shutdown of OCNGS driving the community differences observed (Figure 130).

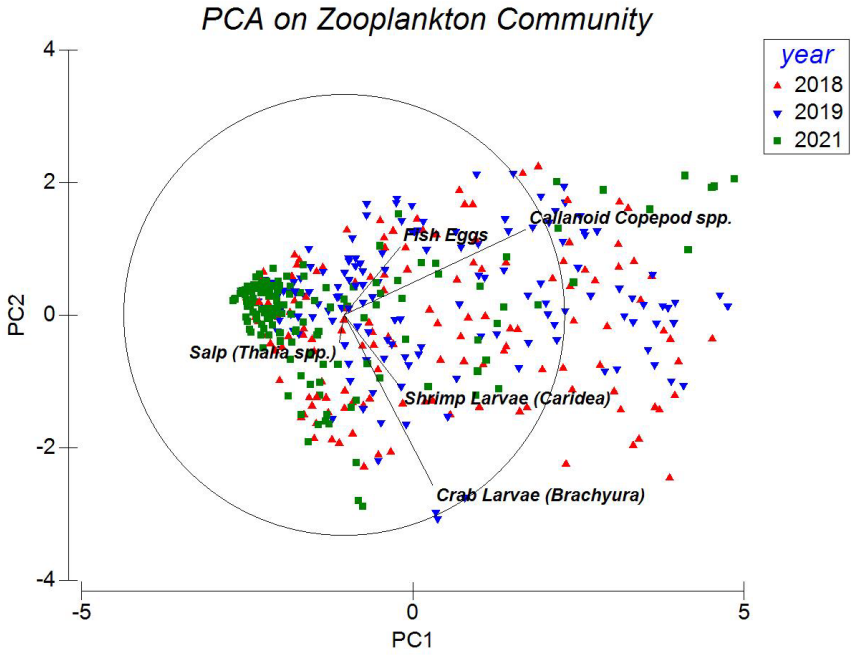

Figure 130. Principal Component Analysis of Zooplankton species identified among all 3 years with the primary taxa loading on PCA 1 and 2.

When only the gelatinous zooplankton taxa were considered, *M. leidyi*, *C. chesapeakei* adults, *C. chesapeakei* ephyrae, and *N. bachei* were the taxa that showed discrimination among the two primary Principal Components (Figure 131). Loading for *C. chesapeakei* adults and ephyrae on PC2 pushed samples from 2021 in a positive direction relating to their increases following the shutdown of OCNGS, but also reflect the high abundances from FRL and FRRT9 observed in 2018. Loading for *M. leidyi* was positive for PC1, which shaped the general pattern of the analysis, given its prominence as a dominant species. These same taxa were critical in discriminating the communities among the months of collection, with early season blooms of *N. bachei* and *M. leidyi* driving strong discrimination among months by loading negatively on PC2, and then their declines and the rise of *C. chesapeakei* in July and into August (Figure 132).

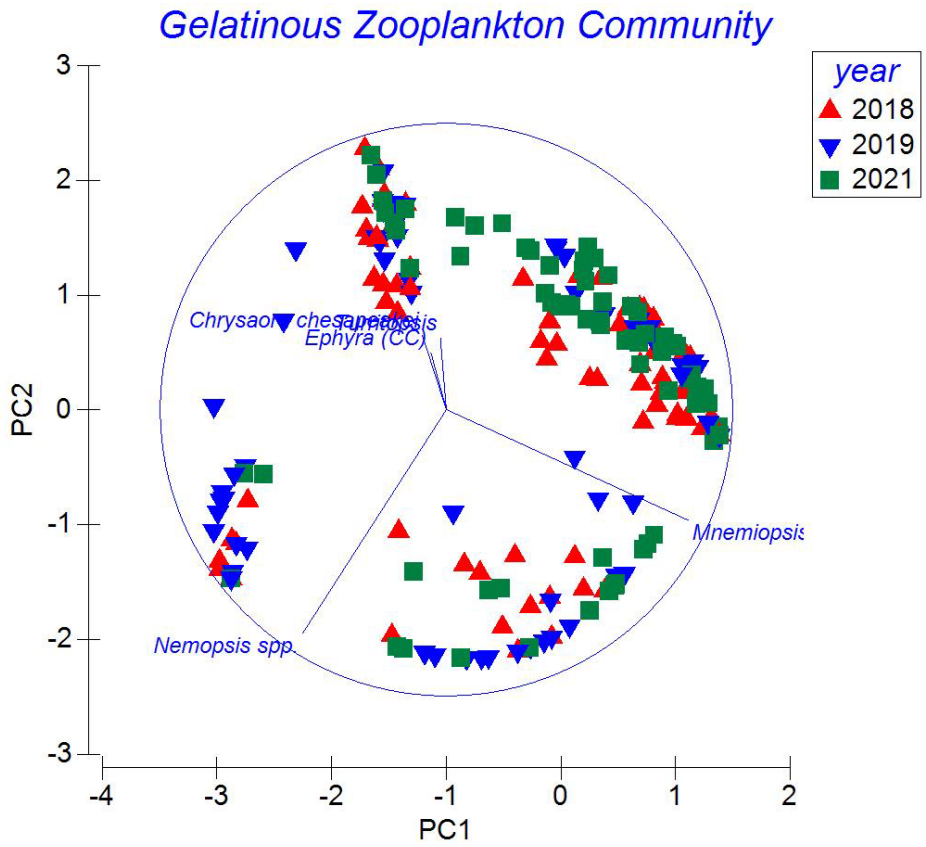

Figure 131. Principal Component Analysis of Gelatinous Zooplankton species identified among all 3 years with the primary taxa loading on PCA 1 and 2.

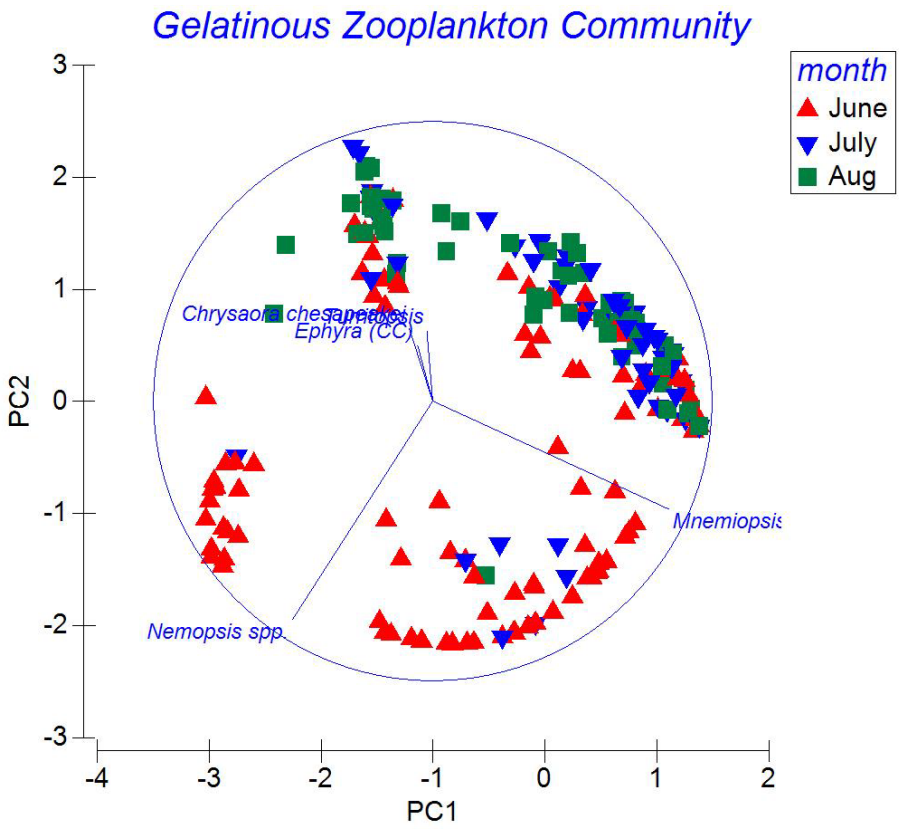

Figure 132. Principal Component Analysis of Gelatinous zooplankton species identified among all 3 years plotted by month of collection.

Metagenomic Analyses among Years

Samples from 2021 contained anywhere from ~700 reads to ~800,000 reads. Over six thousand ASVs were identified across all samples. Of these 1365 were assigned to Metazoa. Samples from the combined dataset (consisting of both the 2018, 2019, and 2021 samples) contained anywhere from ~700 reads to ~4,100,000 reads. Over twenty-five thousand ASVs were identified across all samples. Of these 5012 were assigned to Metazoa.

Statistically significant differences in species diversity as identified by Enspie are given below for analyses with and without Toms River using the combined 2018, 2019 and 2021 samples (Table 10). "All groups" refers to a comparison between all members of a category and pairwise means between two categories: X=No statistical significance; q-value= p-value with a Benjamini & Hochberg correction (Benjamini & Hochberg 1995). Results from these analyses demonstrate that community structure differed significantly among years and among the designated categorical groupings. These results were expected to some degree because data from 2018 incorporate the negative impacts of the OCNGS on faunal community structure. After the closure of the plant, these significant differences among the categorical groupings show the major impact the plant had on the biological community. If we contrast that with the results from the analysis conducted using only data from 2021, we actually see very few differences among all those categorical comparisons (Table 5).

Table 10. Significant differences among categorical analyses for combined analyses of 2018, 2019, and 2021 Samples from NEXGEN Sequencing. "All samples and Years" refers to the grouping of data into categories regardless of collection year. "by year" compares each category by year.

	Toms River Included				**Toms River Excluded**		
CATEGORY		**Enspie (Kruskal-Wallis)**				**Enspie (Kruskal-Wallis)**	
	All Groups (p-value)	**pairwise**	**q-value**		**All Groups (p-value)**	**pairwise**	**q-value**
Location Name	0.07				X		
Geography (All Samples and Years)	0.02	East-North	0.05		X		
		East-West					
		East-Lagoon					
Geography (By Year)	0.0	East_2018 East_2021	0.01		0.0	East_2018-East_2021	0.01
		East_2018-North_2018	0.02				
		East_2018-North_2019	0.04				
		East_2018-North_2021	0.02				

					East_2018-lagoon_2018	0.01
		East_2018-West_2019	0.02		East_2018-West_2019	0.01
		East_2018-West_2021	0.01		East_2018-West_2021	0.00
					East_2018-lagoon_2019	0.05
		East_2018-lagoon_2018	0.01			
		East_2018-lagoon_2021	0.01		East_2018-lagoon_2021	0.00
		East_2019-East_2021	0.01		East_2019-East_2021	0.01
		East_2019-North_2018	0.04			
		East_2019-North_2021	0.02			
		East_2019-West_2021	0.01		East_2019-West_2021	0.01
					East_2019-lagoon_2018	0.05
		East_2019-lagoon_2021	0.01		East_2019-lagoon_2021	0.00
		East_2021-West_2018	0.01		East_2021-West_2018	0.01
		East_2021-West_2019	0.04		East_2021-West_2019	0.04
		West_2018-West_2021	0.01			
		West_2018-lagoon_2021	0.01		West_2018-lagoon_2021	0.01
		West_2019-West_2021	0.04		West_2019-West_2021	0.03
		West_2019-lagoon_2021	0.02		West_2019-lagoon_2021	0.01
					lagoon_2019-lagoon_2021	0.05
Circulation (All Samples and Years)	0.00			X		X
Circulation (By Year)	0.00	Lagoon_2021-River_2018	0.03	0.00	Lagoon_2021-River_2018	0.00
		Lagoon_2021-Tidal open_2018	0.00		Lagoon_2021-Tidal open_2018	0.00
		Lagoon_2021-Tidal open_2019	0.00		Lagoon_2021-Tidal open_2019	0.00

		River_2018-Tidal open_2021	0.04			
					River_2018-River_2019	0.01
		River_2019-Tidal open_2018	0.00		River_2018-Tidal open_2021	0.01
		River_2019-Tidal open_2019	0.00		River_2019-Tidal open_2018	0.00
		River_2021-Tidal open_2018	0.03		River_2019-Tidal open_2019	0.00
		River_2021-Tidal open_2019	0.01		Tidal open_2018-Tidal open_2021	0.00
		Tidal open_2018-Tidal open_2021	0.00		Tidal open_2019-Tidal open_2021	0.00
		Tidal open_2019-Tidal open_2021	0.00		Lagoon_2021-River_2018	0.00
Impact_1 (All Samples and Years)	X			X		X
Impact_1 (By Year)	0.00	Control_2018-Control_2021	0.01	0.00	Control_2018-Control_2021	0.00
		Control_2018-Impact_2021	0.01		Control_2018-Impact_2021	0.00
		Control_2019-Control_2021	0.00		Control_2019-Control_2021	0.00
		Control_2019-Impact_2021	0.00		Control_2019-Impact_2021	0.00
		Control_2021-Impact_2018	0.00		Control_2021-Impact_2018	0.00
		Control_2021-Impact_2019	0.02			
		Impact_2018-Impact_2021	0.00		Impact_2018-Impact_2021	0.00
		Impact_2019-Impact_2021	0.02		Impact_2019-Impact_2021	0.02
Impact_2 (All Samples and Years)	.04	Control-Far Control	.04	X		X

Impact_2 (By Year)	0.00	Control_2018-Control_2021	0.00	0.00	Control_2018-Control_2021	0.00
		Control_2018-Far Control_2018	0.02			
		Control_2018-Far Control_2021	0.01			
		Control_2018-Impact_2019	0.03			
		Control_2018-Impact_2021	0.00		Control_2018-Impact_2021	0.00
		Control_2019-Control_2021	0.00		Control_2019-Impact_2021	0.00
		Control_2019-Far Control_2018	0.02			
		Control_2019-Far Control_2021	0.01			
		Control_2019-Impact_2021	0.00			
		Control_2021-Impact_2018	0.01			
		Far Control_2018-Impact_2018	0.03			
		Far Control_2021-Impact_2018	0.03		Control_2021-Impact_2018	0.02
		Impact_2018-Impact_2021	0.00		Impact_2018-Impact_2021	0.00
		Impact_2019-Impact_2021	0.03		Impact_2019-Impact_2021	0.04
Site-group (All Samples and Years)	0.04			X		X
Site-group (By Year)	0.00	Inflow_2021-Near Control_2018	0.00	0.00	Inflow_2018-Inflow_2021	0.04
		Inflow_2021-Near Control_2019	0.00		Inflow_2021-Near Control_2018	0.00
		Near Control_2018-Near Control_2021	0.01		Inflow_2021-Near Control_2019	0.00
		Near Control_2019-	0.01		Inflow_2021-Outflow_2018	0.04

		Near Control_2021				
					Near Control_2018-Near Control_2021	0.01
					Near Control_2019-Near Control_2021	0.01
Time of Day (All Samples and Years)	0.01	Day-Night	0.01	0.01	Day-Night	0.01
Time of Day (By Year)	0.0	Day_2018-Day_2021	0.00	0.00	Day_2018-Day_2021	0.00
		Day_2019-Day_2021	0.00		Day_2019-Day_2021	0.00
		Day_2021-Night_2018	0.04		Day_2021-Night_2018	0.05
		Day_2021-Night_2019	0.04		Day_2021-Night_2019	0.05
		Day_2018-Day_2021	0.00			
Temperature Regime (All Samples and Years)	X		X	X		X
Temperature Regime (By Year)	0.00	Extreme_2018-High_2021	0.04	0.00		
		Extreme_2018-Low_2021	0.04		Extreme_2018-High_2021	0.04
		Extreme_2018-Medium_2021	0.04			
		High_2019-High_2021	0.04		High_2019-High_2021	0.04
		High_2019-Low_2021)	0.03		High_2019-Low_2021	0.04
		High_2021-Low_2018)	0.04		High_2021-Low_2018	0.03
		High_2021-Low_2019)	0.03		High_2021-Low_2019	0.03
		High_2021-Medium_2018	0.03		High_2021-Medium_2018	0.03
		Low_2018-Low_2021	0.04		Low_2018-Low_2021	0.03

					Low_2018-Medium_2021	0.04
		Low_2019-Low_2021	0.02		Low_2019-Low_2021	0.03
		Low_2019-Medium_2021	0.04		Low_2019-Medium_2021	0.03
		Low_2021-Medium_2018	0.03		Low_2021-Medium_2018	0.04
		Low_2021-Medium_2019	0.04			
		Medium_2018 - Medium_2021	0.04		Medium_2018 - Medium_2021	0.04
Salinity Regime (All Samples and Years)	0.00	Euryhaline - Mesohaline	0.00	0.01	Euryhaline - Polyhaline	0.01
		Euryhaline - Polyhaline	0.01			
Salinity Regime (By Year)	0.0	Euryhaline_2018-Euryhaline_2021	0.00		Euryhaline_2018-Euryhaline_2021	0.00
		Euryhaline_2018-Mesohaline_2018	0.01			
		Euryhaline_2018-Mesohaline_2019	0.03			
		Euryhaline_2018-Mesohaline_2021	0.01			
		Euryhaline_2018-Polyhaline_2018	0.01		Euryhaline_2018-Polyhaline_2018	0.00
		Euryhaline_2018-Polyhaline_2019	0.00		Euryhaline_2018-Polyhaline_2019	0.00
		Euryhaline_2018-Polyhaline_2021	0.00		Euryhaline_2018-Polyhaline_2021	0.00
		Euryhaline_2019-	0.00		Euryhaline_2019-	0.00

		Euryhaline_2021			Euryhaline_2021	
		Euryhaline_2019-Mesohaline_2018	0.01			
		Euryhaline_2019-Mesohaline_2021	0.01			
		Euryhaline_2019-Polyhaline_2019	0.02		Euryhaline_2019-Polyhaline_2019	0.01
		Euryhaline_2019-Polyhaline_2021	0.00		Euryhaline_2019-Polyhaline_2021	0.00
		Euryhaline_2021-Polyhaline_2018	0.01		Euryhaline_2021-Polyhaline_2018	0.01
					Euryhaline_2021-Polyhaline_2019	0.04
		Polyhaline_2018-Polyhaline_2021	0.01		Polyhaline_2018-Polyhaline_2021	0.00
		Polyhaline_2019-Polyhaline_2021	0.01		Polyhaline_2019-Polyhaline_2021	0.00
Power Plant Closing (All Samples and Years)	0.01	After-Before	0.01	0.00	After-Before	0.00
Power Plant Closing (By Year)	0.00	After_2019-After_2021	0.00		After_2019-After_2021	0.00
		After_2021-Before_2018	0.00		After_2021-Before_2018	0.00

Taxonomic Analyses

In the 2021 sample analysis, 228 unique taxa were identified to species level at 0.70 confidence or greater. The combined 2018, 2019, 2021 sample analysis identified 384 unique taxa at 0.70 confidence or greater. Some of the species identifications refer to unique sequences on GenBank that are only given a

designation and no assigned species. Anywhere from 43 (e.g. Sunrise Beach Lagoon) to 114 (e.g. Double Creek East) species were identified from each of the collection sites in 2021. Of the 228 identified metazoan taxa, 193 had defined Genera in the 2021 data set. Of the 384 identified metazoan taxa, 325 had defined Genera in the combined 2018, 2019, and 2021 data set.

Animals identified in 2021 and combined 2018, 2019, and 2021 data sets included representatives from 13 different phylum (see Appendix B) including gelatinous zooplankton identified in plankton tows such as *Chrysaora chesapeakei, Mnemiopsis leidyi, Diadumene spp., Obelia spp., Orthopyxis spp, Nemopsis bachei, Sarsia tubulosa, Moerisia inkermanica, Turritopsis dohrnii, Clytia spp., Gonothyraea loveni, Halopteris diaphana,* and *Haliclystus tenuis.* For the 2021 samples, Double Creek East and Oyster Creek Mouth exhibited the highest species richness (114 and 96 taxa respectively), while the Sunrise Beach Lagoon and Bayshore Lagoon sites had the fewest (43 and 49 respectively; Figure 133). The decrease in species richness at the Oyster Creek Route 9 site, as compared to 2018, agrees with our prior hypothesis that the OCNGS entrained or entrapped water born individuals and DNA in relatively high concentrations, which were picked up during the sampling process.

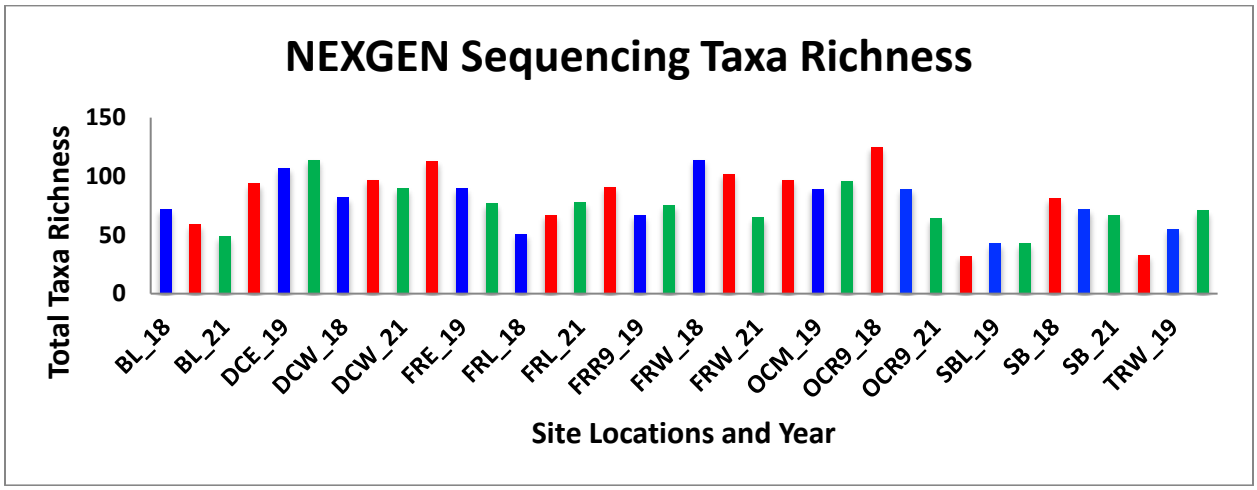

Figure 133. Total Animal Species Richness identified through NEXGEN Sequencing among sample locations for 2018 (_18), 2019 (_19), 2021(_21). Site Abbreviations organized by south to north: BL: Bayshore Lagoon; DCE: Double Creek East; DCW: Double Creek West; FRE: Forked River East; FRL: Forked River Lagoon; FRR9: Forked River RT 9; FRW: Forked River West; OCM: Oyster Creek Mouth; OCR9: Oyster Creek Outflow RT9; SBL: Sunrise Beach Lagoon; SB: Sunrise Beach; TRW: Toms River West.

Assess community structure across temporal scales: comparing baseline data from 2012-2014 with community structure data from 2018, 2019, and 2021

To generate a collective assessment of what has occurred in the last decade regarding gelatinous zooplankton, two series of evaluations were undertaken. The first is a generalized look using complete data sets (all bay sites, all years) to establish large scale patterns. The second evaluation looked to assess the differences among four sites which were used in both sampling efforts, namely Forked River East (FRE), Forked River West (FRW), Double Creek East (DCE), and Double Creek West (DCW). While this second evaluation reduces the robustness of the data collected over this 10-year period, the site-specific results provide the statistical rigor needed to identify significant differences between the two sampling programs (2012-2014 and 2018-2021).

Generalized Patterns: Lift Nets

Comb Jelly, *Mnemiopsis leidyi*

We used data collected from all bay sites among all years to evaluate the changes in density observed of major gelatinous zooplankton among years. The two dominant taxa, from a food web perspective, are the comb jelly *Mnemiopsis leidyi* and the scyphozoan *Chrysaora chesapeakei*. When we look at the aggregate data from all sampling years for *M. leidyi*, we see considerably lower densities in the current evaluation from 2018-2021 (Figure 134). In fact, densities were significantly greater in 2012 and 2013 compared to all other years ($F_{5,5937} = 44.2$; $P < 0.0001$). In our previous work (Bologna et al. 2018), the increase in density observed in 2013 was the result of the declines in *C. chesapeakei*, a major predator of *M. leidyi*, following Superstorm Sandy. The subsequent drop in 2014, despite the continued low densities in *C. chesapeakei* (see Figure 135), was attributed to higher densities of numerous other gelatinous zooplankton species (Bologna et al. 2018). The recent increases from 2018 to 2021 suggest a recovering *M. leidyi* population following the closure of OCNGS.

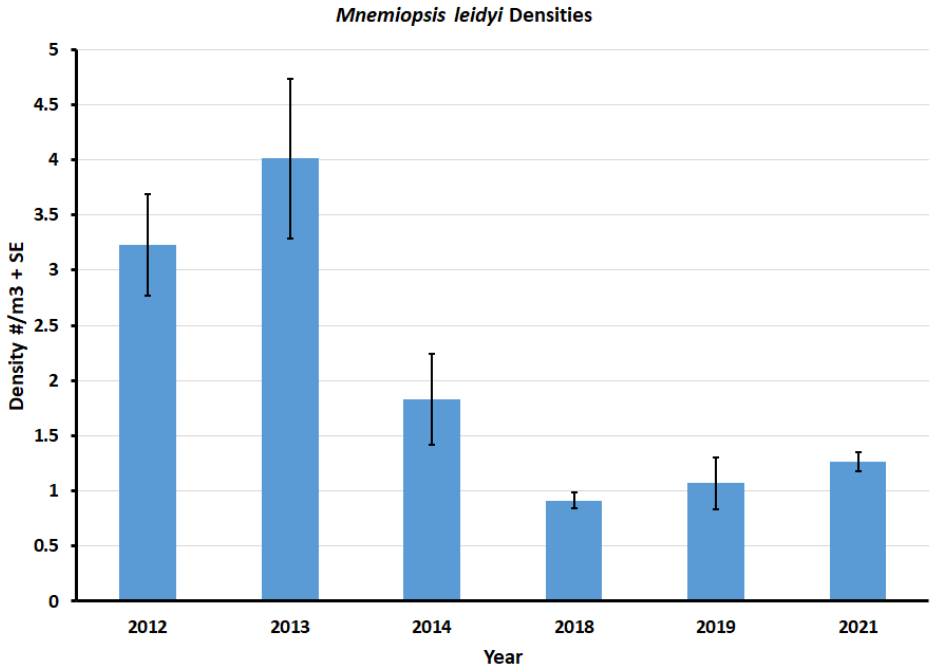

Figure 134. Densities of *M. leidyi* from Lift Net sampling across 2012 to 2021 from all bay stations.

Bay Nettle, *Chrysaora chesapeakei*

When we look at the patterns observed for the bay nettle (Figure 135), the major increases observed in 2019 and 2021 need to be placed in context, since inclusion of all sites has the potential to skew the evaluation, especially between the sampling events of 2012-2014 and the current evaluation of 2018-2021. One pattern that is clear is that *C. chesapeakei* was showing declines in density between 2012 and 2014 following Superstorm Sandy. The other major pattern is the substantial increases from 2018 to 2021, following the closure of the OCNGS. While Superstorm Sandy reduced the density of *C. chesapeakei* in 2013 and 2014, it was not until the plant closure that the significant increases took place ($F_{5,5938} = 20.46$; $P < 0.0001$). So, one concept to consider is that it took seven years post Sandy to allow *C. chesapeakei* populations to recover to pre-storm levels, and with the closure of the plant which had caused the destruction of *C. chesapeakei* ephyrae from major sources like the Forked River and Forked River Lagoon, population growth massively expanded (Figure 64). This was always a concern about the closure of the OCNGS, which would allow Bay Nettle populations to increase, and the data generated from this study confirm those concerns (Figure 135). Perhaps the next question to address is whether their increase will negatively impact the other taxa in the region. Since *C. chesapeakei* is an apex predator in the system, will their increase offset the gains of other species since the shutdown of the plant? At current densities, it is unlikely that in the near future they will exert that pressure. Given the significant increases seen in Fish Eggs, Fish Larvae, *Menidia menidia*, and copepods since the closure of the plant, the trend suggests that the top-down predation pressure by *C. chesapeakei* is dwarfed by the impacts that OCNGS was having on the zooplankton of the bay. Consequently, the shutdown appears to have had a substantial positive effect on the bay.

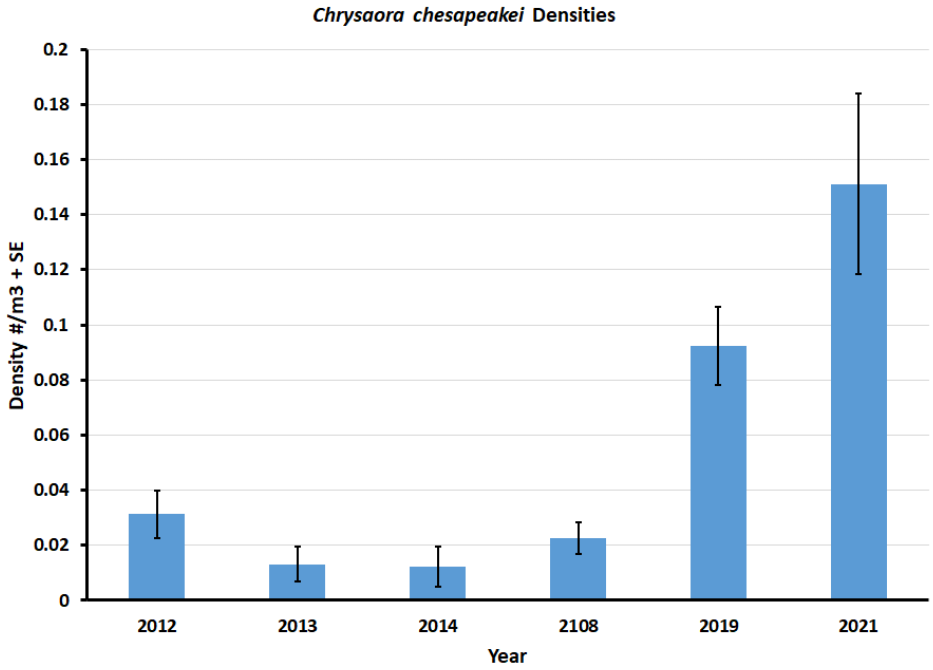

Figure 135. Densities of *C. chesapeakei* from Lift Net sampling across 2012 to 2021 from all bay stations.

Hydrozoan, *Nemopsis bachei*

The hydrozoan *Nemopsis bachei* shows a dramatic increase in density within the lift net sampling events from 2012-2014 to the most recent sampling (Figure 136). In fact, density is significantly greater from 2018, 2019, and 2021 when compared to the sampling completed between 2012-2014 ($F_{5,5938} = 20.9$,

P < 0.0001). This dramatic increase in density is likely a result of the diminished *C. chesapeakei* densities following Hurricane Sandy in 2012 (Figure 135), as no *N. bachei* were recorded in 2012, but they emerged and were present in 2013 samples and continued to increase to their peak in 2018 and stabilizing densities ever since.

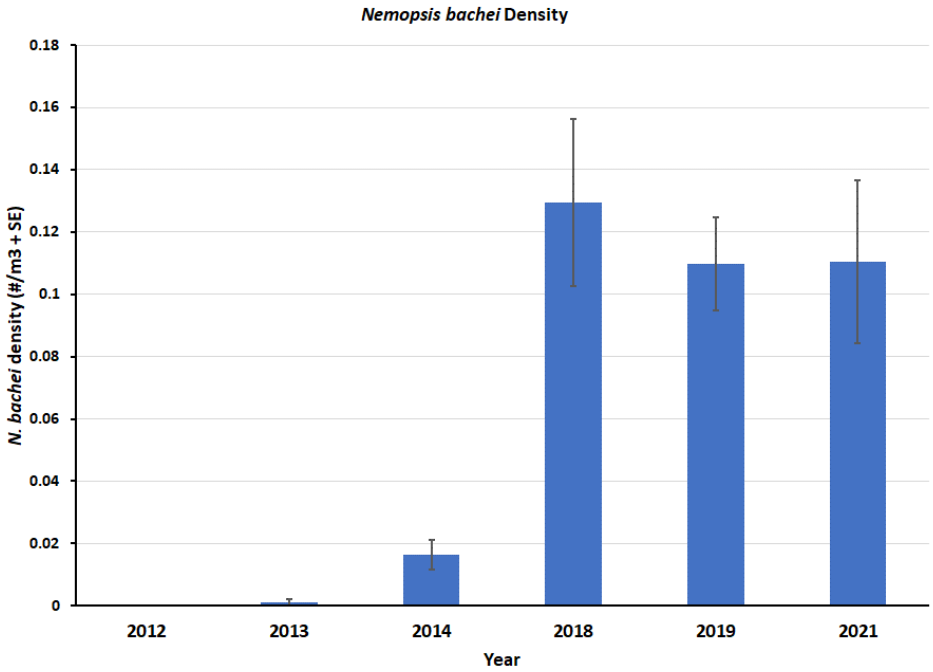

Figure 136. Densities of *N. bachei* from Lift Net sampling across 2012 to 2021 from all bay stations.

Multi year comparisons for Plankton Tow Data

When we evaluate some of the critical taxa among years, we can identify a few clear patterns within. First, Hurricane Sandy in 2012, caused substantial shifts in the density of many organisms and second, the closure of OCNGS showed shifts in the density of organisms in a similar manner. It is advisable to recognize that the sample stations used between 2012-2014 and 2018-2021 are not the same, so interpretation of these results reflect the generality of these differences. Specific site evaluations are provided in the next session for sites which are concordant.

Generalized Patterns: Plankton Tows

Comb Jelly, *Mnemiopsis leidyi*

Analysis of the plankton tows among all years sampled shows significant differences in density among years ($F_{5,1451}$ = 14.7, P < 0.00001). Specifically, densities of *M. leidyi* increased significantly in 2013, post Hurricane Sandy (Figure 137), but were reduced in 2014 due to competition among other gelatinous zooplankton (see Other Gelatinous Zooplankton below) and were lowest in samples from 2018 during the operation of OCNGS. After the closure of the plant, *M. leidyi* again rose substantially in 2019 through 2021 in response to the elimination of the impingement and entrainment of individuals in the plant.

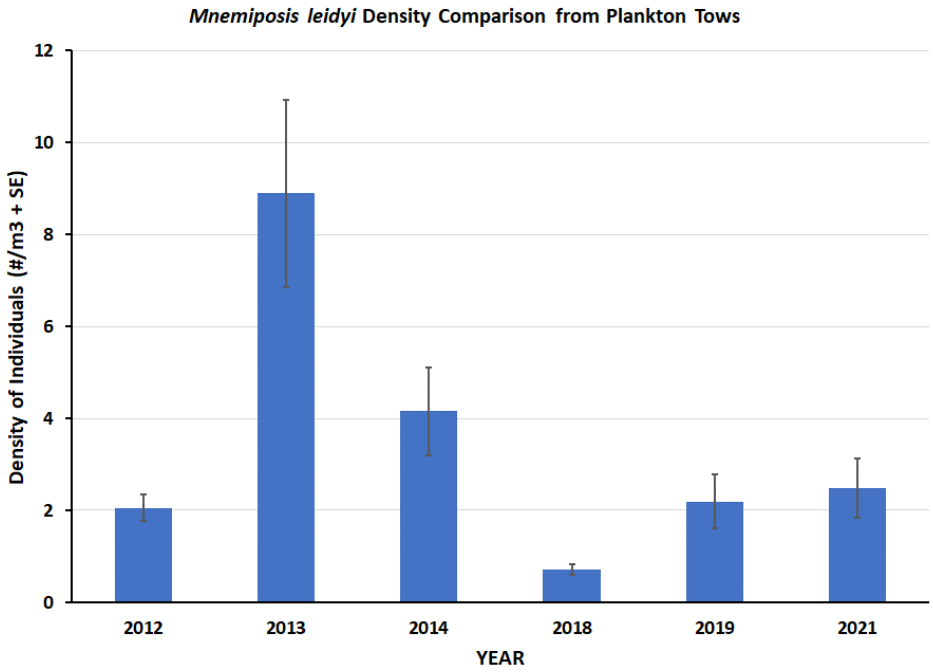

Figure 137. Comparison of *M. leidyi* density among all years sampled from Plankton Tow data collections.

Bay Nettle, *Chrysaora chesapeakei*

Results from the generalized plankton tow data showed that densities of *C. chesapeakei* were substantially higher from 2018-2021 compared to 2012-2014 (Figure 138) and significantly higher in 2019 after the closure of the plant comparted to all other years ($F_{5,1453} = 4.5$, $P < 0.0004$). The differences seen between sampling time frames reflects the broad coverage of 16 stations in the early assessment and the more targeted site evaluation with regards to the closure of OCNGS. The change in density from 2019 through 2021 does not match what was observed in the lift nets (Figure 135), which showed continued increases in density of *C. chesapeakei* in 2021. This is likely a reflection of the early bloom and growth of *C. chesapeakei* in 2021 where individuals were larger and less likely to be captured in plankton tows as compared to lift nets.

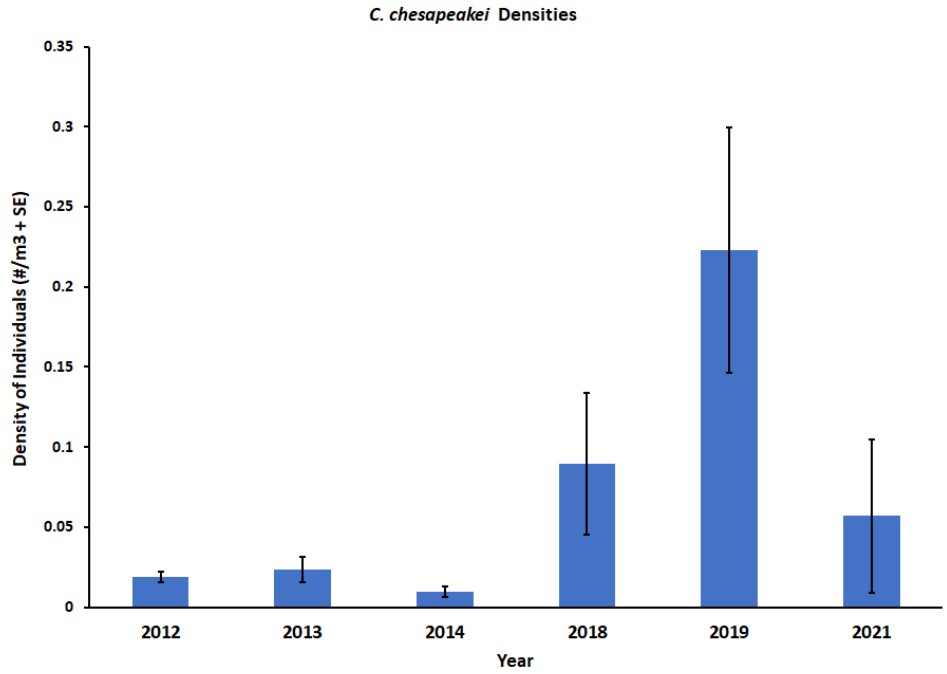

Figure 138. Comparison of *C. chesapeakei* density among all years sampled from Plankton Tow data collections.

Other Gelatinous Zooplankton

Comparisons among years presents challenges to interpret the overall patterns in species distributions given the site differences between the two sampling periods. Regardless of taxa specific differences, it is apparent that after Superstorm Sandy in 2012 and the closure of the OCNGS in 2018, the overall community of minor gelatinous species increased dramatically (Figure 139). Additionally, while there is some variation in the taxa identified among years, the increases in density and species richness have also increased and includes species identified only in 2019 and 2021 (e.g., *Laodicea undulata* and *Eucheilota maculata*). This is interesting because *E. maculata* is another non-native hydrozoan which has been identified in the study, and has shown increases in density from 0 in 2018 to 0.065 m^{-3} in 2019 and 0.199 m^{-3} in 2021, comprising 25% of the minor gelatinous taxa collected. Another species which has shown dramatic changes in their density and contributions to the gelatinous zooplankton community is *Turritopsis dohrnii* (Figure 139). In 2012, *T. dohrnii* was less than 1% of the overall minor gelatinous species, but after Superstorm Sandy and the declines in *C. chesapeakei*, *T. dohrnii* densities began to increase rapidly and now comprise 20-30% of the minor species. While it is difficult to say whether the closure of OCNGS has benefitted *Turritopsis dohrnii* populations, the restructuring of the overall community after Superstorm Sandy shows the power and impact of that event in Barnegat Bay.

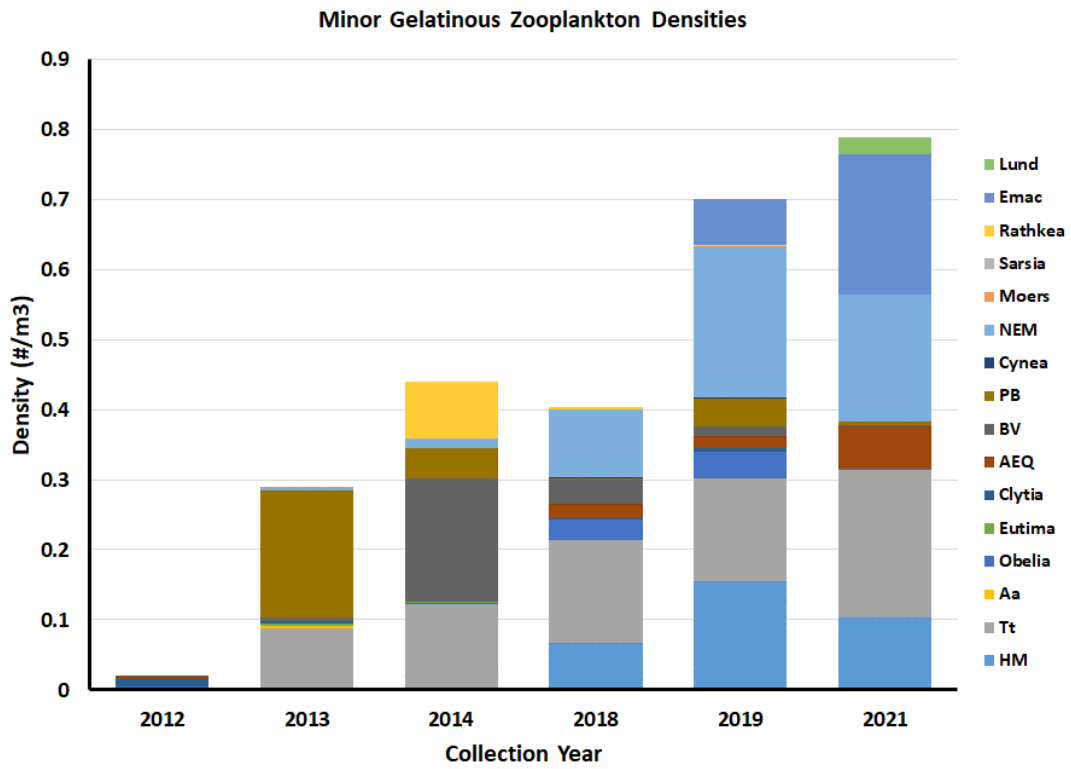

Figure 139. Densities of minor gelatinous zooplankton taxa from plankton sampling across 2012 to 2021 from all bay stations. Taxa Abbreviations: Lund = *Laodicea undulata*, Emac = *Eucheilota maculata*, Rathkea = *Rathkea* sp., Sarsia = *Sarsia tubulosa*, Moers = *Moerisia* spp., NEM = *Nemopsis bachei*, Cynea = *Cyanea capillata*, PB = *Pleurobrachia pileus*, BV = *Bougainvillia carolinensis*, AEQ = *Aequora* sp., Clytia= *Clytia* spp., Eutima = *Eutima* sp., Obelia = *Obelia* spp., Aa = *Aurelia* spp., Tt = *Turritopsis dohrnii*, HM = Hydromedusa unknown.

Calanoid Copepods

Changes in the density of copepods among years shows defining linkages with major disturbances. After Hurricane Sandy in 2012, copepod densities increased dramatically (Figure 140) associated with the significant declines in *C. chesapeakei* during that year. Similarly, after the closure of OCNGS copepod densities again increased in 2019 and were significantly greater in 2021 compared to all other years ($F_{5,1453}$ = 9.05, $P < 0.0001$). This significant increase demonstrates that copepod populations were being substantially suppressed due to the operation of the plant and that these increases really show the improvement in biological conditions in Barnegat Bay.

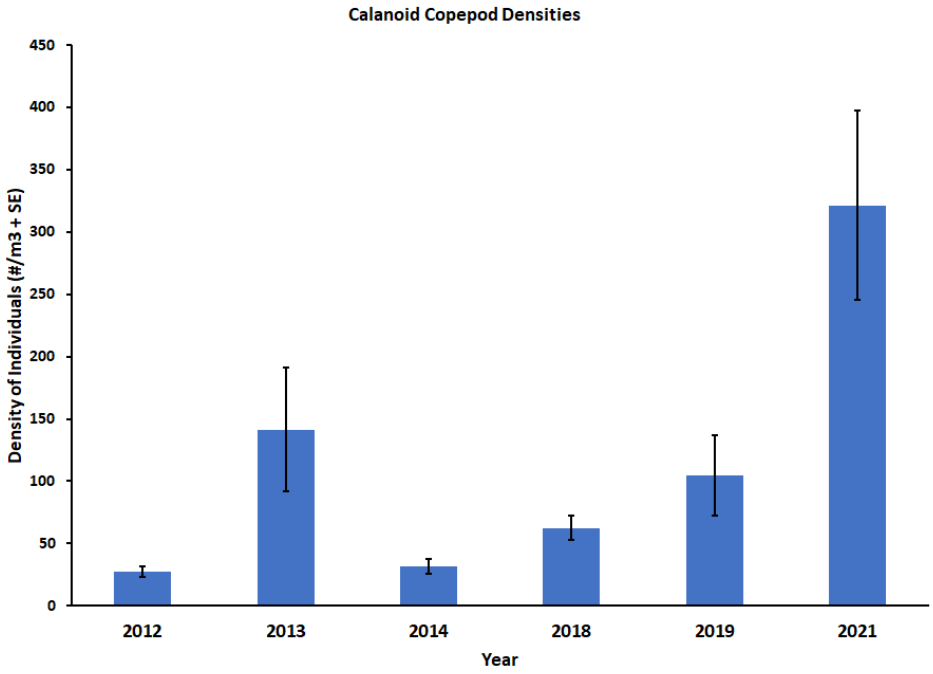

Figure 140. Comparison of Calanoid Copepod density among all years sampled from Plankton Tow data collections.

Exact Site Comparisons: Lift net

The choice of sampling sites allowed for a comparison of changes in gelatinous zooplankton between research completed between 2012 and 2014 with the data collected for this project from 2018 to 2021. Specifically, four sites in proximity to the OCNGS provide a metric to evaluate changes over the last decade. The four sites were Forked River East (FRE), Forked River West (FRW), Double Creek East (DCE), and Double Creek West (DCW). When we analyzed the lift net data using a mixed-model ANOVA, no significant differences in density were observed for the bay nettle *Chrysaora chesapeakei*, as they were only observed from sites in 2014 and 2021 at the Forked River West site. However, significant differences were observed among years and sites for the comb jelly, *Mnemiopsis leidyi*. Specifically, densities from 2012 and 2013 were significantly greater than all other years ($F_{5,1557} = 31.6$, $P < 0.0001$), but 2014 was also significantly greater than 2018 through 2021, which did not differ significantly (Figure 141). It is highly probable that the declines in density observed during 2018 through to 2021 may reflect increases in *C. chesapeakei* density after their significant decline following Superstorm Sandy. Among sites, Forked River East had significantly greater densities than all other sites ($F_{3,1557} = 18.7$, $P < 0.0001$), which may reflect its distance from potential sources of predation by *C. chesapeakei*. Another species which increased significantly in abundance post-Super Storm Sandy and the closure of the OCNGS was the hydrozoan *Nemopsis bachei* (Figure 142), which showed significantly great densities in 2019 and 2021 compared to all other years ($F_{5, 1557} = 6.63$, $P < 0.0001$) and significantly more at the Forked River East location ($F_{3,1557} = 15.15$, $P < 0.0001$).

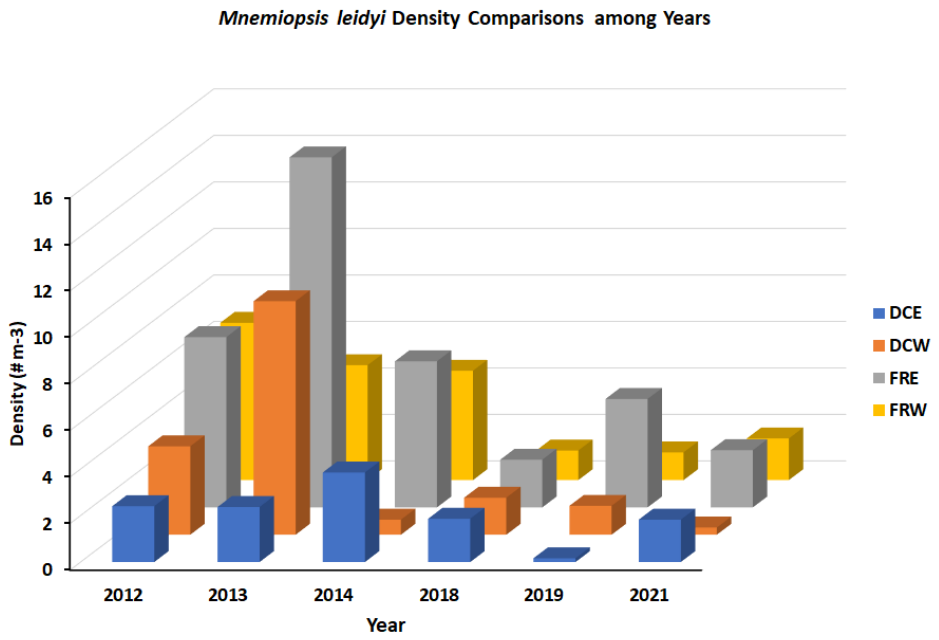

Figure 141. Comparison of *M. leidyi* density from lift nets among all years at the four corresponding sites sampled.

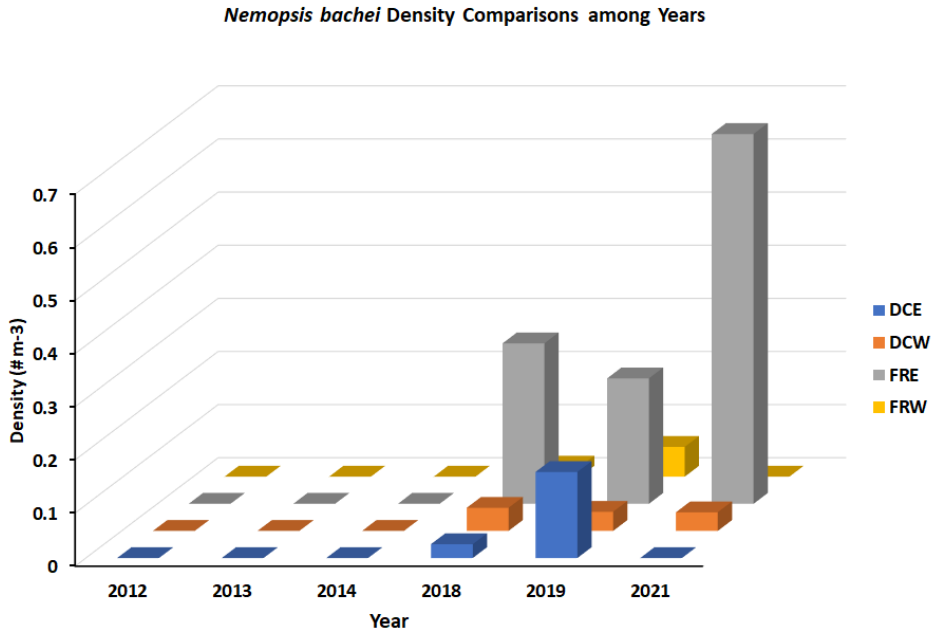

Figure 142. Comparison of *N. bachei* density from lift nets among all years at the four corresponding sites sampled.

Exact Site Comparisons: Plankton Tow

When evaluating the changes in the density of organisms between sampling efforts for the four identical sites, some patterns of abundance are similar to the results from the lift nets. For example, no significant differences in density among years were observed for *C. chesapeakei* densities ($F_{5,401} = 1.19$, $P > 0.3$), nor among sites ($F_{3,401} = 0.98$, $P > 0.4$), as few or no individuals were collected at these four specific sites. Like the results observed in lift nets, *M. leidyi* density was significantly greater in 2013 compared to all other years ($F_{5,399} = 14.27$, $P < 0.0001$) and densities in 2014 were significantly greater than samples collected from 2018 to 2021 (Figure 143). When we evaluate the differences among sites for *M. leidyi* (Figure 143), we can see that DCW had substantially greater densities in 2013 and drove the overall significant differences, but after that peak in 2013, densities were very low for the remainder of the study period, while other sites showed increases after the shutdown of the OCNGS. This small recovery in *M. leidyi* populations may be driven by a combined effect of positive feedback from the closure of the plant, but negative top-down pressure from the increasing *C. chesapeakei* densities observed throughout the region (Figure 135).

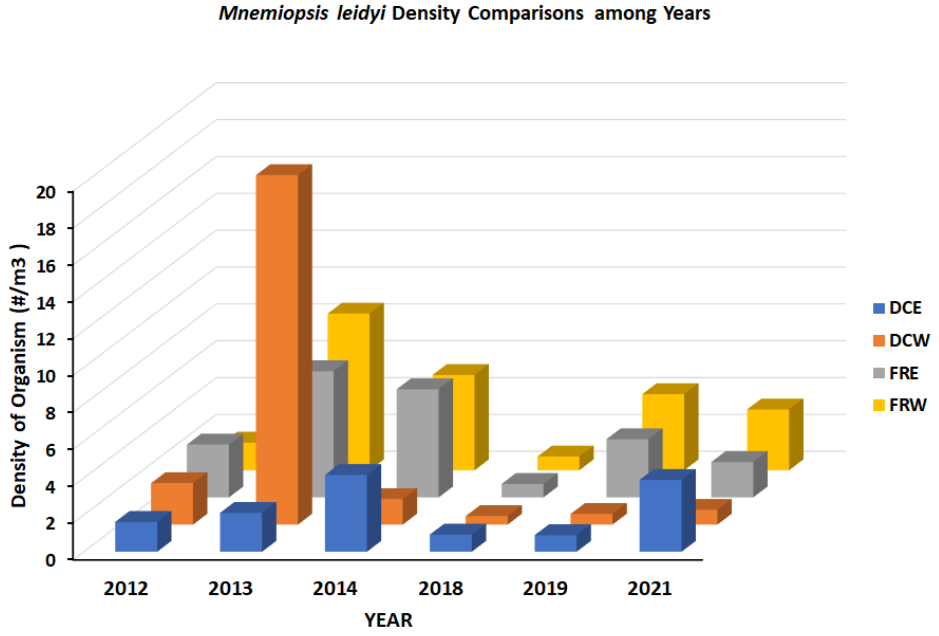

Figure 143. Comparison of *M. leidyi* density among all years at the four corresponding sites sampled from Plankton Tow data collections.

The other abundant gelatinous zooplankton species prevalent among these four sites was *Nemopsis bachei*. Results from the analysis indicated a significant difference among years ($F_{5,400} = 2.9$; $P < 0.014$), with greater densities observed between 2018-2021 compared to 2012-2014 (Figure 144). However, no significant differences were observed among sites ($F_{3,400} = 2.01$; $P > 0.11$), but significantly greater densities were collected in June compared to other months in the mixed model analyses ($F_{22,400} = 2.49$; $P < 0.0003$).

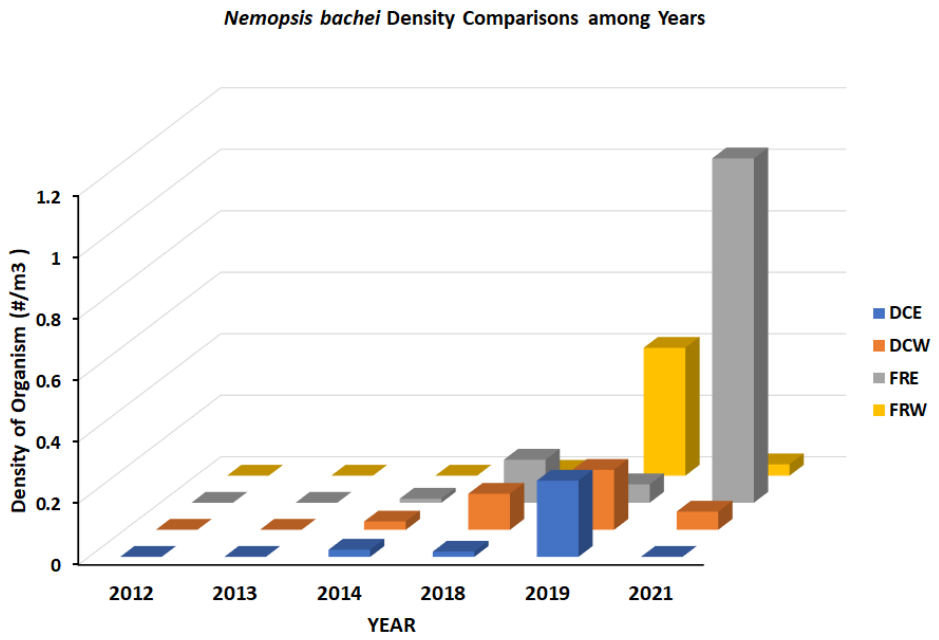

Figure 144. Comparison of *Nemopsis bachei* density among all years at the four corresponding sites sampled from Plankton Tow data collections.

Two critical taxonomic groups which are vital for the health of Barnegat Bay are Calanoid Copepods (Figure 145) and Fish Eggs (Figure 146). The analysis related to the shut-down of the plant showed significant increases in densities from 2018 to 2021 for both of these groups. In the longer-term analyses, Calanoid Copepods were again significantly greater in 2021 compared to all years ($F_{5,400} = 23.3$; $P < 0.0001$) and were significantly greater at Double Creek East ($F_{3,400} = 2.94$; $P < 0.033$). The relatively low densities which occurred from 2012-2014 could relate to combined predation and impacts from the operation of the plant, but the jump in density in 2018 while the plant was functional is not as easily explained. It is possible that the major declines observed for *M. leidyi* and *C. chesapeakei* during these time frames were truly releasing copepods from top down pressure allowing their populations to rebuild. This, coupled with the shutdown could demonstrate the rapid recovery of these critical links in the pelagic food web and aid in the recovery of Barnegat Bay. When we analyzed the densities of fish eggs (Figure 146), we saw a similar pattern with significantly greater densities in 2021 compared to all years ($F_{5,400} = 2.66$; $P < 0.022$) and significantly greater densities at Double Creek East ($F_{3,400} = 3.31$; $P < 0.02$). However, the pattern of densities being suppressed by predators and the operation of the plant do not seem to regulate their abundance in our comparisons for fish eggs, as identified for copepods. The major increase in fish eggs came in 2021, three years after the shutdown. While there was variability among the previous years, the major increase seen suggests that several years were needed for fish populations to begin to recover. This was not unexpected, since this would be directly reflected in slowly growing populations moving towards recovery.

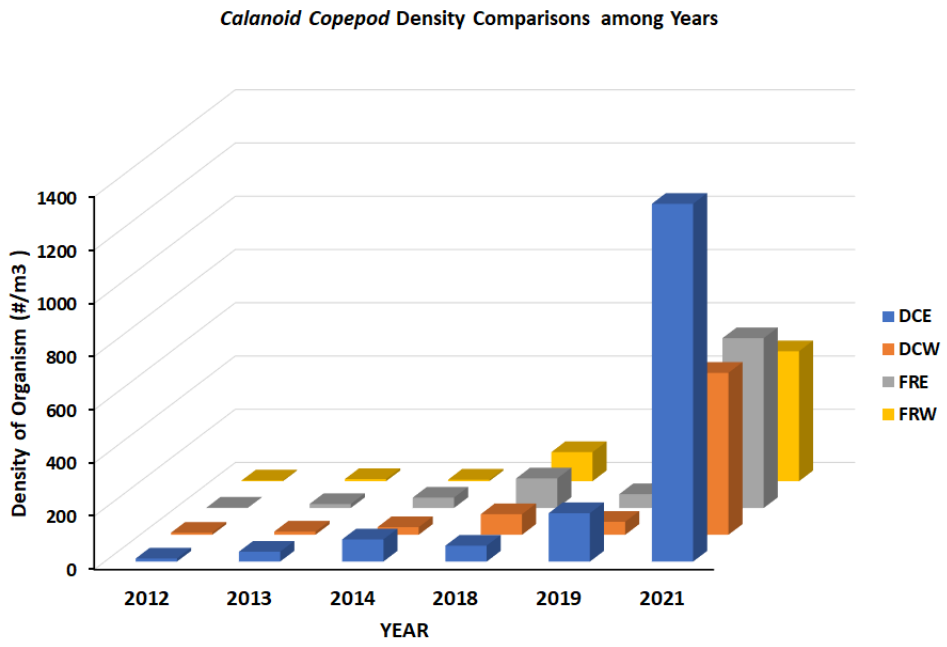

Figure 145. Comparison of Calanoid Copepod density among all years at the four corresponding sites sampled from Plankton Tow data collections.

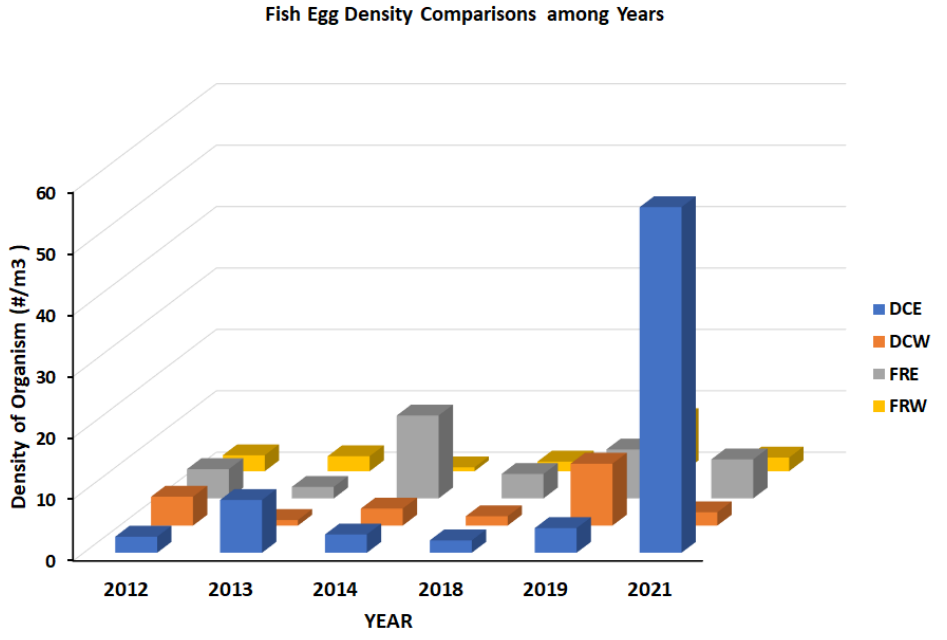

Figure 146. Comparison of Fish Egg density among all years at the four corresponding sites sampled from Plankton Tow data collections.

Conclusions and Recommendations

In the last decade, we have been studying the gelatinous zooplankton community in Barnegat Bay. During this time frame, Barnegat Bay was subjected to a massive, acute disturbance in the form of Hurricane Sandy in 2012, but also a long-term chronic stress from the operation of the Oyster Creek Nuclear Generating station. A major impact of Hurricane Sandy was the significant reduction in the abundance of the apex predator the bay nettle (*Chrysaora chesapeakei*), which allowed the density and diversity of other gelatinous zooplankton to increase. This simple top-down effect is commonplace after these large-scale disturbances. The chronic impingement, entrainment, and thermal loading of OCNGS for more than 50 years has had substantial impacts on the health of Barnegat Bay. Principally, these long-term stresses are felt through the loss of planktonic organisms, but also the loss of eggs, larvae, and juveniles of species who only spend the early part of their life in the plankton. The OCNGS environmental evaluation demonstrated the loss/destruction of substantial numbers of planktonic organism like copepods, as well as fish eggs and larvae. With the closure of the plant, these combined stresses of direct losses and thermal loading are now significantly lower. Regarding thermal stress, we were able to document significantly greater water temperatures in 2018 during the operation of OCNGS at our Oyster Creek Rt. 9 (OCRT9) site, where the outfall from the plant was occurring in comparison to the adjacent sites (Figure 16). After the closure, there was no discernable temperature differences observed among the sites (Figures 17, 18), documenting the minimization or elimination of the thermal stress to Barnegat Bay. Additionally, the massive flow of water that was circulated through the system was significantly reduced, which had impacts on the diversity of organisms from the two sites most impacted by this flow, namely the intake site Forked River Rt. 9 (FRRT9) and the outfall OCRT9. These were the only two sites to show significantly fewer taxa identified after the closure of the plant than during its operation (Figure 129), demonstrating that the artificial waterways created as part of the OCNGS are showing fundamental shifts in overall community structure. However, after the closure of the plant several nearby sites which had been affected by the operation showed increases in their taxa richness, including the Oyster Creek Mouth site which was heavily impacted by the thermal loading from the plant, but also the Double Creek West, Forked River West, and Sunrise Beach sites. Given their proximity to the inflow and outflow corridors of the plant, these increases in taxa richness show the cascading positive effects that the closure has had.

Morphological identification via visual identification methods has been the standard for biodiversity studies (e.g., Kennish 2001; Taghon et al. 2017; Howson et al. 2017). However, this is very time consuming, requires years of training/experience, and often species level identifications aren't possible due in part to undescribed or unidentifiable larval forms. These factors can all lead to an underestimation of true biodiversity (e.g., Beng and Corlett 2020). Molecular techniques (e.g., metagenomics) potentially offer a better methodology. Environmental DNA (eDNA) sampling for biodiversity assessments has received a lot of attention. eDNA is DNA that can be extracted from the environment (e.g., soil, water, air) without targeting specific organism(s) (Taberlet et al. 2012; Thomsen and Willerslev 2015). The eDNA can then be metabarcoded (amplification and sequencing of marker gene(s)) for identification of taxa in a given sample. This can reveal patterns of marine biodiversity on a large scale (e.g., Yang and Zhang 2020). eDNA techniques are therefore productive, relatively cheap, and non-destructive or invasive to both organisms and the environment. In addition, eDNA techniques are highly sensitive to detecting rare, uncommon, or cryptic species, enable early detection of invasive species, and can accurately identify species regardless of developmental stage or environment (summarized in Thomsen and Willerslev 2015; Beng and Corlett 2020). Through use of this technique, we were able to identify a variety of known invasive species (e.g., clinging jellyfish *G. vertens*; tunicate, *Botryllus schlosseri*), but also numerous potential invasive species never recorded in Barnegat Bay or the region including crustaceans (*Crangon franciscorum*, *Panopeus chilensis*), tunicates (*Ascidia ahodori*), polychaetes (*Protula pacifica*), bryozoans (*Tricellaria occidentalis*), and fish (*Zoarces gillii*). Metagenomic analyses also have the advantage over traditional visual identification methods in that they use amplicon sequence variants (ASVs). ASV's are single DNA sequences representing the sequenced COI amplicons. ASVs provide a more accurate estimate of sequence

variation which corresponds to species diversity even if a sample cannot be identified visually or through its DNA sequence (i.e., the species is not in the database). With a potentially more accurate picture of biodiversity through metagenomics, any and all statistical analyses employing that data will also be more reflective of reality. For these reasons, metagenomic analyses offer a potentially more accurate reconstruction of biodiversity and a bellwether of potential invasive species.

Based on the evidence of collected samples, the closure of the Oyster Creek Nuclear Generating Station had several profound impacts on the zooplankton communities and individual taxa. A critical change in water temperature occurred downstream of the plant, reducing potential thermal stresses to the organisms of Barnegat Bay. Additionally, with the closure of the plant, significantly more fish eggs, fish larvae, and several important fish species (e.g., *Menidia menidia*) were reported after the closure. As the plant was known to have had significant impacts on the early life history stages of fish, the increases seen indicate that for some species their populations are recovering and should continue to increase in subsequent years. Other critical groups of zooplankton like Calanoid Copepods showed significant increases in density following the closure and point to rebounding pelagic food webs in Barnegat Bay. Several other prominent gelatinous zooplankton species also saw increasing densities after the closure of the plant. Specifically, increases in density were recorded for the comb jelly, *Mnemiopsis leidyi*, and the cnidarians *Chrysaora chesapeakei* and *Nemopsis bachei*. As these species are important predators of the zooplankton in the bay, the substantial increases observed after the closure may offset the increases in fish and crustacean densities seen in the future. If the populations of these apex predators continue to increase, they have the potential to exert significant top-down pressure on the community and may replace the plant as a critical mortality substitute. Only through continued evaluation of the complete suite of zooplankton in Barnegat Bay can we understand what the lasting impacts of OCNGS are on the bay. Several promising pieces of evidence indicate that the coastal waters can rebound and create a robust and vibrant zooplankton community supporting commercial and recreational fisheries and generalized improved health of Barnegat Bay.

Acknowledgements

Funding for this project was provided by the New Jersey Department of Environmental Protection under contracts SR18-008 for 2018, SR19-004 & SR21-003 for 2019, and SR20-005 & SR21-015 for 2021 to Montclair State University. This work was also supported in part from NSF grant DBI-1725932 to RM, JG, and PB. The Principal Investigators would like to thank the numerous students who assisted in both field and laboratory activities to collect, identify, and analyze samples. In particular, we want to acknowledge Dena Restaino, Alyssa Petitdemange, Seina Stucki, Alorah, Bliese, Erika Bernal, and Sarah Hoffman, for extraordinary efforts in field and laboratory activities. We would also like to acknowledge the Cristina Perez, Dominika Polchowska, Anthony Tamberelli, Angela Chemdlin, and Diana Sisk for research support efforts in field and laboratory activities and data entry and QAQC.

Bibliography

Altschul, S.F., Gish, W., Miller, W., Myers, E.W. and D.J. Lipman. 1990. Basic local alignment search tool. J. Mol. Biol. 215:403-410.

Bayha, K.M. and W. M. Graham. 2009. A new Taqman PCR-based method for the detection and identification of scyphozoan jellyfish polyps. Hydrobiologia. 616:217–228.

Bednarski, M. and A. Morales-Ramirez. 2004. Composition, abundance and distribution of macrozooplankton in Culebra Bay, Gulf of Papagayo, Pacific Coast of Costa Rica and its value as a bioindicator of pollution. Revista de Biologia Tropical. V.52, supl.2,

Beng, K. C., & Corlett, R. T. 2020. Applications of environmental DNA (eDNA) in ecology and conservation: opportunities, challenges and prospects. Biodiversity and Conservation, 29(7), 2089-2121.

Boero, F. Bouillon J., Gravili C., Miglietta M. P, Parsons T., and Piraino S. 2008. Gelatinous plankton: irregularities rule the world (sometimes). Marine Ecology Progress Series. 356: 299–310.

Bologna, P.A.X.; Gaynor, J.J.; Barry C.L., and Restaino, D.J., 2017. Top-down impacts of sea nettles (*Chrysaora quinquecirrha*) on pelagic community structure in Barnegat Bay, New Jersey, U.S.A. In: Buchanan, G.A.; Belton, T.J., and Paudel, B. (eds.), A Comprehensive Assessment of Barnegat Bay–Little Egg Harbor, New Jersey. Journal of Coastal Research, Special Issue No. 78, pp. 193–204. Coconut Creek (Florida), ISSN 0749-0208.

Bologna, P. Gaynor, J. and Meredith, R. 2015. Impacts of Invasive Sea Nettles (*Chrysaora quinquecirrha*) and Ctenophores on Planktonic Community Structure and Bloom Prediction of Sea Nettles Using Molecular Techniques. NJDEP Final Project Report. 137p.

Bologna, P., Gaynor, J.J., Meredith, R., Restaino, D. and Barry, C. 2018. Stochastic event alters gelatinous zooplankton community structure: impacts of Hurricane Sandy in a Mid-Atlantic estuary. Mar. Ecol. Prog. Ser. 591: 217-227. DOI: https://doi.org/10.3354/meps12262

Bouillon, J.; Seghers, G.; Boero, F. 1988. Notes additionnelles sur les méduses de Papouasie Nouvelle-Guinée (Hydrozoa, Cnidaria). III. Indo-Malayan Zoology. 5(2): 225-253.

Braley, M., Goldsworthy, S.D., Page, B., Steer, M., and J.J. Austin. 2012. Assessing morphological and DNA-based diet analysis techniques in a generalist predator, the arrow squid *Nototodarus gouldi*. Molecular Ecology 10:466-474.

Bridge, D., C. W. Cunningham, B. Schierwater, R. Desalle, and L. W. Buss. 1992. Class-level relationships in the phylum Cnidaria - evidence from mitochondrial genome structure. Proceedings of the National Academy of Science. 89:8750-8753.

Brodeur, R., Decker, M., Ciannelli, L., Purcell, J., Bond, N., Stabeno, P., Acuna, E., Hunt, G., 2008. Rise and fall of jellyfish in the eastern Bering Sea in relation to climate regime shifts. Progress in Oceanography 77:103-111

Cargo, D. and Rabenold, G. 1980. Observation on the asexual reproductive activities of the sessile stages of the sea nettle *Chrysaora quinquecirrha* (Scyphozoa). Estuaries 3: 20-27.

Champalbert, G., M. Pagano, P. Sene, and D. Corbin. 2007. Relationships between meso- and macro-zooplankton communities and hydrology in the Senegal River Estuary. Estuarine, Coastal and Shelf Science 74: 381-394.

Clesceri, L., A. Greenberg, A. Eaton, and M.A. Franson. 1998. Standard Methods for the Examination of Water and Wastewater. Prepared and published jointly by American Public Health Association, American Water Works Association and Water Environment Federation. American Public Health Association, Washington, D.C.

Dawson, M. N., and D.K. Jacobs. 2001. Molecular evidence for cryptic species of *Aurelia aurita* (Cnidaria, Scyphozoa). The Biological Bulletin, 200(1), 92-96.

de Almeida e Silva, T., S. Neumann-Leitao, R. Schwamborn, L.M. de Oliveira, and D.A do Nascimento-Vieira. 2003. Diel and seasonal changes in the macrozooplankton community of a Tropical Estuary in Northeastern Brazil. Revista Brasileira de Zoologia 20: 439-446.

Dhanasekaran, S., Doherty, T.M., and J. Kenneth. 2010. Comparison of different standards for real-time PCR-based absolute quantification. Immunological Methods. 354 (1–2): 34–39.

Gaynor, J.J., Bologna, P.A.X., Restaino, D., and C.L. Barry. 2016. First occurrence of the invasive hydrozoan *Gonionemus vertens* A. Agassiz, 1862 (Cnidaria: Hydrozoa) in New Jersey, USA. BioInvasions Records, 5:233-237.

GO. 2006. General Oceanics Digital Flow Meter Mechanical and Electronic Operators Manual. General Oceanics, Inc. Miami, FL.

Grove, M.W. and Breitburg, D.L. 2005. Growth and reproduction of gelatinous zooplankton exposed to low dissolved oxygen. Marine Ecology Progress Series 301: 185-198.

Hay, S. 2006. Marine ecology: gelatinous bells may ring change in marine ecosystems. Current Biology 16: R679-R682.

Hong, J., He-Qin, C., Hai-Gen, X., Arreguin-Sanchez, F., Zetina-Rejon, M., Del Monte Luna, P., LeQuesne, W. 2008. Trophic controls of jellyfish blooms and links with fisheries in the East China Sea. Ecological Modeling 212: 492-503

Hoover, R., and Purcell, J. 2009. Substrate preferences of scyphozoan *Aurelia labiata* polyps among common dock-building materials. Hydorbiologia 616: 259-267.

Howson, U. Buchanan, G. A., and James A. Nickels, J.A. 2017. Zooplankton community dynamics in a western mid-Atlantic lagoonal estuary. Journal of Coastal Research. Special Issue 78: pp. 141-168.

Javidpour, J., Molinero JC, Peschutter Sommer U. 2009. Seasonal changes and population dynamics of the ctenophore *Mnemiopsis leidyi* after its first year of invasion in the Kiel Fjord, Western Baltic Sea. Biological Invasions. 11:873–882

Johnson, W. and D. Allen. 2005. Zooplankton of the Atlantic and Gulf Coasts: A Guide to Their Identification and Ecology. Johns Hopkins University Press. Baltimore, MD.

Kaufman, R., E. Fisher, W. Gill, A. King, M. Laubacher, and B. Sullivan. 2003. Temporal patterns in the distribution, biomass and community structure of macrozooplankton and micronekton within Port Foster, Deception Island, Antarctica. Deep-Sea Research II 50: 1765-1785.

Kennish, M. 2001. Barnegat Bay – Little Egg Harbor, New Jersey: Estuary and Watershed Characterization. Journal of Coastal Research. Vol. SI, No. 32, 2001:163-167.

Kennish MJ 2001. Physical description of the Barnegat Bay−Little Egg Harbor estuarine system. Journal of Coastal Research. 32: 13−27.

Kideys A.E., Roohi, A,. Bagheri, S., Finenko, G., Kamburska, L. 2005. Impacts of invasive ctenophores on the fisheries of the Black Sea and Caspian Sea. Oceanography (Black Sea Spec Issue) 18(2):76–85.

Kirby, RR and Beaugrand, G. 2009. Trophic amplification of climate warming. Proceedings of the Royal Society B 276: 4095-4103.

Kirby, RR, Beaugrand, G and Lindley, JA. 2009. Synergistic effects of climate and fishing in a marine ecosystem. Ecosystems 12: 548-561.

Leray M, Knowlton N. DNA barcoding and metabarcoding of standardized samples reveal patterns of marine benthic diversity. Proceedings of the National Academy of Sciences of the United States of America. 2015;112(7):2076-2081. doi:10.1073/pnas.1424997112.

Lynam, C.P., Gibbons, M.J., Axelsen, B.E., Sparks, C.A.J., Coetzee, J., Heywood, B.G. and Brierley, A.S. 2006. Jellyfish overtake fish in a heavily fished ecosystem. Current Biology 16: R492-R493.

Mountford, K. 1984. Phytoplankton. Chapter in: M. Kennish and R. Lutz. Ecology of Barnegat Bay, New Jersey. Springer-Verlag. Lecture Notes on Coastal and Estuarine Studies. New York, NY.

Nelson, T. 1925. On the occurrence and food habits of ctenophores in New Jersey incland coastal waters. Biological Bulletin 48:92-111.

Newell, G. and R. Newell. 1973. Marine Plankton: A Practical Guide. Hutchinson Educational. London, WI.

Nailis H, Coenye T, Van Nieuwerburgh F, Deforce D, Nelis HJ. 2006. Development and evaluation of different normalization strategies for gene expression studies in *Candida albicans* biofilms by real-time PCR. BMC Molecular Biology. 7: 25-32.

Newell, G. and R. Newell. 1973. Marine Plankton: A Practical Guide. Hutchinson Educational. London, WI.

Pauly, D., Christensen, V., Dalsgaard, J., Froese, R., and Torres, F. Jr. 1998. Fishing down marine food webs. Science 279: 860-863.

Pauly, D., Watson, R., and Alder, J. 2005. Global trends in world fisheries: impacts on marine ecosystems and food security. Philosophical Transactions of the Royal Society of London B. 360: 5-12.

Pompanon, F., Deagle, B.E., Symondson, W.O.C., Brown, D.S., Jarman, S.N., and P. Taberlet. 2012. Who is eating what: diet assessment using next generation sequencing. Molecular Ecology 21:1931-1950.

Purcell, J.E., Arai, M.N., 2001. Interactions of pelagic cnidarians and ctenophores with fish: a review. Hydrobiologia 451, 27–44.

Purcell, J.E., Breitburg, D.L. Decker, M.B., Graham, W.M., Youngbluth, M.J. and Raskoff, K.A. 2001. In: Coastal hypoxia: consequences for living resources and ecosystems (Rabalais, N.N. and Turner, R.E., eds.) American Geophysical Union, Washington, DC.

Purcell, J.E. and Decker, M.B. 2005. Effects of climate on relative predation by scyphomedusae and ctenophores on copepods in Chesapeake Bay during 1987-2000. Limnology and Oceanography 50: 376-387.

Purcell, J., Uye, S., Lo, W., 2007. Anthropogenic causes of jellyfish blooms and their direct consequences for humans: a review. Marine Ecology Progress Series 350:153-174

Reeve, M. R., Walter, M. A., Ikeda, T. 1978. Laboratory studies of ingestion and food utilization in lobate and tentaculate ctenophores. Limnology and Oceanography. 23: 740-751

Restaino, D.J., Bologna, P.A.X., Gaynor, J.J. Buchanan, G., and J. Bilinski. 2018a. Who's lurking in your lagoon? First occurrence of the invasive hydrozoan Moerisia inkermanica (Cnidaria: Hydrozoa) in New Jersey, USA. In review, BioInvasions Records.

Restaino, D.J., Bologna, P.A.X., and J.J. Gaynor. 2018b. Molecular Identification of Nudibranch Predation on Cnidarians. In review, Marine Ecology.

Richardson, A.J., Bakun, A., Hays, G.C., and Gibbons, M.J. 2009. The jellyfish joyride: causes, consequences and management responses to a more gelatinous future. Trends in Ecology and Evolution 24(6): 312-322.

Sandine, P. 1984. Zooplankton. Chapter in: Kennish, M. and R. Lutz. 1984. Ecology of Barnegat Bay, New Jersey. Lecture Notes on Coastal and Estuarine Studies. Springer-Verlag. New York, NY.

Schroth, W., Jarms, G., Streit, B., and B. Schierwater. 2002. Speciation and phylogeography in the cosmopolitan marine moon jelly, *Aurelia* sp. BMC Evolutionary Biology, 2(1), 1.

Shehzad, W., Riaz, T., Nawaz, M.A., Miquel, C., Poillot, C., Shah, S.A., Pompanon, F., Coissac, E., and P. Taberlet. 2012. Carnivore diet analysis based on next-generation sequencing: application to the leopard cat (Prionailurus bengalensis) in Pakistan. Molecular Ecology 21:1951-1965.

Smith, D. and K. Johnson. 1996. A Guide to Marine Coastal Plankton and Marine Invertebrate Larvae (second edition). Kendall/Hunt Publishing Co. Dubuque, IW.

Sullivan, BK, Van Keuren, D and Clancy, M. 2001. Timing and size of blooms of the ctenophore *Mnemiopsis leidyi* in relation to temperature in Narragansett Bay, RI. Hydrobiologica 451: 113-120.

Taberlet P., Coissac, E., Hajibabaei, M., Rieseberg, L.H. 2012. Environmental DNA. Molecular Ecology 21:1789–1793

Taghon, G.L., Ramey, P.A., Fuller, C.M., Petrecca, R.F., Grassle, J.P., and Belton, T.J. 2017. Benthic invertebrate community composition and sediment properties in Barnegat Bay, New Jersey, 1965−2014. In: Buchanan, G.A.; Belton, T.J., and Paudel, B. (eds.), A Comprehensive Assessment of Barnegat Bay–Little Egg Harbor, New Jersey.

Thomsen PF, Willerslev E (2015) Environmental DNA—an emerging tool in conservation for monitoring past and present biodiversity. Biological Conservation 183:4–18

Todd, C., M. Laverack and G Boxshall.1996. Coastal Marine Zooplankton: A Practical Manual for Students. Cambridge University Press. Cambridge, UK.

USEPA. 1994. Standard Operating Procedures for Phytoplankton Sample Collection and Preservation. U.S. Environmental Protection Agency. Grace Analytical Lab. Chicago, IL.

USEPA. 2002. Standard Operating Procedures for Phytoplankton Sample Collection and Preservation (Revised). U.S. Environmental Protection Agency. Grace Analytical Lab. Chicago, IL.
Walsh, P.G., Metzger, D.A., and R. Higuchi. 1991. Chelex R100 as a medium for simple extraction of DNA for PCR-based typing from forensic material. Biotechniques 10:506-513.
Yang, J., Zhang, X. 2020. eDNA metabarcoding in zooplankton improves the ecological status assessment of aquatic ecosystems. Environ Int 134:105230
Young, C. (ed) and M. Sewell and M. Rice (assoc. eds.). 2006. Atlas of Marine Invertebrate Larvae. Academic Press. Burlington, MA.

APPENDIX A. CTAB/NACL DNA EXTRACTION PROTOCOL

CTAB/NaCl DNA Extraction Protocol for NGS of Plankton Tow Samples*

Reagent	[Final]	Volume (for 100 mL)	# of sets	Total Volume or weight	Checklist
CTAB (solid)	2% (w/v)	2 g			
ddH_2O		57.8 mL			
1 M Tris (pH 8.0)	100 mM	10 mL			
5 M NaCl	1.4 M	28 mL			
0.5 M EDTA	20 mM	4 mL			
□-mercaptoethanol (14.3 M stock)	0.2% (v/v) (28.6 mM)	200 □L			
Proteinase K (20 mg/mL stock)	0.1 mg/mL	500 □L			
		100 mL	Total		

*To make 100 mL of CTAB extraction buffer. For typical plankton tow samples use 10 mL per jar. 100 mL should do 10 plankton tow samples.

1. Combine CTAB[3] and water in 100 mL graduated cylinder. Cover with Parafilm and run under hot tap water with gentle rocking until CTAB has dissolved (1 to 2 min).
2. Add other reagents in order. Move to hood to add the □-mercaptoethanol[1].
3. Add proteinase K last. Cover with Parafilm and invert to mix. Good for 24 hrs. if kept @4C (may need to warm up prior to use to redissolve CTAB).

Plankton Tow Extraction

1. Transfer each plankton tow sample to a pre-weighed 250 mL centrifuge bottle[2].
2. Top off all samples with 70% (v/v) EtOH[1] to bring all to same level.
3. Centrifuge for 10 min @10,000 rpm (15,000 x g @bottom of tube) @4C in Beckman-Coulter J2HS Centrifuge (using JLA-16.250 rotor).
4. Decant off supernatant into original plankton tow bottle and store @-20C for later use. Any small amount of remaining ethanol should be removed with a disposable Pasteur pipette.
5. Briefly (10 – 20 min) dry in Savant Speed-Vac (with rotor removed) to remove all traces of ethanol. Do NOT use heat and do not overdry.
6. Take weight of dried bottles (to calculate fresh weight of plankton tow).
7. Add 10 mL of freshly-prepared CTAB extraction mix to each sample in 250 mL centrifuge bottle.
8. Grind each sample using the Pro Scientific (PRO200 – Biogen Series) hand homogenizer for 30 sec @full speed (35,000 rpm). Move tip around in sample to fully homogenize material. (Use 7-mm x 95-mm saw-tooth generator probe; https://proscientific.com).
9. Cover with bottle cap.
10. Incubate @ 60°C in a water bath for 60 minutes. Invert tubes occasionally to mix.
11. Add 10 mL of chloroform:isoamyl alcohol (24:1) to each bottle.
12. Cover with cap and gently mix for 2 minutes by inverting the tube.
13. Transfer all liquid from each bottle to a pre-labelled 50 mL centrifuge tube.
14. Spin for 10 minutes @ 6,000 rpm (3,904 x g) in Hermle Z400K centrifuge using the 6 x 50 mL rotor (Hermle 220.97) @4°C.

15. Carefully pipette off upper aqueous phase (6 mL) into new 15 mL blue-capped tube. Do not transfer any solid material at the interface to new tube. Measure volume removed. Usually you can recover between 6 to 8 mL, depending on the amount of debris at the interface.
16. Add 1 µL RNase A (10 mg/mL) for every 1 mL of supernatant and incubate 30 minutes @37°C. (This step is optional; or could be done later).
17. Add 2/3 volume of isopropanol[1]. Close cap and gently invert to mix.
18. Store tubes overnight @-20C. Solution should turn cloudy immediately.
19. Spin for 15 minutes @6,000 rpm (3,904 x g) in Hermle Z400K centrifuge using the 6 x 50 mL rotor (Hermle 220.97) @4°C.
20. Decant off supernatant carefully so as to not lose the pellet. Then wash 2X with 10 mL of 70% (v/v) EtOH[1]. Each time spin for 5 minutes @6,000 rpm @4°C to pellet the DNA.
21. Remove supernatant and dry pellet briefly (5 min) in Speed-Vac **without** heating.
22. Re-suspend pellet in minimum volume of TE (pH 8.0).
23. Determine concentration and purity by UV absorption with NanoDrop. May also do Qubit 3.0 and Bioanalyzer analyses.
24. Store in aliquots at -20°C.
25. Run small aliquot on 1.0% agarose gel to check for quality and size of DNA.
26.

[1]Chloroform:isoamyl alcohol (24:1), isopropanol, □-mercaptoethanol and 70% (v/v) ethanol are stored in the explosion-proof refrigerator/freezer in SH 326.

[2]Use only PP or PPCO 250-mL plastic bottles. All others will collapse when using 15,000 X g.

[3]CTAB = Cetrimonium bromide [$(C_{16}H_{33})N(CH_3)_3$]Br; cetyltrimethyl-ammonium bromide; hexadecyltrimethylammonium bromide; CTAB] is a quaternary ammonium surfactant.

Appendix B. Taxa identified from the 2021 sample NEXGEN Sequence analysis and their presence at the 10 field sampling locations. Site Abbreviations organized by south to north: BL: Bayshore Lagoon; DCE: Double Creek East; DCW: Double Creek West; FRE: Forked River East; FRL: Forked River Lagoon; FRR9: Forked River RT 9; FRW: Forked River West; OCM: Oyster Creek Mouth; OCR9: Oyster Creek Outflow RT9; SBL: Sunrise Beach Lagoon; SB: Sunrise Beach; TRW: Toms River West

Phylum	**Class**	***Taxa Identified***	**BL**	**DCE**	**DCW**	**FRE**	**FRL**	**FRR9**	**FRW**	**OCM**	**OCR9**	**SBL**	**SB**	**TRW**
Annelida	Polychaeta	*Alitta succinea*			X		X		X					
Annelida	Polychaeta	*Amphitrite ornata*		X										
Annelida	NA	*Annelida sp. BOLD:ACQ1279*			X		X		X				X	X
Annelida	NA	*Annelida sp. BOLD:ACR0235*	X	X	X	X	X	X	X	X	X	X	X	X
Annelida	NA	*Annelida sp. VAFIV223-14*		X	X	X				X				
Annelida	Polychaeta	*Capitella teleta*			X									
Annelida	Polychaeta	*Dasybranchus sp. DH1*	X					X			X			X
Annelida	Polychaeta	*Diopatra cuprea*		X	X				X				X	
Annelida	Polychaeta	*Echiura sp. Polychaete2009PCR3G1*					X							
Annelida	Polychaeta	*Ficopomatus enigmaticus*	X				X							
Annelida	Polychaeta	*Glycinde multidens*			X			X						X
Annelida	Polychaeta	*Hesionidae sp. WCH 2331*		X										
Annelida	Polychaeta	*Hypereteone heteropoda*					X					X		X
Annelida	Polychaeta	*Loimia medusa*	X		X					X	X		X	
Annelida	Polychaeta	*Marphysa sanguinea*										X		
Annelida	Polychaeta	*Mediomastus sp. DNAS-464-60PM*		X										
Annelida	Polychaeta	*Neanthes sp. RP2011-N*						X						
Annelida	Polychaeta	*Nereididae SERC INVERT 1199*	X	X	X	X								
Annelida	Clitellata	*Paranais litoralis*					X							
Annelida	Polychaeta	*Parasabella microphthalma*								X		X		X
Annelida	Polychaeta	*Phyllodocidae sp. BMOO-13076*		X										
Annelida	Polychaeta	*Pileolaria sp. 11BIOAK-0893*	X					X						
Annelida	Polychaeta	*Polychaeta sp. BOLD:ACQ0474*			X					X				
Annelida	Polychaeta	*Polychaeta sp. BOLD:ACQ8109*		X										
Annelida	Polychaeta	*Polydora cornuta*		X	X	X	X	X	X	X				X

Annelida	Polychaeta	*Polydora websteri*	X				X							X
Annelida	Polychaeta	*Prionospio steenstrupi*		X	X	X							X	
Annelida	Polychaeta	*Protula pacifica*				X			X					X
Annelida	Polychaeta	*Serpulidae sp. BOLD:AAG0874*		X					X			X		
Annelida	Polychaeta	*Streblospio benedicti*					X	X		X	X	X		X
Arthropoda	Hexanauplia	*Acartia hudsonica*		X	X	X	X	X	X	X			X	X
Arthropoda	Hexanauplia	*Acartia tonsa*	X	X	X	X	X	X	X	X	X	X	X	X
Arthropoda	Hexanauplia	*Amphibalanus eburneus*	X		X		X	X	X	X	X	X	X	X
Arthropoda	Hexanauplia	*Amphibalanus improvisus*	X			X	X	X	X		X	X	X	X
Arthropoda	Malacostraca	*Amphipoda sp. DNAS-1B6-193928*	X	X										
Arthropoda	Malacostraca	*Amphipoda sp. LP-2009*					X			X	X	X		
Arthropoda	Malacostraca	*Ampithoe longimana*		X					X					
Arthropoda	Branchiopoda	*Artemia franciscana*	X	X	X	X	X	X	X	X	X	X	X	X
Arthropoda	Malacostraca	*Callinectes sapidus*				X				X				
Arthropoda	Malacostraca	*Caprella penantis*		X					X	X				
Arthropoda	Malacostraca	*Carcinus maenas*											X	
Arthropoda	Hexanauplia	*Centropages chierchiae*		X										
Arthropoda	Hexanauplia	*Centropages hamatus*	X	X	X	X	X	X	X	X	X	X	X	
Arthropoda	Hexanauplia	*Centropages typicus*		X	X									
Arthropoda	Hexanauplia	*Copilia quadrata*	X		X									
Arthropoda	Malacostraca	*Crangon franciscorum*		X		X	X							
Arthropoda	Malacostraca	*Crangon hakodatei*		X			X							
Arthropoda	Malacostraca	*Crangon septemspinosa*		X		X	X	X		X				
Arthropoda	Hexanauplia	*Cyclopoida sp. HE-654.1*					X	X			X	X		
Arthropoda	Malacostraca	*Cymadusa compta*		X	X									
Arthropoda	Malacostraca	*Dyspanopeus sayi*	X	X	X	X		X	X	X		X	X	X
Arthropoda	Hexanauplia	*Ectinosomatidae sp. SR-2019*		X	X	X				X				X
Arthropoda	Malacostraca	*Erichsonella filiformis*			X									
Arthropoda	Malacostraca	*Eurypanopeus depressus*					X				X	X	X	X
Arthropoda	Malacostraca	*Eurythenes gryllus*									X			

Arthropoda	Branchiopoda	*Evadne nordmanni*		X	X	X	X	X	X	X		X		
Arthropoda	Malacostraca	*Gammarus mucronatus*					X			X			X	
Arthropoda	Hexanauplia	*Harpacticoida sp. 10BIOBC-00687*						X	X					
Arthropoda	Hexanauplia	*Harpacticoida sp. DNZ085*		X	X	X	X		X	X			X	
Arthropoda	Malacostraca	*Hemigrapsus sanguineus*									X			
Arthropoda	Malacostraca	*Hexapanopeus angustifrons*								X				
Arthropoda	Malacostraca	*Hippolyte zostericola*		X	X	X	X	X		X			X	
Arthropoda	Malacostraca	*Hyalella azteca*						X						
Arthropoda	Malacostraca	*Idotea sp. BEB-2013*		X	X	X	X							
Arthropoda	Merostomata	*Limulus polyphemus*												X
Arthropoda	Branchiopoda	*Macrothrix sp. HE-364*	X				X	X		X	X	X	X	
Arthropoda	Malacostraca	*Metasesarma obesum*			X									
Arthropoda	Malacostraca	*Minuca minax*									X			X
Arthropoda	Malacostraca	*Minuca pugnax*		X	X			X		X	X		X	X
Arthropoda	Malacostraca	*Neomysis americana*		X					X	X				
Arthropoda	Hexanauplia	*Oithona similis*		X										
Arthropoda	Hexanauplia	*Onychocorycaeus catus*	X		X					X	X	X	X	X
Arthropoda	Malacostraca	*Ovalipes ocellatus*		X										
Arthropoda	Malacostraca	*Pagurus exilis*				X								
Arthropoda	Malacostraca	*Pagurus longicarpus*		X	X	X				X				
Arthropoda	Malacostraca	*Palaemon sp. DNAS-14F-145035*		X									X	X
Arthropoda	Malacostraca	*Palaemon gravieri*									X			
Arthropoda	Malacostraca	*Palaemon macrodactylus*	X		X		X		X	X	X			X
Arthropoda	Malacostraca	*Palaemon pugio*												X
Arthropoda	Malacostraca	*Palaemon vulgaris*		X		X		X			X			X
Arthropoda	Malacostraca	*Panopeus herbstii*						X			X		X	X
Arthropoda	Hexanauplia	*Paracalanus sp. F AC-2013*		X										
Arthropoda	Malacostraca	*Paracaprella tenuis*			X		X	X		X				
Arthropoda	Branchiopoda	*Pleopis polyphemoides*		X	X	X	X	X		X	X	X	X	
Arthropoda	Branchiopoda	*Podon intermedius*		X										

Arthropoda	Branchiopoda	*Podon leuckartii*								X				
Arthropoda	Malacostraca	*Proasellus coiffaiti*		X	X	X	X		X	X	X		X	X
Arthropoda	Hexanauplia	*Pseudocalanus moultoni*		X										
Arthropoda	Malacostraca	*Rhithropanopeus harrisii*	X				X	X			X	X	X	X
Arthropoda	Malacostraca	*Sesarma reticulatum*								X				
Arthropoda	Hexanauplia	*Temora longicornis*		X	X	X		X		X	X			X
Arthropoda	Hexanauplia	*Tigriopus californicus*		X	X					X				X
Arthropoda	Malacostraca	*Upogebia affinis*		X	X	X				X			X	
Bryozoa	Gymnolaemata	*Amathia sp. n. 2 AW-2014*	X	X	X		X	X	X	X	X	X		X
Bryozoa	Gymnolaemata	*Bugulina stolonifera*										X		
Bryozoa	Gymnolaemata	*Conopeum tenuissimum*	X	X	X	X	X	X	X	X			X	X
Bryozoa	Gymnolaemata	*Membranipora tenuis*									X			
Bryozoa	Gymnolaemata	*Tricellaria occidentalis*		X	X				X	X				
Chordata	Actinopteri	*Anchoa mitchilli*			X	X	X	X		X		X	X	X
Chordata	Actinopteri	*Apeltes quadracus*									X			
Chordata	Ascidiacea	*Ascidia ahodori*	X	X	X		X	X	X	X			X	X
Chordata	Actinopteri	*Bairdiella chrysoura*		X		X		X		X				
Chordata	Ascidiacea	*Botrylloides violaceus*	X	X	X	X	X	X	X	X	X	X	X	
Chordata	Ascidiacea	*Botryllus schlosseri*		X		X	X		X	X				
Chordata	Actinopteri	*Brevoortia aurea*		X				X						
Chordata	Actinopteri	*Cynoscion regalis*		X			X	X		X		X		
Chordata	Actinopteri	*Engraulidae sp. BOLD:AAB7044*	X	X	X	X	X	X	X	X			X	X
Chordata	Actinopteri	*Fundulus heteroclitus*									X			
Chordata	Actinopteri	*Fundulus similis*									X			
Chordata	Actinopteri	*Gobiesox sp. BOLD:AAE7082*						X	X					X
Chordata	Actinopteri	*Gobiosoma ginsburgi*				X								
Chordata	Actinopteri	*Membras martinica*		X					X	X	X	X	X	X
Chordata	Actinopteri	*Menidia beryllina*						X						
Chordata	Actinopteri	*Menidia menidia*	X	X	X	X	X	X	X	X	X	X	X	X
Chordata	Actinopteri	*Menticirrhus saxatilis*							X					

Chordata	Actinopteri	*Oncorhynchus kisutch*									X			
Chordata	Actinopteri	*Ophidion marginatum*						X						
Chordata	Actinopteri	*Pogonias courbina*					X			X			X	
Chordata	Actinopteri	*Pogonias cromis*		X		X		X		X			X	X
Chordata	Actinopteri	*Sphoeroides nephelus*	X	X	X	X	X	X	X	X	X	X	X	X
Chordata	Actinopteri	*Syngnathus fuscus*		X			X	X	X	X	X	X	X	X
Chordata	Actinopteri	*Tautoga onitis*	X	X	X		X	X	X	X	X	X		
Chordata	Actinopteri	*Trinectes maculatus*											X	X
Chordata	Actinopteri	*Zoarces gillii*	X											
Cnidaria	Anthozoa	*Arachnactis albida*		X										
Cnidaria	Hydrozoa	*Bougainvillia carolinensis*		X									X	
Cnidaria	Scyphozoa	*Chrysaora sp. MXTBARR*			X		X							
Cnidaria	Scyphozoa	*Chrysaora chesapeakei*	X	X	X	X	X	X	X	X	X	X	X	X
Cnidaria	Scyphozoa	*Chrysaora quinquecirrha*					X	X						
Cnidaria	Hydrozoa	*Clytia gracilis*	X											
Cnidaria	Hydrozoa	*Clytia hemisphaerica*	X							X				
Cnidaria	Hydrozoa	*Clytia xiamenensis*							X					
Cnidaria	NA	*Cnidaria sp. C 0241*				X								
Cnidaria	Anthozoa	*Diadumene leucolena*		X	X	X	X		X	X	X		X	X
Cnidaria	Hydrozoa	*Gonionemus sp. GS JRH-2014*	X	X	X	X	X		X	X	X	X		
Cnidaria	Hydrozoa	*Halopteris diaphana*		X							X			
Cnidaria	Hydrozoa	*Kirchenpaueria halecioides*		X										
Cnidaria	Hydrozoa	*Lovenella assimilis*						X						
Cnidaria	Hydrozoa	*Nemopsis bachei*	X	X	X	X	X	X	X	X	X	X	X	X
Cnidaria	Hydrozoa	*Obelia bidentata*	X		X	X		X	X	X			X	X
Cnidaria	Hydrozoa	*Obelia dichotoma*	X	X						X				
Cnidaria	Anthozoa	*Sagartiogeton laceratus*			X									
Cnidaria	Hydrozoa	*Sarsia tubulosa*		X	X	X	X	X	X	X				
Cnidaria	Hydrozoa	*Turritopsis dohrnii*						X						
Ctenophora	Tentaculata	*Mnemiopsis leidyi*	X	X	X	X	X	X	X	X	X	X	X	X
Echinodermata	Holothuroidea	*Leptosynapta tenuis*		X										
Echinodermata	Ophiuroidea	*Microphiopholis atra*	X						X					
Echinodermata	Holothuroidea	*Pentamera calcigera*		X									X	

Echinoderm ata	Holothuroidea	*Sclerodactyla briareus*		X	X									
Mollusca	Bivalvia	*Ameritella agilis*				X								
Mollusca	Bivalvia	*Ameritella mitchelli*						X	X					X
Mollusca	Gastropoda	*Astyris lunata*		X		X								
Mollusca	Gastropoda	*Bittiolum varium*	X	X		X				X	X		X	
Mollusca	Gastropoda	*Corambe obscura*								X				
Mollusca	Gastropoda	*Costoanachis avara*				X			X				X	
Mollusca	Bivalvia	*Crassostrea virginica*	X											
Mollusca	Gastropoda	*Ercolania fuscata*				X								
Mollusca	Gastropoda	*Gyroscala rupicola*							X					
Mollusca	Gastropoda	*Haminoea solitaria*					X	X		X				X
Mollusca	Bivalvia	*Kelliopsis elevata*		X										
Mollusca	Gastropoda	*Lunatia heros*		X										
Mollusca	Bivalvia	*Mercenaria mercenaria*				X		X						
Mollusca	Bivalvia	*Mulinia lateralis*								X				
Mollusca	Gastropoda	*Nassarius vibex*				X			X				X	X
Mollusca	Bivalvia	*Tagelus divisus*		X	X	X	X		X	X	X		X	
Mollusca	Gastropoda	*Tritia obsoleta*								X				
Mollusca	Gastropoda	*Tritia trivittata*		X	X									
Nemertea	Enopla	*Monostilifera sp. WCH 2441*		X	X									
Nemertea	Enopla	*Tetrastemma wilsoni*		X						X				
Platyhelminthes	Monogenea	*Ancyrocephalinae sp. FA-2017*					X						X	
Platyhelminthes	Rhabditophora	*Microstomum compositum*			X									
Platyhelminthes	Rhabditophora	*Microstomum septentrionale*		X										
Porifera	Demospongiae	*Callyspongia siphonella*									X			
Porifera	Demospongiae	*Cliona celata*		X	X		X			X				
Porifera	Demospongiae	*Halichondria panicea*				X								
Rotifera	Bdelloidea	*Rotaria tardigrada*									X			

Appendix C. Pair-wise comparison differences in community structure among all Site-Year combinations based on the ANOSIM analysis of faunal density from plankton tows.

Site-Year	Site-Year Comparison	R Statistic	Significance (P-value)
DCE 2018	DCW 2018	0.012	0.274
DCE 2018	FRE 2018	-0.019	0.582
DCE 2018	FRL 2018	0.26	0.002
DCE 2018	FRRT9 2018	-0.022	0.592
DCE 2018	FRW 2018	-0.056	0.961
DCE 2018	OCM 2018	0.008	0.311
DCE 2018	OCRT9 2018	0.105	0.04
DCE 2018	SB 2018	0.009	0.317
DCE 2018	DCE 2019	0.108	0.036
DCE 2018	DCW 2019	0.096	0.063
DCE 2018	FRE 2019	0.099	0.049
DCE 2018	FRL 2019	0.343	0.001
DCE 2018	FRRT9 2019	0.372	0.001
DCE 2018	FRW 2019	0.05	0.134
DCE 2018	OCM 2019	0.108	0.038
DCE 2018	OCRT9 2019	0.245	0.005
DCE 2018	SB 2019	0.118	0.022
DCE 2018	DCE 2021	0.261	0.001
DCE 2018	DCW 2021	0.175	0.013
DCE 2018	FRE 2021	0.292	0.002
DCE 2018	FRL 2021	0.421	0.001
DCE 2018	FRRT9 2021	0.285	0.002
DCE 2018	FRW 2021	0.191	0.013
DCE 2018	OCM 2021	0.113	0.033
DCE 2018	OCRT9 2021	0.201	0.009
DCE 2018	SB 2021	0.011	0.3
DCE 2018	TRW 2018	0.065	0.104
DCE 2018	TRW 2019	0.059	0.105
DCE 2018	TRW 2021	0.124	0.035
DCW 2018	FRE 2018	0.078	0.085
DCW 2018	FRL 2018	0.126	0.029
DCW 2018	FRRT9 2018	0.029	0.204
DCW 2018	FRW 2018	-0.037	0.771
DCW 2018	OCM 2018	0.04	0.158
DCW 2018	OCRT9 2018	0.164	0.01
DCW 2018	SB 2018	-0.061	0.946
DCW 2018	DCE 2019	0.174	0.01
DCW 2018	DCW 2019	0.08	0.083
DCW 2018	FRE 2019	0.148	0.011
DCW 2018	FRL 2019	0.251	0.002
DCW 2018	FRRT9 2019	0.277	0.001

DCW 2018	FRW 2019	0.034	0.175
DCW 2018	OCM 2019	0.106	0.042
DCW 2018	OCRT9 2019	0.188	0.005
DCW 2018	SB 2019	0.08	0.068
DCW 2018	DCE 2021	0.192	0.004
DCW 2018	DCW 2021	0.05	0.142
DCW 2018	FRE 2021	0.166	0.012
DCW 2018	FRL 2021	0.295	0.003
DCW 2018	FRRT9 2021	0.212	0.003
DCW 2018	FRW 2021	0.091	0.056
DCW 2018	OCM 2021	0.022	0.239
DCW 2018	OCRT9 2021	0.151	0.02
DCW 2018	SB 2021	-0.01	0.418
DCW 2018	TRW 2018	0.017	0.257
DCW 2018	TRW 2019	0.022	0.234
DCW 2018	TRW 2021	0.034	0.148
FRE 2018	FRL 2018	0.401	0.001
FRE 2018	FRRT9 2018	0.096	0.039
FRE 2018	FRW 2018	-0.019	0.599
FRE 2018	OCM 2018	0.074	0.061
FRE 2018	OCRT9 2018	0.198	0.004
FRE 2018	SB 2018	0.16	0.02
FRE 2018	DCE 2019	0.097	0.034
FRE 2018	DCW 2019	0.166	0.006
FRE 2018	FRE 2019	0.119	0.015
FRE 2018	FRL 2019	0.464	0.001
FRE 2018	FRRT9 2019	0.473	0.001
FRE 2018	FRW 2019	0.177	0.009
FRE 2018	OCM 2019	0.212	0.001
FRE 2018	OCRT9 2019	0.359	0.001
FRE 2018	SB 2019	0.182	0.002
FRE 2018	DCE 2021	0.252	0.001
FRE 2018	DCW 2021	0.246	0.002
FRE 2018	FRE 2021	0.321	0.001
FRE 2018	FRL 2021	0.569	0.001
FRE 2018	FRRT9 2021	0.404	0.001
FRE 2018	FRW 2021	0.266	0.002
FRE 2018	OCM 2021	0.176	0.01
FRE 2018	OCRT9 2021	0.275	0.003
FRE 2018	SB 2021	0.092	0.039
FRE 2018	TRW 2018	0.235	0.004
FRE 2018	TRW 2019	0.213	0.004
FRE 2018	TRW 2021	0.26	0.001
FRL 2018	FRRT9 2018	0.273	0.002
FRL 2018	FRW 2018	0.147	0.014

FRL 2018	OCM 2018	0.248	0.001
FRL 2018	OCRT9 2018	0.397	0.001
FRL 2018	SB 2018	0.108	0.043
FRL 2018	DCE 2019	0.567	0.001
FRL 2018	DCW 2019	0.312	0.001
FRL 2018	FRE 2019	0.383	0.001
FRL 2018	FRL 2019	0.121	0.019
FRL 2018	FRRT9 2019	0.201	0.003
FRL 2018	FRW 2019	0.29	0.003
FRL 2018	OCM 2019	0.377	0.001
FRL 2018	OCRT9 2019	0.148	0.009
FRL 2018	SB 2019	0.283	0.001
FRL 2018	DCE 2021	0.369	0.001
FRL 2018	DCW 2021	0.138	0.013
FRL 2018	FRE 2021	0.171	0.019
FRL 2018	FRL 2021	0.177	0.008
FRL 2018	FRRT9 2021	0.148	0.01
FRL 2018	FRW 2021	0.188	0.004
FRL 2018	OCM 2021	0.135	0.011
FRL 2018	OCRT9 2021	0.183	0.006
FRL 2018	SB 2021	0.22	0.005
FRL 2018	TRW 2018	0.115	0.035
FRL 2018	TRW 2019	0.242	0.006
FRL 2018	TRW 2021	0.081	0.061
FRRT9 2018	FRW 2018	0.053	0.12
FRRT9 2018	OCM 2018	-0.041	0.862
FRRT9 2018	OCRT9 2018	0.016	0.289
FRRT9 2018	SB 2018	0.028	0.255
FRRT9 2018	DCE 2019	0.266	0.001
FRRT9 2018	DCW 2019	0.12	0.031
FRRT9 2018	FRE 2019	0.179	0.007
FRRT9 2018	FRL 2019	0.332	0.002
FRRT9 2018	FRRT9 2019	0.379	0.001
FRRT9 2018	FRW 2019	0.089	0.062
FRRT9 2018	OCM 2019	0.102	0.045
FRRT9 2018	OCRT9 2019	0.24	0.001
FRRT9 2018	SB 2019	0.166	0.005
FRRT9 2018	DCE 2021	0.327	0.001
FRRT9 2018	DCW 2021	0.214	0.002
FRRT9 2018	FRE 2021	0.363	0.001
FRRT9 2018	FRL 2021	0.489	0.001
FRRT9 2018	FRRT9 2021	0.306	0.001
FRRT9 2018	FRW 2021	0.239	0.003
FRRT9 2018	OCM 2021	0.133	0.014
FRRT9 2018	OCRT9 2021	0.214	0.003

FRRT9 2018	SB 2021	0.047	0.15
FRRT9 2018	TRW 2018	0.079	0.087
FRRT9 2018	TRW 2019	0.076	0.078
FRRT9 2018	TRW 2021	0.14	0.028
FRW 2018	OCM 2018	0.015	0.264
FRW 2018	OCRT9 2018	0.166	0.009
FRW 2018	SB 2018	-0.022	0.586
FRW 2018	DCE 2019	0.145	0.023
FRW 2018	DCW 2019	0.068	0.084
FRW 2018	FRE 2019	0.031	0.193
FRW 2018	FRL 2019	0.207	0.001
FRW 2018	FRRT9 2019	0.204	0.001
FRW 2018	FRW 2019	0.075	0.093
FRW 2018	OCM 2019	0.123	0.023
FRW 2018	OCRT9 2019	0.125	0.006
FRW 2018	SB 2019	0.05	0.138
FRW 2018	DCE 2021	0.146	0.012
FRW 2018	DCW 2021	0.051	0.096
FRW 2018	FRE 2021	0.098	0.033
FRW 2018	FRL 2021	0.314	0.001
FRW 2018	FRRT9 2021	0.18	0.001
FRW 2018	FRW 2021	0.08	0.062
FRW 2018	OCM 2021	0.003	0.364
FRW 2018	OCRT9 2021	0.112	0.017
FRW 2018	SB 2021	0.033	0.195
FRW 2018	TRW 2018	0.062	0.097
FRW 2018	TRW 2019	0.097	0.065
FRW 2018	TRW 2021	0.037	0.182
OCM 2018	OCRT9 2018	-0.015	0.548
OCM 2018	SB 2018	0.036	0.215
OCM 2018	DCE 2019	0.255	0.001
OCM 2018	DCW 2019	0.087	0.057
OCM 2018	FRE 2019	0.11	0.032
OCM 2018	FRL 2019	0.287	0.001
OCM 2018	FRRT9 2019	0.266	0.001
OCM 2018	FRW 2019	0.044	0.17
OCM 2018	OCM 2019	0.088	0.054
OCM 2018	OCRT9 2019	0.15	0.004
OCM 2018	SB 2019	0.128	0.01
OCM 2018	DCE 2021	0.305	0.001
OCM 2018	DCW 2021	0.231	0.001
OCM 2018	FRE 2021	0.337	0.001
OCM 2018	FRL 2021	0.459	0.001
OCM 2018	FRRT9 2021	0.308	0.001
OCM 2018	FRW 2021	0.27	0.001

OCM 2018	OCM 2021	0.144	0.013
OCM 2018	OCRT9 2021	0.21	0.003
OCM 2018	SB 2021	0.057	0.118
OCM 2018	TRW 2018	0.056	0.1
OCM 2018	TRW 2019	0.072	0.086
OCM 2018	TRW 2021	0.165	0.012
OCRT9 2018	SB 2018	0.166	0.014
OCRT9 2018	DCE 2019	0.33	0.001
OCRT9 2018	DCW 2019	0.178	0.01
OCRT9 2018	FRE 2019	0.204	0.005
OCRT9 2018	FRL 2019	0.443	0.001
OCRT9 2018	FRRT9 2019	0.466	0.001
OCRT9 2018	FRW 2019	0.137	0.02
OCRT9 2018	OCM 2019	0.162	0.013
OCRT9 2018	OCRT9 2019	0.299	0.001
OCRT9 2018	SB 2019	0.231	0.001
OCRT9 2018	DCE 2021	0.372	0.001
OCRT9 2018	DCW 2021	0.373	0.001
OCRT9 2018	FRE 2021	0.554	0.001
OCRT9 2018	FRL 2021	0.662	0.001
OCRT9 2018	FRRT9 2021	0.479	0.001
OCRT9 2018	FRW 2021	0.436	0.001
OCRT9 2018	OCM 2021	0.281	0.001
OCRT9 2018	OCRT9 2021	0.375	0.001
OCRT9 2018	SB 2021	0.218	0.002
OCRT9 2018	TRW 2018	0.162	0.008
OCRT9 2018	TRW 2019	0.182	0.013
OCRT9 2018	TRW 2021	0.328	0.001
SB 2018	DCE 2019	0.305	0.001
SB 2018	DCW 2019	0.091	0.088
SB 2018	FRE 2019	0.15	0.023
SB 2018	FRL 2019	0.269	0.001
SB 2018	FRRT9 2019	0.274	0.001
SB 2018	FRW 2019	0.021	0.234
SB 2018	OCM 2019	0.142	0.029
SB 2018	OCRT9 2019	0.136	0.039
SB 2018	SB 2019	0.08	0.083
SB 2018	DCE 2021	0.21	0.005
SB 2018	DCW 2021	0.084	0.071
SB 2018	FRE 2021	0.178	0.02
SB 2018	FRL 2021	0.296	0.002
SB 2018	FRRT9 2021	0.16	0.016
SB 2018	FRW 2021	0.06	0.125
SB 2018	OCM 2021	0.006	0.35
SB 2018	OCRT9 2021	0.108	0.04

SB 2018	SB 2021	-0.019	0.522
SB 2018	TRW 2018	-0.001	0.395
SB 2018	TRW 2019	0.025	0.237
SB 2018	TRW 2021	-0.021	0.521
DCE 2019	DCW 2019	0.226	0.005
DCE 2019	FRE 2019	0.163	0.003
DCE 2019	FRL 2019	0.671	0.001
DCE 2019	FRRT9 2019	0.652	0.001
DCE 2019	FRW 2019	0.213	0.002
DCE 2019	OCM 2019	0.261	0.001
DCE 2019	OCRT9 2019	0.591	0.001
DCE 2019	SB 2019	0.165	0.004
DCE 2019	DCE 2021	0.208	0.005
DCE 2019	DCW 2021	0.302	0.001
DCE 2019	FRE 2021	0.548	0.001
DCE 2019	FRL 2021	0.789	0.001
DCE 2019	FRRT9 2021	0.689	0.001
DCE 2019	FRW 2021	0.392	0.001
DCE 2019	OCM 2021	0.264	0.002
DCE 2019	OCRT9 2021	0.61	0.001
DCE 2019	SB 2021	0.29	0.001
DCE 2019	TRW 2018	0.32	0.001
DCE 2019	TRW 2019	0.186	0.003
DCE 2019	TRW 2021	0.424	0.001
DCW 2019	FRE 2019	0.022	0.238
DCW 2019	FRL 2019	0.473	0.001
DCW 2019	FRRT9 2019	0.443	0.001
DCW 2019	FRW 2019	-0.048	0.892
DCW 2019	OCM 2019	-0.045	0.857
DCW 2019	OCRT9 2019	0.34	0.001
DCW 2019	SB 2019	0.007	0.372
DCW 2019	DCE 2021	0.301	0.001
DCW 2019	DCW 2021	0.301	0.002
DCW 2019	FRE 2021	0.404	0.001
DCW 2019	FRL 2021	0.579	0.001
DCW 2019	FRRT9 2021	0.501	0.001
DCW 2019	FRW 2021	0.375	0.001
DCW 2019	OCM 2021	0.215	0.001
DCW 2019	OCRT9 2021	0.44	0.001
DCW 2019	SB 2021	0.076	0.08
DCW 2019	TRW 2018	0.118	0.05
DCW 2019	TRW 2019	0.08	0.082
DCW 2019	TRW 2021	0.178	0.01
FRE 2019	FRL 2019	0.542	0.001
FRE 2019	FRRT9 2019	0.476	0.001

FRE 2019	FRW 2019	0.006	0.341
FRE 2019	OCM 2019	0.087	0.053
FRE 2019	OCRT9 2019	0.353	0.001
FRE 2019	SB 2019	0.057	0.089
FRE 2019	DCE 2021	0.263	0.001
FRE 2019	DCW 2021	0.305	0.001
FRE 2019	FRE 2021	0.363	0.001
FRE 2019	FRL 2021	0.608	0.001
FRE 2019	FRRT9 2021	0.531	0.001
FRE 2019	FRW 2021	0.39	0.001
FRE 2019	OCM 2021	0.239	0.002
FRE 2019	OCRT9 2021	0.429	0.001
FRE 2019	SB 2021	0.159	0.009
FRE 2019	TRW 2018	0.166	0.012
FRE 2019	TRW 2019	0.14	0.02
FRE 2019	TRW 2021	0.264	0.004
FRL 2019	FRRT9 2019	0.031	0.219
FRL 2019	FRW 2019	0.447	0.001
FRL 2019	OCM 2019	0.518	0.001
FRL 2019	OCRT9 2019	0.063	0.061
FRL 2019	SB 2019	0.455	0.001
FRL 2019	DCE 2021	0.483	0.001
FRL 2019	DCW 2021	0.229	0.001
FRL 2019	FRE 2021	0.3	0.001
FRL 2019	FRL 2021	0.208	0.003
FRL 2019	FRRT9 2021	0.095	0.032
FRL 2019	FRW 2021	0.269	0.001
FRL 2019	OCM 2021	0.178	0.002
FRL 2019	OCRT9 2021	0.174	0.005
FRL 2019	SB 2021	0.291	0.001
FRL 2019	TRW 2018	0.174	0.007
FRL 2019	TRW 2019	0.336	0.001
FRL 2019	TRW 2021	0.191	0.003
FRRT9 2019	FRW 2019	0.364	0.001
FRRT9 2019	OCM 2019	0.519	0.001
FRRT9 2019	OCRT9 2019	0.064	0.086
FRRT9 2019	SB 2019	0.403	0.001
FRRT9 2019	DCE 2021	0.457	0.001
FRRT9 2019	DCW 2021	0.291	0.001
FRRT9 2019	FRE 2021	0.313	0.001
FRRT9 2019	FRL 2021	0.232	0.001
FRRT9 2019	FRRT9 2021	0.17	0.009
FRRT9 2019	FRW 2021	0.287	0.001
FRRT9 2019	OCM 2021	0.238	0.001
FRRT9 2019	OCRT9 2021	0.202	0.003

FRRT9 2019	SB 2021	0.258	0.001
FRRT9 2019	TRW 2018	0.218	0.004
FRRT9 2019	TRW 2019	0.319	0.001
FRRT9 2019	TRW 2021	0.222	0.002
FRW 2019	OCM 2019	-0.015	0.526
FRW 2019	OCRT9 2019	0.277	0.002
FRW 2019	SB 2019	0.021	0.267
FRW 2019	DCE 2021	0.3	0.001
FRW 2019	DCW 2021	0.275	0.001
FRW 2019	FRE 2021	0.368	0.002
FRW 2019	FRL 2021	0.515	0.001
FRW 2019	FRRT9 2021	0.44	0.001
FRW 2019	FRW 2021	0.311	0.002
FRW 2019	OCM 2021	0.173	0.016
FRW 2019	OCRT9 2021	0.377	0.001
FRW 2019	SB 2021	0.063	0.119
FRW 2019	TRW 2018	0.064	0.093
FRW 2019	TRW 2019	0.012	0.282
FRW 2019	TRW 2021	0.15	0.019
OCM 2019	OCRT9 2019	0.408	0.001
OCM 2019	SB 2019	0.048	0.144
OCM 2019	DCE 2021	0.329	0.001
OCM 2019	DCW 2021	0.324	0.001
OCM 2019	FRE 2021	0.489	0.001
OCM 2019	FRL 2021	0.646	0.001
OCM 2019	FRRT9 2021	0.543	0.001
OCM 2019	FRW 2021	0.402	0.001
OCM 2019	OCM 2021	0.23	0.005
OCM 2019	OCRT9 2021	0.486	0.001
OCM 2019	SB 2021	0.093	0.067
OCM 2019	TRW 2018	0.171	0.022
OCM 2019	TRW 2019	0.105	0.05
OCM 2019	TRW 2021	0.212	0.008
OCRT9 2019	SB 2019	0.337	0.001
OCRT9 2019	DCE 2021	0.397	0.001
OCRT9 2019	DCW 2021	0.219	0.001
OCRT9 2019	FRE 2021	0.247	0.001
OCRT9 2019	FRL 2021	0.205	0.006
OCRT9 2019	FRRT9 2021	0.041	0.148
OCRT9 2019	FRW 2021	0.234	0.001
OCRT9 2019	OCM 2021	0.124	0.009
OCRT9 2019	OCRT9 2021	0.079	0.073
OCRT9 2019	SB 2021	0.192	0.002
OCRT9 2019	TRW 2018	0.077	0.058
OCRT9 2019	TRW 2019	0.231	0.003

OCRT9 2019	TRW 2021	0.127	0.024
SB 2019	DCE 2021	0.21	0.002
SB 2019	DCW 2021	0.167	0.008
SB 2019	FRE 2021	0.305	0.001
SB 2019	FRL 2021	0.495	0.001
SB 2019	FRRT9 2021	0.425	0.001
SB 2019	FRW 2021	0.227	0.005
SB 2019	OCM 2021	0.131	0.018
SB 2019	OCRT9 2021	0.378	0.001
SB 2019	SB 2021	0.084	0.047
SB 2019	TRW 2018	0.161	0.012
SB 2019	TRW 2019	0.103	0.044
SB 2019	TRW 2021	0.149	0.007
DCE 2021	DCW 2021	0.132	0.017
DCE 2021	FRE 2021	0.241	0.001
DCE 2021	FRL 2021	0.516	0.001
DCE 2021	FRRT9 2021	0.426	0.001
DCE 2021	FRW 2021	0.199	0.007
DCE 2021	OCM 2021	0.085	0.047
DCE 2021	OCRT9 2021	0.415	0.001
DCE 2021	SB 2021	0.231	0.002
DCE 2021	TRW 2018	0.309	0.001
DCE 2021	TRW 2019	0.269	0.003
DCE 2021	TRW 2021	0.292	0.001
DCW 2021	FRE 2021	0.021	0.237
DCW 2021	FRL 2021	0.211	0.001
DCW 2021	FRRT9 2021	0.167	0.001
DCW 2021	FRW 2021	-0.008	0.479
DCW 2021	OCM 2021	-0.023	0.638
DCW 2021	OCRT9 2021	0.141	0.005
DCW 2021	SB 2021	0.097	0.034
DCW 2021	TRW 2018	0.163	0.006
DCW 2021	TRW 2019	0.212	0.009
DCW 2021	TRW 2021	0.045	0.118
FRE 2021	FRL 2021	0.177	0.009
FRE 2021	FRRT9 2021	0.191	0.003
FRE 2021	FRW 2021	0.075	0.059
FRE 2021	OCM 2021	0.037	0.171
FRE 2021	OCRT9 2021	0.15	0.013
FRE 2021	SB 2021	0.148	0.011
FRE 2021	TRW 2018	0.266	0.002
FRE 2021	TRW 2019	0.35	0.002
FRE 2021	TRW 2021	0.089	0.055
FRL 2021	FRRT9 2021	0.102	0.048
FRL 2021	FRW 2021	0.168	0.006

FRL 2021	OCM 2021	0.206	0.002
FRL 2021	OCRT9 2021	0.162	0.012
FRL 2021	SB 2021	0.278	0.001
FRL 2021	TRW 2018	0.338	0.001
FRL 2021	TRW 2019	0.443	0.001
FRL 2021	TRW 2021	0.164	0.012
FRRT9 2021	FRW 2021	0.13	0.013
FRRT9 2021	OCM 2021	0.12	0.017
FRRT9 2021	OCRT9 2021	0.011	0.296
FRRT9 2021	SB 2021	0.178	0.003
FRRT9 2021	TRW 2018	0.182	0.004
FRRT9 2021	TRW 2019	0.367	0.001
FRRT9 2021	TRW 2021	0.068	0.067
FRW 2021	OCM 2021	-0.04	0.825
FRW 2021	OCRT9 2021	0.105	0.028
FRW 2021	SB 2021	0.051	0.104
FRW 2021	TRW 2018	0.223	0.007
FRW 2021	TRW 2019	0.231	0.009
FRW 2021	TRW 2021	0.041	0.161
OCM 2021	OCRT9 2021	0.109	0.024
OCM 2021	SB 2021	0.032	0.195
OCM 2021	TRW 2018	0.103	0.047
OCM 2021	TRW 2019	0.124	0.025
OCM 2021	TRW 2021	0.034	0.189
OCRT9 2021	SB 2021	0.076	0.056
OCRT9 2021	TRW 2018	0.205	0.003
OCRT9 2021	TRW 2019	0.354	0.002
OCRT9 2021	TRW 2021	0.053	0.129
SB 2021	TRW 2018	0.14	0.02
SB 2021	TRW 2019	0.134	0.029
SB 2021	TRW 2021	0.022	0.234
TRW 2018	TRW 2019	-0.003	0.397
TRW 2018	TRW 2021	0.055	0.132
TRW 2019	TRW 2021	0.148	0.024